2012

THE ROLE OF p62 IN OSTEOCLASTOGENESIS AND PAGET'S DISEASE OF BONE

Tamer Hadi
Virginia Commonwealth University

THE ROLE OF p62 IN OSTEOCLASTOGENESIS AND PAGET'S DISEASE OF BONE

A dissertation submitted in partial fulfillment of the requirements for the degree of
Doctor of Philosophy at Virginia Commonwealth University

by

Tamer Mahmoud Abdel Hadi

Bachelor of Science, University of California, Berkeley, 1998
Master of Science, University of California, Davis, 2007

Director: Jolene J. Windle, Ph.D.
Irene Shaw Grigg Distinguished Professor, Department of Molecular and Human Genetics
Director, VCU Transgenic/Knock-out Mouse Core
Cancer Molecular Genetics Program Co-leader, Massey Cancer Center

Virginia Commonwealth University
Richmond, VA
April, 2014

ACKNOWLEDGEMENTS

I would like to begin by thanking my wife, Marwa, and children, Ismael and Maryam. Thank you for your patience, companionship, encouragement, and love over the past several years. I could not have done it without you.

I also want to thank my mentor and advisor Dr. Jolene Windle. Jolene, I began my research career as an undergraduate in the late 1990s, worked as a technician in a research lab for three years, then completed a Master's research project that took another two and a half years. I have never seen an advisor like you. For your mentorship, financial support, and patience over the many long months and years, I am truly grateful.

I would also like to gratefully acknowledge and thank my dissertation committee: Dr. Straus for all of your help in teaching me how to optimize my Western blots and Co-IPs and insightful comments on preliminary drafts of this dissertation, Dr. Fawcett for patiently working with me to understand and interpret my microarray data, Dr. Beckman for guiding me in how I should follow up on this data, and Dr. Barbour for your advice in all aspects of my work and unfettered access to your laboratory and office, thank you.

I would also like to thank my fellow members of the Windle lab: Dr. Mark Subler for teaching me how to do my first PCR (the right way) and for his insights, suggestions, and good company while commiserating about our terrible sports teams over the past several years; Greg Campbell for his help and friendship in and out of the lab; Christina Boykins, Jillian Stafflinger, and Pam Weller for their diligence in maintaining all of our mouse colonies and always making sure I had whatever I needed to get my research done.

Scientific endeavors are growing increasingly collaborative, and my work as a member of Dr. Windle's research team was no exception. I owe a special debt of gratitude to Dr. G. David Roodman of IUPUI for his willingness to answer my questions, and to his staff, including Judy Anderson, Ken Patrene, and long-time collaborator Dr. Noriyoshi Kurihara, who patiently taught

me how to generate osteoclasts in vitro and contributed directly to this project by performing bone resorption assays for us. I would also like to gratefully acknowledge Dr. Deb Galson and her staff at UPMC including Drs. Benedicte Sammut and Fengming Wang, for their willingness to share insight, protocols, and supplies. Finally I would like to thank Dr. David Dempster at Columbia University, and, in particular, his collaborator Dr. Hua Zhou, who performed all of the histomorphometric analysis included in this research project.

I would also like to gratefully acknowledge Dr. Gordon Archer, director of the MD-PhD program at VCU, who took a chance on me; Sandra Sorrell and Magdalena Nopova for their kindness and assistance in making sure that my time in the program was as smooth and stress-free as possible; Dr. Gail Christie for her mentorship and guidance in the MBG program, and Naty Chaimowitz, Julie Farnsworth, and Dr. Dan Conrad, who facilitated my access to a Flow Cytometry core of the highest caliber here at VCU. I would also like to thank the graduate students and post-doctoral researchers in the Sarkar and Fisher labs, including Tim Kegelman, Bridget Quinn, Dong Chen, and especially Chadia Robertson who all helped me with supplies and expertise in many experiments.

I owe a special debt of gratitude to my colleague and friend Hoon Shim for more things than I can enumerate. From teaching me how to do my first Western blot years ago to patiently answering countless questions about homework and laboratory techniques to innumerable rides to the airport, Hoon has always been there for me and I am truly grateful.

I would like to thank my sisters, Dina and Rania, for all of their love and support over the years.

Finally, to my parents, Mahmoud and Moshira, you instilled a love of learning in me when I was young, nurtured it throughout my youth (maybe too long!), and inspired me to pursue my dreams with your hard work and dedication. I love you both very much and dedicate this PhD to you.

TABLE OF CONTENTS

LIST OF TABLES

LIST OF FIGURES

ABBREVIATIONS

$1,25\text{-}(OH)_2D_3$ – 1,25-dihydroxy-vitamin D_3

AKT – protein kinase B (Akt originally referred to a mouse strain, Ak, that develops thymomas)

ANOVA – two-way analysis of variance

aPKCζ – atypical protein kinase C ζ

BMU – basic multicellular unit

C/EBPβ – CCAAT/enhancer binding protein β

CDV – canine distemper virus

CFU-GM – colony-forming unit - granulocyte, monocyte/macrophage

CSF-1R – M-CSF receptor

CTR – calcitonin receptor

CYLD – cylindromatosis

DAVID – Database for Annotation, Visualization and Integrated Discovery

EDTA – ethylenediaminetetraacetic acid

ELISA – enzyme-linked immunosorbent assay

ER – endoplasmic reticulum

ERK – extracellular signal-related kinase (also called MAPK)

GAPDH – glyceraldehyde 3-phosphate dehydrogenase

IκB – inhibitor of NFκB

IKK – IκB kinase

JNK – Jun N-terminal kinase

KEAP1 – kelch-like ECH-associated protein 1

KI – knock-in

KO – knock-out

MAPK – mitogen-activated protein kinase

M-CSF – macrophage colony-stimulating factor

MITF – microphthalmia-associated transcription factor

MMP – matrix metalloproteinase

MTT – thiazolyl blue tetrazolium blue

MV – measles virus

MVNP – measles virus nucleocapsid protein

NFATc1 – nuclear factor of activated T-cells

NFκB – nuclear factor kappa-light-chain-enhancer of activated B-cells

NMR – nuclear magnetic resonance

NRF2 – nuclear factor (erythroid-derived 2)-like 2, also called NFE2L2

OPG – osteoprotegerin

PCA – principal component analysis

PCR – polymerase chain reaction

PDB – Paget's disease of bone

PMA – present-marginal-absent

PTHrP – parathyroid hormone-related protein

RANK – receptor activator of NFκB

RANKL – RANK ligand

RER – rough endoplasmic reticulum

ROS – reactive oxygen species

RSV – respiratory syncytial virus

RT-PCR – reverse transcriptase - polymerase chain reaction

SQSTM1 – sequestosome 1

TAB2 – TGF-beta activated kinase 1/MAP3K7 binding protein 2

TAF12 – transcription initiation factor TFIID subunit 12

TAK1 – TGF-beta activated kinase, also called MAP3K7

TNFα – tumor necrosis factor α

TRAF6 – TNF receptor-associated factor 6

TRAP – tartrate resistant acid phosphatase

Ub – ubiquitin

UBA – ubiquitin associated

UPR – unfolded protein response

ABSTRACT

THE ROLE OF p62 IN OSTEOCLASTOGENESIS AND PAGET'S DISEASE OF BONE

by Tamer M. A. Hadi, M.S., Ph.D.

A dissertation submitted in partial fulfillment of the requirements for the degree of Doctor of Philosophy at

Virginia Commonwealth University, 2014

Director: Jolene J. Windle, Ph.D.
Irene Shaw Grigg Distinguished Professor, Department of Molecular and Human Genetics
Director, VCU Transgenic/Knock-out Mouse Core
Cancer Molecular Genetics Program Co-leader, Massey Cancer Center

Paget's disease (PDB) is the second most common metabolic bone disease after osteoporosis, affecting up to 3% of adults over age 55. It is characterized by focal lesions of bone resorbed by hyperactive osteoclasts coupled with rapid formation of highly disorganized, low quality bone formed by osteoblasts. Such lesions cause skeletal deformity, fractures, and other symptoms that significantly decrease quality of life. In 2001, mutations in the SQSTM1/p62 gene were found in a subset of Paget's patients. The work summarized in this dissertation sought to answer two broad questions: what is the function of p62 in normal bone homeostasis and how do PDB-associated

mutations alter it? These studies took advantage of two mouse models: p62 knock-out (KO) mice, and p62P394L "knock-in" (KI) mice carrying the most common PDB-associated mutation.

KO, KI, and wildtype (WT) controls were aged to one year for skeletal-histological characterization. No differences were observed in a variety of bone parameters between WT and KO bones, while bones from age-matched KI mice exhibited a 33% decrease in bone volume and a 25% increase in osteoclast formation. In vivo, TNF-α caused a potent induction of osteoclastogenesis in calvariae of WT and KI, but not KO, mice. In vitro, RANKL induced osteoclast formation in a dose-dependent manner in WT and KI, but not KO, cultures.

Gene expression profiling of RANKL-treated osteoclast progenitors from WT, KO, and KI mice was then performed to identify the changes in signaling pathways responsible for these effects. Surprisingly, gene expression patterns from all three groups were consistent with robust activation of NFκB signaling in RANKL-treated samples, indicating that p62 is dispensable for RANKL activation of NFκB. Interestingly, gene expression patterns in KO cells suggested impaired proliferation and response to reactive oxygen species (ROS), a finding which was confirmed in cell culture experiments. In contrast, KI cells displayed enrichment for genes associated with the unfolded protein response, consistent with p62's role in ubiquitin-mediated protein degradation via proteolysis and autophagy. These studies have therefore generated several novel hypotheses concerning the role of p62 in both normal bone homeostasis and Paget's disease of bone.

CHAPTER 1

INTRODUCTION

1.1 Background and Significance: Paget's disease of bone

Paget's disease is a focal metabolic bone disease that affects up to 3% of adults over the age of 60 (Siris et al., 1990; Hamdy, 1995; Kanis, 1998). Though often asymptomatic, PDB is associated with significant morbidity in a substantial number of patients. Symptoms include bone pain, skeletal deformity (Figure 1.1), neurological complications, pathologic fractures, deafness, and osteosarcoma at a 1000-fold greater incidence than in the general population (Kanis, 1998; Meunier et al., 1980; Chapuy et al., 1982; Siris et al., 1989; Hansen et al., 1999; Roodman and Windle, 2005). At the tissue level, such symptoms correlate with the presence in one or more bones of characteristic pagetic lesions, or focal areas of highly exaggerated bone remodeling (Figure 1.2). It is now known that these lesions form in a stereotypical manner. Initially, PDB is characterized by excessive bone resorption by abnormal osteoclasts in a focal region. Subsequently, rapid, haphazard bone formation by increased numbers of hyperactive osteoblasts results in a highly disorganized mosaic of poor quality, woven bone (Roodman and Windle, 2005).

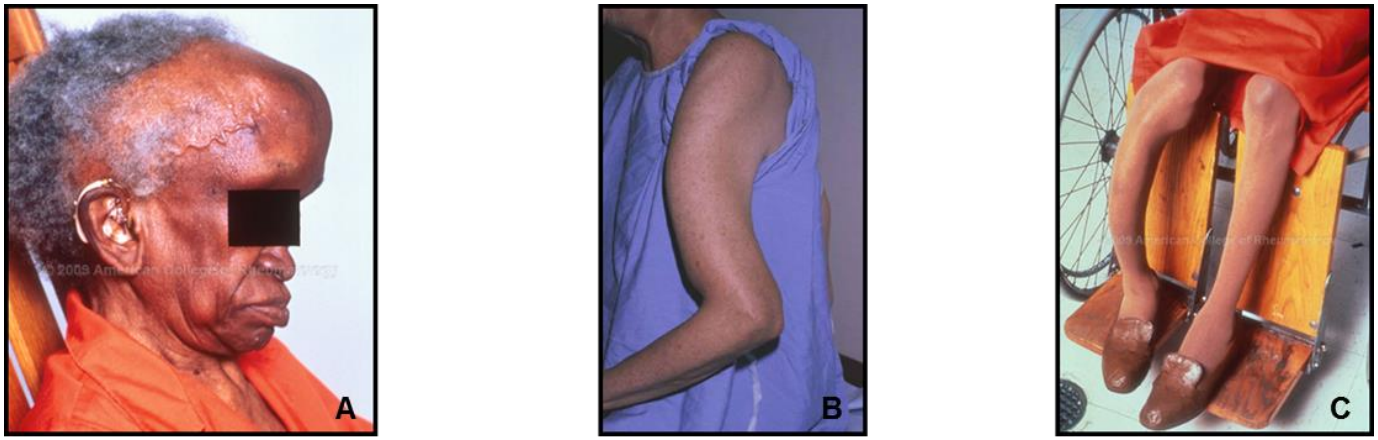

Figure 1.1. Clinical manifestations of Paget's disease of bone. (A) Typical changes in the skull associated with Paget's disease include diffuse enlargement, and dilated scalp veins. Involvement of the skull in PDB can lead to cranial nerve compression, optic atrophy, and nerve deafness (note the presence of a hearing aid). Bowing deformities can also occur in the long bones of the arm (B) and leg (C) leading to arthritic bone pain, limb shortening and gait abnormalities. Images from American College of Rheumatology image bank and The Paget Foundation.

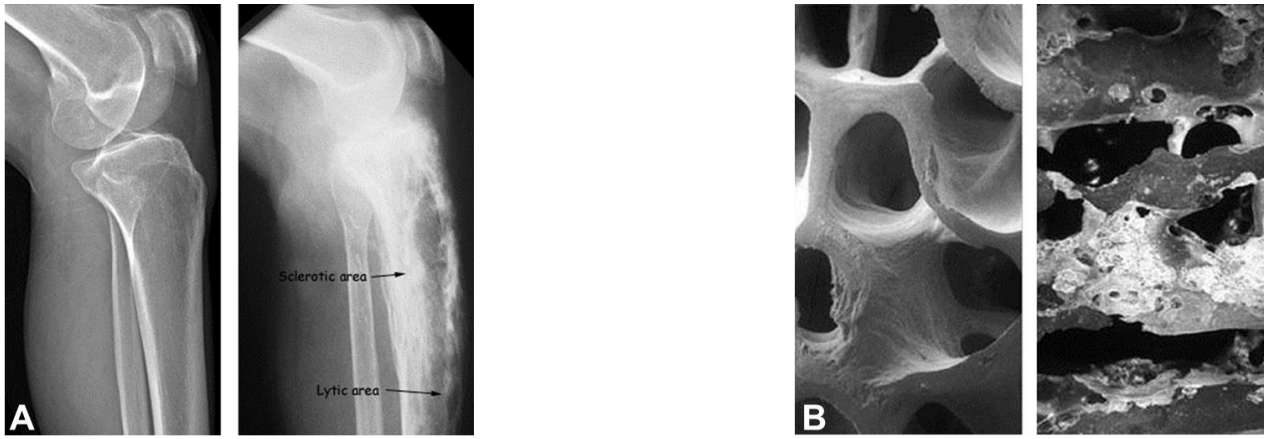

Figure 1.2. Normal and pagetic bone. (A) Radiomicrograph contrasting normal bone (left) with the sclerotic and lytic lesions characteristic of PDB (right). (B) Scanning electron micrograph showing intact trabecular plates and marrow spaces in healthy bone (left) and extensive pitting and loss of normal architecture in pagetic bone (right). Photographs from Siris ES, Canfield RE 1995 Paget's disease of bone. In Becker KL (ed.) Principles and Practice of Endocrinology and Metabolism, 2nd ed. © 1995 Lippincott. All rights reserved.

1.2 Bone remodeling and osteoclastogenesis

Over forty years ago, Harold Frost first deduced that the process of skeletal remodeling, and indeed, the very internal structure of bone, is created, maintained, and altered by the cells that populate it – osteoclasts, osteoblasts, and osteocytes – in teams of "Basic Multicellular Units" or BMUs (Figure 1.3; Martin et al., 1998).

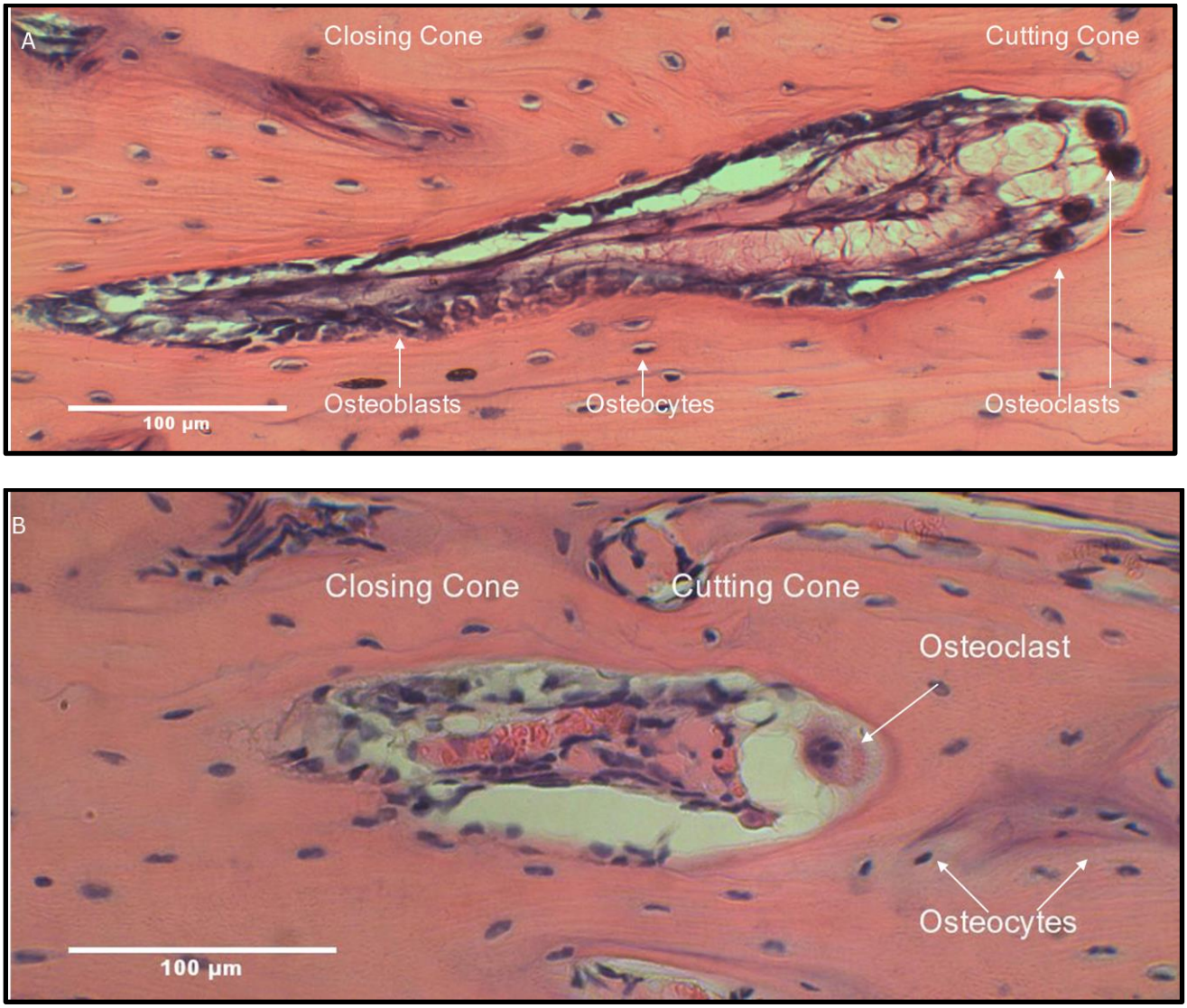

Figure 1.3. Basic Multicellular Units. Hematoxylin and eosin stained longitudinal sections of Basic Multicellular Units (BMUs) taken from rabbit tibial midshafts. Note the presence of several prominent nuclei in the labeled osteoclasts in the cutting cones.

Each BMU is composed of an advancing cutting cone populated by bone-resorbing, multinucleated osteoclasts, followed by a closing cone lined by scores of bone-forming, mononuclear osteoblasts (Martin et al., 1998). In the cortices of long bones, osteoclasts in the cutting cone tunnel in one direction, approximately aligned with the longitudinal axis of the bone, while osteoblasts lay down osteoid, a collagenous precursor to mineralized bone, in an orthogonal, radial direction (Martin et al., 1998).

Osteoclasts are structurally and functionally anomalous in pagetic lesions

The osteoclast plays a central role in the pathogenesis of PDB (Hosking, 1981). Under normal conditions, mononuclear precursor cells in the monocyte-macrophage lineage of hematopoietic cells fuse to form multinucleated osteoclasts (~ 3 to 20 nuclei) that are then activated to resorb bone in a tightly regulated progression (Figure 1.4; Takayanagi, 2008).

In PDB, however, osteoclasts in pagetic lesions are characterized by abnormal morphology, exhibiting unusual cytoplasmic and nuclear inclusion bodies whose composition remains a source of controversy (Meunier et al., 1980; Chapuy et al., 1982; Hosking 1981; Rebel et al., 1981; Kukita et al., 1990). Moreover, such osteoclasts are abnormally increased in number and size and contain up to 100 nuclei per cell (Hosking 1981; Rebel et al., 1981). Evidence for the central role played by osteoclasts in PDB is provided by the finding that treatment of Paget's patients with agents that block osteoclast formation and bone resorption, such as calcitonin or bisphosphonates, induces clinical remission (Langston and Ralston, 2004). Abnormal structure and function in PDB are, however, not limited to fully differentiated osteoclasts. In vitro studies of marrow cell cultures obtained from involved bones of PDB patients have identified several unique characteristics of pagetic osteoclast precursors. Compared with precursors formed in normal marrow cultures, these

pagetic precursors: (a) form osteoclasts much more rapidly, in far greater numbers (10 to 100 fold), with many more nuclei (Kukita et al., 1990), (b) express higher levels of tartrate acid resistant phosphatase (TRAP) (Kukita et al., 1990) and TAF12 (formerly TAFII-17), a component of the vitamin D receptor transcription complex (Kurihara et al., 2004), and (c) exhibit hyper-responsivity to osteoclastogenic stimuli such as 1,25-$(OH)_2D_3$, RANKL (receptor activator of nuclear factor-κB ligand), and TNF-α (Neale et al., 2002; Menaa et al., 2000; Demulder et al., 1993).

Osteoclastogenesis depends upon cooperative M-CSF, RANKL and co-stimulatory signaling

To explore these findings in greater detail, we will now take a moment to introduce the cellular physiology underlying basal osteoclast formation and activation (Figure 1.4). Specifically, mouse models of osteopetrosis (i.e. in which osteoclasts are structurally or functionally absent) have revealed a number of genes that are essential for osteoclastogenesis and may be broadly divided into those that are required for the generation of osteoclast precursors and those that are required for the differentiation process (reviewed in Teitelbaum and Ross, 2003; Takayanagi, 2008). The former include M-CSF, c-Fms, bcl-2, PU.1, and the MITF family of transcription factors. Early binding of M-CSF to its receptor, c-Fms, activates the proliferation, survival and cytoskeletal reorganization of osteoclast precursor cells and up-regulates RANK expression, which is required for further differentiation. PU.1 binds to the promoter of c-Fms, up-regulating its expression (Zhang et al., 1994), while MITF binds the promoter of anti-apoptotic Bcl-2, regulating its expression (McGill et al., 2002). Mice deficient in any of these genes exhibit osteopetrosis, increased skeletal mass due to abnormally dense bone, due to an absence of the common precursor for both osteoclasts and macrophages (Takayanagi, 2008).

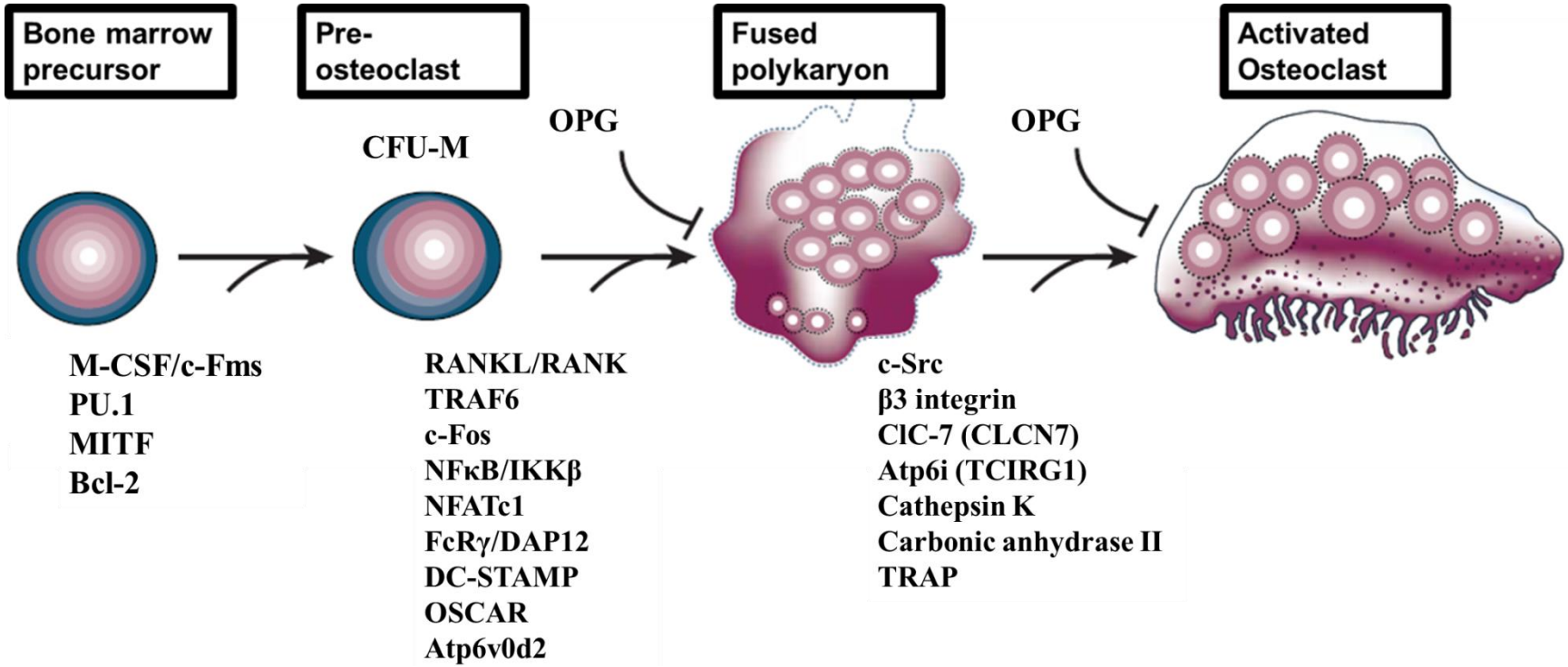

Figure 1.4 Osteoclast formation and activation. Osteoclasts are formed by the fusion of hematopoietic precursors in a manner that is induced by M-CSF, RANKL and its co-stimulatory immunoglobulin-like receptor, and opposed by the RANKL-decoy receptor OPG. Ultimately, the mature, multinucleated osteoclast is activated by signals that lead to the initiation of bone remodeling. These include rearrangements of the actin cytoskeleton, formation of a tight junction between the bone surface and surrounding tissue, and secretion of hydrogen ion and proteolytic enzymes to resorb bone.

Abbreviations: M-CSF, macrophage colony-stimulating factor; c-Fms, Colony stimulating factor 1 receptor also known as macrophage colony-stimulating factor receptor; PU.1, Transcription factor PU.1; MITF, microphthalmia-associated transcription factor; Bcl-2, B-cell CLL/lymphoma 2; RANK, receptor activator of nuclear factor-κB; RANKL, RANK ligand; TRAF6, tumor necrosis factor receptor-associated factor 6; c-Fos, Proto-oncogene c-Fos; NFκB, nuclear factor-κB; IKKβ; Inhibitor of NFκB kinase subunit beta; NFATc1, nuclear factor of activated T-cells cytoplasmic 1; DAP12, DNAX-activating protein; FCRγ, Fc receptor common γ subunit; DC-STAMP, dendritic cell-specific transmembrane protein; OSCAR, osteoclast-associated receptor; ATP6v0d2, ATPase, H+ Transporting, Lysosomal 38kDa, V0 Subunit D2; c-Src, Proto-oncogene tyrosine-protein kinase Src; ClC-7, chloride channel 7; ATP6i, V-proton pump, H+ transporting (vacuolar proton pump) member I; TRAP, Tartrate resistant acid phosphatase; OPG, osteoprotegerin. Adapted from Figure 1 in Boyle et al., 2003 and Figure 1 in Takayanagi, 2008.

A second group of genes that are essential for osteoclast differentiation include: RANKL, its receptor RANK, c-Fos, NFκB, NFATc1, DC-STAMP, OSCAR, and ATP6i, among others (reviewed in Teitelbaum and Ross, 2003; Takayanagi, 2008). Binding of RANKL to RANK results in the recruitment of TRAF6 (responsible for downstream NFκB signaling), the induction of the transcription factor c-Fos, and the concomitant phosphorylation of co-stimulatory ITAM in DAP12 and FcRγ (adaptor proteins associated with critical calcium signaling in both immune cells and osteoclasts), committing the hematopoietic precursors to the osteoclast lineage. TRAF6-mediated NFκB signaling ultimately induces NFATc1, the master transcription factor for genes such as DC-STAMP and ATP6v0d2, responsible for cell-cell fusion (Kim et al., 2008); β3 integrin, responsible for cytoskeletal changes and matrix-derived intracellular signaling (McHugh et al., 2000); carbonic anhydrase and vacuolar proton pumps, responsible for secretion of hydrogen ion that solubilizes hydroxyapatite or the mineral component of bone (Kim, Y et al., 2005; Yang et al., 2012); cathepsin K, TRAP, and matrix metalloproteinases 9 and 14, responsible for proteolytic cleavage of the organic component of bone (Takayanagi et al., 2002 Sundaram et al., 2007; Song et al., 2009); and NFATc1 itself and OSCAR or osteoclast-associated receptor, responsible for calcium-dependent auto-amplification of NFATc1 signaling (Kim, Y et al., 2005).

Osteoblasts in pagetic lesions are increased in number but exhibit no structural abnormalities

Briefly, osteoblasts and their precursors are also thought to play an important role in PDB. Pagetic lesions are characterized by increased numbers of both mature and immature osteoblasts (Roodman and Windle, 2005). While these cells exhibit no structural abnormalities akin to those in pagetic osteoclasts, they do display signs of increased cellular activity, including abundant rough

endoplasmic reticulum (RER) and well-developed Golgi, consistent with the increased bone formation that occurs in active pagetic lesions (Hosking, 1981). Traditionally, it has been thought that this increase in osteoblast number and activity reflects a response to increased osteoclast activity, since bone resorption and formation remain tightly coupled in PDB (Chapuy, 1982). More recent studies, however, suggest that osteoblasts and their precursors may also enhance the osteoclastogenic microenvironment in pagetic lesions intrinsically (Menaa et al., 2000; Demulder et al., 1993; Sun et al., 2006; Naot et al., 2007; Hiruma et al., 2008).

1.3 Etiology of Paget's Disease of Bone

Though the cause of PDB remains the object of intensive investigation, it is generally accepted that both genetic and environmental factors contribute to the pathogenesis of this disease. On the one hand, familial clustering is observed, with up to 40% of affected patients having at least one first-degree relative with PDB (Sofaer et al., 1983; Siris et al., 1991; Morales-Piga, 1995) and numerous studies have described extended families exhibiting an autosomal dominant mode of inheritance (Leach et al., 2001; Daroszeswska and Ralston, 2005). On the other hand, the findings that PDB exhibits incomplete penetrance in these families (Leach et al., 2001; Daroszeswska and Ralston, 2005), presents in a clinically variable manner, even within families, and is highly localized to a particular bone or bones and not systemic in nature, all suggest the presence of some mediating environmental factor that acts locally in bone (Roodman and Windle, 2005).

Paramyxoviral infection in the etiology of PDB

Among the best studied environmental stimuli for the manifestation of PDB is slow virus infection by the members of the family paramyxoviridae (Roodman and Windle, 2005; Roodman and Singer 2012). Beginning in the early 1980s and through the next decade, several groups published independent accounts of unusual nuclear and cytoplasmic inclusions in giant osteoclasts (but not osteoblasts or osteocytes) obtained from histological sections of patients with PDB (Mirra et al., 1981; el-Labban et al., 1984; Carles et al., 1989; Singer et al., 1993; DeChiara et al., 1998; Singer, 1996). In parallel, a growing body of literature arose suggesting that these inclusions were viral in origin. In osteoclasts cultured from pagetic lesions, evidence was found for the presence of antigens immunologically akin to those of several viruses including measles virus (MV) (Baslé et al., 1979; Rebel et al., 1980), respiratory syncytial virus (RSV) (Mills et al., 1981), and canine distemper virus (CDV) (Gordon et al., 1991), all paramyxoviruses. In the subsequent decade, further support for a viral etiology was provided by the detection of viral transcripts in both affected (where they were enriched) and non-affected bone cells of PDB patients (Baslé et al., 1986; Reddy, et al., 1995; Mee et al., 1998).

Over the next decade, several additional important developments arose in Paget's research – most notably, the publication of the earliest reports of genetic models of viral contributions to PDB pathogenesis (reviewed in Singer and Roodman, 2012). In one study, normal osteoclast precursors were transfected with the measles virus nucleocapsid protein (MVNP) gene and subsequently formed osteoclasts that were increased in number, nuclei per osteoclast, bone resorptive capacity, and sensitivity to 1,25-$(OH)_2D_3$ (Kurihara et al., 2000) – they key characteristics of osteoclasts from pagetic lesions. In a later study, nearly one-third of transgenic mice with osteoclast-targeted expression of MVNP developed characteristic pagetic lesions (Kurihara et al., 2006).

The proposition that viruses play an important role in the etiology of PDB is not, however, without controversy. As long ago as 1994, the *absence* of measles and canine distemper viral transcripts and paramyxoviral sequences in pagetic samples was reported in the UK (Birch et al., 1994) and later confirmed by another group in New Zealand (Matthews et al., 2008). Subsequently, it was suggested that direct evidence of viral causality was scant, that the indirect evidence presented was poor because molecular targets for probes used to evince paramyxoviral infection in pagetic osteoclasts could have been endogenous mRNA and proteins rather than viruses, and that independent, double-blinded replication of the findings was sorely needed before an association or causal relationship between paramyxoviral infection and PDB could be asserted (Ralston and Helfrich, 1999). In the subsequent year, this group published yet another negative result, finding no evidence for measles virus, RSV, or CDV via immunocytochemistry, in situ hybridization, and RT-PCR in a large sample (n = 53) of PDB patients in the UK (Helfrich et al., 2000). Interestingly, ultrastructural studies of pagetic osteoclasts revealed:

> intranuclear inclusion bodies, similar to those described by others previously…. The pagetic inclusions were straight, smooth tubular structures packed tightly in parallel bundles and differed from nuclear inclusions, known to represent MV nucleocapsids, in a patient with subacute sclerosing panencephalitis (SSPE) in which undulating, diffuse structures were found, arranged loosely in a nonparallel fashion.

Finally, this group spearheaded a multi-center, blinded study aimed at detecting transcripts of measles or canine distemper viruses in PDB patient samples and controls via RT-PCR with sensitivity to 16 copies (Ralston et al., 2007). Despite including groups that had previously shown the presence of CDV in pagetic lesions, they were unable to detect any evidence of paramyxoviruses, concluding that previously published positive reports were likely due to laboratory cross-contamination (Ralston et al., 2007). While these studies did not end the controversy, they did catalyze interest in alternative etiologies for PDB – and in the intervening

years, a more formal appreciation for the genetic contributions to PDB began to emerge (reviewed in Ralston and Layfield, 2012).

1.4 *SQSTM1* / p62 is the gene most frequently linked to PDB

It had already been well understood at this point that genetic factors played a role in the pathogenesis of PDB, for several reasons. First, up to 40% of patients report a positive family history with first-degree relatives affected at a frequency approximately 7 times greater in cases than in controls (Sofaer et al., 1983; Siris et al., 1991). Moreover, it was also well known that PDB exhibited an autosomal dominant mode of transmission with incomplete penetrance (Siris et al., 1991; Morales-Pigga et al., 1995). Finally, multiple susceptibility loci had been identified and confirmed (Fotino et al., 1977; Cody et al., 1997; Haslam et al., 1998). In 2001, a breakthrough was made. Research groups in Canada and the UK independently published reports of a strong susceptibility locus for PDB on chromosome 5q35 identified by genomewide linkage scans in affected families (Laurin et al., 2001; Hocking et al., 2001). Subsequent mutation screening in a critical 300kb locus therein led to the identification of a recurrent nonconservative Proline to Leucine change at residue 392 (P392L) flanking the ubiquitin-associated domain of the protein sequestosome 1 (SQSTM1/p62) that was not present in 291 control individuals in a French-Canadian cohort (Laurin et al., 2002) – a finding confirmed later that year in a British cohort (Hocking et al., 2002). What made this discovery unique and important was that it was the first time mutation of a specific gene was uniquely associated with PDB.

p62 structure and function

First cloned in 1996, p62 was identified as a p56lck binding partner (Joung et al., 1996), ubiquitin binding protein (Vadlamudi et al., 1996), and oxidative stress sensor (Ishii et al., 1996; Ishii et al., 1997). It is now known that p62 is a 440 amino acid protein characterized by an abundance of motifs that mediate distinct interactions with binding partners in several different signaling pathways (Figure 1.5), most critically, those related to ubiquitin binding, autophagy, inflammation, and the oxidative stress response (reviewed in Chen and White, 2011; Chung and Van Hul, 2012; Salminen et al., 2012; Nezis and Stenmark, 2012).

UBA domain mutations and PDB

Over the course of the past decade, nearly thirty mutations (missense and truncating) in p62 have been identified in PDB patient populations all over the world (Table 1.1). It is now estimated that mutation in p62 is associated with 40 to 50% of familial cases and up to 10% of sporadic cases of PDB (Daroszewska and Ralston, 2005; Ralston and Layfield, 2012; Chung and Van Hul, 2012). Importantly, essentially all PDB-associated mutations reside in the 7th and 8th exons, encoding the UBA domain, which has been shown to possess ubiquitin binding function.

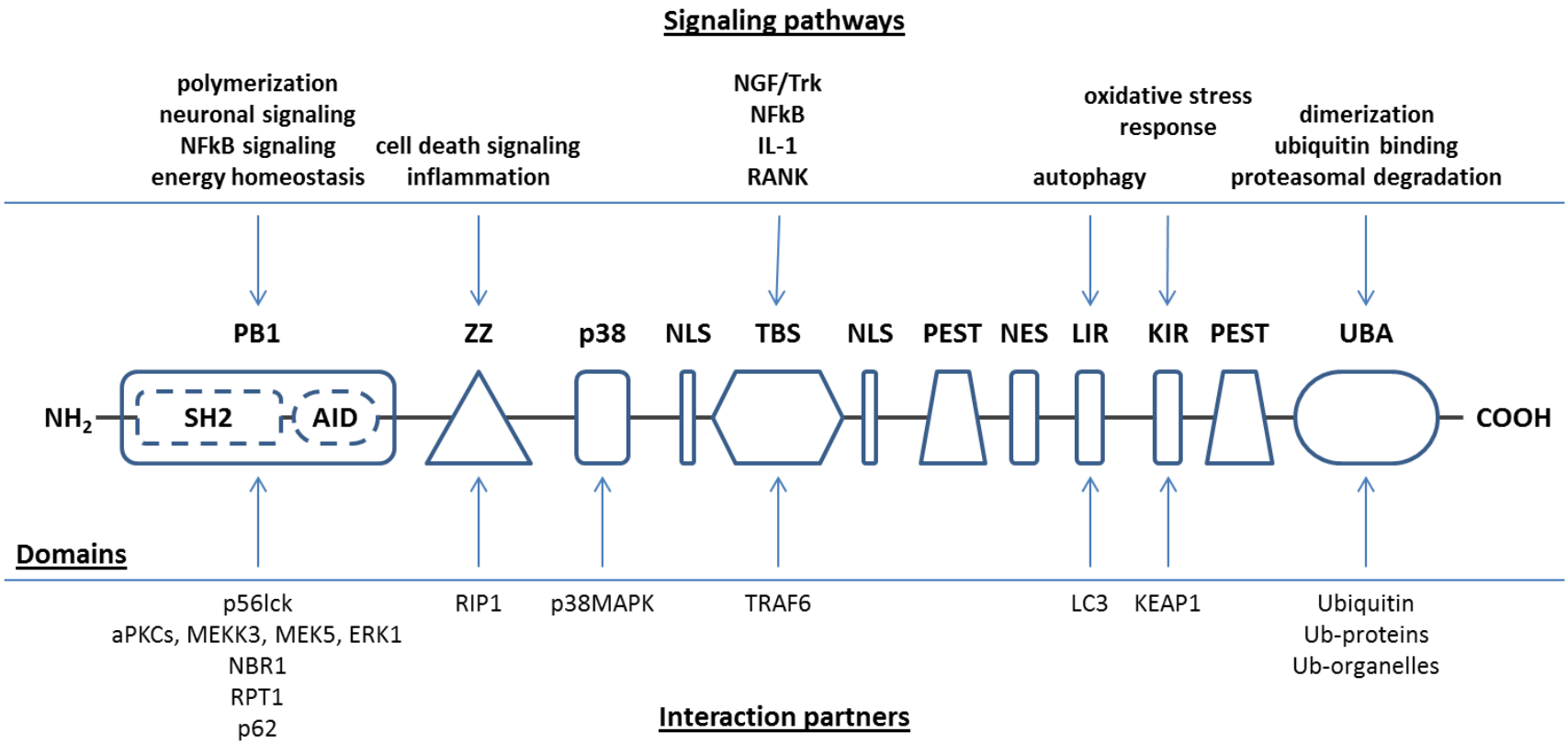

Figure 1.5. Signaling pathways, interaction motifs, and binding partners of p62. Starting from its N-terminus, p62 has a PB1 (Phox and Bem 1p) domain that is composed of a p56lck-interacting Src homology 2 domain (SH2), and an acidic interaction domain (AID) that interacts with the autophagy receptor neighbor of BRCA1 (NBR1), the ATPase subunit of 19S regulatory particle of 26S proteasome (Rpt1), p62 itself to facilitate polymerization, and several classes of kinases including the extracellular signal-regulated kinase (ERK1), atypical protein kinase Cs (aPKCs), mitogen-activated protein kinase kinase kinase 3 (MEKK3), and mitogen-activated protein kinase kinase 5 (MEK5). This is followed by a zinc finger domain (ZZ) that binds the scaffold protein RIP1 (receptor interacting serine-threonine kinase 1) that recruits aPKCs to tumor necrosis factor-(TNF)-signaling complexes, a p38MAPK binding domain important for p38-MAPK-induced PPARα phosphorylation as well as to LIM-domain containing proteins. The remaining domains include a TNF receptor-associated factor 6 (TRAF6)-binding domain (TBS), which is thought to transduce TRAF6 signaling in a variety of pathways, an LC3-interacting domain (LIR) that binds autophagic effector proteins, a KEAP1-interacting domain (KIR) that plays an important role in facilitating the NRF2-antioxidant response, and, ultimately, a C-terminal ubiquitin-associated domain, that binds ubiquitin, polyubiquitinated proteins, and organelles. Additional domains include nuclear export and localization signals (NES, NLS) that play an important role in nuclear-cytoplasmic shuttling of p62, and PEST domains, peptide sequences rich in proline (P), glutamate (E), serine (S), and threonine (T) that are putative signals for rapid proteolytic degradation.

Table 1.1. Mutations in p62 associated with Paget's disease of bone. Adapted from Table 2 in Chung PY, Van Hul W. Paget's disease of bone: Evidence for complex pathogenetic interactions. Semin Arthritis Rheum. 2012 Apr;41(5):619-41.

	Position from ATG	Reported Position	Protein Change
Exon 7			
	T1005A	T1046A	D335E
	T1045A	T1085A	S349T
	C1090T	C1090T	P364S
	A1132T	A1132T	K378X
	C1142T	C1182T	A381V
	C1149A	C1190A	Y383X
	C1160T	C1200T	P387L
	G1165C	G1205C	A390X
	C1169T	C1209T	A390V
	IVS7+1G/A	IVS7+1G/A	A390X
Exon 8			
	1170delT	1210delT	L394X
	C1175T	C1215T	P392L
	1175delC	1215delC	L394X
	1185/6insT	1224/5insT	E396X
	T1189G	T1229G	S397A
	T1195C	T1235C	S399P
	C1198T	C1238T	Q400X
	A1201G	A1241G	M401V
	A1210G	A1250G	M404V
	T1211C	-	M404T
	G1231A	-	G411S
	C1237T	C1277T	L413F
	T1250A	T1290A	I417q
	1267insT	130insT	D423X
	T1271G	T1311G	I424S
	G1273A	G1313A	G425R
	G1274A	G1312A	G425E
	C1280A	-	A427D

Several bio-physical studies have been undertaken to elucidate the effect of mutations in the UBA domain of p62 (Cavey et al., 2005; Cavey et al., 2006; Long et al., 2010; Garner et al., 2011; Isogai et al., 2011). Most notably, NMR relaxation dispersion experiments, isothermal titration calorimetry, and fluorescence kinetic measurements, have demonstrated that the p62 UBA domain forms a highly stable dimer, and that the dimer interface partially occludes the Ub-binding surface of p62, impairing the ability of p62 to bind ubiquitin (Long et al., 2010). More recently, the crystal structure of the UBA domain of mouse p62 and the solution structure of its ubiquitin-bound form

have been solved (Isogai et al., 2011). Subsequent NMR analyses from this group corroborate the earlier finding that p62's UBA domain exists in equilibrium between mutually exclusive monomeric and dimeric forms, and that ubiquitin binding shifts the equilibrium toward the active monomeric form (Isogai et al., 2011). Interestingly, certain PDB-associated point mutations, such as S399P and M404V/T, are associated with impaired UBA structural integrity and reduced dimer stability, while others, such G425R, have increased stabilization and dimerization, and others still, such as the common P392L mutation, seem to have no significant effect on either of these factors (Garner et al., 2011). However, all PDB-associated mutations in p62 lead to varying degrees of loss of ubiquitin binding capacity in the context of full-length p62 (Searle et al., 2012).

To summarize: at least twenty-eight different mutations, all localized within the C-terminal UBA domain of p62, have been identified, each of which is associated with a phenotypic gain of function (i.e. increased osteoclast number and activity) in pagetic lesions. Bio-structural studies have revealed that these PDB-associated mutations have differing effects on dimer stability, but that all are associated with a loss of full length p62's capacity to bind ubiquitin.

1.5 Mouse models and p62

What are the downstream effects of such mutations in the context of skeletal architecture and bone cell function? To answer this question we begin with a review of the relevant mouse models. As noted earlier, research groups in Canada and the UK independently published reports of a recurrent nonconservative Proline to Leucine change at residue 392 (P392L) flanking the UBA domain of p62 (Laurin et al., 2002; Hocking et al., 2002). Shortly thereafter, the first mouse models aimed at clarifying the role played by p62 in osteoclastogenesis began to emerge.

p62 -/- mice

One of the earliest models generated was that in which p62 was ablated genetically. In 2004, Durán and colleagues observed that p62-/- mice were born in Mendelian proportions, were grossly normal, showed no sign of osteopetrosis (failure to form functional osteoclasts) in 6 to 8 week old mice, or radiological or histological abnormalities in cortical or trabecular bone. They therefore concluded that basal osteoclastogenesis is not affected by the loss of p62. Next they treated mice or bone marrow-derived progenitors with osteoclastogenic factors, such as PTHrP in vivo, or RANKL in vitro, and observed impaired osteoclast formation and activation in the p62-/- mice, but not in mice deficient for the atypical protein kinase C, ζ (aPKCζ), to which p62 binds, as compared to wildtype controls (Durán et al., 2004). The authors offered a potential mechanism for this effect – presenting evidence that p62 binds TRAF6 and, most likely, acts at the level of IKK to facilitate NFκB translocation, activation, and ultimately, NFATc1 induction (Durán et al., 2004). Importantly, in a subsequent publication, this group demonstrated that that p62-/- mice develop mature-onset obesity, first statistically detectable at the age of 5 months, in addition to systemic glucose intolerance and insulin resistance (Rodriguez et al., 2006). They also suggested that p62-/- mice exhibit increased bone mineral density as they age, implying a possible osteopetrotic phenotype, but provided no evidence of this effect (Rodriguez et al., 2006). While at least one group suggests that mature-onset obesity in p62-/- mice is attributable to hyperphagia secondary to deficient central-leptin signaling (Harada et al., 2013), tissue specific p62-/- mouse lines have revealed: (a) that lack of p62 specifically in adipose tissue recapitulates the metabolic syndrome phenotype, (b) that impaired p62-mediated mitochondrial function in brown adipose tissue is responsible for this phenotype, and (c) that the likeliest mechanism for this regulation is diminished p38 MAPK activation and signaling (Müller et al., 2013).

To summarize, early evidence obtained from p62-/- mouse models demonstrates that p62 plays an important role in induced osteoclastogenesis and the likeliest mechanism for this effect is the RANK-TRAF6-NFκB signaling pathway (this pathway will be discussed in greater detail in the following section). Whether p62 also plays a role in basal osteoclastogenesis and the most relevant signaling pathways by which it might do so have not yet been firmly established, and form the basis for the first set of our experimental studies in chapter two. Before proceeding, however, it should be noted that the p62-/- mouse does not accurately model the p62 mutations seen in PDB, which invariably result in the production of a full-length or near full-length protein carrying alterations in the UBA domain, and thus the knock-out mice were not expected to model PDB phenotypically.

Mouse models of PDB

To create a genetically accurate model of PDB, two groups have generated knock-in mice in which the endogenous p62 gene was modified to carry the murine equivalent of the most common PDB mutation, P394L. In 2008, Hiruma and colleagues described the first p62 P394L (KI) mouse. Osteoclast precursors from these mice were hypersensitive to several osteoclastogenic stimuli including RANKL, TNF-α, and 1α,25-$(OH)_2D_3$. However, the mice failed to develop pagetic lesions in the axial skeleton, although the bones displayed minor osteopenia, an indication of increased osteoclastogenesis. In terms of an underlying mechanism, they found that the mutation exerts effects both on osteoclasts and supporting stromal cells – i.e. the effect of the mutation is both cell autonomous (increasing osteoclast precursor sensitivity to RANKL and TNF-α) and non-

autonomous, increasing stromal cell production of RANKL in response to 1α,25-$(OH)_2D_3$ through an increase in p38MAPK signaling (Hiruma et al., 2008).

More recently, another group also generated a p62 P394L mouse in a similar fashion. In contrast to Hiruma et al., the Ralston group reported that the mutant mice developed (a) focal lesions on lower long bones (on 95% of tested 12-month old homozygous mutants, ~75% of heterozygotes, and 0% of wildtype littermates) that were characterized by (b) increases in bone turnover, disruption of normal architecture, and accumulation of woven bone, and (c) osteoclast progenitors that were hypersensitive to RANKL in vitro, resulting in larger, more nucleated osteoclasts than those generated from wildtype littermates. In terms of mechanism, they observed increased transcripts of autophagy related genes, such as microtubule-associated protein 1 light chain 3 gene (lc3) and the autophagy-related gene 5 (atg5) in RANKL-treated mutant cells. They therefore hypothesized that impaired autophagy might explain the increase in nuclear inclusion bodies characteristic of pagetic osteoclasts (Daroszewska et al., 2011).

In the most recent contribution to this dialogue, Kurihara and colleagues bridged the historical divide between the genetic and viral etiologies for PDB. They reported that (a) bone marrow from eight of twelve PDB patients who harbored the p62 P392L mutation also tested positive for the expression of measles virus nucleocapsid protein (MVNP), (b) osteoclast progenitors from these patients formed pagetic osteoclasts in vitro, which were inhibited by antisense-MVNP, and (c) that osteoclast progenitors from the four case patients who harbored the p62 P392L mutation but did not test positive for MVNP formed osteoclasts that were hyper-responsive to RANKL but unaffected by antisense-MVNP (Kurihara et al., 2011). A parallel set of experiments was also conducted on equivalent murine models. Mice expressing MVNP in the osteoclast-lineage developed pagetic osteoclasts in vitro and rare pagetic lesions in vivo, while the p62 knock-in mice

formed increased numbers of osteoclasts that were hypersensitive to RANKL, but did not develop pagetic lesions. However, when these two lines of mice were interbred, the resulting MVNP/p62 P394L mice developed more frequent and pronounced pagetic lesions.

To summarize, p62 is thought to play an important role in the signaling pathways that regulate osteoclast differentiation largely based on the abundant epidemiological studies associating mutation in p62's UBA domain with PDB (a disease characterized by dysregulated, overly exuberant osteoclast formation), and the aforementioned study conducted by Durán and associates in 2004 in which p62 was genetically ablated in mice, resulting in impaired osteoclastogenesis in vitro (Durán et al., 2004). More recent mouse models of the most common PDB-associated p62 UBA domain mutation (P392L) have been generated and characterized by two independent groups. There is consensus among the researchers that osteoclasts generated from these mice are hyper-responsive to RANKL, but little agreement on anything else (the mechanisms underlying this increased sensitivity and activity, the presence or absence of true pagetic lesions in these genetic mouse models, and the putative role of a key viral contributor to the development of frank PDB). To help unravel the role p62 mutation plays in the pathogenesis of PDB, we will turn to a discussion of some of the key pathways and cellular processes that: (a) are putatively regulated by p62, (b) may be differentially affected by PDB associated mutations, and (c) thereby alter osteoclastogenesis. These include: the NFκB signaling pathway, autophagic protein degradation pathways, and reactive oxygen species-generating and oxidative stress response pathways.

1.6 p62 and the NFκB signaling pathway

If the key signaling mediators responsible for the initiation and maintenance of osteoclastogenesis include M-CSF, RANK, its ligand RANKL, and their inhibitor, RANK decoy protein OPG, what role does p62 play? First, we observe that RANK's intracellular domain has been shown to lack intrinsic enzymatic activity (Darnay et al., 1998). Structural analyses of this domain and the molecules that associate with it reveal that RANK's cytoplasmic tail contains three TRAF-binding sites, and that RANKL-initiated signaling is transduced downstream by recruiting adaptor molecules from the TRAF family of proteins (Darnay et al., 1998; Galibert et al., 1998; Wong et al., 1999; Takahashi et al., 2008). Further phenotypic characterization of TRAF knock-out mice has demonstrated that TRAF6 is the major adaptor molecule linking RANK to osteoclastogenesis (Lomaga et al., 1999; Naito et al., 1999). TRAF6 knock-out mice were generated by three independent groups. Lomaga and associates found that osteoclasts in these mice were normal in number but functionally defective (Lomaga et al., 1999), Naito and colleagues reported a complete absence of TRAP+ osteoclasts in their TRAF6-/- mice (Naito et al., 1999), while a third group, found that osteoclast numbers were considerably reduced but still detectable (Kim, N et al., 2005).

Functionally, the binding of TRAF6 to RANK induces TRAF6 trimerization and activation. TRAF6 undergoes Lysine 63-linked autoubiquitination and the resultant polyubiquitin chains facilitate the formation of an activated signaling complex containing upstream RANK and downstream TAK-1-binding protein (TAB)2, which results in TGFβ-activated kinase (TAK)1 activation (Gohda et al., 2005; Mizukami et al., 2002; Lamothe et al., 2007). In this manner, TRAF6 transduces the RANK-mediated signal by activating multiple downstream signaling pathways, including NFκB, AKT, JNK, p38 MAPK, and ERK, that in turn induce expression of genes that regulate osteoclast differentiation, survival, and activity (Roodman and Windle, 2005;

Wong et al., 1999; Lamothe et al., 2008). In particular, NFκB signaling up-regulates expression of the master osteoclastogenic regulator, nuclear factor of activated T-cells c1 (NFATc1), which in turn promotes the expression of numerous genes needed for bone resorption, while directly inhibiting OPG expression (Kobayashi et al., 2001; Takayanagi et al., 2007; Yamashita et al., 2007; Aliprantis, 2008).

p62 positively regulates TRAF6 signaling

Several studies have elucidated the structural and functional associations between TRAF6 and p62. Through its TBS domain, p62 binds TRAF6, mediating TRAF6-dependent activation of NFκB (Geetha et al., 2002; Wooten et al., 2005). Through its UBA domain, p62 recruits polyubiquitin then mediates TRAF6 ubiquitination and ubiquitin-chain transfer to downstream substrates (Wooten et al., 2005, Seibenhener et al., 2007). Finally, through its PB1 domain, p62 may dimerize and thereby function in the formation of multimeric protein complexes that are critical for TRAF6 activation (Lamark et al., 2003) or interact with other PB1 domain proteins such as atypical protein kinase C (aPKC), which phosphorylates and activates downstream mediators in the NFκB pathway (Lamark et al., 2003; Durán et al., 2004). Deletion constructs that remove any of these three domains from p62 (TBS, UBA, or PB1), reveal that each is necessary for the activation of TRAF6 and NFκB in neuronal cell lines (Wooten et al., 2005).

In the context of osteoclastogenesis, Durán and colleagues provided the first evidence of a role for p62 in mediating TRAF6 signaling in the RANK-NFκB signaling pathway (Durán et al., 2004). First, the authors demonstrated that p62 is induced and remains elevated after RANKL treatment during osteoclastogenesis. Next, they developed and bred p62 knock-out mice and characterized

them phenotypically. Interestingly, under basal conditions, they did not detect an osteopetrotic phenotype at 6 to 8 weeks of age, as had been demonstrated in TRAF6 knock-out mice, nor were differences found in cortical thickness, trabecular size and distribution, or osteoclast number in H&E stained tibiae between wildtype and p62 knock-out mice.

However, when the p62 knock-out mice were treated with the osteoclastogenic parathyroid hormone related protein (PTHrP, which increases RANKL production and signaling), they demonstrated significantly impaired osteoclastogenesis, increased bone volume, trabecular number and thickness. Moreover, culture of precursors obtained from p62 knock-out mice with M-CSF and RANKL were significantly deficient in osteoclast production, generating approximately one-third the number of osteoclasts as wildtype precursors. Mechanistically, the authors presented additional data suggesting that osteoclast precursors from p62 knock-out mice have impaired formation of a critical signaling complex involving TRAF6, p62, and aPKC, which results in impaired NFκB signaling, NFATc1 up-regulation, and ultimately osteoclast formation (Durán et al., 2004).

What then accounts for the phenotypic gain of osteoclast function that characterizes PDB in patients and mouse models? As noted earlier, the vast majority of PDB-associated mutations isolated thus far are located in the carboxy-terminal UBA domain of p62 (Chung and Van Hul, 2012). Truncating mutations remove significant portions of the UBA domain and result in more severe pagetic phenotypes than missense mutations (Layfield et al., 2007; Hocking et al., 2004). These observations suggest two possible resolutions: (1) enhanced positive regulation, whereby each of these mutations produces enhanced RANK signaling, or (2) impaired negative regulation, whereby binding of a negative mediator of RANK signaling that acts at p62's UBA domain is attenuated. As detailed below, this latter explanation is supported by several lines of recent experimental evidence.

p62 also plays a role in the negative regulation of TRAF6 signaling

In particular, p62 has been shown to bind the tumor suppressor CYLD, and recruit it to the RANK-TRAF6 complex in neuronal cells (Wooten et al., 2008), osteoclasts (Jin et al., 2008), and macrophages (Kim et al., 2009). CYLD is a deubiquitinating enzyme that digests Lysine 63-linked polyubiquitin chains (Kovalenko et al., 2003) and has previously been shown to negatively modulate both TRAF and TRAF-mediated downstream molecules such as IKK kinase (Kovalenko et al., 2003; Courtois, 2008). It has been further demonstrated that NFκB activation is required for CYLD induction, suggesting that CYLD acts as a negative feedback modulator in NFκB autoregulation (Jono et al., 2009). Jin and colleagues demonstrated that CYLD knock-out mice develop severe osteoporosis (loss of > 50% trabecular bone volume at 14 weeks of age) and that this phenotype is caused primarily by an increased number of osteoclasts (Jin et al., 2008). Further in vitro characterization of pre-osteoclasts derived from these CYLD-/- mice demonstrated that these cells are hypersensitive to RANKL stimulation and accumulate substantially more ubiquitinated TRAF6 than wildtype controls. Moreover, pre-osteoclasts obtained from wildtype controls showed that CYLD is induced 24 hours after RANKL stimulation. Finally, transfection of CYLD into HEK 293 cells potently inhibited RANKL-induced TRAF6 ubiquitination and co-immunoprecipitated with TRAF6 in the presence of p62, but not a p62ΔUBA deletion mutant (Jin et al., 2008).

One year later, Kim and Ozato analyzed temporal expression and association patterns of p62, TRAF6, and CYLD in macrophages (Kim et al., 2009). Using sequential co-immunoprecipitations, they demonstrated that within 15 minutes of activation by stimulatory cytokines, TRAF6 was both ubiquitinated and bound to p62 in RAW cells. At one hour post-activation, though, both TRAF6's ubiquitination and its association with p62 were diminished, replaced by a strong p62-CYLD

interaction (Kim et al., 2009). Finally, Sundaram and colleagues recently confirmed that CYLD binds p62 in both wildtype and mutant osteoclast progenitor cells in which PDB-associated, though non-UBA, $p62^{A381V}$ is overexpressed, but not when the most common PDB-associated $p62^{P392L}$ is overexpressed (Sundaram et al., 2011). Furthermore, they demonstrated elevated levels of ubiquitinated TRAF6 in $p62^{P392L}$ transfected cells during osteoclastogenesis (Sundaram et al., 2011).

NFκB signaling, p62, and PDB – a unifying hypothesis

Taken together with earlier findings that RANKL induces CYLD expression and that CYLD acts as a deubiquitinase, the results noted above suggest a hypothesis in which p62 coordinates the orderly ubiquitination and deubiquitination of TRAF6, sequentially activating then attenuating downstream signaling. PDB-associated mutations in the carboxy-terminal UBA domain of p62 may result in impaired CYLD binding or activity and decreased deubiquitination, thereby predisposing affected cells to diminished negative feedback regulation of TRAF6 mediated signaling (Figure 1.6). In osteoclasts this may lead to enhanced activation of NFκB and NFATc1, increased osteoclastogenesis and a permissive environment in which exposure to a second insult (e.g. viral agent) may lead to abnormal bone resorption and formation – the hallmarks of PDB.

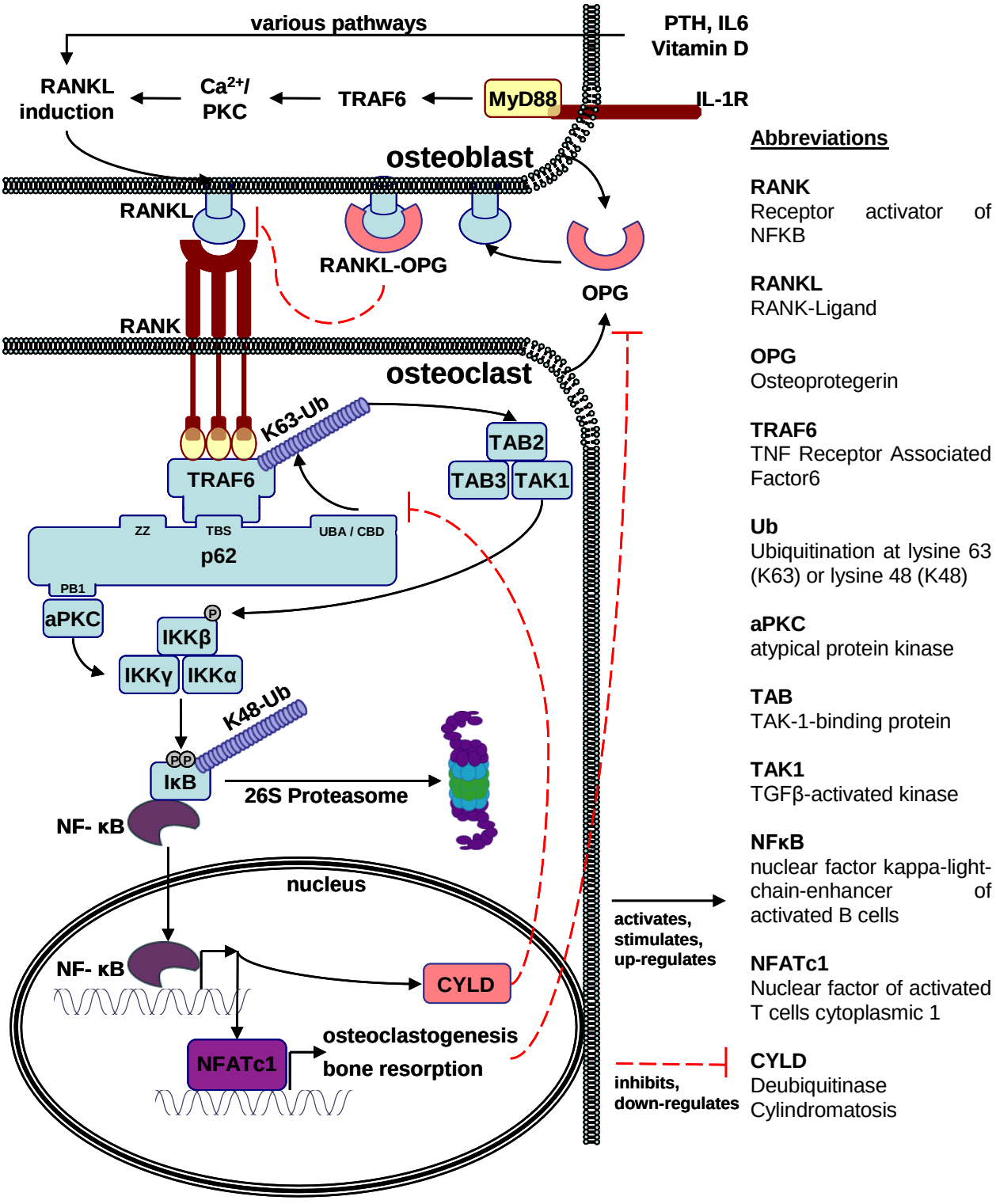

Figure 1.6. Putative roles of p62, TRAF6, and CYLD in osteoclast formation and activation.

NFκB signaling and p62 – important caveats

While this hypothesis integrates several findings in the literature, several questions remain. First, if TRAF6-/- mice are osteopetrotic (Lomaga et al., 1999; Naito et al., 1999), CYLD-/- mice are osteoporotic (Jin et al., 2008), and p62 mediates both TRAF6 and CYLD signaling, then why do p62-/- mice demonstrate structurally normal bone under basal conditions (Durán et al., 2004)? As noted in the discussion about p62 P394L mouse models above, interpretation of phenotypic data may vary despite models being generated in identical ways. One potential confounder among these studies is heterogeneity of experimental method. Early studies on TRAF6-/- mice were conducted on animals ranging from 2 (Naito et al., 1999) to 4 weeks (Lomaga et al., 1999) of age, while p62 -/- mice were characterized at 6 to 8 weeks of age (Durán et al., 2004), and CYLD-/- mice at 14 weeks of age (Jin et al., 2008). This is significant because, while mice reach sexual maturity at 6 to 8 weeks of age, they do not achieve peak bone mass until 16 to 24 weeks of age in the majority of mouse strains (Jilka, 2013) and continue to accrue bone for months afterwards. Moreover, citing unpublished results, investigators have suggested that p62-/- mice exhibit mature-onset obesity accompanied by increased bone mineral density, which implies osteopetrosis (Rodriguez et al., 2006). These deficiencies in our knowledge highlight the need for further experiments, and in particular, for standardization in phenotypic characterization by comparing mice with genotypes of interest on the same genetic background at the same stage of skeletal maturation. While this challenge is taken up in chapter two, we must also acknowledge that though such experiments may resolve many unknowns, the possibility that p62 affects skeletal homeostasis via alternative pathways must also be explored.

1.7 p62 and autophagy

In this light, it has been proposed that p62 mediates osteoclast formation and activity through its role as a mediator of autophagy (Daroszewska et al., 2011), an evolutionarily conserved intracellular degradation process. Most broadly, autophagy is a catabolic process in which intracellular components are sequestered in double-membraned components, autophagosomes, and delivered to the lysosome for degradation (Mizushima et al., 2009). This process may be non-selective, as in so called "bulk autophagy" which is induced by starvation to provide the cell with essential nutrients. It may also be selective, in which targets, such as misfolded proteins, protein aggregates, damaged organelles (mitophagy), or even pathogens (xenophagy), are tagged by post-translational modification (protein ubiquitination, in particular) and cleared by the autophagolysosome (Kirkin et al., 2009; Ashrafi and Schwarz, 2011). In this process, particular molecular chaperones or autophagy receptors have been identified that bind ubiquitinated targets and shuttle them to the autophagosome for selective degradation (Kirkin et al., 2009). While it has been known that p62 binds both mono- and poly-ubiquitinated protein aggregates through its C-terminal UBA domain since it was first cloned nearly twenty years ago, (Vadlamudi et al., 1996), it was only in 2007 that researchers showed that p62 also serves as an autophagy receptor, proving that it was required for the formation of ubiquitinated aggregates in cytosolic bodies, that LC3 or microtubule-associated protein 1A/1B-light chain 3 (found on the inner sheath of autophagosomes and a key marker of autophagy) co-localized with these aggregates, and that both elements were required for their formation and degradation in autophagolysosomes (Komatsu et al., 2007; Pankiv et al., 2007; Nezis et al., 2008). The physiological roles of selective autophagy are the subject of continued investigation, but it is interesting to note that targets may be very specific. For example, in *C. elegans*, SQST-1 (the homolog of p62) has been shown to specifically mediate the

degradation of a core component of the micro RNA induced gene silencing complex (miRISC) through selective autophagy (Zhang and Zhang, 2013), while in mammalian cells, selective autophagy mediated by the adaptor NDP52, rather than p62, has been shown to degrade the primary miRNA processing enzyme and effector, DICER and AGO2, respectively, in the regulation of microRNA activity (Gibbings et al., 2012).

How PDB-associated mutation to UBA domains might alter normal cellular homeostasis has not been elucidated mechanistically, but we may speculate that bulk degradation and cellular energy homeostasis may be altered. Remarkably, it has been demonstrated that severe ATP-depletion leads to increased bone resorbing activity and accelerated apoptosis, while the release of ATP from intracellular stores diminishes bone resorption through an autocrine/ paracrine feedback loop (Miyazaki et al., 2012). This is particularly noteworthy in fully differentiated, bone-resorbing osteoclasts, which are characterized by an over-abundance of mitochondria, required to power energy-taxing activities as bone resorption (Gonzales and Karnovsky, 1961). We might hypothesize that toxic byproducts of oxidative phosphorylation (reactive oxygen species such as superoxide anion, hydrogen peroxide, and hydroxyl radicals) accumulate in osteoclasts, damaging lipids, nucleic acids, and proteins. PDB-associated mutations to p62's UBA domain might impair p62's ability to bind accumulating damaged organelles, misfolded proteins, and ubiquitinated aggregates, and shuttle them to autophagosomes, which may then result, in an increased resorptive burst (due perhaps to fewer potential substrates for intracellular ATP production), accompanied by more rapid accumulation of toxic byproducts, and ultimately apoptosis. Alternatively, degradation of a very specific target or regulator that is normally selectively degraded by autophagy during cellular differentiation, akin to the miRISC component in *C. elegans*, may be perturbed by PDB-associated mutations to p62's UBA domain, resulting in altered osteoclast structure and function.

1.8 p62, reactive oxygen species, and the oxidative stress response

A third potential mechanism by which p62 might mediate osteoclastogenesis, alluded to above, is the cellular response to oxidative stress. It has been known for nearly two decades that osteoclast formation is enhanced by superoxide dismutase and suppressed by catalase, which catalyze the production and degradation, respectively, of H_2O_2 in a dose-dependent manner (Bax et al., 1992; Suda et al., 1993). Sodium nitroprusside, a nitric oxide donor, significantly increases the generation of osteoclasts when added to cultures in low concentrations (Chae et al., 1997). Moreover, RANKL stimulation of osteoclast progenitors transiently increases intracellular ROS through a signaling cascade involving TRAF6 (Lee et al., 2005), while application of the antioxidant N-acetylcysteine (NAC) or suppressing the activity of Nox (an enzyme that catalyzes the production of ROS) inhibit the responses of progenitors to RANKL, including JNK signaling, p38MAPK signaling, ERK signaling, and ultimately osteoclast differentiation (Lee et al., 2005). The importance of ROS-mediated signaling, however, is not limited to the formation of osteoclasts. Indeed, fully formed osteoclasts are often characterized by expression of tartrate resistant acid phosphatase (TRAP) which catalyzes production of elevated levels of hydroxyl radicals and partially co-localizes with late endosomal/lysosomal markers (Räisänen et al., 2001). Interestingly, altering redox status by varying concentrations of H_2O_2 within controlled ranges (that do not alter cellular viability, 0 to 40 μM), yields a biphasic pattern in osteoclasts: moderate concentrations enhance formation of TRAP-positive osteoclasts in a dose-dependent manner, while excessive concentrations decrease the number of TRAP-positive osteoclasts (Kim et al., 2006).

Given the requirement for an optimal level of ROS production in intracellular signaling in the differentiation and activation of osteoclasts, it is not surprising that cells exert exquisite control

over cellular redox status. The cell's primary defense against oxidative stress is the KEAP1-NRF2 pathway. KEAP1 is a cytoplasmic inhibitor of NRF2 (Nuclear factor (erythroid-derived 2)-like 2, also known as NFE2L2), a transcription factor and master regulator of cellular redox homeostasis (Stępkowski and Kruszewski, 2011). Under non-stressed conditions, KEAP1 mediates the constitutive ubiquitination and proteasomal degradation of NRF2 (Nezis and Stenmark, 2012), while in the presence of electrophiles or ROS, KEAP1's cysteine residues are modified leading to its inactivation. Free of KEAP1, NRF2 is stabilized (its half-life goes from 7 minutes to 70 minutes) translocates into the nucleus, and, after heterodimerizing with small Maf proteins, induces expression of genes responsible for (a) intracellular redox-balance (e.g. glutamate cysteine ligase), (b) elimination of ROS (e.g. thioredoxin reductase 1, peroxiredoxin), (c) phase II detoxification (e.g. NQO1, glutathione S-transferase), and (d) transport (multidrug resistance protein 1) (Stępkowski and Kruszewski, 2011; Nezis and Stenmark, 2012; Taguchi et al., 2012).

Through its evolutionarily-conserved KEAP1-interacting region (KIR, corresponding to residues 344-356 in humans and 346-358 in mice), p62 interacts with the NRF2-binding site on KEAP1, competitively displacing the KEAP1-NRF2 interaction under conditions of oxidative stress (Ishii et al., 1996, Ishii et al., 1997; Nezis and Stenmark, 2012; Wright et al., 2013). Remarkably, p62 is also induced by NRF2, forming a positive-feedback loop in the antioxidant response (Jain et al., 2010). Moreover, it has been reported that p62 controls basal levels of KEAP1. In one study, overexpression of p62 led to a decrease in the basal protein level of KEAP1 in several cell lines, while RNAi mediated depletion of p62 resulted in: (a) an increase KEAP1 protein levels (its half-life nearly doubling from 11 to 21 hours) and (b) a concomitant decrease in NRF2 protein levels (and downstream targets), absent changes in KEAP1 or NRF2 mRNA levels (Copple et al., 2010).

A subsequent study has confirmed that KEAP1 is degraded by autophagy rather than the proteasome in a p62-dependent manner (Figure 1.7; Taguchi et al., 2012).

In this light, we may speculate that PDB-associated mutations to p62 may alter its ability to competitively displace KEAP1, thereby decreasing NRF2 translocation into the nucleus, and diminishing the antioxidant response that is so critical in metabolically active osteoclasts. Two recent publications reinforce this hypothesis. In 2013, Wright and colleagues, demonstrated that a rare, PDB-associated, p62 KIR-domain mutant, p62 S349T, was associated with impaired p62-KEAP1 interaction and decreased NRF2 activity via Co-IP and NQO1-promoter driven reporter assays, respectively, in transfected HEK293T cells, while ubiquitin binding and NFκB signaling were indistinguishable from wildtype (Wright et al., 2013). A second research group has provided a plausible molecular basis for this observation, demonstrating: (a) that the p62-KIR interaction with KEAP1 was two orders of magnitude weaker than that between NRF2 and KEAP1 in its native state, but when S351 (the murine equivalent of S349 in humans) was phosphorylated, its binding affinity for KEAP1 increased 30-fold (Ichimura et al., 2013). Furthermore, they demonstrated that oxidative stressors increased the expression of p62, its phosphorylation at residue 351, its aggregation in cytosolic autophagosomes, the time-dependent sequestration of KEAP1 in these structures, and a concomitant increase in nuclear fraction of NRF2 and expression of cytoprotective downstream targets (Ichimura et al., 2013).

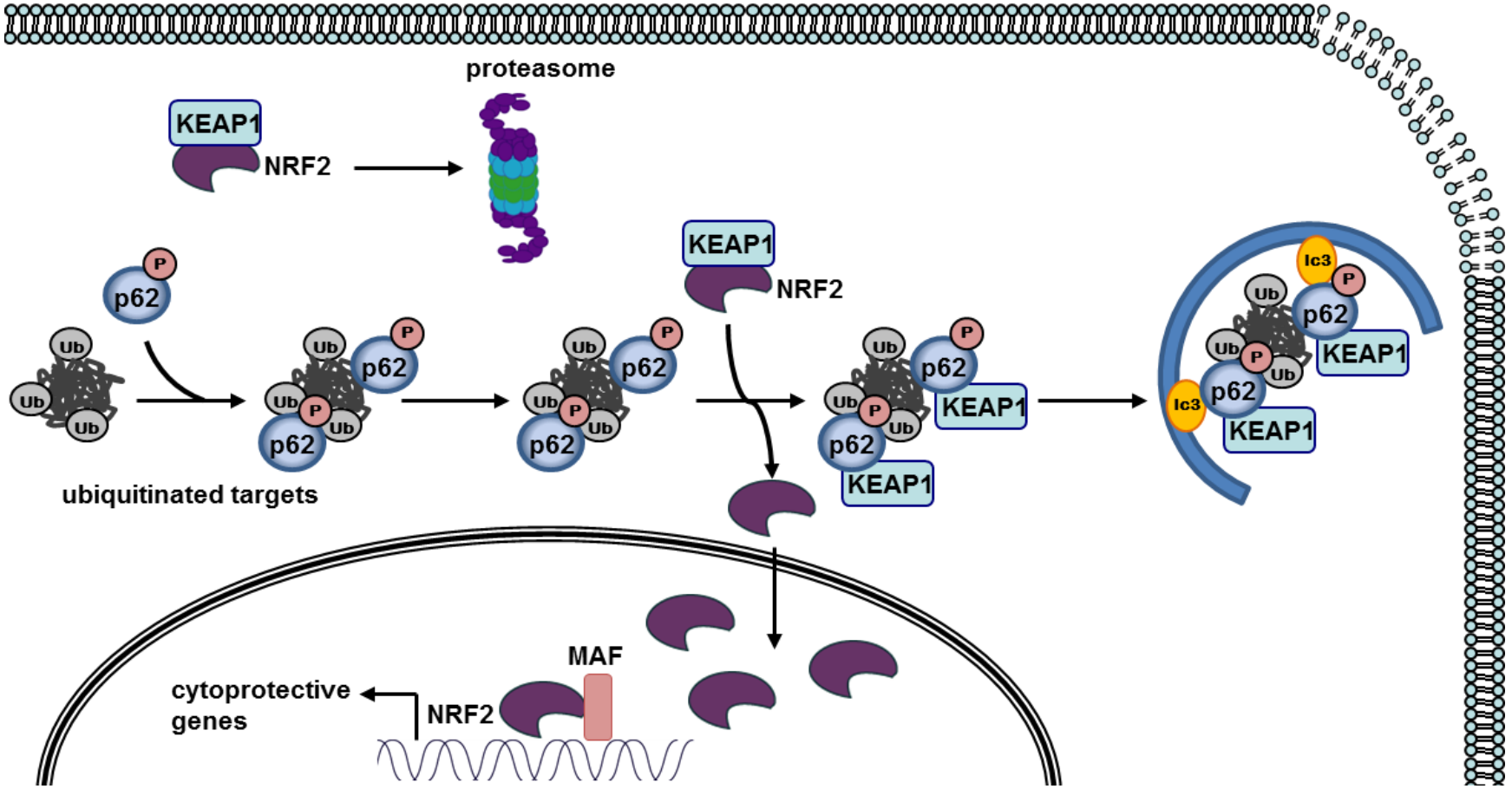

Figure 1.7. The role of p62 in the oxidative stress response. Under normal conditions, KEAP1 constitutively mediates the proteasomal degradation of NRF2. Under conditions of oxidative stress, KEAP1 is destabilized or competitively displaced by phosphorylated p62 and degraded by the autophagosome. Meanwhile, NRF2 is stabilized, translocates and accumulates in the nucleus where it induces the expression of antioxidant genes and p62, in a positive feedback loop. Figure adapted from Ichimura et al., Phosphorylation of p62 activates the Keap1-Nrf2 pathway during selective autophagy. Mol Cell. 2013 Sep 12;51(5):618-31.

1.9 Summary and dissertation overview

Although first identified over a century ago, surprising gaps remain in our knowledge of PDB. Genetic factors, for example, irrefutably contribute to disease pathophysiology. Yet, PDB manifests in a highly focal manner, often affecting a single site in a single bone in the body, and is generally not at all systemic or diffuse as we might expect of a "genetic bone disease." Furthermore, evidence for environmental contributors, such as viruses, to PDB etiology has been presented for at least 30 years, yet the identity and nature of these contributors still evokes heated debate among specialists in the field. The research described in this dissertation was undertaken specifically to shed light on one such gap in our understanding of PDB – the role played by the multifunctional adaptor protein p62 in the cellular physiology of osteoclasts in health and disease.

In particular, it is well established that osteoclasts, bone's principal resorptive cells, are both structurally and functionally anomalous in the focal lesions characteristic of PDB. Dysregulated osteoclast activity accounts for the clinical manifestations of the disease, which may include bone pain, skeletal deformity, neurological complications, pathologic fractures, deafness, and osteosarcoma at a 1000-fold greater incidence than in the general population. Genetic analyses published over one decade ago, and corroborated epidemiologically since, have shown that p62 is the gene product most frequently linked to Paget's and, when mutated, is associated with up to 50% of familial cases and 10% of sporadic cases of the disease.

But what is known of p62's basal function? What specific functions does it play in osteoclasts? The literature paints an interesting yet confounding picture – and our primary objective in this dissertation was to elucidate it. To help and model understand the role p62 plays in osteoclastogenesis and PDB, our group has obtained mice from which p62 has been genetically

knocked-out (p62 KO) and generated mice harboring a mutation causing a proline to leucine substitution at residue 394 of p62 (p62 KI), the murine equivalent of the most common PDB-associated mutation in humans. We then initiated breeding colonies, back-crossing our mice and wildtype controls (WT) to a common C57Bl/6 background, and undertook careful characterization experiments in vivo and in vitro to confirm reported phenotypes about skeletal architecture and cellular function, before proceeding to a detailed study of underlying mechanisms.

We did so primarily by employing hypothesis generating techniques during the course of this project. Specifically, we aimed at further elucidating our understanding of p62 function during osteoclastogenesis in an unbiased and global manner using DNA Microarray gene expression profiling paired with pathway analysis tools to identify critical transcriptional regulators and signaling pathways that are altered when p62 is mutated, as in PDB, or knocked-out. We validate these results functionally testing predictions about specific signaling pathways culled from the microarray results. In this context, we pay particular attention to the RANK-TRAF6-NFκB pathway, reactive oxygen species and the oxidative stress response, and general measures of proliferation and survival, using the tools of Western Blotting, Co-Immunoprecipitation, and ELISA to help elucidate the role of p62 in osteoclastogenesis and Paget's disease of bone.

CHAPTER 2

EFFECTS OF p62 ABLATION AND MUTATION ON BONE STRUCTURE AND OSTEOCLASTOGENESIS

2.1 Introduction

Over one decade ago, the first correlations between mutations in p62 and Paget's disease of bone in patient populations were made. In the intervening years, genetic manipulation of mouse models, biochemical studies on progenitors derived therefrom, and epidemiological studies in patient populations the world over, have drawn a fascinating, if confounding, portrait of the complex role played by p62 in osteoclastogenesis. As detailed in the previous chapter, different research groups have shown that full length p62: (a) does not affect basal osteoclastogenesis, but (b) regulates osteoclastogenesis in response to stimulating cytokines such as PTHrP in vivo, and RANKL in vitro; and that a common PDB-associated p62 UBA-domain mutation: (c) is responsible for cell autonomous increases in progenitor sensitivity and activity, and (d) may or may not be sufficient to generate pagetic lesions in mouse models. In the present chapter, we highlight our efforts to clarify the effect of genotype on skeletal phenotype, cellular morphology, and activity. To do so, we obtained mouse models in which p62 has been ablated (p62-/- or KO) or mutated genetically (p62

P394L knock-in or KI), backcrossed them onto a common C57Bl/6 background, and conducted careful phenotypic studies, as detailed below.

2.2 Methods

Generation of p62 P394L KI mice[1]

p62 P394L mice were previously generated in the laboratory of Dr. Jolene Windle in the Virginia Commonwealth University School of Medicine and published in an account in the journal Human and Molecular Genetics (Hiruma et al., 2008). Briefly, a line of KI mice with a targeted mutation in the endogenous p62 gene encoding a proline-to-leucine substitution at amino acid residue 394 was generated by homologous recombination (Figure 2.1). For the purposes of maintaining a standard genetic background for all experiments in this project, the mutation at the p62 gene locus was transferred onto the inbred strain C57BL/6J by backcrossing more than 6 times, and homozygous mutants (p62P394L/P394L, KI) were used for subsequent experiments. Mouse tail DNA was used for genotyping by PCR using a pair of primers that flank the introduced loxP site: 5`-ACT CCA GTC TCT ACA GAT GCC AG-3` and antisense (intron 7): 5`-GTT GCC AAG ACT AGA CAG GAC AGG-3`, yielding a product of 182 bp for the WT allele and 226 for the p62-P394L KI allele. Water and regular chow were available ad libitum and all mice were handled in accordance with IACUC approved procedures at the VCU School of Medicine.

1 Both this section and the accompanying figures are adapted from the paper in which they first appeared (Hiruma et al., 2008) and are included for the sake of reference and comparison in this dissertation. No credit for the generation or initial characterization of these mice is claimed by the author.

Generation of p62-/- KO mice[2]

p62-/- (KO) mice were also generated by homologous recombination, but in the lab of Dr. Jaekyoon Shin at Sungkyunkwan Medical School in South Korea and obtained by the laboratory of Dr. Windle at the Virginia Commonwealth University School of Medicine. Although Dr. Windle's lab first obtained the p62-/- (KO) mice, which were already on the C57Bl/6J genetic background, and initiated its own breeding colony of these mice in 2006, the targeting strategy was published only recently in the EMBO journal (Figure 2.1, adapted from Kwon et al., 2012). Homozygous mutants (p62-/- or KO) were used for subsequent experiments. These mice were genotyped using the following primers: p62 (1822-1845): GCT AAC AAA ATG AAG CCA GAT GGG, p62 (2222-2199): GCC TGG CAT CTA AGT TGT TCT GAG, and PGK (353-332): CTGA GCC CAG AAA GCG AAG GAG, yielding a product of 401 bp for the WT allele and 583 bp for the p62 -/- allele. Water and regular chow were available ad libitum and all mice were handled in accordance with IACUC approved procedures at the VCU School of Medicine.

Bone Histomorphometry

The term bone histomorphometry refers to the science and craft of the histological assessment of bone phenotypes. Its practice facilitates the visualization and quantification of bone cells in tissue – i.e., osteoblasts, osteoclasts, osteocytes in the context of the organic and mineral milieu in which they reside – permitting the comparison of groups (baseline vs. disease, transgenic vs. wildtype, etc.) even when differences are not grossly evident.

2 Both this section and the accompanying figures are taken directly, with little change to the text, from the papers in which they first appeared (Kwon et al., 2012) and are only included for the sake of reference and comparison in this dissertation. No credit for the generation or initial characterization of these mice is claimed by the author.

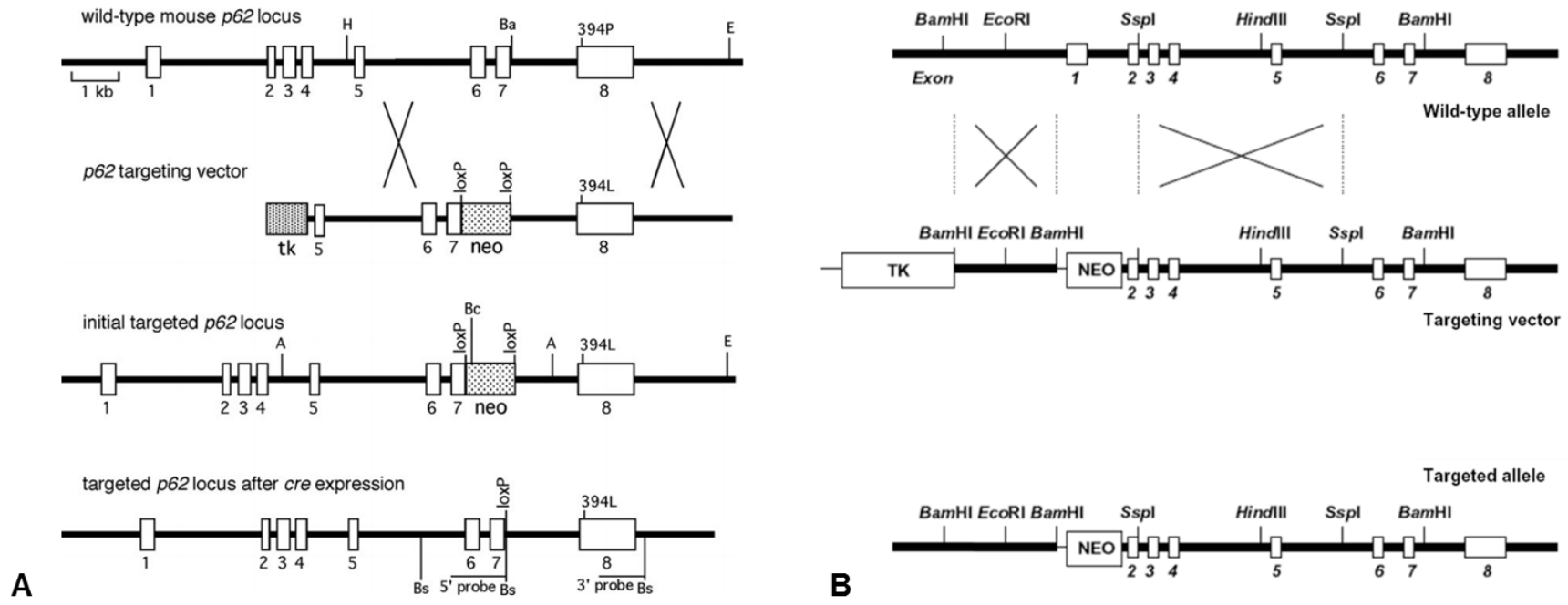

Figure 2.1. Targeting strategies for the generation of p62 P394L knock-in and p62-/- mice.

(A) Targeting strategy for the generation of p62 P394L knock-in (KI) mice, as previously published by the Windle lab. Schematic representation of the murine p62 gene (indicating the location of codon 394 in exon 8), targeting vector, initial targeted p62 locus, and final targeted p62 locus following transient cre expression in ES cells. Adapted from Figure 1 in Hiruma et al., A SQSTM1/p62 mutation linked to Paget's disease increases the osteoclastogenic potential of the bone microenvironment. Hum Mol Genet. 2008 Dec 1;17(23):3708-19.

(B) Targeting strategy for the generation of p62-/- (KO) mice, as previously published by the Shin lab. Schematic representation of the murine p62 gene, targeting vector for knocking out exon 1, and final targeted locus. Please note, sequencing conducted by Dr. Mark Subler has demonstrated the presence of an intact full-length exon 2 in the targeted p62 locus. More specifically, the deletion extends from 310 bp 5` of the first AUG start codon, and extends approximately 2 kb, through most of intron 1 concluding 44 bp 5` of the start of exon 2 (personal communication). The figure has been modified to reflect this correction. Adapted from Figure S1 in Kwon et al., Assurance of mitochondrial integrity and mammalian longevity by the p62-Keap1-Nrf2-Nqo1 cascade. EMBO Rep. 2012 Feb 1;13(2):150-6.

Histomorphometry Specimen Preparation and Processing

Ten 12 to 14-month old p62-/- (KO), p62 P394L/P394L (KI), and age-matched wildtype (WT) controls were weighed and sacrificed. After euthanasia, their hindlimbs and spinal columns were manually dissected free of soft tissue, fixed in 50mL of neutral buffered 10% formalin, and submitted to Dr. Hua Zhou at the Helen Hayes Hospital, New York for histomorphometric analysis. Tissue fixation, decalcification, and processing followed previously published methods (Kurihara et al., Cell Metabolism, 2011) and all procedures were conducted with approval from the Institutional Animal Care and Use Committee at Virginia Commonwealth University.

Specifically, after initial fixation, spinal segments from lumbar vertebrae 1 through 4 were isolated, fixed in 10% neutral buffered formalin for a minimum of two weeks, rinsed in running distilled water for 1-3 days, fixed in 70% EtOH, rinsed in running distilled water for 1-3 days, then decalcified in 250mL of 15% disodium EDTA (Fisher Chemical) at 4°C under constant agitation for 10 weeks. The EDTA solution was changed daily for the first month, and every 3 to 4 days thereafter. When decalcification was complete, each spinal column segment was removed from EDTA, rinsed in running distilled water, dehydrated in graded ethanol solutions, cleared in xylene, and infiltrated then embedded in paraffin (TissuePrep) using a vacuum infiltration processor (Tissue-Tek VIP).

Tartrate Resistant Acid Phosphatase (TRAP) Staining

Among bone cells, differentiated osteoclasts uniquely express tartrate resistant acid phosphatase (TRAP). To illustrate these cells in section, samples are incubated in a solution containing naphthol AS-BI phosphoric acid and freshly diazotized fast garnet GBC. Enzymatic hydrolysis by tartrate

resistant acid phosphatase releases Naphthol AS-BI which immediately couples with fast garnet GBC, forming insoluble maroon deposits at sites of activity. Cells with tartrate sensitive acid phosphatases are devoid of activity and therefore do not stain red. Accordingly, decalcified sections obtained from experimental animals were assayed for TRAP activity according to manufacturer specifications (Sigma 387A, Sigma-Aldrich).

Specifically, all slides were dewaxed in xylene (5min x 2), then rehydrated in graded ethanol baths to water (5min 100% EtOH x 2, 3min 95% EtOH x 2, 3min 70% EtOH, 5min deionized H_2O), then incubated for one hour at 37°C in freshly made TRAP solution (diazotized Fast Garnet GBC, Naphthol AS-BI phosphate, acetate, tartrate, and deionized water). All sections were evaluated by light microscopy and red-stained cells were counted as OCLs.

Histomorphometry Quantification

Another set of sections was stained with 0.1% toluidine blue. Histomorphometry was performed on the region of cancellous bone between the cranial and caudal growth plates of the third lumbar vertebral body under bright field and polarized light at a magnification of ×200, using OsteoMeasure 4.00C morphometric program (OsteoMeasure; OsteoMetrics). Osteoclast surface was defined as the area of bone surface covered with TRAP-positive and mono- and multinuclear cells. Osteoblast surface, cancellous bone volume, trabecular width, trabecular number, and trabecular separation were also quantified and calculated. All variables were expressed and calculated according to the recommendations of the American Society for Bone and Mineral Research Nomenclature Committee (Parfitt et al., 1987).

TNF-α Specimen Preparation and Processing

Acute, intermittent application of TNF-α over the calvariae of mice has been long known to induce osteoclast formation by directly acting on receptors on the cell surface of osteoclast progenitors, unlike PTHrP which is thought to induce RANKL expression in stromal cells, and thereby increase osteoclastogenesis indirectly. Application of TNF-α was performed as described previously (Ishizuka et al., JBMR 2011). In brief, murine TNF-α (Millipore, 1.5μg in 50μL of saline) or the same volume of saline was injected once daily for 5 consecutive days into the subcutaneous layer overlaying the calvariae of 2-month-old KO (n = 11), KI (n = 10), and WT control (n = 8) mice. On day 6, calvariae were harvested, fixed in 10% neutral buffered formalin, and processed for histology. Tissue fixation, decalcification, processing, and TRAP staining followed previously published methods (Kurihara et al., Cell Metabolism, 2011) and procedures were conducted with approval from the Institutional Animal Care and Use Committee at Virginia Commonwealth University.

Osteoclast formation and bone resorption

Non-adherent marrow cells (1 x 10^5cells/well: 96-well plate; 2.6 to 3 x 10^6cells/well: 6-well, 6cm plate, and 10cm plates) were prepared as previously described (Hiruma et al., 2008) and cultured in α-MEM + 10% FBS + 1% antibiotic/antimycotic for 2 days in the presence of recombinant murine M-CSF (20ng/mL, R&D), and then an additional bolus of various concentrations of M-CSF and recombinant murine RANK (R&D), as noted. Cells were then stained for TRAP using a leukocyte acid phosphatase kit (Sigma), and TRAP-positive cells were quantitated. For bone resorption,

Non-adherent marrow cells were cultured on mammoth dentin slices (Wako, Osaka, Japan) in cultured in α-MEM + 10% FBS containing 10ng/mL M-CSF and 50ng/mL RANKL. After 14 days

of culture, the dentin slices were stained with acid hematoxylin, and areas of dentin resorption were determined using image analysis techniques (Image J, NIH).

Statistical Analysis

Significance was evaluated using the StatView Software package (StatView for Windows, SAS Institute, v5.0.1) by a two-sided, unpaired Student's t test or two-way analysis of variance (ANOVA) where indicated. The criterion for statistical significance was $p < 0.05$. Post-hoc analysis was performed using the Tukey-Kramer test as appropriate.

2.3 Results

Genetic manipulation at the p62 locus alters mRNA expression

During individual crosses between KI heterozygotes on the C57Bl/6J background, offspring of each of the three possible genotypes (wildtype or p62 +/+, heterozygous knock-ins or p62 +/P394L, and homozygous knock-ins or p62 P394L/P394L) were generated in the expected ratio, indicating that this mutation had no discernible effect on normal embryonic development. Further, both KI heterozygotes and homozygotes were viable and had no grossly apparent phenotypic abnormalities up to 1.5 years of age. The same was true of crosses between KO heterozygotes, in that offspring of each of the three possible genotypes (wildtype, p62 +/-, p62 +/+) were generated in the expected ratio, indicating that this knock-out also had no discernible effect on normal embryonic development. Further, both KO heterozygotes and homozygotes were viable. Interestingly, by four to five months of age, an obesity phenotype is readily discernible in these mice, similar to that previously published and documented by the lab of Dr. Jorge Moscat (Rodriguez et al., 2006), whose group published the first p62-/- mouse, generated through an alternative targeting strategy (Durán et al., 2004).

To confirm that p62 expression was absent in the KO mice, and to compare expression levels in the WT and KI mice, osteoclast progenitors were generated from mice of each genotype by treating marrow cultures with M-CSF (20ng/mL) for 3 days, and then culturing for an addition 8 hours with M-CSF (20ng/mL) ± RANKL (100ng/mL). Protein extracts were then prepared, and p62 levels assessed by western blot analysis (Figure 2.2). Relative p62 mRNA levels were determined from the microarray studies described in chapter three. As expected, no p62 mRNA or

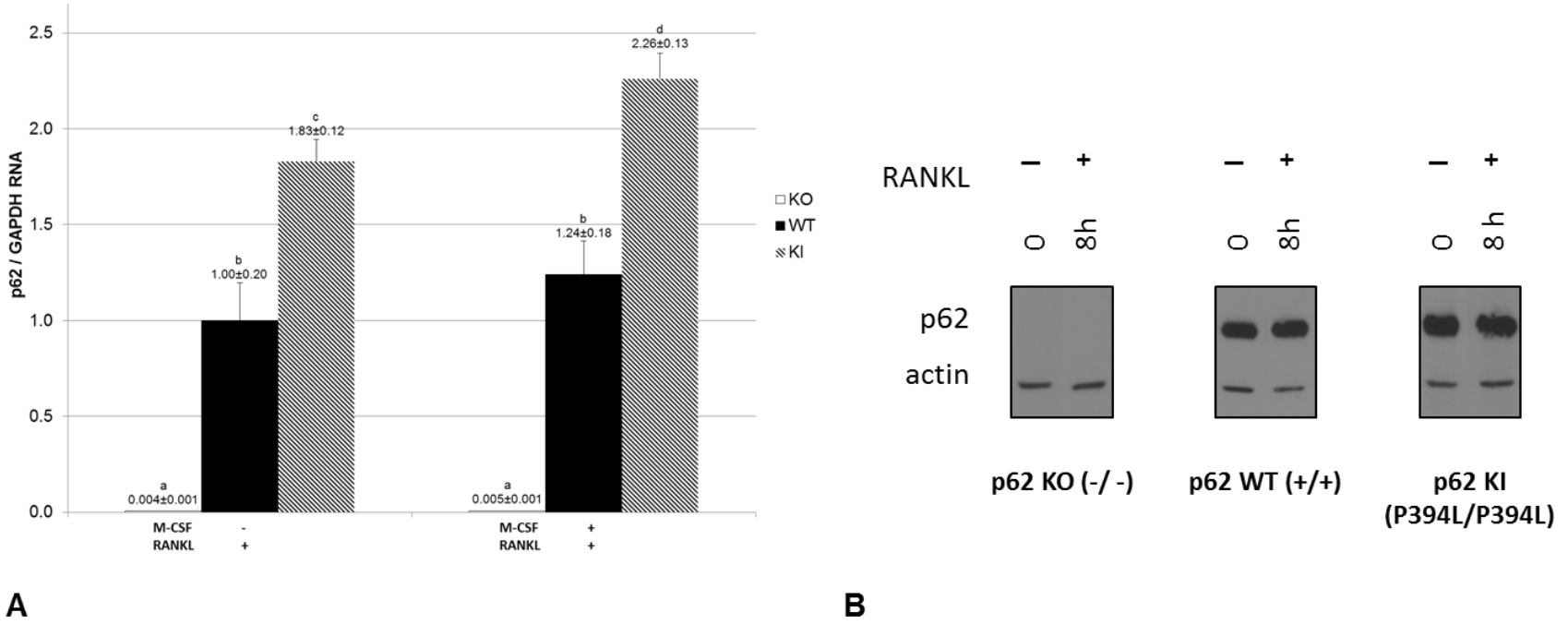

Figure 2.2a. Expression of p62 mRNA and protein in KO, WT, and KI osteoclast progenitors.

(A) Relative p62 mRNA levels quantified from microarray experiment. Transcript intensity levels were normalized to internal GAPDH levels on each Chip. SEM derived from n = 3 genotype-treatment combinations. (a, b, c, d, $p < 0.05$ using one-way ANOVA, Bonferroni corrected)

(B) Effect of p62 genotype on p62 protein levels. A representative immunoblot showing the levels of p62 and actin, obtained from whole cell lysates of osteoclast progenitors from KO, WT, and KI mice cultured in the presence or absence M-CSF and RANKL.

protein was detected, either in the presence or absence of RANKL in the KO cells, consistent with the fact the entire first exon, including the translation start site, has been deleted in the KO mice (Figure 2.2a). In the WT and KI osteoclast progenitors, p62 protein levels were indistinguishable, indicating that the P394L mutation does not have a significant effect on p62 protein stability. Interestingly, the KIs expressed p62 mRNA at 1.8 and 2.4 fold higher levels than WT in the presence and absence of RANKL, respectively (Figure 2.2a). However, the significance of this finding is unclear, since the difference is not reflected at the protein level.

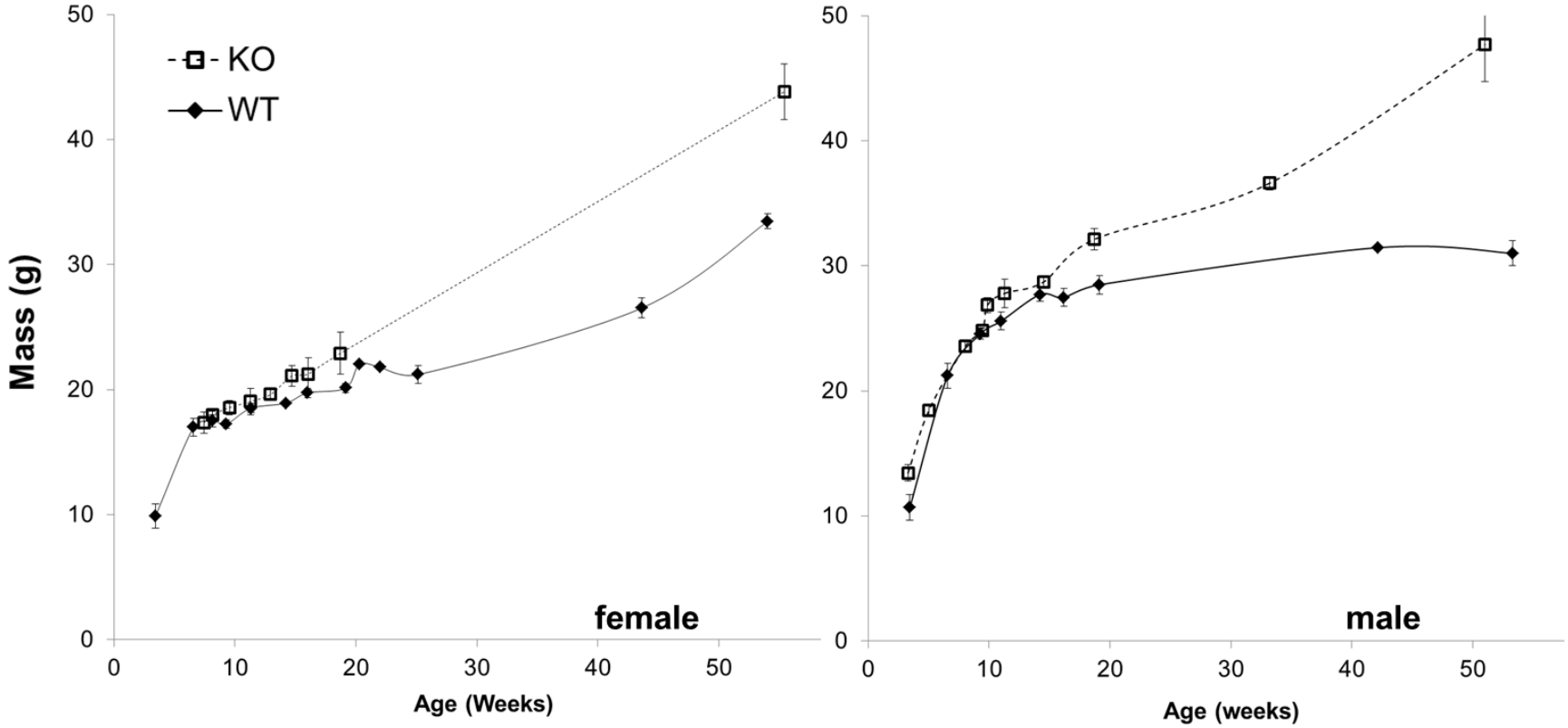

Figure 2.2b. p62 KO mice develop mature-onset obesity.

The masses of various sets of female (left panel, n = 34 KO, n = 30 WT) and male (right panel, n = 34 KO, n = 19 WT) mice were measured intermittently. As observed in previous studies, p62 -/- mice develop mature-onset obesity that, in our hands, is first detectable at 3 months of age. Results shown are the mean ± SEM. The masses of KI mice were indistinguishable from WT (data not shown).

Histomorphometric analysis of bones from one-year-old mice of each genotype

KO and KI mice, backcrossed onto the C57Bl/6J genetic background, along with WT control mice from the same colonies, were aged for one year and their weights were measured intermittently (Figure 2.2b). Of particular note, p62 KO mice developed mature-onset obesity that is first detectable as soon as three months of age, but becomes particularly prominent at 5 months of age (Figure 2.2b), confirming a previously published finding (Rodriguez et al., 2006).

For histomorphometry, animals were sacrificed, and spinal columns were harvested, fixed, processed for histology, and assessed for measures of bone structure. All histomorphometric analysis was conducted by Dr. Hua Zhou at the Helen Hayes Hospital, New York. Interestingly, no PDB-like pagetic lesions were observed in bones from mice of any genotype.

While there was a trend suggesting that osteoclast formation was impaired in KO mice, it did not reach statistical significance ($p = 0.075$, Figure 2.3a). On balance, for measures of both (a) bone cellular activity, such as osteoblast surface, and (b) bone structure and cancellous bone microarchitecture, such as bone volume, trabecular thickness, number, and spacing – there were no statistically significant differences between WT and KO mice, under basal, unstimulated conditions (Figure 2.3a). In contrast, there was a pronounced structural phenotype in p62 KI mice compared to WT controls (Figure 2.3b): bone volume was reduced by approximately 33% ($p = 0.005$), while trabecular number was reduced by 25% ($p = 0.02$), and resulting spacing between

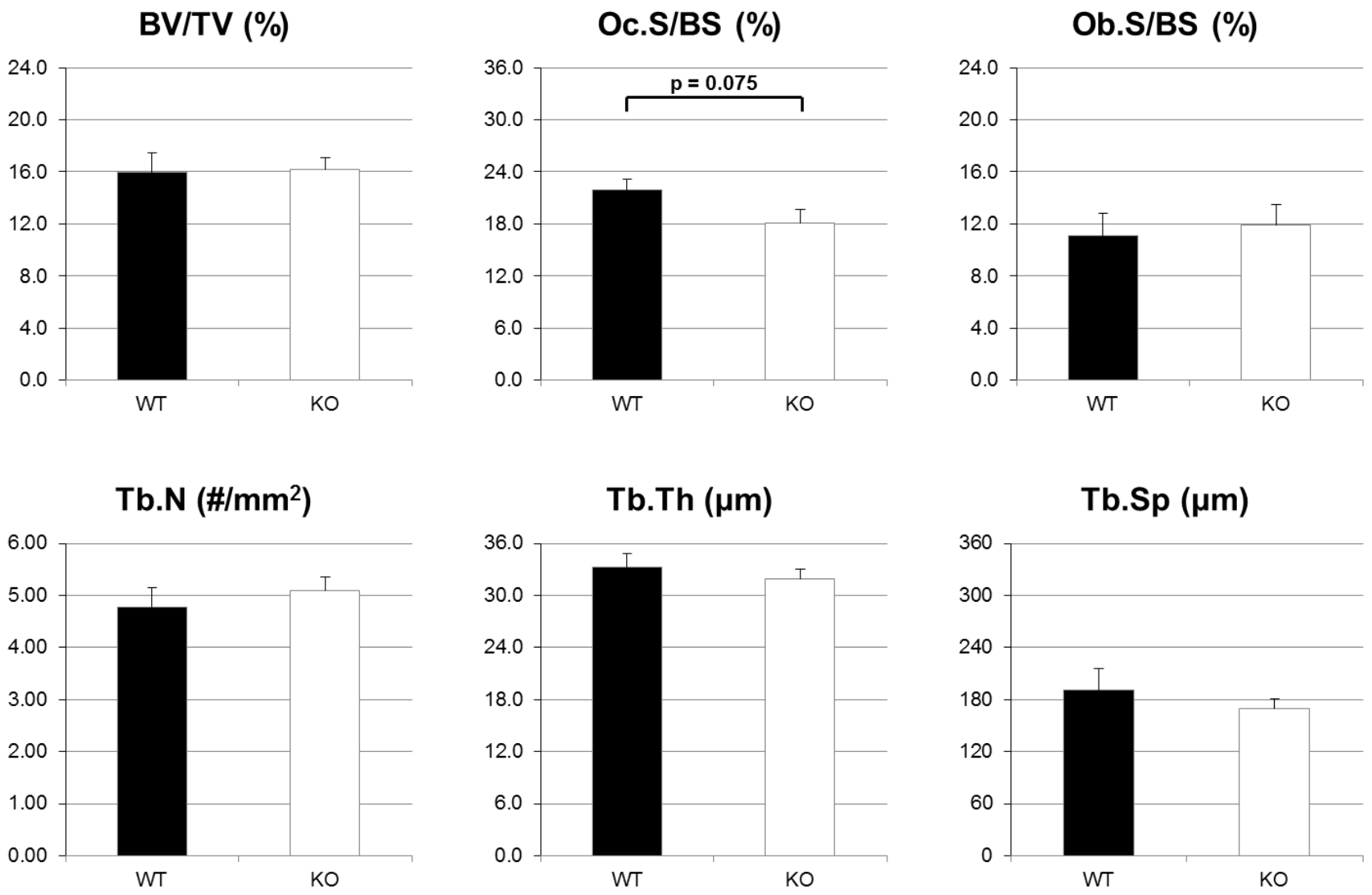

Figure 2.3a. Effect of genotype on bone histomorphometric parameters in p62 KO mice (n = 10) and age-matched WT (n = 10) control mice. Results shown are the mean ± SEM. * $p < 0.05$, ** $p < 0.005$. Abbreviations: BV, bone volume; TV, tissue volume; Oc.S, osteoclast surface; Ob.S, osteoblast surface; BS, bone surface; Tb.N, trabecular number; Tb.Th, trabecular thickness; Tb.Sp, trabecular spacing.

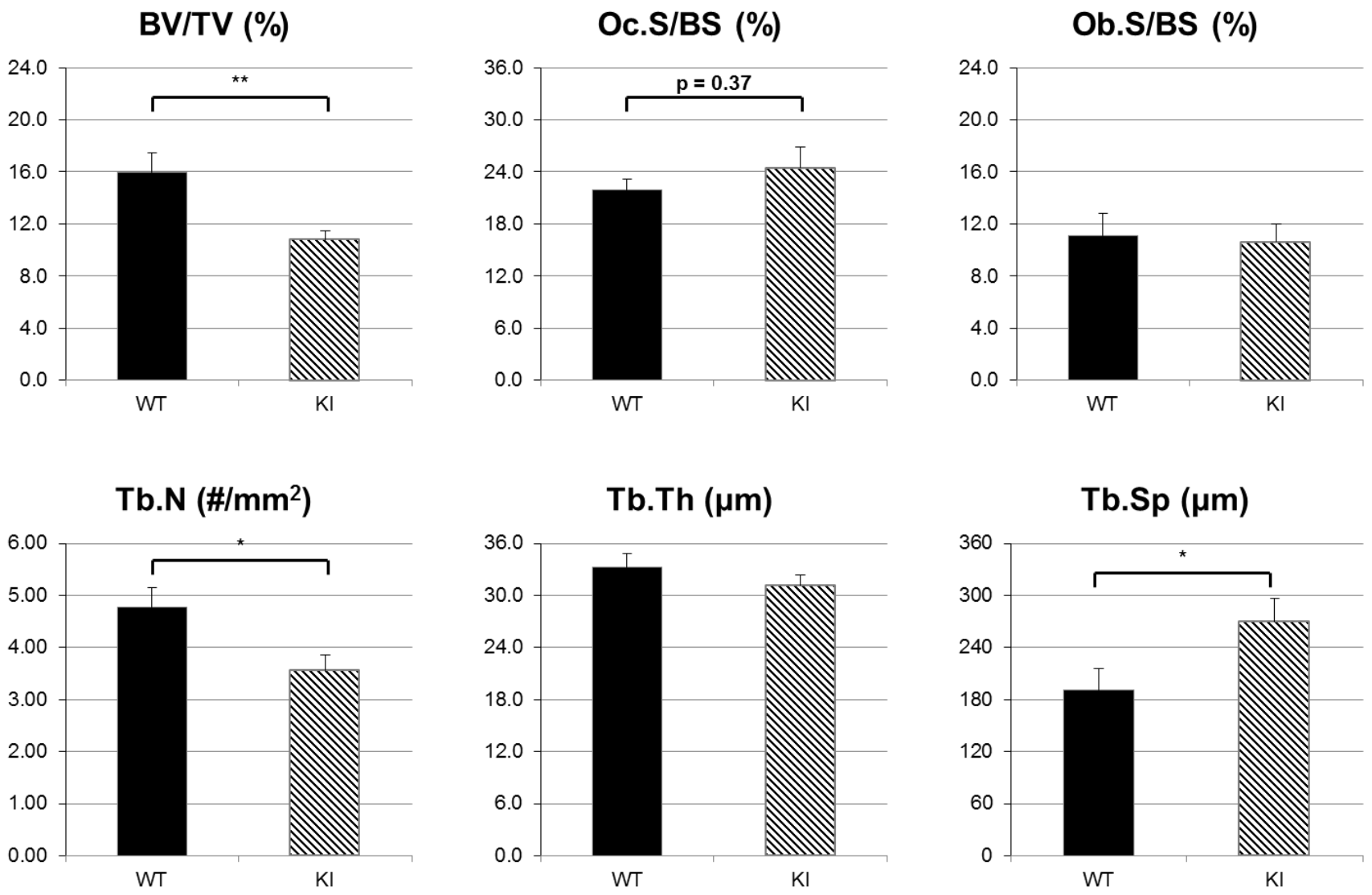

Figure 2.3b. Effect of genotype on bone histomorphometric parameters in p62 P394L KI mice (n = 9) and age-matched WT (n = 10) control mice. Results shown are the mean ± SEM. * $p < 0.05$, ** $p < 0.005$. Abbreviations: BV, bone volume; TV, tissue volume; Oc.S, osteoclast surface; Ob.S, osteoblast surface; BS, bone surface; Tb.N, trabecular number; Tb.Th, trabecular thickness; Tb.Sp, trabecular spacing.

trabeculae increased by approximately 40% ($p < 0.05$). Interestingly, osteoclast surface was not statistically distinguishable between KI and WT controls when the data are pooled by gender (Figure 2.3b, $p = 0.37$). However, osteoclast formation in female KI mice exceeded that in WT females by approximately 25% (data not shown, $p = 0.04$), while no differences in osteoblast surface were observed, even when separated out by gender (data not shown).

Effect of TNF-α on in vivo osteoclastogenesis in mice of each genotype

Eight-week-old female KO, WT, and KI mice were subjected to supracalvarial, subcutaneous injection of TNF-α, a potent, direct inducer of osteoclast formation and activity, and osteoclast numbers in sections of the treated calvariae were counted (Figure 2.4). As expected, TNF-α caused a potent induction of osteoclastogenesis in WT mice (↑80%, $p < 0.005$, Figure 2.4a), while this effect was completely absent in the KO mice (↓8.7%, $p = 0.46$). KI mice demonstrated a trend toward increased osteoclast formation in response to TNF-α, although it did not reach statistical significance in our sample (↑50%, $p = 0.11$, Figure 2.4b).

Effect of RANKL on formation of osteoclasts from bone marrow derived progenitors from mice of each genotype

In vitro studies on osteoclastogenesis induced by RANKL, performed on bone marrow derived progenitors obtained from age and gender-matched KO, WT, and KI mice, yielded similar results (Figure 2.5). Notably, osteoclast formation increased in a significant, dose-dependent manner in WT and KI cultures, while KO cultures were less sensitive to osteoclastogenic cytokines, producing approximately 50% fewer osteoclasts at equivalent doses of RANKL (Figure 2.5b). Moreover, KI cultures produced osteoclasts that were greater in individual size than those formed in the WT cultures, while KO osteoclasts were smaller than WT (Figure 2.5a).

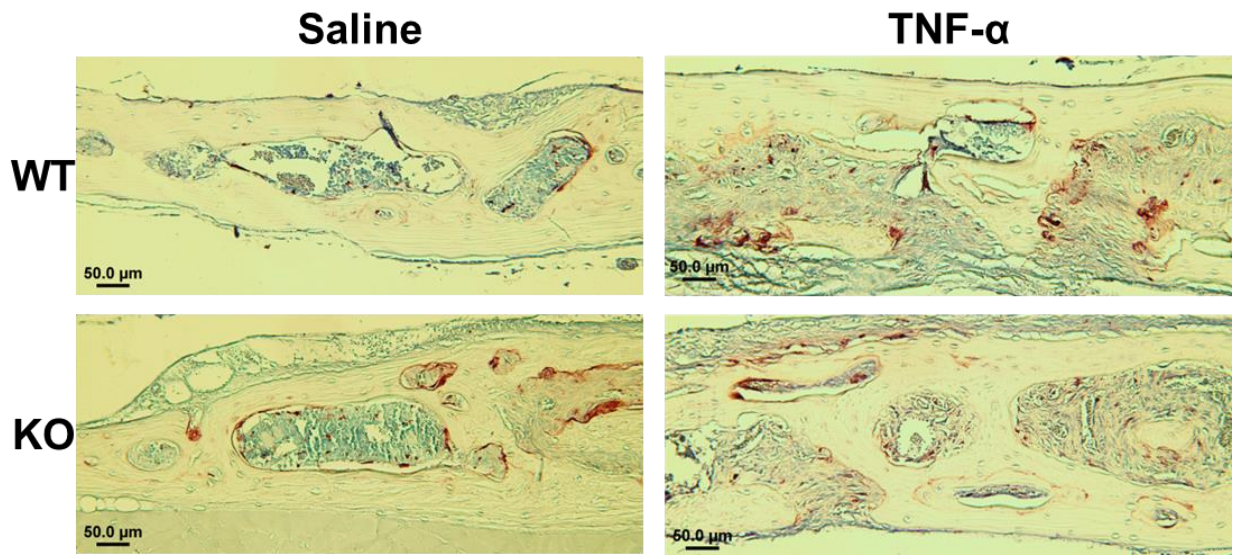

Figure 2.4a. Effect of genotype on induced osteoclastogenesis in p62 KO mice and WT control mice treated with TNF-α or saline. Murine TNF-α (1.5µg in 50µL of saline) or the same volume of saline was injected once daily for 5 consecutive days into the subcutaneous layer overlaying the calvariae of 2-month-old KO (n = 11) or WT control female mice (n = 8). On day 6, calvariae were harvested, fixed in 10% neutral buffered formalin, processed for histology, and stained for tartrate resistant acid phosphatase activity (TRAP). TRAP+ cells with three or more nuclei were counted as osteoclasts and quantified. Results shown are the mean ± SEM. * $p < 0.05$, ** $p < 0.005$

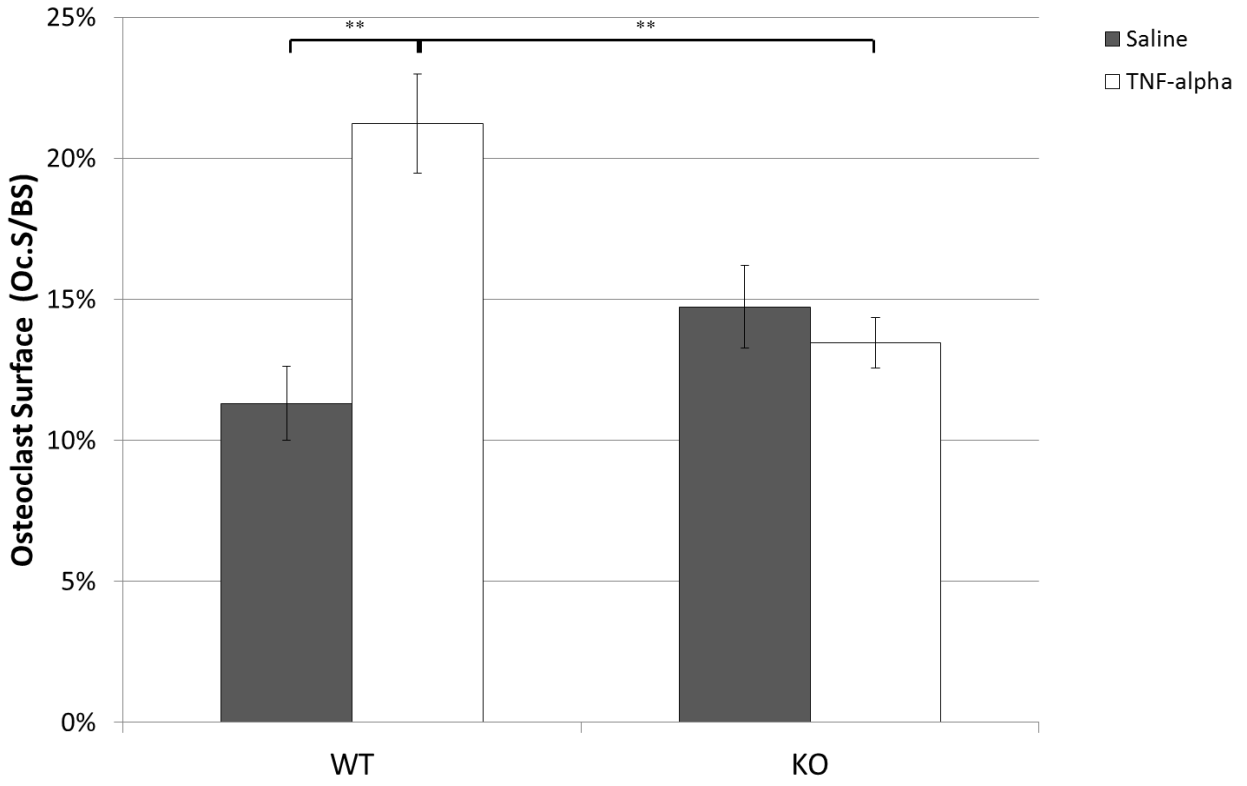

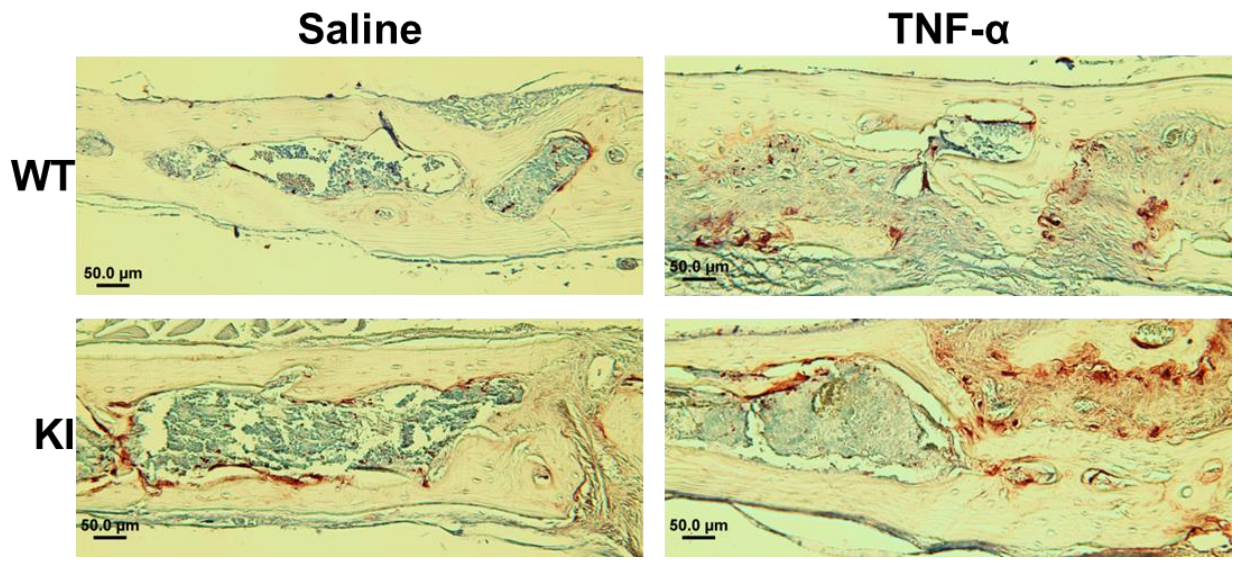

Figure 2.4b. Effect of genotype on induced osteoclastogenesis in p62 P394L KI mice and WT control mice treated with TNF-α or saline. Murine TNF-α (1.5µg in 50µL of saline) or the same volume of saline was injected once daily for 5 consecutive days into the subcutaneous layer overlaying the calvariae of 2-month-old KI (n = 10) or WT control female mice (n = 8). On day 6, calvariae were harvested, fixed in 10% neutral buffered formalin, processed for histology, and stained for tartrate resistant acid phosphatase activity (TRAP). TRAP+ cells with three or more nuclei were counted as osteoclasts and quantified. Results shown are the mean ± SEM. * $p < 0.05$

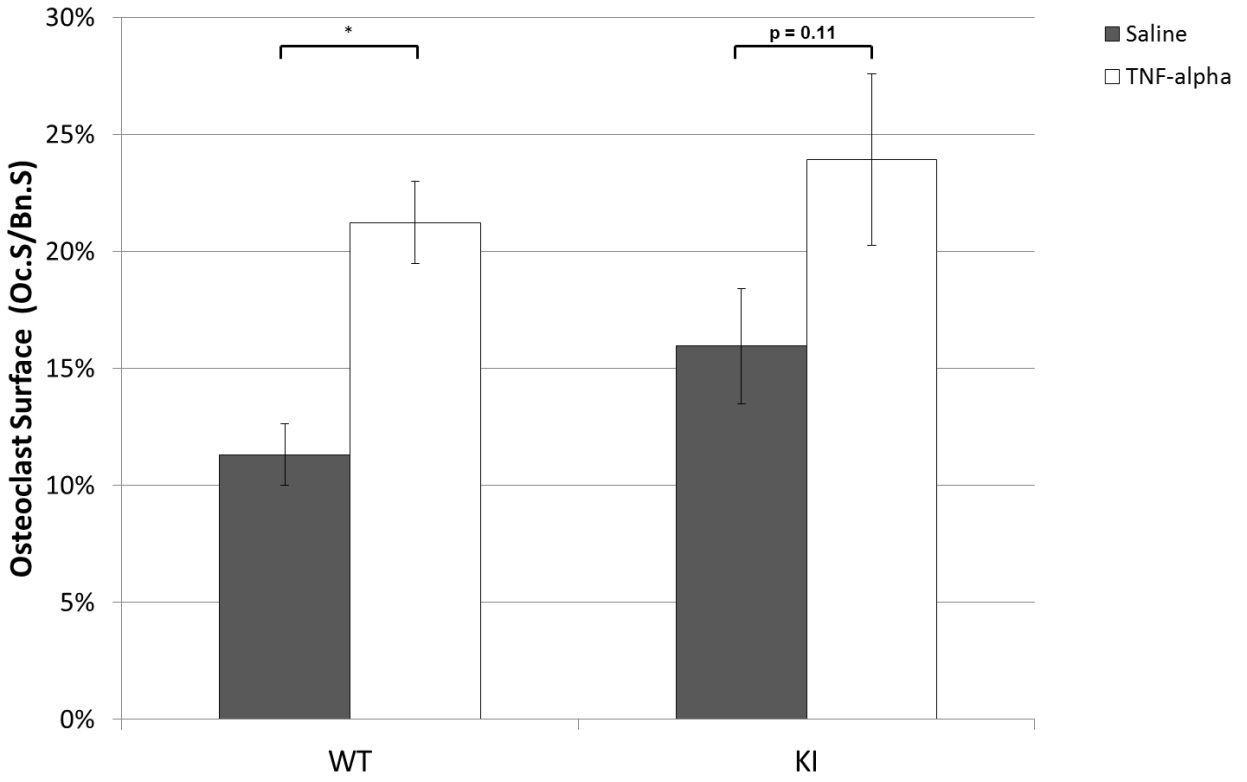

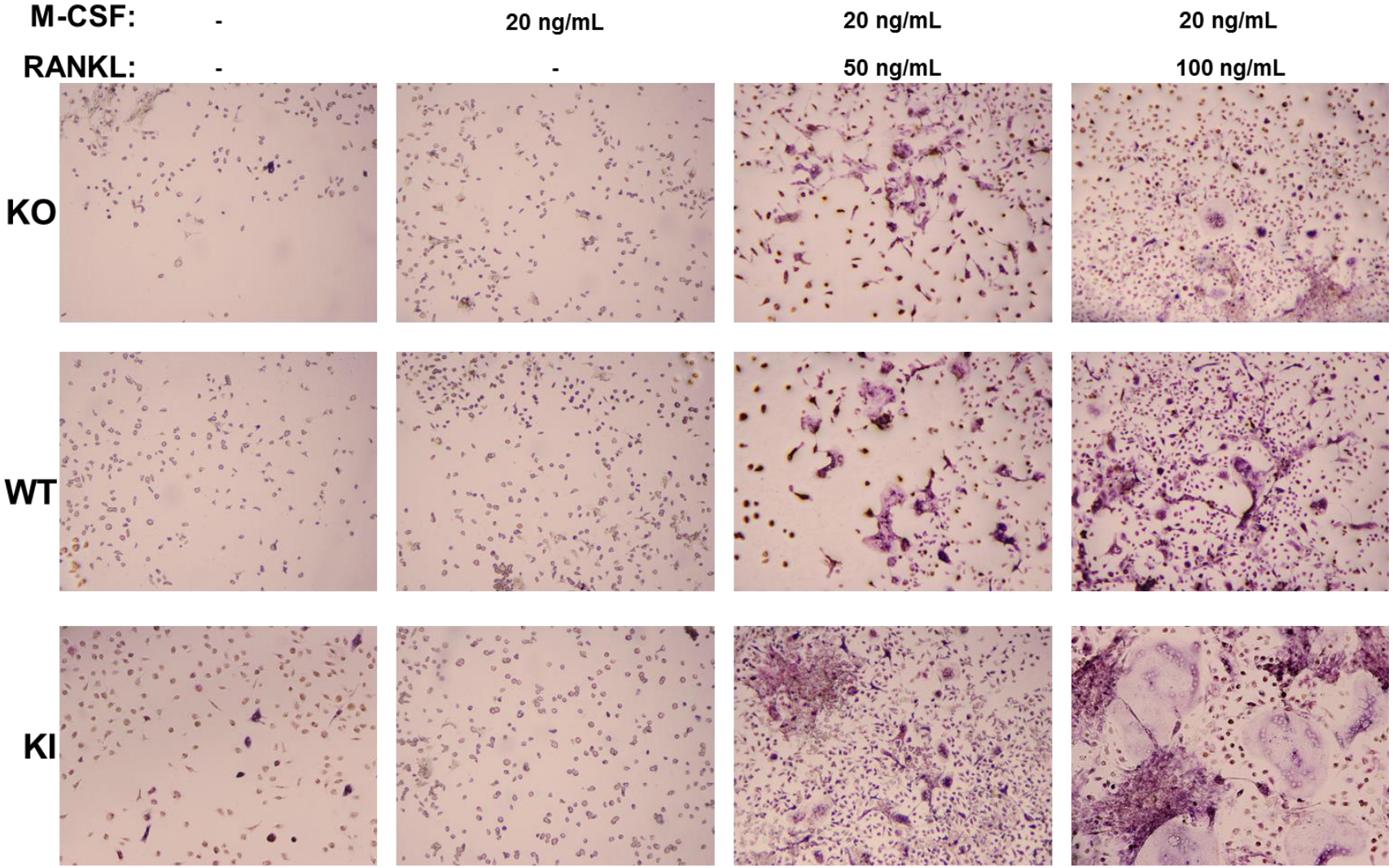

Figure 2.5a. Effect of genotype and RANKL dose on induced osteoclastogenesis in vitro. Bone marrow derived progenitors obtained from p62 –/– (KO), wildtype (WT), and p62 P394L (KI) mice were primed with M-CSF for two days then cultured in the presence of varying quantities of M-CSF ± RANKL for three days. Osteoclasts were then fixed in 10% neutral buffered formalin and stained for tartrate resistant acid phosphatase activity (TRAP) and imaged (representative images included). TRAP+ cells with three or more nuclei were counted as osteoclasts and quantified. Note the enlarged size of osteoclasts in the KI genetic background.

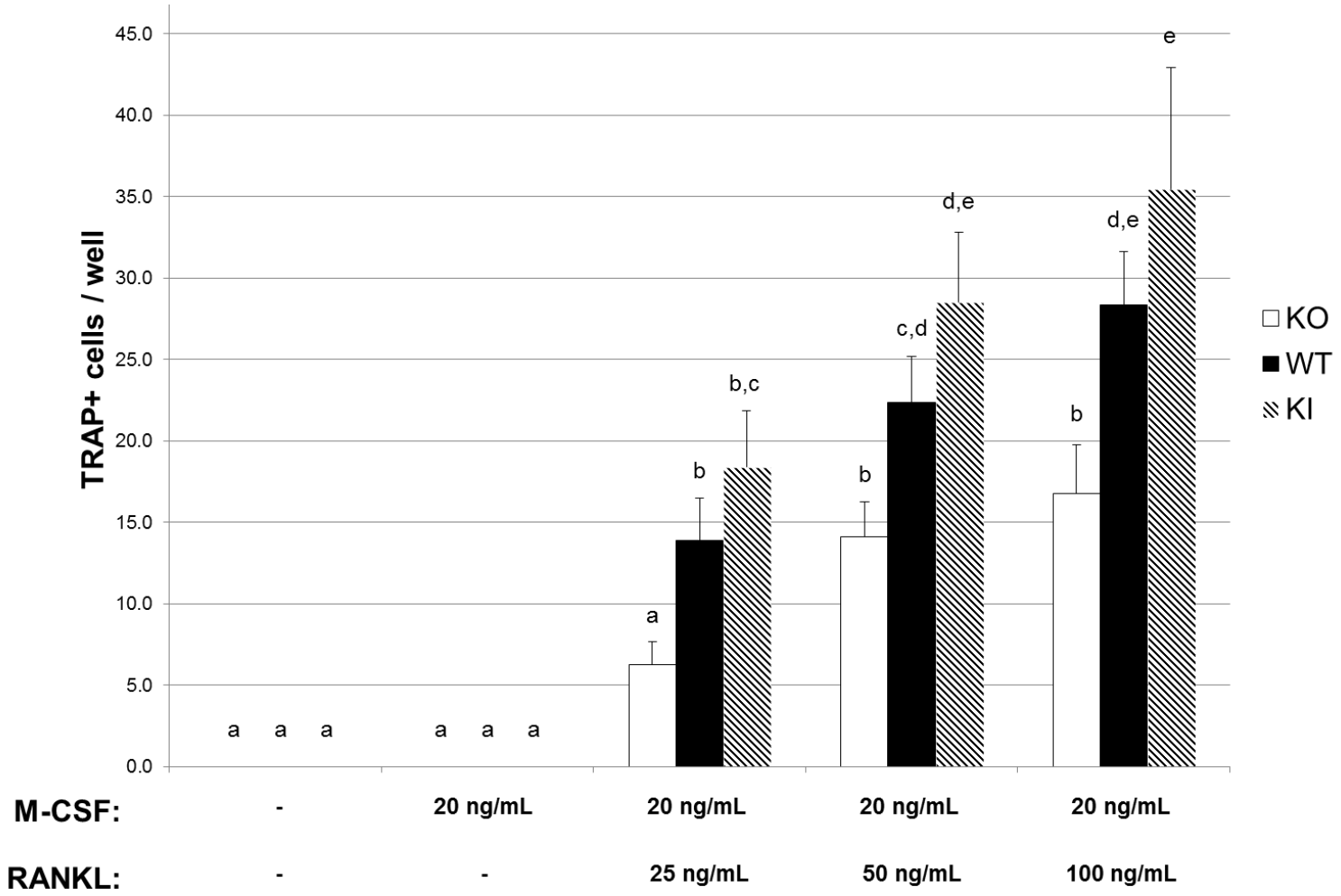

Figure 2.5b. Quantitation of effect of genotype and RANKL dose on induced osteoclastogenesis in vitro. Bone marrow derived progenitors obtained from p62 –/– (KO), wildtype (WT), and p62 P394L (KI) mice were primed with M-CSF for two days then cultured in the presence of varying quantities of M-CSF ± RANKL for three days. Osteoclasts were then fixed in 10% neutral buffered formalin and stained for tartrate resistant acid phosphatase activity (TRAP). TRAP+ cells with three or more nuclei were counted as osteoclasts and quantified. Results, aggregated from 6 independent experiments (n = 6), are the mean ± SEM. a, b, c, d, e, represent $p < 0.05$ using one-way ANOVA, Bonferroni corrected.

Bone resorption capacity of osteoclasts from mice of each genotype

To determine whether the osteoclasts from mice of each genotype differed functionally, bone resorption was measured from osteoclasts grown on dentin slices. This analysis was performed by our collaborator, Dr. Noriyoshi Kurihara at Indiana University. KO cultures produced functionally deficient osteoclasts which generated resorption lacunae totaling approximately one-third the area of WT cultures, while KI osteoclasts resorbed area in excess of two fold greater than WT cultures. In each instance, KO vs. WT. or KI vs. WT, the effect of p62 alteration had a more profound effect on osteoclast function than the effects on osteoclast number (Figure 2.6).

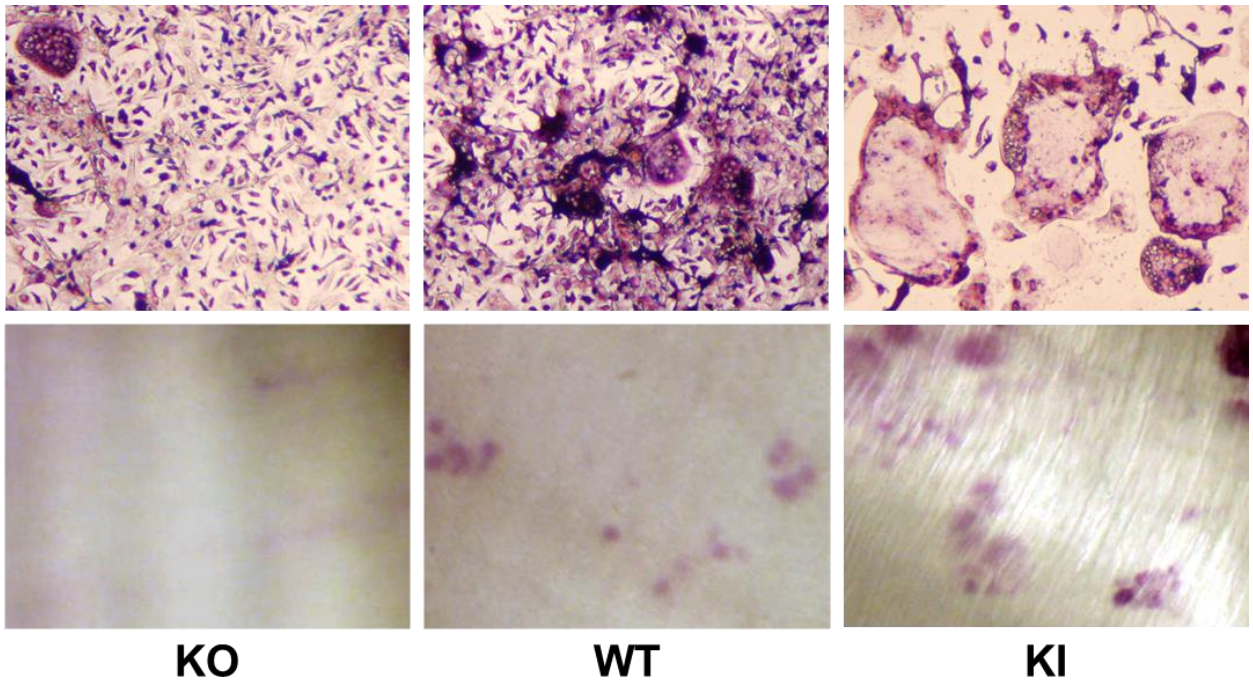

Figure 2.6. Effect of genotype on osteoclast formation and activity.

(Top panel) **Representative images of differentiated osteoclasts**. Bone marrow derived progenitors obtained from p62 –/– (KO), wildtype (WT), and p62 P394L (KI) mice were primed with M-CSF for two days then cultured in the presence of 20ng/mL M-CSF and 100 ng/mL RANKL for three days. Osteoclasts were fixed in 10% neutral buffered formalin and stained for tartrate resistant acid phosphatase (TRAP) activity. TRAP+ cells with 3+ nuclei were counted as osteoclasts. Bone resorption assays (bottom three panels) were performed by Dr. Noriyoshi Kurihara at Indiana University (IUPUI).

(Bottom panel) **Resorption lacunae formed by osteoclasts**. Bone marrow derived progenitors obtained from p62 –/– (KO), wildtype (WT), and p62 P394L (KI) mice were cultured on dentin slides in the presence of M-CSF and RANKL for 14 days. Cells were then removed and the dentin slices were stained with acid hematoxylin, photographed, and resorption area quantified using ImageJ software (Bottom panel).

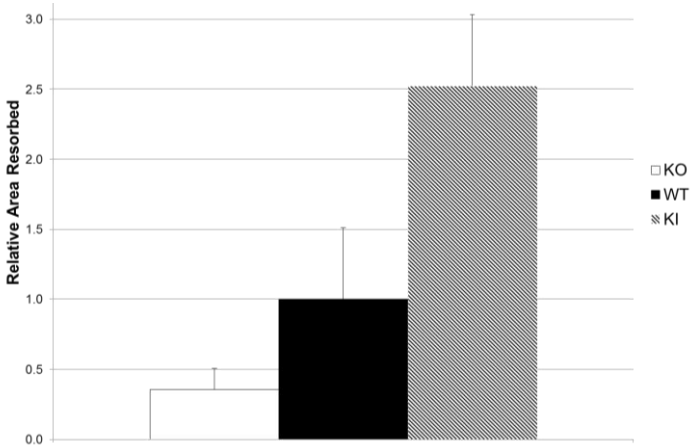

2.4 Discussion

Paget's disease is a common metabolic bone disease associated with exuberant osteoclast formation and activity (Roodman and Windle, 2005). Though its etiology has not been precisely delineated, it is commonly accepted that there are both environmental and genetic bases for the disease. In particular, over twenty independent case reports and epidemiological studies – conducted in North America, Europe and Australia – have demonstrated that mutation in the C-terminal ubiquitin-associated domain of p62 is very highly associated with Paget's disease (Ralston and Layfield, 2012; Chung and Van Hul, 2012). But what is known about the function of p62 during normal osteoclastogenesis, and how is its function perturbed by such mutations?

Some attempts to answer these questions have already been made. Specifically, mouse models in which p62 is genetically abrogated or mutated to match a common PDB-associated mutation were previously generated on separate genetic backgrounds and individually assessed histologically for a selection of bone structural and cellular phenotypes (Durán et al., 2004; Hiruma et al., 2008; Daroszewska et al., 2011).

In the present chapter we summarize a series of experiments in which we have united these mouse models onto a common genetic background, C57Bl/6J, to eliminate strain-dependent variance, and supplemented or re-configured previously conducted experiments on these mice to eliminate confounding effects of signaling intermediaries, increase confidence in cell autonomous effects of genetic manipulations, improve statistical power, and, ultimately, advance our understanding of p62's effect on bone structure and cellular function.

We may begin by noting that the genetic ablation of p62 resulted in no statistically appreciable differences in skeletal microarchitecture or cellular activity in year-old mice in the absence of

pharmacological intervention in vivo or cytokine stimulation in vitro, confirming results previously reported using eight-week old p62-/- mice (generated by a separate group, Durán et al., 2004) and extending them. This latter point is particular important. That is, the Moscat group, which had initially characterized the first p62-/- mouse in 2004, went on to demonstrate that p62-/- mice develop mature-onset obesity, systemic glucose intolerance, and insulin resistance (Rodriguez et al., 2006). They also intimated, but never published that p62-/- mice exhibit increased bone mineral density as they age, implying a possible osteopetrotic phenotype (Rodriguez et al., 2006). In the present study, we confirmed the mature-onset obesity phenotype in p62-/- mice, but found no statistically significant differences in bone volume from age and gender-matched wildtype mice.

In contrast, the P394L PDB-associated mutation of p62 resulted in a significant osteopenic phenotype under basal conditions, unlike previously reported results (Hiruma et al., 2008; Daroszewska et al., 2011). While it is possible that this result is strain dependent, we suspect that this discrepancy is better accounted for by the fact that we characterized older (12 to 14 months of age vs. 4 month old mice in Daroszewska et al., 2011) and greater numbers of mice (n = 9 KI and 10 WT vs. n = 4 KI and 3 WT in Hiruma et al., 2008) in the present study.

In terms of induced-osteoclastogenesis in vivo, our results confirm what has been previously published, i.e. that KO mice fail to mount an appropriate osteoclastogenic response to pharmacological induction, while removing a potential confounder. More specifically, previously published experiments used PTHrP (parathyroid hormone-related peptide) – a prohormone that acts only indirectly on cells of the osteoclast lineage – to demonstrate that induced osteoclastogenesis was impaired in p62-/- mice (Durán et al., 2004). PTHrP is natively produced by osteoblast progenitors and acts in a paracrine and autocrine manner through the PTHR1 receptor on (1) pre-osteoblasts to enhance their differentiation to mature, matrix-producing

osteoblasts, (2) reduce osteoblast and osteocyte apoptosis, and (3) increase production of RANKL in cells of this lineage (Martin, 2005). It might be argued that given that their p62-/- mouse was a global knock-out, the in vivo effects they demonstrated might, however unlikely, have emerged from an osteoblast-specific failure to up-regulate RANKL in response to PTHrP. To remove this confounding effect we utilized subcutaneous administration of TNF-α, a direct inducer of osteoclast formation (Kobayashi et al., J Exp Med. 2000) and demonstrated a failure to induce osteoclastogenesis in KO mice – a result that differed substantially from WT and KI mice.

These results were confirmed in vitro. Bone marrow derived progenitors from KO cultures failed to form osteoclasts as efficiently or as functionally active as WT cultures, confirming what had been previously published (Durán et al., 2004), while KI cultures formed robust, hyperactive osteoclasts, confirming previous results (Hiruma, et al., 2008; Daroszewska et al., 2011).

These results are significant for several reasons. First, p62-/- mice develop an obese phenotype that it is first evident at approximately 3 to 4 months of age. It has been further suggested that p62 plays a critical role in the activation of the RANK-TRAF6-NFκB signaling pathway (Durán et al., 2004). Yet genetic knock-out models of: (a) upstream intermediaries in this pathway, including RANKL, RANK, TRAF6, and (b) downstream targets such NFκB1 and NFκB2 (when knocked out simultaneously), among many others, have a pronounced osteopetrotic phenotype (Kong et al., Nature 1999; Dougall et al., Genes Dev 1999; Naito et al., Genes Cells 1999; Iotsova et al., Nature Med 1997). That the absence of p62 does not alter bone structure or activity, either before or after the development of this phenotype, suggests that either p62 plays a minor role in normal bone homeostasis – and, importantly, is likely not the key mediator of RANK-TRAF6 signaling during basal conditions – or that a sufficient number of compensatory pathways are active to mask the effects of its loss. On the other hand, clear impairment of induced-osteoclastogenesis is evident,

both in vivo and in vitro. That our KI mice exhibit a phenotype very similar to knock-out models of competitive inhibitors of the NFκB pathway, such as OPG (Bucky et al., Genes Dev, 1998) or feedback inhibitors such as CYLD (Jin et al., 2008) – i.e. a demonstrable osteoporotic phenotype – strengthens the hypothesis that PDB-associated mutations result in a true physiologic gain of osteoclast function.

To summarize, we have united two important mouse models aimed at elucidating the role of p62 in osteoclastogenesis and Paget's disease of bone on a common C57bl/6J background, and characterized the effects of mutation at the p62 locus in vivo and in vitro. Taken together, the results of this study beget several important questions. Does p62 play an important role in physiologic RANK-TRAF6 signaling or not? Does mutation at the UBA domain amplify NFκB signaling, and if so what is the mechanism? Given p62's multiple domains, what alternative pathways might be account for these phenotypes, if any? It is to these questions that we now turn in the following chapter.

CHAPTER 3

A GLOBAL INVESTIGATION INTO THE MECHANISMS BY WHICH p62 MEDIATES OSTEOCLASTOGENESIS

3.1 Introduction

In the preceding chapter, we focused on defining the phenotypes of two important mouse models generated to help elucidate the role played by the multifunctional adaptor protein p62 during osteoclastogenesis and in the pathophysiology of Paget's disease of bone (PDB). These models – in which p62 was genetically ablated (p62-/- or KO) or mutated (p62 P394L or KI) to match a common mutation found in familial PDB patients – were backcrossed onto a common genetic background, C57Bl/6J. Isolated bones were then subjected to careful histomorphometric measurements, and bone marrow derived osteoclast precursors were characterized in vitro.

Experiments conducted on p62-/- mice suggest that p62 is dispensable for in vivo basal osteoclast formation, absent any external stimuli or cytokines. At the same time, osteoclastogenesis induced by any of the cytokines tested or published – TNF-α, PTHrP, or RANKL – appears to be significantly impaired in these mice and their cells, which suggests that p62 may yet play an important role in induced osteoclast differentiation and activation.

Bones from p62 P394L mutant mice, on the other hand, reveal an osteopenic phenotype under basal conditions, with increased trabecular spacing, and decreased bone volume and trabecular number. Although impaired osteoblast function cannot be ruled out as a possible explanation, subsequent experiments in which the cytokine-induced response was characterized suggest that overly exuberant osteoclastogenesis plays an important role in this process. These results further strengthen the notion that p62 plays a complex mediatory role during osteoclastogenesis and that the mechanisms underlying this regulation merit further investigation.

While several hypotheses have been proposed to explain this role, the one that has gained the broadest acceptance asserts that p62 forms a complex with TRAF6 to integrate and transduce RANKL signaling, leading to the degradation of the NFκB inhibitor, IκB, and the nuclear translocation and activation of NFκB (Figure 3.1). In chapter one, we elaborated on the lines of evidence linking p62 to the positive regulation of TRAF6 signaling and how this may pertain to osteoclastogenesis (Figure 1.6). We return to this discussion now, investigating its experimental bases more closely.

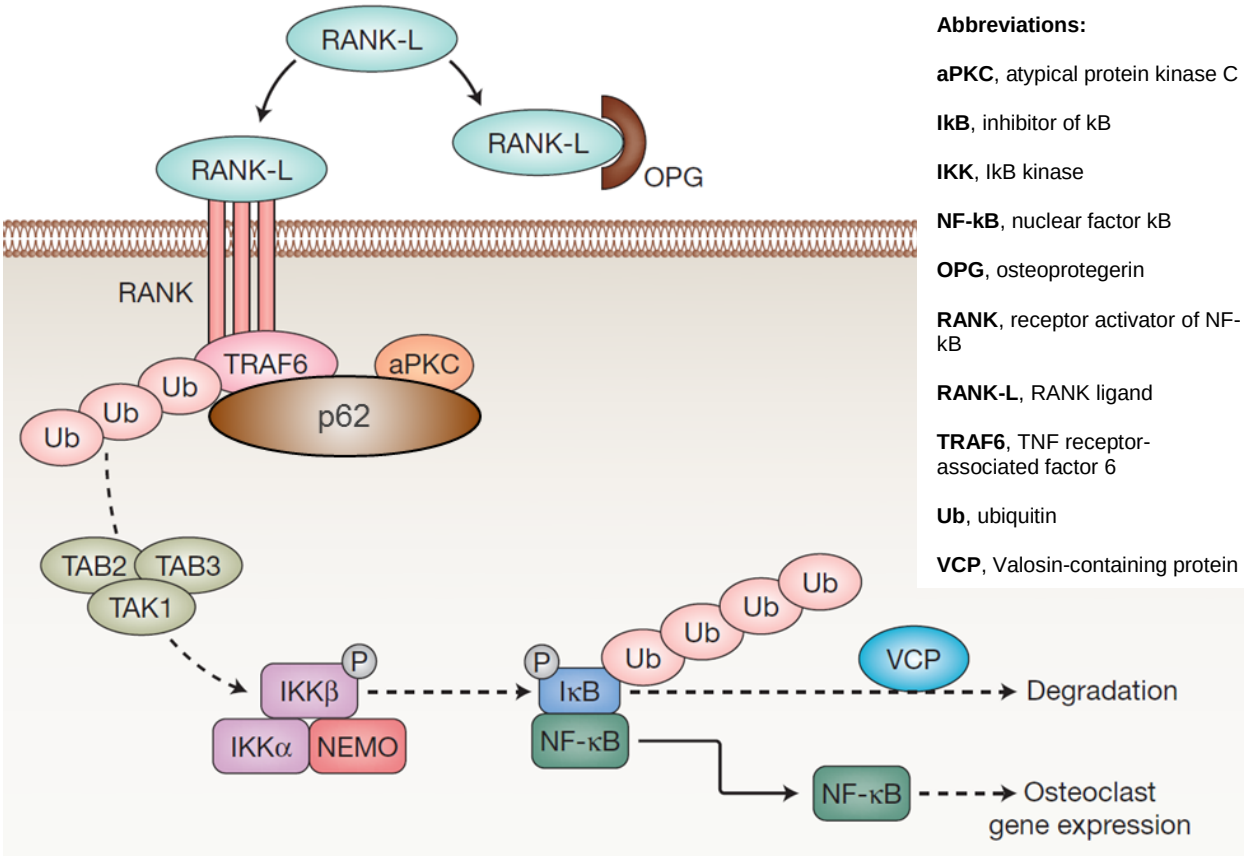

Figure 3.1. Overview of the RANK-TRAF6-p62-NFκB signaling pathway hypothesis.

RANKL binds to its receptor RANK in an interaction antagonized by OPG. On receptor stimulation, TRAF6 associates with RANK, and p62 with TRAF6. Lys63-linked autoubiquitination of TRAF6 is catalyzed by its intrinsic E3 ubiquitin ligase activity. Through its N-terminal PB1 domain p62 binds aPKC, stimulating the activation of IκB kinaseß (IKKß) as does activation of the TAB1-TAB2-TAK1 complex by binding ubiquitinated TRAF6. Phosphorylation of IκB by the activated IKKß complex, and subsequent Lys48-linked polyubiquitination, leads to 26S proteasomal degradation of IκB, permitting NFκB to enter the nucleus and activate target gene expression. Adapted from Layfield, The molecular pathogenesis of Paget disease of bone, Expert Rev Mol Med. 2007 Oct 1;9(27):1-13.

As noted earlier, Durán and colleagues provided the first evidence that p62 plays a role in induced osteoclastogenesis by: (a) demonstrating that p62 is up-regulated and remains elevated during RANKL-mediated osteoclast formation, (b) generating p62-/- mice, that despite being histomorphologically indistinguishable from wildtype mice at 6-8 weeks of age under basal conditions, demonstrated significantly decreased osteoclast formation and increased bone volume in response to PTHrP, and (c) culturing p62-/- osteoclast progenitors that demonstrated inefficient up-regulation of NFATc1 and poor responsiveness to M-CSF and RANKL (Durán et al., 2004). Durán and colleagues proposed a model in which p62-/- mice are unable to form a critical signaling complex involving TRAF6, p62, and aPKC, which results in impaired NFκB signaling, supported by the following evidence (Figure 4, Durán et al., 2004).

Experimentally, the authors observed that nuclear NFκB-DNA binding, as measured by EMSA, was diminished in the absence of p62, not upon initial stimulation with M-CSF and RANKL, but only after a period of days. To explain this, they reasoned that p62 contributes to this signaling pathway only later in the cycle of RANKL-mediated differentiation, during which p62 is itself up-regulated. Next, they observed changes in another surrogate for NFκB activity, phosphorylated-IκB (which is phosphorylated, then ubiquitinated and degraded via the 26S proteasome). P- IκB levels were found to be diminished in KO cells after 6 days of RANKL treatment compared to WT cells. The authors explained that this finding may be have been due to deficient formation of a complex between TRAF6 and p62, which co-precipitated within 10 minutes of RANKL treatment, and between p62 and the atypical protein kinase C member, aPKCζ, which co-precipitated after 6 days of RANKL treatment. The relevance of this potential pathway is unclear, however, for as the authors point out "aPKCζ-/- BMDMs do not have osteoclastogenic defects" (Durán et al., 2004; Leitges et al., 2001).

With respect to Paget's disease of bone, the authors next provided the first evidence that PDB-associated mutations enhance NFκB signaling by transfecting 293 cells with either wildtype or P392L mutant expression vectors and a κB dependent reporter and assessing for luciferase activity. Interestingly, they observed that NFκB transcriptional activity was twice as high in cells in which mutant p62 was overexpressed compared to those in which wildtype p62 was overexpressed (Figure S1, Durán et al., 2004). Notbaly, this experiment has since served as the archetype for at least five subsequent published analyses that link PDB-associated mutations to enhanced NFκB signaling.

In 2006, for example, Yip and colleagues transiently transfected RAW264.7 cells stably expressing p62-WT, p62-UBA domain mutant (p62-ΔUBA), or pcDNA3.1 control with an NFκB luciferase reporter for 24 hours, then stimulated cells with 100 ng/ml of RANKL for 10 and 40 hours, before harvesting them and measuring luciferase activity. Interestingly, NFκB transcriptional activity peaked at 10 hours, then fell back to near unstimulated levels at 40 hours, in cells of all 3 groups (Figure 5A, Yip et al., 2006). Here, overexpression of wildtype p62 was associated with persistent, significant decreases in NFκB transcriptional activity in response to RANKL compared to control from the outset. Moreover, ectopic expression of p62-ΔUBA domain mutant protein appears to have suppressed this inhibition and even enhanced NFκB transcriptional activity compared to control in response to RANKL (Yip et al., 2006).

Using a similar model, reports in 2006 and 2009 demonstrated that ectopic expression of wildtype p62 impaired NFκB transcriptional activity compared to control, whereas overexpression of 4 different PDB-associated mutations (K378X, P392L, E396X in one study; P364S, K378X, P392L in the other) each individually only partially suppressed this inhibition compared to control after 24 hours of treatment (Figure 3, Rea et al., 2006; Figure 6, Rea et al., 2009). These findings were

corroborated in a similar manner by Najat and colleagues for a different mutant (A381) that exerts only nominal effects on ubiquitin binding (Figure 6, Najat et al., 2008, not included) and by Wright and associates in the absence of RANKL stimulation in known UBA domain mutants, E396X and G425R, but not for a non-UBA domain mutant, S349T (Figure 1, Wright et al., 2013).

Finally, in an underappreciated report published in 2009, Chamoux and associates used immunofluorescence and Western blot to probe the association between NFκB transcriptional activity and p62. In human osteoclasts that were either left un-transfected or transfected with empty vector, they demonstrated: (a) that p50 (an NFκB subunit) was detectable both in the cytoplasm and nucleus under basal conditions, (b) that p50 aggregated exclusively in the nucleus after 30 minutes of RANKL stimulation, and (c) that IκB (NFκB's inhibitor) levels fell at approximately 15 minutes of RANKL stimulation. In contrast, in human osteoclasts overexpressing wildtype p62, p50 levels were "barely detectable before or after stimulation" and these cells had significantly lower levels of IκB that dropped even further with stimulation. Finally, osteoclasts overexpressing the PDB-associated P392L p62 mutant demonstrated high levels of nuclear p50 staining and IκB under basal conditions, both of which remained essentially unchanged after RANKL stimulation (Figure 8, Chamoux et al., 2009).

To summarize, a pioneering early study demonstrated that ablation of p62 was associated with diminished NFκB-DNA binding only after 24 hours or more of RANKL stimulation, and that overexpression of a common PDB-associated mutant resulted in increased NFκB transcriptional activity compared to wildtype (Durán et al., 2004). In contrast, several subsequent studies have demonstrated that ectopic expression of: (a) wildtype p62 is associated with inhibited NFκB transcriptional activity compared to control, (b) most PDB-associated p62 mutants suppress this inhibition back to control levels or higher, and (c) that this inhibition (and suppression of

inhibition) may be detected in the absence of RANKL treatment, or in its presence after 4, 10, 24 and even 40 hours (Yip et al., 2006; Rea et al., 2006; Najat et al., 2008; Rea et al., 2009; Wright et al., 2013). Discrepancies in these results raise significant questions. Is p62 required for NFκB transcriptional activity in differentiating osteoclasts or not? What are the kinetics of this regulation? Why is overexpression of wildtype p62 associated with impaired NFκB transcriptional activity in so many models? Are additional binding partners required to mediate this inhibition? Finally, are models in which p62 is overexpressed appropriate for drawing conclusions about what occurs physiologically? On this last question, we maintain that results in at least one study cast some doubt on the suitability of these models, suggesting that overexpression of p62 or PDB-associated mutants may alter NFκB signaling in a non-physiologic manner (Chamoux et al., 2009).

Taken together with additional hypotheses proposed to explain p62's role in osteoclastogenesis outside of the NFκB narrative – including preferential activation of downstream kinases (Hiruma et al., 2008), autophagy (Daroszewska et al., 2011), and or the KEAP1/NRF2 antioxidant response (Wright et al., 2013) – these gaps in our knowledge have prompted the present study.

In this chapter, we describe our efforts to assess the mechanisms by which p62 regulates osteoclastogenesis in an unbiased and global manner. Specifically, we employed gene expression profiling via DNA Microarray paired with commercial and open source pathway analysis tools to identify critical transcriptional regulators and signaling pathways that are activated and repressed during RANKL-mediated osteoclastogenesis and determine how these are altered, both qualitatively and quantitatively, when p62 is knocked-out or mutated as in PDB.

3.2 Methods

Mouse colonies and genotyping

First, we established independent colonies of p62-/- (KO), p62 P394L/P394L (KI), and wildtype (WT) controls, with our loci of interest backcrossed onto the C57Bl/6J background for at least 6 generations to generate congenic strains, as detailed in chapter two. Mouse tail DNA was used for genotyping by PCR. KI mice were genotyped using a pair of primers that flank the introduced loxP site: sense (exon 7): 5`-ACT CCA GTC TCT ACA GAT GCC AG-3` and antisense (intron 7): 5`-GTT GCC AAG ACT AGA CAG GAC AGG-3`, yielding a product of 182 bp for the WT allele and 226 for the p62-P394L KI allele. KO mice were genotyped using the following primers: p62 (1822-1845): GCT AAC AAA ATG AAG CCA GAT GGG, p62 (2222-2199): GCC TGG CAT CTA AGT TGT TCT GAG, and PGK (353-332): CTGA GCC CAG AAA GCG AAG GAG, yielding a product of 401 bp for the WT allele and 583 bp for the p62 -/- allele.

Microarray pipeline

Next, we harvested hindlimbs from each of 6 age and gender-matched mice (mean age of each group: 4 months; range: 3 to 7 months) for each of the 3 aforementioned genotypes, KO, WT, and KI. Hindlimbs were flushed of bone marrow, red blood cells were lysed (ACK buffer), and remaining cells were resuspended in conditioning media (α-MEM supplemented with 10% Gemcell FBS + 1% antibiotic), and cultured overnight (37°C, 5% CO_2) to select for non-adherent hematopoietic precursors.

On the following day, cells were pooled by genotype then subjected to magnetic antibody cell sorting (MACS, Miltenyi) to enrich cell populations for CD11b+ osteoclast precursors of the monocyte lineage. To generate osteoclast precursors, cells were re-suspended in conditioning media supplemented with macrophage colony stimulating factor (M-CSF, 20ng/mL) and split into six 60mm plates at a concentration of 3 x 10^6 cell/mL (Cellometer) and volume of 4 mL/plate. This yielded a total of 6 plates per genotype (n = 3 experimental replicates and n = 3 control replicates).

Two days later, floating cells were discarded, and a fresh bolus of 20ng/mL M-CSF in conditioning media was added, followed 12 hours later by the addition of a 100ng/mL bolus of RANK-ligand (the primary osteoclastogenic cytokine, receptor activator of NFκB ligand or RANKL) or volume equivalent vehicle control, as appropriate. Cells were placed back into the incubator for 8 hours, at the end of which total RNA from each plate was obtained using Trizol (Invitrogen). The resulting 18 vials of Trizol + cells were frozen at -80°C and submitted to the VCU Molecular Diagnostics Core for RNA purification, reverse transcription, processing, hybridization and scanning on the Affymetrix genechip platform (Mouse genome 430A 2.0 array, Affymetrix).

In this manner, each replicate came from a separate pool of cells that were biologically related, but not identical. The Molecular Diagnostics Core then generated RNA quality control measures and raw .CEL files for each of the 18 scanned arrays, and submitted them to the Windle lab for data processing and analysis as described below (Figure 3.2).

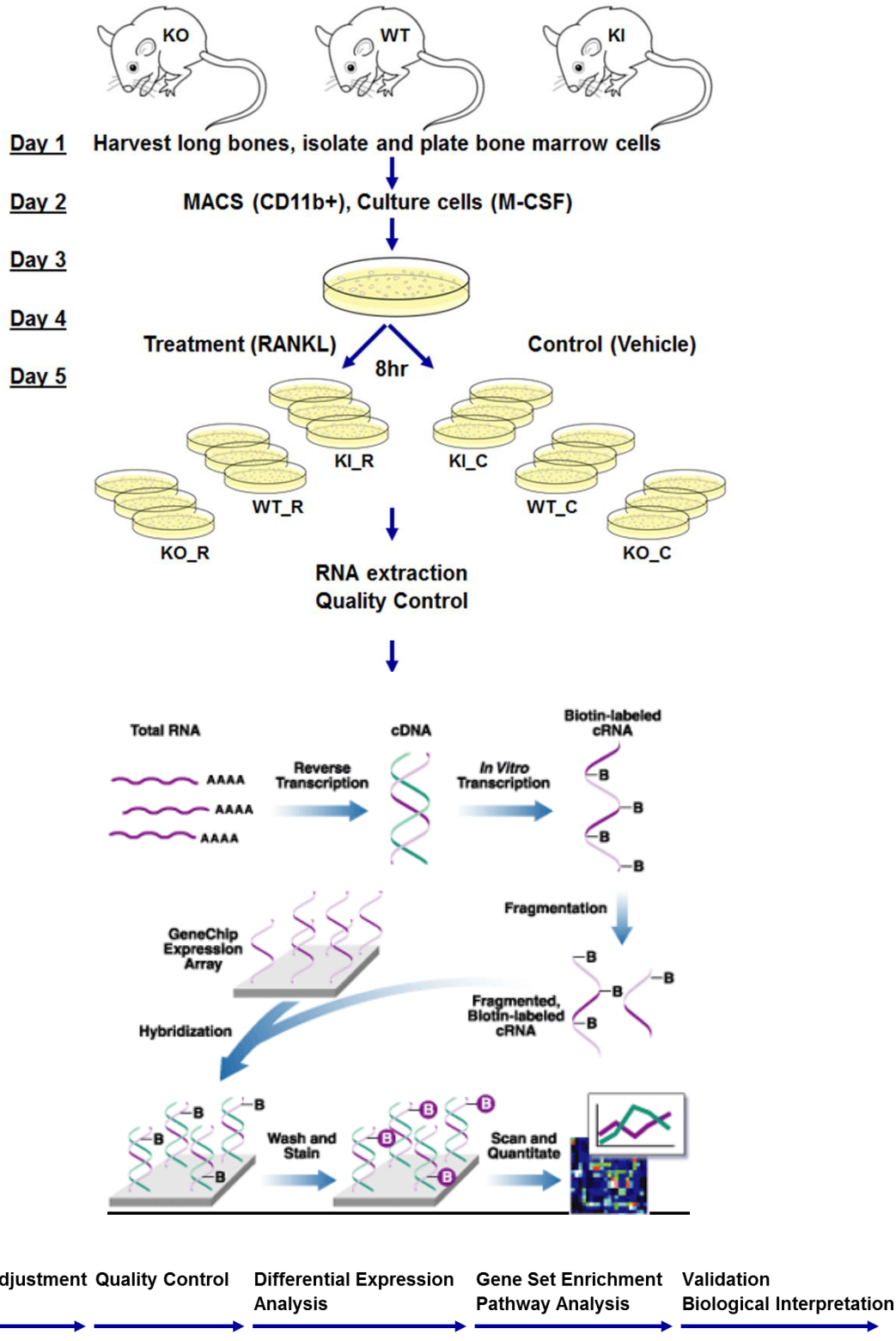

Figure 3.2. Pipeline for microarray experiment. Abbreviations: WT, wildtype; KO, p62 -/-; KI, p62 P394L; C, control; R, RANKL treated; 1, 2, 3 replicate arrays.

Pre and post-processing, volcano plots, and threshold selection

The Affymetrix Mouse genome 430A 2.0 genechip is a single array that contains over 22,600 probe sets representing transcripts from approximately 14,000 mouse genes. For each of these probe sets, 11 pairs of oligonucleotide probes are used to measure the transcription level of each sequence on the array. Each of these probes consists of 25-mers that are perfect matches for target mRNA sequences.

The treated and untreated RNA samples we generated were subjected to the Affymetrix pipeline by the VCU Molecular Diagnostics Core facility. RNA was initially reverse transcribed to cDNA, then in vitro transcribed into cRNA, which was fragmented, biotin-labeled, and washed over the Affy chip, facilitating cRNA-oligo hybridization. Areas of increased hybridization accumulate biotinylated cRNA, which was then bound by a fluorescent dye in the next wash over the genechip. Subsequent fluorescent scan of the chip provided a fluorescence value for each probe that is directly related to specifically hybridized cRNA abundance. From this scan we infer the relative abundance of specific mRNA sequences, and thereby obtain a snapshot of the transcriptome – and in the case of our experiment, how the transcriptome of osteoclast progenitors changes with p62 genotype and RANKL treatment.

To summarize the probes into a probe set, deal with the various sources of noise (e.g. non-specific binding of cRNA to probes, processing effects such as deposits left after wash stages, or optical noise from the scanner) and technical variation (e.g. due to slight discrepancies between hybridization length, sample volume, or other processes for each array that lead to scaling differences between fluorescence intensity levels), we made use of the gcRMA algorithm as implemented on the Bioconductor software package in the R statistical programming environment.

The primary comparisons made in the present study were mean intensity data for RANKL-treated cells normalized by intensity of vehicle control treated cells, by genotype. Log2 transformed data were filtered for present-marginal-absent calls (only probe sets for which 3 of 3 replicates were present were retained), and pairwise p-values and real-space fold changes were calculated using two-tailed t-tests via Microsoft Excel. To correct for multiple hypothesis testing in our large data sets, we used the C++ program QVALITY to calculate the false discovery rate, q, which corresponds to the probability that a given observation is drawn from the null distribution (Kall et al., 2009). Next we performed a preliminary visualization of our data using volcano plots, in which biological fold change data (fc) between RANKL and vehicle treated samples is plotted on the x-axis against the false discovery rate (q) on the y-axis for all three genotypes. This facilitated a broad view of the data and provided a sense of the extent to which setting different cut-offs for further analysis (by these surrogates for biological and statistical significance, respectively) would capture or lose important blocks of data.

After examining multiple thresholds for significance in fold change data and false discovery rates, we set thresholds at $fc \geq 1.3$ and $q \leq 0.11$, respectively. These appear, at face value, to be relatively relaxed criteria. We reasoned, however, that there may be constellations of genes that while only altered modestly individually, can, in aggregate, produce significant biological effects.

Estimation of data quality before and after processing, hybridization, and analysis

Microarray technology provides a powerful tool for defining gene expression profiles in many physiological and pathophysiological conditions. Yet our conviction for the validity of these profiles and confidence in their biological interpretation are tempered by the fact that many sources of variation and bias, or noise, can obscure true effects, or signal. To quantify confidence in microarray results, and if need be, repeat experiments, several quality control measures were quantified using the arrayQualityMetrics Bioconductor package in the R programming environment. In the present experiment neither pre-processing errors, such as RNA contamination or degradation, nor concurrent errors, such as unacceptably low efficiency in amplification, reverse transcription, or hybridization, were problematic in control or RANKL-treated samples (Figures 3.3, 3.4). Moreover, there is strong evidence that the individual arrays cluster by both experimental genotype and treatment with RANKL or vehicle, strongly suggesting that the experimental effects are much larger than any noise in the experiment. More specifically, in a heatmap showing relative distance between normalized arrays (Figure 3.5), no single array was found in which the sum of distances to all other arrays was beyond the 95% confidence interval of the distribution of the sums for all arrays (i.e. there were no outliers). As a final quality control measure, we investigated the signal intensity distributions of our normalized arrays, and observed that there were no outliers using the Kolmogorov-Smirnov test between each array's distribution and the distribution of the pooled arrays (Figure 3.6).

Taken together, these results indicate that sources of noise were relatively minimal in our experiment, while the experimental effects of both genotype and treatment were comparatively large and distinct.

#	Name/Levels	Sample	Initial Level No.	260/280	260/270	[ ]1	28S/18S	% of rRNA	[ ]2	Sample Quality Control (QC)	RIN
42	KI_C1			2.1	1.3	0.65	2.0	67.4	0.73	PASS QC	10.0
43	KI_C2			2.1	1.3	0.54	2.0	60.6	0.50	PASS QC	10.0
44	KI_C3			2.1	1.2	0.78	2.2	74.6	0.74	PASS QC	10.0
45	WT_C1			2.1	1.2	0.51	2.1	58.5	0.59	PASS QC	9.9
46	WT_C2			2.1	1.2	0.38	2.3	66.1	0.38	PASS QC	9.9
47	WT_C3			2.1	1.2	0.57	2.3	56.2	0.73	PASS QC	9.9
48	KO_C1			2.1	1.3	0.49	2.0	61.7	0.50	PASS QC	10.0
49	KO_C2			2.1	1.2	0.55	2.1	63.2	0.58	PASS QC	10.0
50	KO_C3			2.1	1.3	0.55	2.3	59.7	0.57	PASS QC	10.0

#	Name/Levels	%DNA	YIELD		µg input RNA	cDNA Size Dist.	IVT 260/280	IVT yield	cRNA Size Dist.	Synthesis QC (Pre-Hybridization)
42	KI_C1	0.00	7.9	SUFFICIENT	0.5	N/A	2.0	145.5	PASS QC	PASS QC
43	KI_C2	0.00	6.5	SUFFICIENT	0.5	N/A	2.0	109.3	PASS QC	PASS QC
44	KI_C3	0.00	9.3	SUFFICIENT	0.5	N/A	2.0	106.7	PASS QC	PASS QC
45	WT_C1	0.00	6.2	SUFFICIENT	0.5	N/A	2.0	137.1	PASS QC	PASS QC
46	WT_C2	0.00	4.5	SUFFICIENT	0.5	N/A	2.0	112.2	PASS QC	PASS QC
47	WT_C3	0.00	6.9	SUFFICIENT	0.5	N/A	2.0	118.6	PASS QC	PASS QC
48	KO_C1	0.00	5.9	SUFFICIENT	0.5	N/A	2.0	101.6	PASS QC	PASS QC
49	KO_C2	0.00	6.6	SUFFICIENT	0.5	N/A	2.0	102.8	PASS QC	PASS QC
50	KO_C3	0.00	6.6	SUFFICIENT	0.5	N/A	2.0	103.6	PASS QC	PASS QC

Alias*	Name/Levels	Noise (RawQ)	SF	Bkgd (Avg)	TGT Value	% Present	GAPDH (3'/5')	β-actin (3'/5')	Hybridization QC	PolyA Spike Ctrls 3'/5'	Overall QC (Post-Hybridization)
JW42	KI_C1	1.210	0.376	37.53	100	56.7	0.77	1.38	PASS QC	4.59±3.84	PASS QC
JW43	KI_C2	1.400	0.399	48.25	100	56.5	0.81	1.30	PASS QC	3.59±2.62	PASS QC
JW44	KI_C3	1.290	0.408	42.67	100	55.9	0.81	1.26	PASS QC	3.91±2.96	PASS QC
JW45	WT_C1	1.490	0.331	51.95	100	58.4	0.87	1.43	PASS QC	3.94±2.48	PASS QC
JW46	WT_C2	1.420	0.307	46.96	100	58.9	0.85	1.39	PASS QC	4.95±4.29	PASS QC
JW47	WT_C3	1.390	0.327	44.89	100	59.1	0.87	1.35	PASS QC	4.49±3.6	PASS QC
JW48	KO_C1	1.410	0.331	46.37	100	58.6	0.80	1.42	PASS QC	4.6±3.95	PASS QC
JW49	KO_C2	1.470	0.283	47.92	100	58.9	0.80	1.36	PASS QC	4.46±3.85	PASS QC
JW50	KO_C3	1.370	0.343	44.53	100	58.0	0.78	1.39	PASS QC	4.86±4.39	PASS QC

*Make sure the Alias matches the Report file name

Run performed by: TBB (Initials)

Run reviewed by: Catherine Dumur, Ph.D. Date: 11/7/2011

Figure 3.3a. Quality control measures for control (non-RANKL treated) data.
Abbreviations: WT, wildtype; KO, p62 -/-; KI, p62 P394L; C, control; 1, 2, 3 replicate arrays.

#	Name/Levels	Sample	Initial Level No.	260/280	260/270	[ ]1	28S/18S	% of rRNA	[ ]2	Sample Quality Control (QC)	RIN
54	KI_R1			2.1	1.2	0.69	2.2	56.8	0.81	PASS QC	9.8
55	KI_R2			2.1	1.2	0.78	2.3	74.0	0.86	PASS QC	10.0
56	KI_R3			2.2	1.3	0.68	2.0	65.8	0.70	PASS QC	10.0
57	WT_R1			2.1	1.2	0.57	2.3	66.2	0.56	PASS QC	10.0
58	WT_R2			2.1	1.2	0.46	2.2	66.1	0.48	PASS QC	10.0
59	WT_R3			2.1	1.2	0.65	2.4	64.1	0.55	PASS QC	9.9
60	KO_R1			2.1	1.2	0.68	2.2	59.0	0.71	PASS QC	9.9
61	KO_R2			2.1	1.2	0.70	2.3	60.7	0.73	PASS QC	9.7
62	KO_R3			2.1	1.2	0.93	2.4	71.0	0.95	PASS QC	10.0

#	Name/Levels	%DNA	YIELD		µg input RNA	cDNA Size Dist.	IVT 260/280	IVT yield	cRNA Size Dist.	Synthesis QC (Pre-Hybridization)
54	KI_R1	0.00	8.3	SUFFICIENT	0.5	N/A	2.0	160.5	PASS QC	PASS QC
55	KI_R2	0.00	9.4	SUFFICIENT	0.5	N/A	2.0	121.2	PASS QC	PASS QC
56	KI_R3	0.00	8.2	SUFFICIENT	0.5	N/A	2.0	119.4	PASS QC	PASS QC
57	WT_R1	0.00	6.8	SUFFICIENT	0.5	N/A	2.0	128.7	PASS QC	PASS QC
58	WT_R2	0.00	5.5	SUFFICIENT	0.5	N/A	2.0	133.6	PASS QC	PASS QC
59	WT_R3	0.00	7.8	SUFFICIENT	0.5	N/A	2.0	107.7	PASS QC	PASS QC
60	KO_R1	0.00	8.2	SUFFICIENT	0.5	N/A	2.0	98.6	PASS QC	PASS QC
61	KO_R2	0.00	8.4	SUFFICIENT	0.5	N/A	2.0	90.4	PASS QC	PASS QC
62	KO_R3	0.00	11.2	SUFFICIENT	0.5	N/A	2.0	100.6	PASS QC	PASS QC

Alias*	Name/Levels	Noise (RawQ)	SF	Bkgd (Avg)	TGT Value	% Present	GAPDH (3'/5')	β-actin (3'/5')	Hybridization QC	PolyA Spike Ctrls 3'/5'	Overall QC (Post-Hybridization)
JW54	KI_R1	1.050	0.460	35.40	100	57.1	0.77	1.36	PASS QC	3.85±3.43	PASS QC
JW55	KI_R2	1.240	0.362	40.77	100	58.1	0.76	1.24	PASS QC	3.75±3.01	PASS QC
JW56	KI_R3	1.170	0.408	38.90	100	57.3	0.78	1.34	PASS QC	3.71±3.1	PASS QC
JW57	WT_R1	1.300	0.328	44.72	100	59.2	0.79	1.30	PASS QC	3.63±2.78	PASS QC
JW58	WT_R2	1.290	0.301	42.94	100	60.1	0.83	1.29	PASS QC	3.78±2.82	PASS QC
JW59	WT_R3	1.220	0.361	41.00	100	58.8	0.87	1.30	PASS QC	4.15±3.39	PASS QC
JW60	KO_R1	1.310	0.370	43.99	100	57.9	0.81	1.35	PASS QC	3.82±2.84	PASS QC
JW61	KO_R2	1.290	0.347	42.69	100	57.6	0.79	1.33	PASS QC	4.06±3.29	PASS QC
JW62	KO_R3	1.340	0.343	43.36	100	57.6	0.77	1.37	PASS QC	4.1±3.48	PASS QC

*Make sure the Alias matches the Report file name

Run performed by: TBB (Initials)

Run reviewed by: Catherine Dumur, Ph.D. Date: 11/7/2011

Figure 3.3b. Quality control measures for RANKL-treated data.
Abbreviations: WT, wildtype; KO, p62 -/-; KI, p62 P394L; R, RANKL treated; 1, 2, 3 replicate arrays.

Figure 3.4. General quality control measures.

(Left panel) **RNA degradation plot.** This plot demonstrates the intensity trend over the probes of each probeset, ordered from the 5` to 3` ends of the gene. Probesets are averaged to produce a single 5` to 3` trendline for each array. Affymetrix arrays are 3` biased, so it is expected that the RNA will show degradation and therefore less hybridization towards the 5` end of the probeset. As such, a positive slope is normal. An aberrant slope for a single array or arrays could indicate that RNA was degraded or otherwise mishandled, but there is no evidence of this in our samples.

(Right panel) **Scaling factors and housekeeping genes.** Different chips are separated by horizontal grey lines in the plot. The numbers on the left report the number of probesets with present flag, and the average background on the chip. The blue region in the middle denotes the area where scaling factors are less than 3-fold of the mean scale factors of all chips. Bars that end with a point denote scaling factors for the chips. The triangles denote beta-actin 3`:5` ratio, and open circles are GAPDH 3`:5` ratios. If the scaling factors or ratios fall within the 3-fold region (1.25-fold for GAPDH), they are colored blue, otherwise they are colored red and the deviant chips are therefore easy to select (by their red coloring). Here, all scaling factors and housekeeping genes are within the acceptable range.

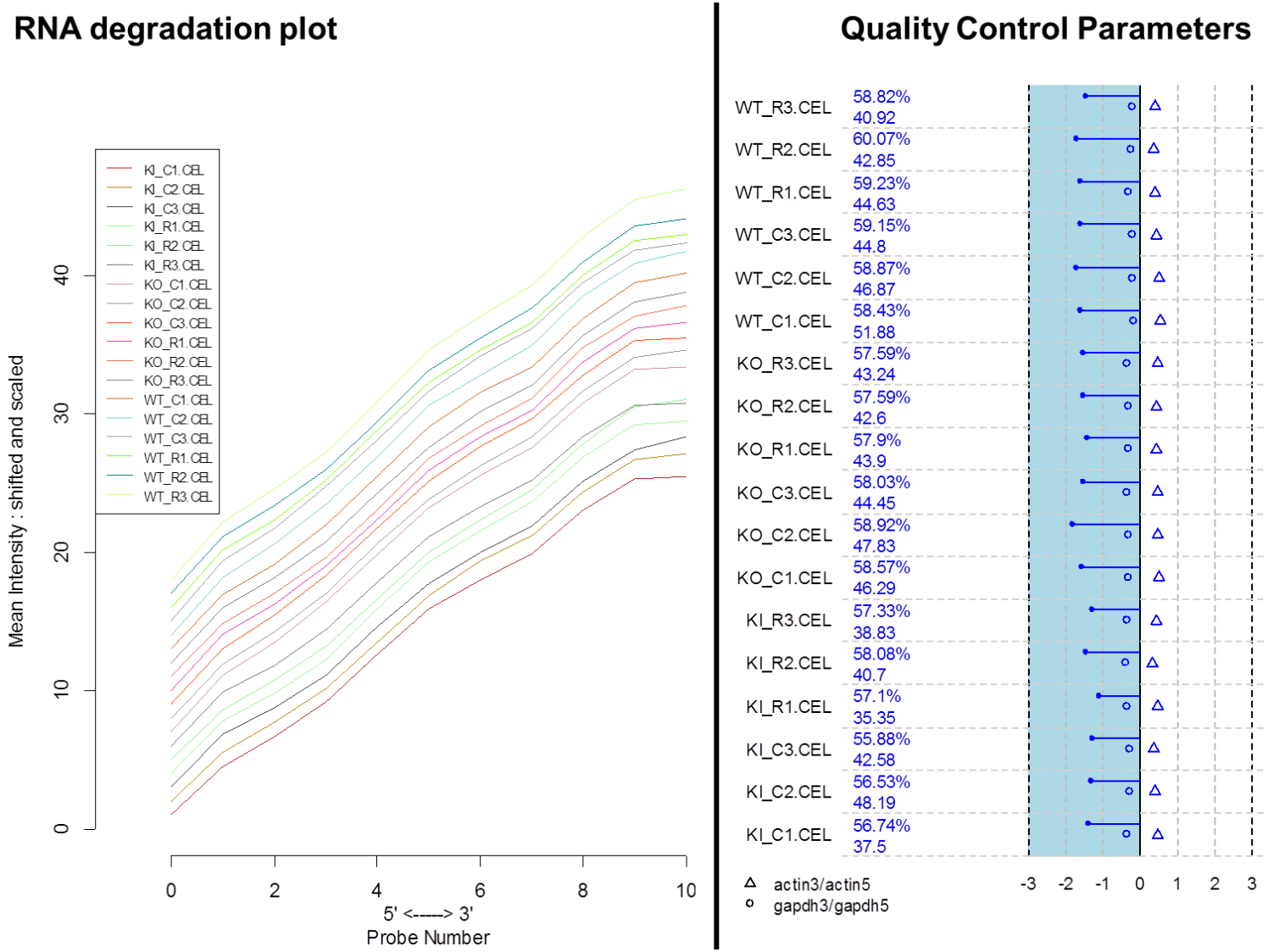

Figure 3.4. General quality control measures.
Abbreviations: WT, wildtype; KO, p62 -/-; KI, p62 P394L; C, control; R, RANKL treated; 1, 2, 3 replicate arrays.

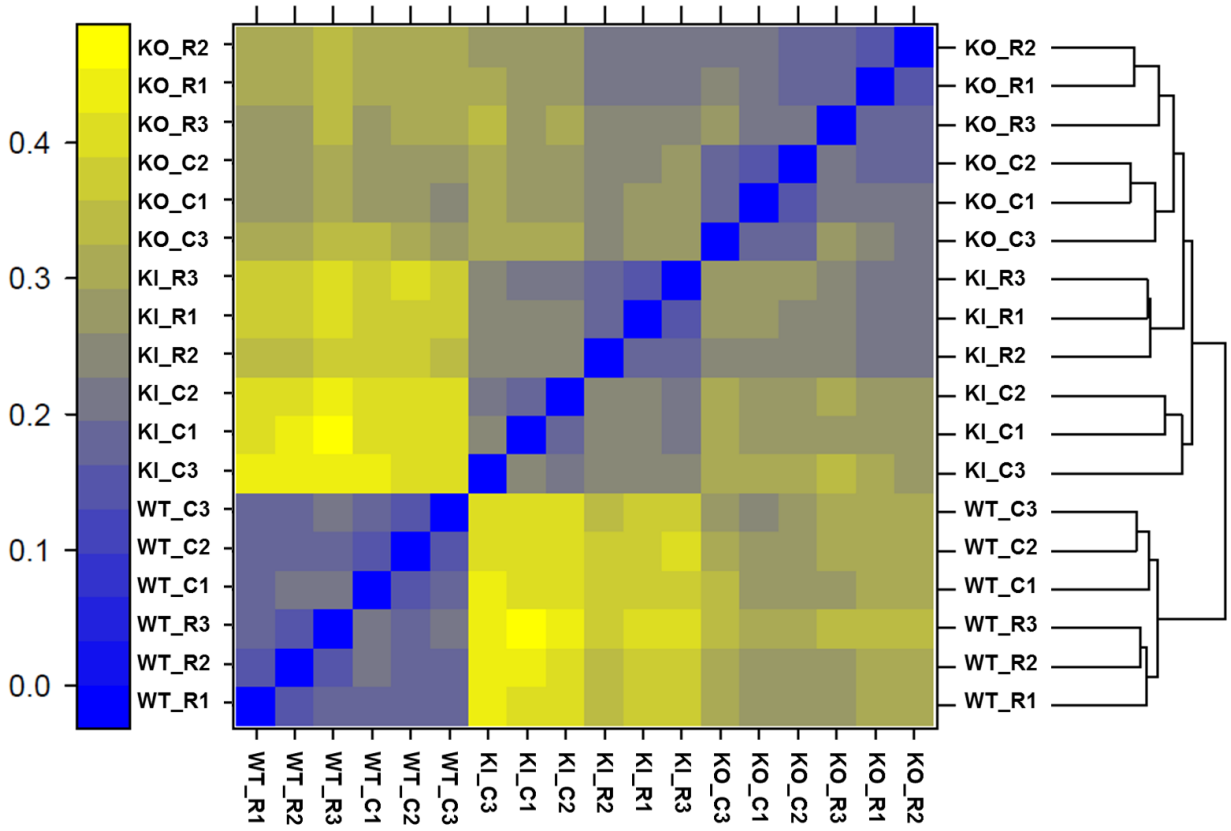

Figure 3.5. Between-array sample heatmap.

Patterns in this plot indicate clustering of the arrays by the biological experimental factors (genotype and treatment). The distance, d_{ab}, between two arrays a and b, for example, is computed as the mean absolute difference (L1-distance) between the data of the arrays (using the data from all probes without filtering). Outlier detection was performed by looking for arrays for which the sum of the distances to all other arrays, Sa = Σb dab was exceptionally large. No such array outliers were detected in this dataset. Abbreviations: WT, wildtype; KO, p62 -/-; KI, p62 P394L; C, control; R, RANKL treated; 1, 2, 3 replicate arrays.

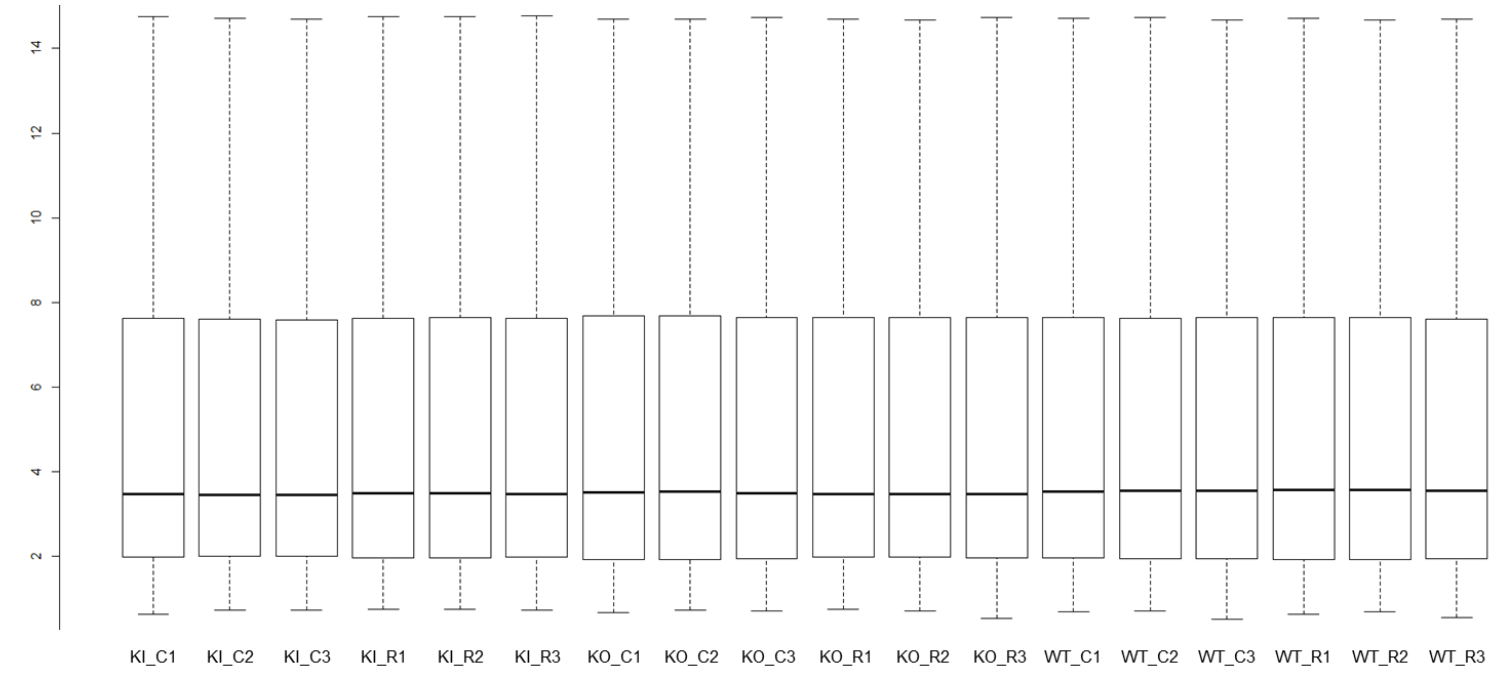

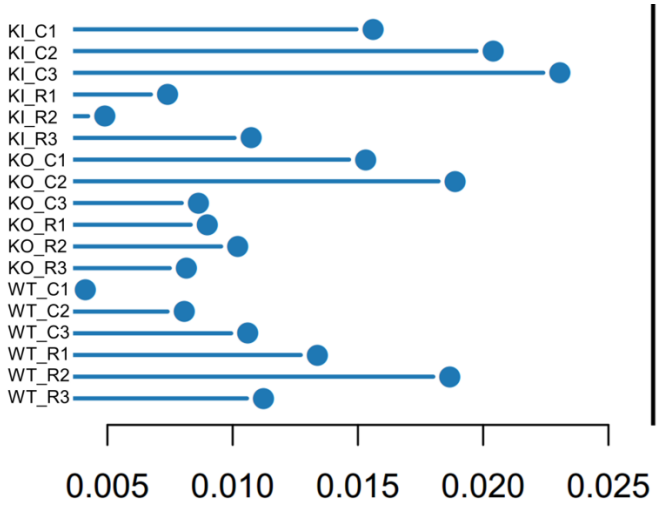

Figure 3.6. Signal intensity distributions of arrays.

(Top panel) Each box corresponds to one array. Because the boxes have similar positions and widths no experimental problems were suspected. Outlier detection performed by computing the Kolmogorov-Smirnov statistic K_a between each array's distribution and the distribution of the pooled data confirmed this suspicion.

(Left panel) A bar chart of the Kolmogorov-Smirnov statistic Ka, the outlier detection criterion from the picture above is shown to the left. Based on the distribution of the values across all arrays, a threshold of 0.0268 was determined, which is indicated by the vertical line. None of the arrays exceeded the threshold and was considered an outlier. Abbreviations: WT, wildtype; KO, p62 -/-; KI, p62 P394L; C, control; R, RANKL treated; 1, 2, 3 replicate arrays.

Data visualization by principal component analysis and unsupervised clustering

Having gained confidence that our data was not confounded by the various sources of noise, our next task was to visualize our microarray data, identify meaningful underlying experimental variables, and explore patterns of relationship between them. To do this we began with common techniques, such as dimension reduction through principal component analysis and investigation of similarities via cluster analysis.

Principal component analysis (PCA) is a widely used statistical tool used to reduce the dimensionality of large data sets that consist of many interrelated variables, while simultaneously keeping as much of the variation present in the data set as possible. This is achieved by transforming the original data into a new set of variables or principal components (PC) that are ordered such that the greatest proportion of variance is captured in the first PC, followed by the second PC, and so on. To illustrate how PCA works we may take an example from the literature (Agilent technologies):

> Say that you measure 10,000 genes in 8 different patients. These values could form a matrix of 8 x 10,000 measurements. Now imagine that each of these 10,000 genes is plotted in a multi-dimensional on a scatter plot consisting of 8 axes, 1 for each patient. The result is a cloud of values in multi-dimensional space. To characterize the trends exhibited by this data, PCA extracts directions where the cloud is more extended. For instance, if the cloud is shaped like a football, the main direction of the data would be a midline or axis along the length of the football. This is called the first component, or the principal component. PCA will then look for the next direction, orthogonal to the first one, reducing the multidimensional cloud into a two-dimensional space. The second component would be the axis along the football width. In this particular example, these two components explain most of the cloud's trends. In a more complex data set, more components might add information about interesting trends in the data.

It is common to complement PCA with additional techniques, and in particular, those whose primary aim is data clustering. If the aim of ordination in reduced space via PCA is to highlight general gradients and patterns, the aim of exploratory cluster analysis is to organize data into similar groups, such that items within a cluster are closer, or more similar, to one another than they are to members of other groups – in short, to discover potential patterns of fine relationship. Typically, clustering is performed in the absence of definitive information about which data should sort into which group, how similarity between groups is measured, or even how many groups there should be. Approaches can broadly be divided into hierarchical, which seeks to build hierarchies of clusters, or nonhierarchical. Hierarchical clustering methods can be further divided into approaches that are agglomerative, in which each data point begins as its own observation or cluster, and pairs of clusters are merged as one proceeds up the hierarchy, or divisive, which proceeds in the opposite direction, i.e. all data start in one cluster and are split recursively down the hierarchy. In the present experiment, we used R to conduct an unsupervised, agglomerative clustering algorithm which minimizes the total within-cluster variance (Ward's criteria) on our microarray data. Finally, we made extensive use of Microsoft Excel and the TIGR Multiexperiment Viewer (http://www.tm4.org/mev.html) for generation of fold-change and signal intensity plots and heatmaps.

Gene annotation enrichment analysis using DAVID, gene ontology, and Fisher's exact test

To gain an appreciation for the meanings and themes that were most heavily represented in our gene lists, we employed gene annotation enrichment techniques. The Database for Annotation, Visualization and Integrated Discovery (DAVID) is an open access, web-based program that

provides investigators a set of functional annotation tools that facilitate understanding of the biological meanings behind gene lists (Huang et al., 2009).

Typically, a user submits an enriched gene list to the web server, which then retrieves the most significant themes, including: Gene Ontology (GO) terms, protein-protein interactions, functional domains, disease associations, bio-pathways, sequence general features, homologies, and so on.

Gene ontology ascription, among the most important tools for gene expression set analysis, is not done in ad hoc manner. Rather, there is a formal Gene Ontology (GO) project, a collaborative effort aimed at providing consistent descriptions of gene products across different databases (http://www.geneontology.org). The GO project began as collaboration between databases for model organisms drosophila, saccharomyces, and mouse in 1998, and has "grown to include many databases, including several of the world's major repositories for plant, animal and microbial genomes" since then. The basic approach taken by the GO project is to describe gene products in terms of their associated (a) cellular component, i.e., the relevant part or parts of a cell, or its extracellular environment, (b) elemental molecular function, i.e., activities of a gene product at the molecular level, such as binding or catalysis, and (c) biological processes, or "operations or sets of events with a defined beginning and end, pertinent to the functioning of integrated living units: cells, tissues, organs, and organisms." An example given by the consortium is the gene product cytochrome c, which "can be described by the molecular function term oxidoreductase activity, the biological process terms oxidative phosphorylation and induction of cell death, and the cellular component terms mitochondrial matrix and mitochondrial inner membrane." We should also note that GO does not purport to cover all functions or components that are unique to mutants or disease, sequence domains, protein-protein interactions, and so on. This explains, in part, why

DAVID and other software programs supplement GO terms with additional enrichment elements as noted above.

Now, having associated GO and other biologically relevant terms to a user-specified gene list of prescribed length, DAVID calculates the statistical significance of this association using a modified Fisher's exact test called the EASE score – to determine levels and patterns of enrichment. A hypothetical example modified from the DAVID website helps clarify how this is done.

Let us assume that in the human genome background (30,000 genes total), a total of 40 have been deemed to participate in the NFκB signaling pathway, based upon findings reported in the literature. Now let us assume that in a given gene list, 3 out of 300 have been associated with NFκB signaling through DAVID's retrieval of GO terms. We pose the question – is our list enriched for the NFκB signaling pathway, i.e., is 3/300 more than we would expect to find by random chance alone compared to the human background of 40/30,000? This question is answered by the use of a 2x2 contingency table, as follows:

Fisher's Exact Test	**User Genes**	**Background**	Totals
In Pathway	**a = 3**	**b = 40**	a + b = 43
Not In Pathway	**c = 297**	**d = 29960**	c + d = 30257
Totals	a + c = 300	b + d = 30000	n = a + b + c + d = 30,300

The Fisher's exact p-value is calculated by the hypergeometric distribution (Wikipedia), expressed by the following equation:

$$p = \frac{\binom{a+b}{a}\binom{c+d}{c}}{\binom{n}{a+c}} = \frac{(a+b)!(c+d)!(a+c)!(b+d)!}{a!b!c!d!n!}$$

where $\binom{n}{k}$ is the binomial coefficient and ! indicates the factorial operator.

Assuming the null hypothesis, we would obtain this result approximately 8 times in one thousand (p-value = 0.008), using the Fisher's exact test, and approximately 6 times in one hundred (p = 0.06), using DAVID's more conservative EASE score (where the equations and terms identical to those in Fisher's exact score except for a, which becomes a` = a-1). In this example, DAVID's EASE score exceeds the common threshold of p = 0.01, suggesting that the user-generated list is not enriched for the NFκB signaling pathway any more than we would expect by random change alone.

Upstream regulator analysis by Ingenuity Systems

Ultimately, gene annotation enrichment such as that provided by DAVID provides very valuable information about gene ontologies including cellular components, molecular function, basic biological processes, and pathways that are over-represented in user-generated lists. However, what is often desired by investigators is information about whether changes in gene expression are consistent with activation or inhibition to signaling pathways. Let us return to the simplified example above to illustrate this issue.

Say that in a subsequent assay, a user-generated list (once again 300 genes long) is submitted to DAVID. This time 10 of the 300 genes are associated with the NFκB signaling pathway, which corresponds to a DAVID EASE score of $p = 1.1 \times 10^{-9}$. This result suggests that the NFκB signaling pathway is unmistakably enriched in the data set, but it is silent as to whether NFκB is activated or inhibited in the gene expression data set. It may be, for example, that among the 10 genes, 5 are up-regulated with respect to control, and, in the literature, known to be induced by NFκB signaling, and the other 5 genes are also up-regulated in the data set, but, according to the literature, known to be repressed downstream of the NFκB signaling cascade. In this instance, statistical significance alone misses the fact that NFκB signaling may be neither activated nor inhibited in this experiment, on balance.

What is needed, then, is a tool that retains DAVID's ability to ascribe or retrieve GO terms and pathways to genes in gene lists, and attributes statistical significance about that enrichment, but, in addition, permits a prediction to be made about the net activation or inhibition status of these terms and pathways, when appropriate. This is precisely what Ingenuity Systems, a private corporation that provides bioinformatics solutions for researchers in the biological and life sciences, has created with its novel IPA upstream regulator analysis (URA) tool.

Briefly, this tool (a) can predict upstream regulators from gene expression data and (b) determine whether those regulators are likely to be activated or inhibited based on a cumulative, regularly - updated and curated knowledge base, culled from the literature. In practice two independent values or metrics are reported. First, a p-value of overlap which corresponds to a modified Fisher's exact test similar to DAVID's EASE score is provided, giving a statistical assessment of the significance

of enrichment of a particular regulator. Next, an independently generated activation z-score is given, which (IPA's "A Novel Approach to Upstream Regulators" whitepaper):

> …indicates the degree of consistent agreement or disagreement of the actual versus predicted direction of change among the downstream gene targets. A prediction about the state of the upstream regulator, either activated or inhibited, is made based on the z-score. For example, if most of the targets of an upstream regulator are expected from the literature to be up-regulated and there is an observed increase in their measured gene expression in the analyzed dataset, this would lead to a positive activation z-score and an "activation" prediction. Conversely, if most of the genes were expected to be up-regulated and the observed expression was down-regulated (or vice-versa), this anti-correlation would lead to a negative z-score and a prediction of "inhibited" for the upstream regulator.

In the present project, we have made use of both DAVID's functional analysis and IPA's URA to analyze gene lists generated from the pipeline described above. Because these values are provided in number alone, we have used Microsoft Excel to generate bar graphs to illustrate statistical and biological significance in offset horizontal bar graphs. For statistical significance, modified Fisher's exact scores are represented by the negative log of the p-value, such that increased significance corresponds to longer bar lengths. For biological predictions about activation state for these upstream regulators, we have labeled offset bars, whose length also corresponds to the strength of the prediction, either orange (activated) or blue (inhibited). Finally, we have included detailed graphical depictions of selected URA pathways (with gene target abbreviations and fc levels) for future reference and experimentation in the appendices at the end of this dissertation.

Pattern determination

Venn diagrams were generated using the Venny web-based program found at the following website: (http://bioinfogp.cnb.csic.es/tools/venny/index.html (Oliveros, 2007).

3.3 Results

Experiment overview

As noted above, we generated osteoclast precursors using M-CSF (20ng/mL) on MACS sorted CD11b+ murine bone marrow derived hematopoietic precursors obtained from age and gender-matched p62-/- (KO), p62+/+ (WT), and p62 P394L/P394L (KI) mice (Figure 3.2). We then treated the cells with a 100ng/mL bolus of the primary osteoclastogenic cytokine, receptor activator of NFκB ligand (RANKL) or volume equivalent vehicle control. After 8 hours, Trizol-generated total RNA was prepared, processed, and scanned on the Affymetrix genechip (Mouse genome 430A 2.0 array, Affymetrix) by the VCU Molecular Diagnostics Core, who generated RNA quality control measures and raw .CEL files for each of 18 scanned arrays (2 treatments x 3 genotypes x 3 replicates/genotype), and submitted them to the Windle lab for data processing and analysis as described.

Principal component analysis and unsupervised clustering suggest that array data cluster by genotype and treatment

Our first task after confirming that our data passed quality control standards (Figures 3.2 through 3.6) was to visualize our microarray data, identify meaningful underlying experimental variables, and explore patterns of relationship between them. We began this analysis with a more global view using two common techniques, principal component analysis and unsupervised clustering.

As noted earlier, the goal of principal component analysis (PCA) is to reduce the dimensionality of large data sets, and thereby gain a general appreciation for gradients and patterns in the data. In our

data set, PCA showed that, by-far, the greatest variance in data (first principal component) corresponded very well with genotype, with wide separation between WT, KO, and KI on the first principal component (Figure 3.7, top panel). The second, orthogonal axis, which corresponds to the next largest amount of variance in the data, corresponds to treatment with RANKL vs. controls (Figure 3.7, top panel).

Unsupervised clustering results bolstered our confidence in these results, showing that array replicates agglomerated tightly by genotype and replicate, as expected, within clusters (Figure 3.8). As noted in the methods, replicates were generated from cells pooled at the level of individual plates, but the RNA obtained from each plate was not pooled (i.e. the samples were not simply technical replicates), which further bolsters our confidence in these results. What was unexpected was the close proximity between the KI and KO clusters (Figure 3.8). We had assumed that the broad pattern of genotypic expression might parallel what we had previously seen in our phenotypic characterization studies. That is, we expected that knocking out p62, a multifunctional adaptor which has many binding partners that play roles in many important signaling pathways and leads to a clear loss of osteoclast function in vitro – would result in a significant divergence in gene expression between KO and WT cells. That much is clear from the distance between clusters in Figure 3.8. On the other hand, introduction of a single amino acid substitution resulting in an increase in osteoclast and function might be expected to result in gene expression changes that cluster closer to WT than to KO. That this was not so, i.e. that KI and KO clustered more closely to one another than to wildtype, suggests that the p62's UBA domain plays an important role in gene expression in differentiating osteoclast progenitors. To gain a deeper understanding of how this might occur, we will now look more closely at these gene expression profiles.

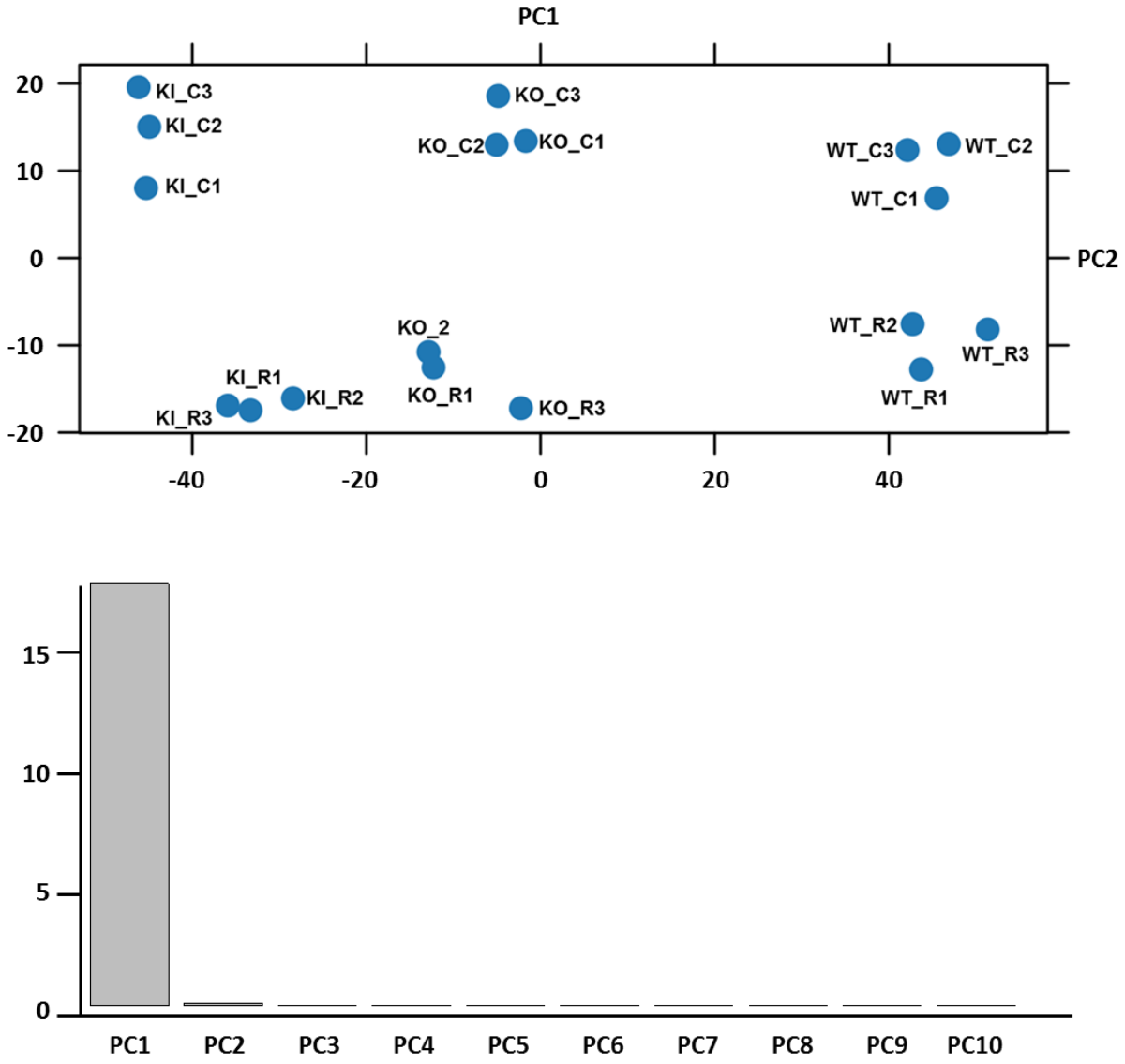

Figure 3.7. Principal component analysis and scree plot.

Abbreviations: WT, wildtype; KO, p62 -/-; KI, p62 P394L; C, control; R, RANKL treated; 1, 2, 3 replicate arrays.

(Top panel) The first principal component, PC1 (horizontal axis), corresponds best to genotype, while the second principal component, best corresponds with treatment (RANKL or vehicle control), suggesting that this is a relatively low noise experiment with large experimental effects.

(Bottom panel) Scree plot of variance vs. principal component demonstrates that the variation explained by each principal component drops dramatically after PC1.

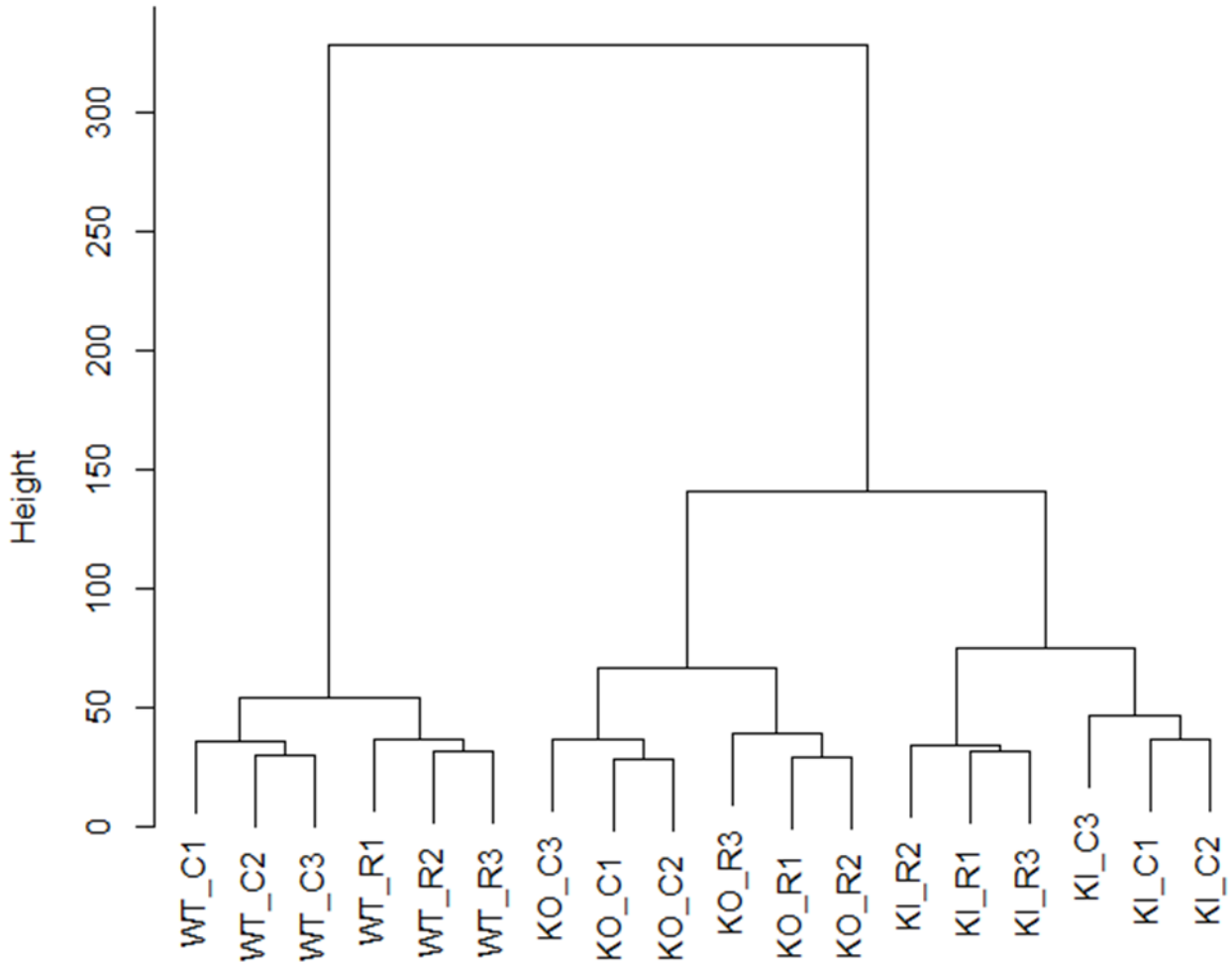

Figure 3.8. Cluster dendrogram.

Abbreviations: WT, wildtype; KO, p62 -/-; KI, p62 P394L; C, control; R, RANKL treated; 1, 2, 3 replicate arrays.

Unsupervised cluster dendrogram (Ward's criteria) confirms that arrays cluster by genotype and treatment. Intriguingly, KO and KI subgroups clustered in much closer proximity to one another than to WT.

Knock-out and P394L mutation of p62 differentially alter gene expression profiles of bone marrow derived osteoclast progenitors treated with RANKL

We next turned our attention to changing our raw data into interpretable gene expression profiles. Given that we were most interested in the biological processes underlying osteoclastogenesis, we focused primarily on the induction of genes in response to RANKL normalized by vehicle treated controls in each of the three genotypes, WT, KO, and KI. Before doing so, however, we had to grapple with the perennial question of what it means for a gene to be differentially expressed. On the one hand, a gene may be termed differentially expressed in the language of statistics if its expression levels change systemically from one condition to the next (p-value, or, in the case of large data sets, false discovery rate or q-value), irrespective of how small the biological difference (fold change, fc) might be. On the other, a gene is likely to be called differentially expressed, in the language of biology, only if its expression levels change by a meaningful amount (fc) between the two treatment conditions. In an attempt to balance these dual concerns, we made use of the following cut-offs: $q \leq 0.11$ false discovery rate and $fc \geq 1.3$ (Figure 3.9), reasoning that (a) there may be constellations of genes that are only modestly altered individually, but taken in aggregate, represent a significantly altered group, and (b) selecting a fold-change cut-off much higher than this may erroneously bias us away from these potentially significant results. Implementing these criteria, we were immediately struck by two general findings. First, the number of genes that were differentially regulated in the presence of RANKL was substantially greater in each of the genetically altered backgrounds, KO and KI, than in WT, by a ratio of between 3:1 and 4:1 in a pattern that was robust to choice of fc and q cut-offs (Figure 3.9a and Figure 3.9b). This is not altogether that surprising in the case of the KO cells, as the abrogation of expression of a multifunctional adaptor protein with roles in many signaling pathways is bound to impair a cell's

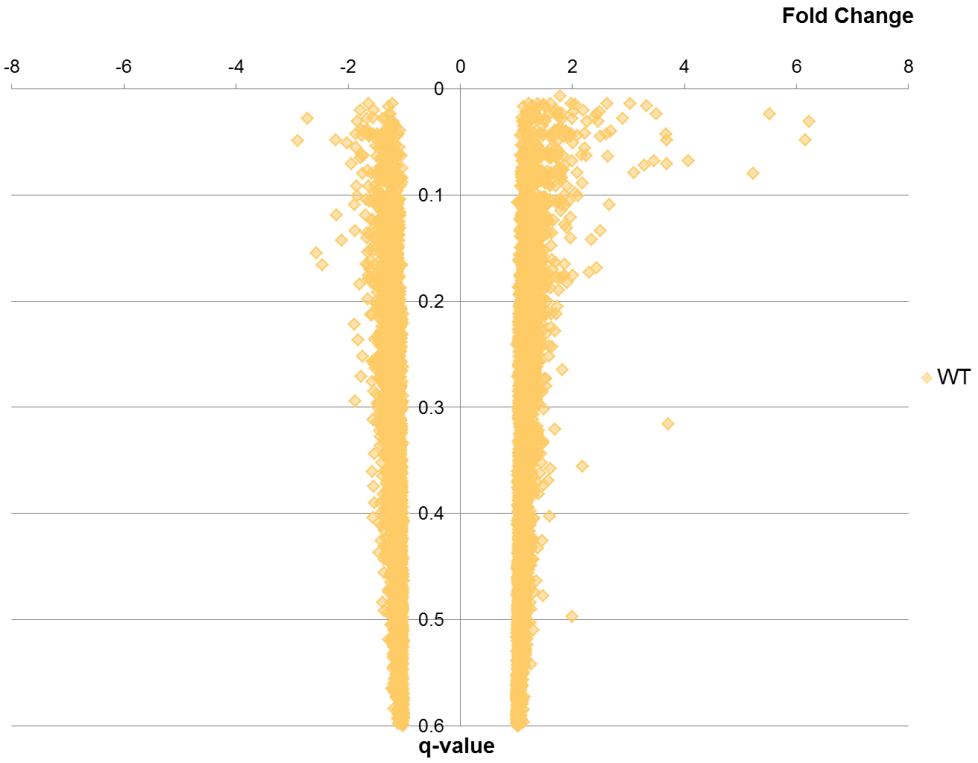

Figure 3.9a. Volcano plots illustrating gene induction in RANKL treated cells relative to controls. (Top panel) Wildtype (WT) only. (Bottom panel) WT data with p62-/- (KO) and p62 P394L (KI) data superimposed. Significance for fold change and false discovery rate was set at fc ≥ 1.3 and q ≤ 0.11, respectively.

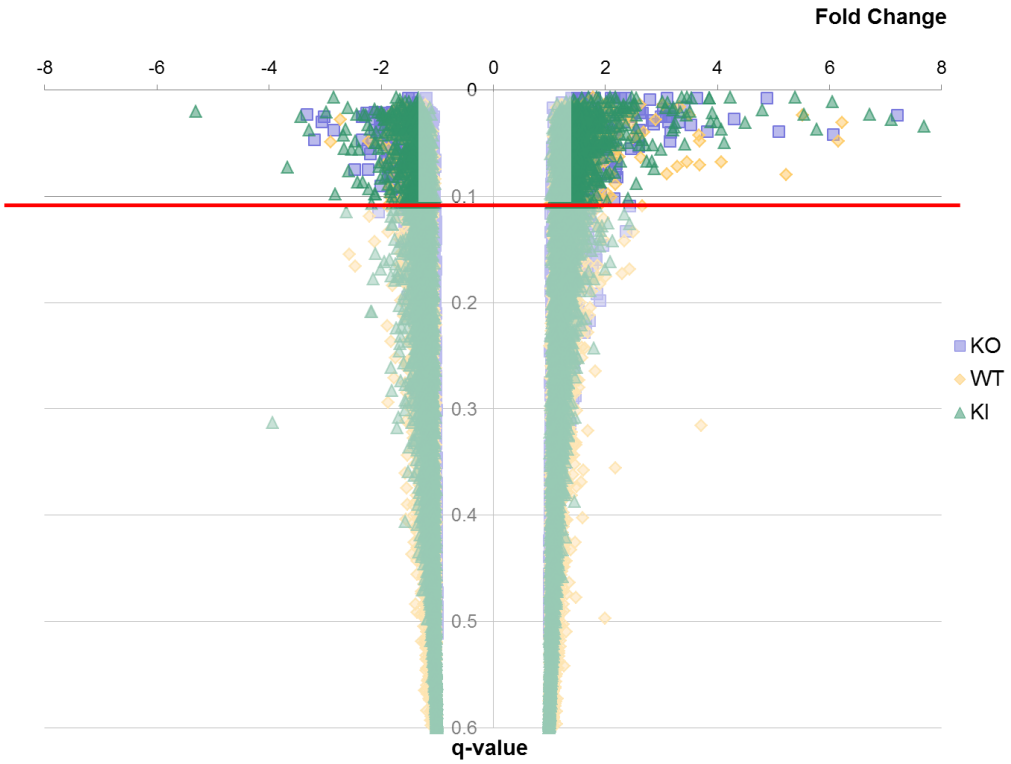

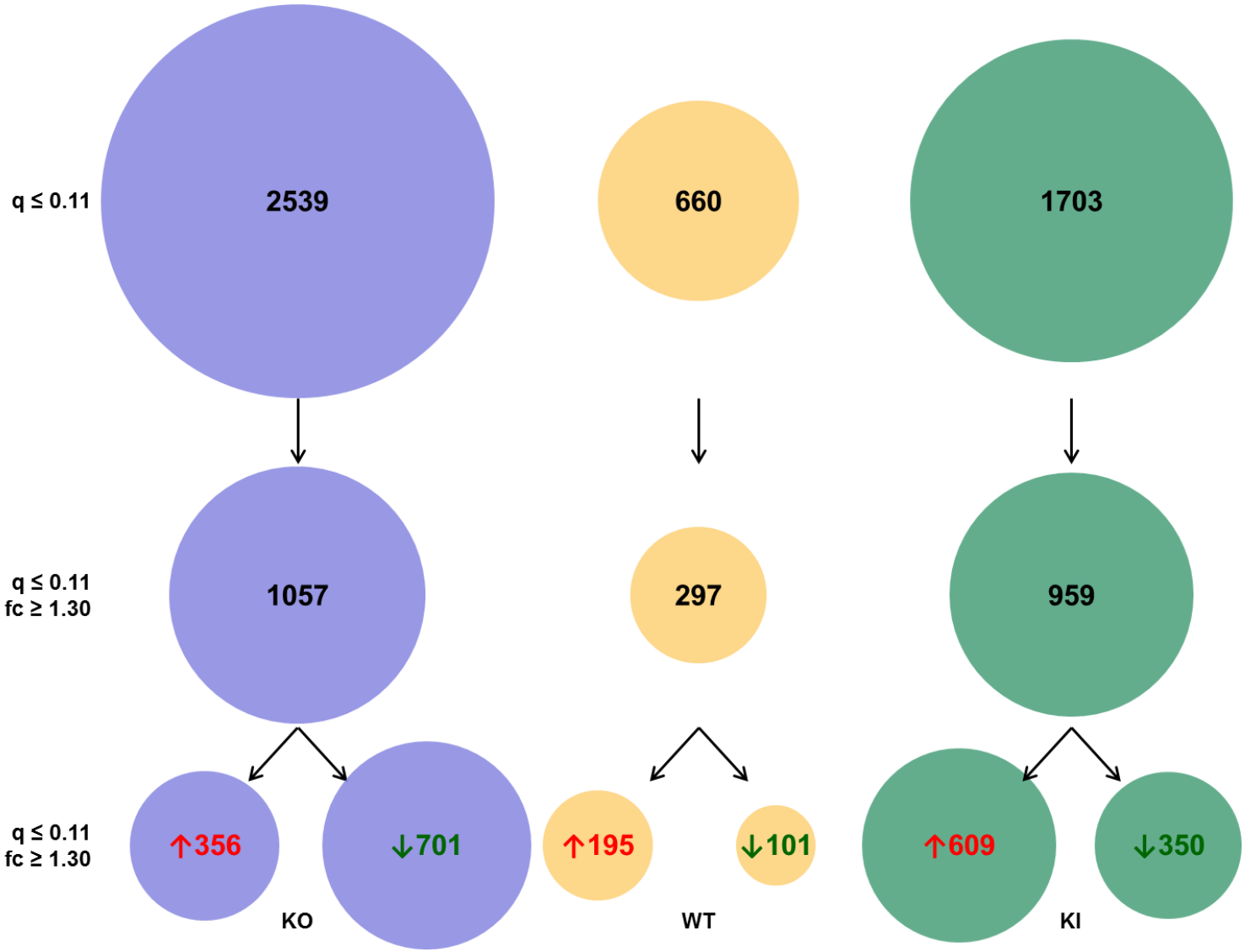

Figure 3.9b. Numbers of genes induced or repressed in bone marrow derived osteoclast progenitors from KO, WT, and KI mice in response to RANKL. Note that many more genes are differentially regulated in cells obtained from transgenic mice compared to WT, and that the ratio of induced to repressed genes is uniquely suppressed in KO cells.

ability to efficiently maintain homeostatic balance in response to cytokine challenge. It also stands to reason that the KI cells might behave like KO cells in some respects, like WT in others, and uniquely in still others. In the case of osteoclast progenitors cultured in vitro, disruption of p62's UBA domain has clearly altered the normal WT response to RANKL challenge (Figures 3.9a, b).

To begin to answer how this has occurred, we turn to a simple inspection of the ratio of genes induced to genes repressed in response to RANKL in each of the genetic backgrounds (Figure 3.9b). For WT and KI cells, many more genes were induced than repressed in response to RANKL. The opposite is true for KO cells, which are characterized by a nearly inverse ratio of genes induced to repressed in response to RANKL (Figure 3.9b). Several possibilities may explain this phenomenon. These include impaired down-regulation of genes in KO cells under basal conditions, impaired induction of genes in response to RANKL, or some combination of the two. To help clarify which of these conditions pertain, we turned next to a specific analysis of highly expressed genes and known osteoclastogenic gene products.

Analysis of select genes suggests that p62 mediates gene expression both in the absence and in the presence of RANKL

First, we plotted the fold change levels of the most highly up-regulated genes from each genetic background (Figure 3.10a).

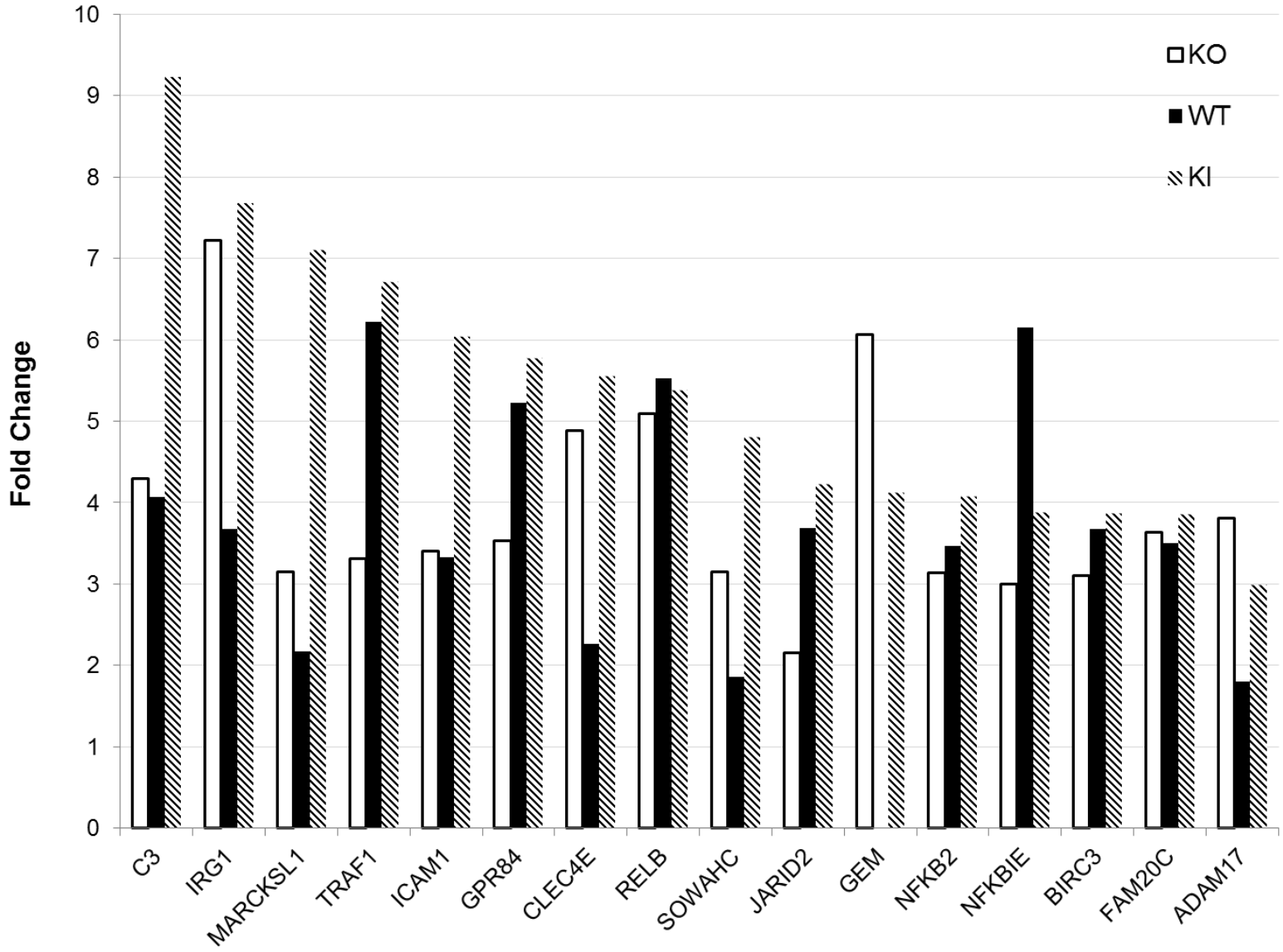

Figure 3.10a. Fold induction of most highly up-regulated genes from KO, WT, and KI RANKL-treated cells.

While many of these genes are well known to play a role in survival and NFκB signaling in osteoclastogenesis (e.g. TRAF1, NFκB2, RelB), there was no obvious correlation between up-regulation and genotype; that is, the genes most highly up-regulated by RANKL tended to be up-regulated in all three genotypes, and thus in what appeared to be a p62-independent fashion. Next we looked at selected genes known to be involved in osteoclastogenesis (Figure 3.10b).

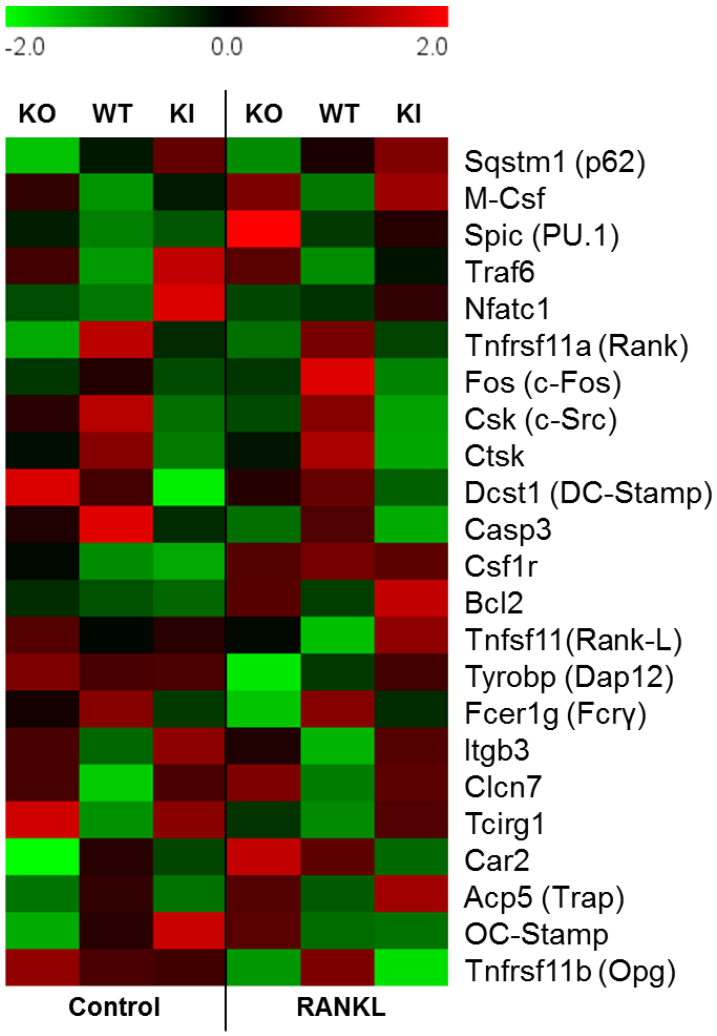

Figure 3.10b Heatmap of select genes differentially expressed after 8 hours treatment of RANKL or vehicle in microarray experiment. Abbreviations: M-Csf, macrophage colony-stimulating factor); Csf1r, macrophage colony-stimulating factor receptor; PU.1, Transcription factor PU.1; Bcl-2, B-cell CLL/lymphoma 2; c-Fos, Proto-oncogene c-Fos; DAP12, DNAX-activating protein; FCRγ, Fc receptor common γ subunit; c-Src, Proto-oncogene tyrosine-protein kinase Src; Itgb3, Integrin β3; ClC-7, Chloride channel 7; Tcirg1, T cell, immune regulator 1, ATPase, H+ transporting, lysosomal V0 protein A3; Ctsk, Cathepskin K; Car2, Carbonic anhydrase II; Trap, Tartrate resistant acid phosphatase; DC-Stamp, dendritic cell-specific transmembrane protein; OC-Stamp, osteoclast-specific transmembrane protein; OPG, osteoprotegerin

In this data subset we expected to find a pattern of gene expression that might help explain the phenotypic data we generated in chapter two, i.e., increased expression of pro-osteoclastogenic genes in WT and KI cells compared with KO cells. This, however, was not the case.

Gene expression levels of pro-osteoclastogenic M-CSF, PU.1, and TRAF6 were greater in KO cells than in WT cells under control conditions (fold changes of 1.9, 1.5, 1.5, respectively), yet the same pattern was true of KI cells relative to WT (fold changes of 1.8, 1.2, and 2.4, respectively) for these genes (Figure 3.10b). Conversely, pro-osteoclastogenic RANK, c-Fos, and c-Src were expressed at much lower levels in both KO (fc = 0.4, 0.07, and 0.53, respectively) and KI (fc = 0.6, 0.02, and 0.30, respectively) cells compared to WT under basal conditions (Figure 3.10b). Finally, expression of the master regulator of osteoclastogenesis, NFATc1, was significantly higher in KI than in WT cells under basal conditions (fc = 1.4), which is consistent with the expected phenotype, yet DC-STAMP (fc = 0.5) levels were not (Figure 3.10b).

Of note, two recent studies asked similar questions using an alternative approach. In 2008, Nagy and associates examined gene expression profiles of 15 known genes via RT-PCR in monocytes and lymphocytes of 23 known PDB patients compared to healthy controls. They found that, of these, eight were up-regulated in PDB patient-derived cultures, including interferons-α, β, γ, p38 β2 MAPK, interferon-γR1, interferon-γR2, STAT1, one, TNF-α, was found to be significantly down-regulated, and in the remainder, RANK, TRAF6, p62, JAK, STAT2, STAT3, and GCR, no differences were found compared to healthy controls (Nagy et al., 2008). In 2010, Michou and colleagues selected 48 osteoclast-expressed candidate genes with known roles in signaling, survival, bone resorption, and adhesion, and used RT-PCR to compare their expression levels in cultures of peripheral blood mononuclear cells obtained from twelve known PDB-patients (who harbored the P392L mutation) versus non-mutated healthy controls. Interestingly, they found that

genes encoding proteins associated with apoptosis (CASP3 and TNFRSF10A), cell-signaling (RANK), and bone resorption including TRAP and Cathepsin K were down-regulated in PDB patients compared to healthy controls (Michou et al., 2010). Of the individual genes that were up-regulated in PDB patients compared to controls in these studies, many of the equivalent murine genes in our microarray analysis were either not queried on our array (TNFRSF10A, p38 β2 MAPK or murine MAPK11), were undetectable under vehicle and experimental conditions (IFN-α, β, γ, TNF-α), or were expressed at levels that were indistinguishable between wildtypes and mutants (IFN-γR1, STAT2, STAT3, TRAP or murine ACP5, GCR or murine NR3C1).

Interestingly, though, our data confirmed a subset of these findings despite significant differences in experimental design. RANK, cathepsin K, and caspase-3 were down-regulated (Figure 3.10b, fc = 0.6, 0.2, 0.6, respectively), and IFN-γR2 (fc = 1.9) was up-regulated, in KI cells compared to WT cells under control conditions. With respect to these genes, caspase-3 plays a well-known role in the induction of cellular apoptosis (Jänicke et al., 1998). Is its down-regulation associated with decreased apoptosis in pagetic osteoclasts? Some studies have shown that bisphosphonate-induced osteoclast apoptosis is caspase-3-dependent (Benford et al., 2001), while others have shown that activated caspase-3 is required for osteoclast differentiation (Szymczyk et al., 2006). Moreover, interferon-γR2 does not have a well-established role in the formation or activation of osteoclasts, yet its relative abundance and induction upon RANKL-stimulation suggest that it deserves further inquiry. Finally, RANK and Cathepsin K are typically associated with increased osteoclast formation and activation, yet transcript levels are relatively diminished in the very cells (KI) that demonstrate the greatest osteoclastogenic potential.

To summarize, on the one hand, the partial concordance between our results and those obtained from patient samples strengthens our confidence in their validity. On the other, the fact that patterns of expression for many of these transcripts do not correlate with known phenotypes confirms the complex regulation at work in our cells of interest, and raises several important questions. Are differences at the level of transcription manifest at the protein level? Do unanticipated expression patterns reflect negative feedback, impaired transcription, or post-transcriptional modification? These questions are addressed in greater detail in the subsequent chapter. Methodologically, though, we are forced to re-examine the approach adopted so far. Investigating the most highly expressed genes in our study or examining a pre-identified selection of genes of interest may provide some insight into p62's regulatory role during osteoclastogenesis, but these are not systematic, comprehensive, or unbiased approaches.

Gene annotation enrichment helps build hypotheses

To this end, we turned next to gene annotation enrichment techniques. The Database for Annotation, Visualization and Integrated Discovery, or DAVID, is an open access, web-based program that provides investigators a set of functional annotation tools that facilitate understanding the biological meanings behind gene lists, such as the ones generated by our data pipeline (Huang et al., 2009). We submitted each of the six gene lists represented graphically in the bottom panel of Figure 3.9b to DAVID and identified several gene ontology terms that were enriched in each data set (Figures 3.11a, 3.11b). Many themes normally associated with hematopoietic cells were universally enriched, irrespective of genotype, including genes related to: the immune response, hematopoiesis, inflammation, and signaling in the apoptotic pathway, while others appeared to be

preferentially enriched in specific genotypes: namely down-regulation of genes related to the cell cycle, mitochondria, and M-phase in KO cells, and up-regulation of genes associated with the endoplasmic reticulum in KI cells (Figures 3.11a, 3.11b).

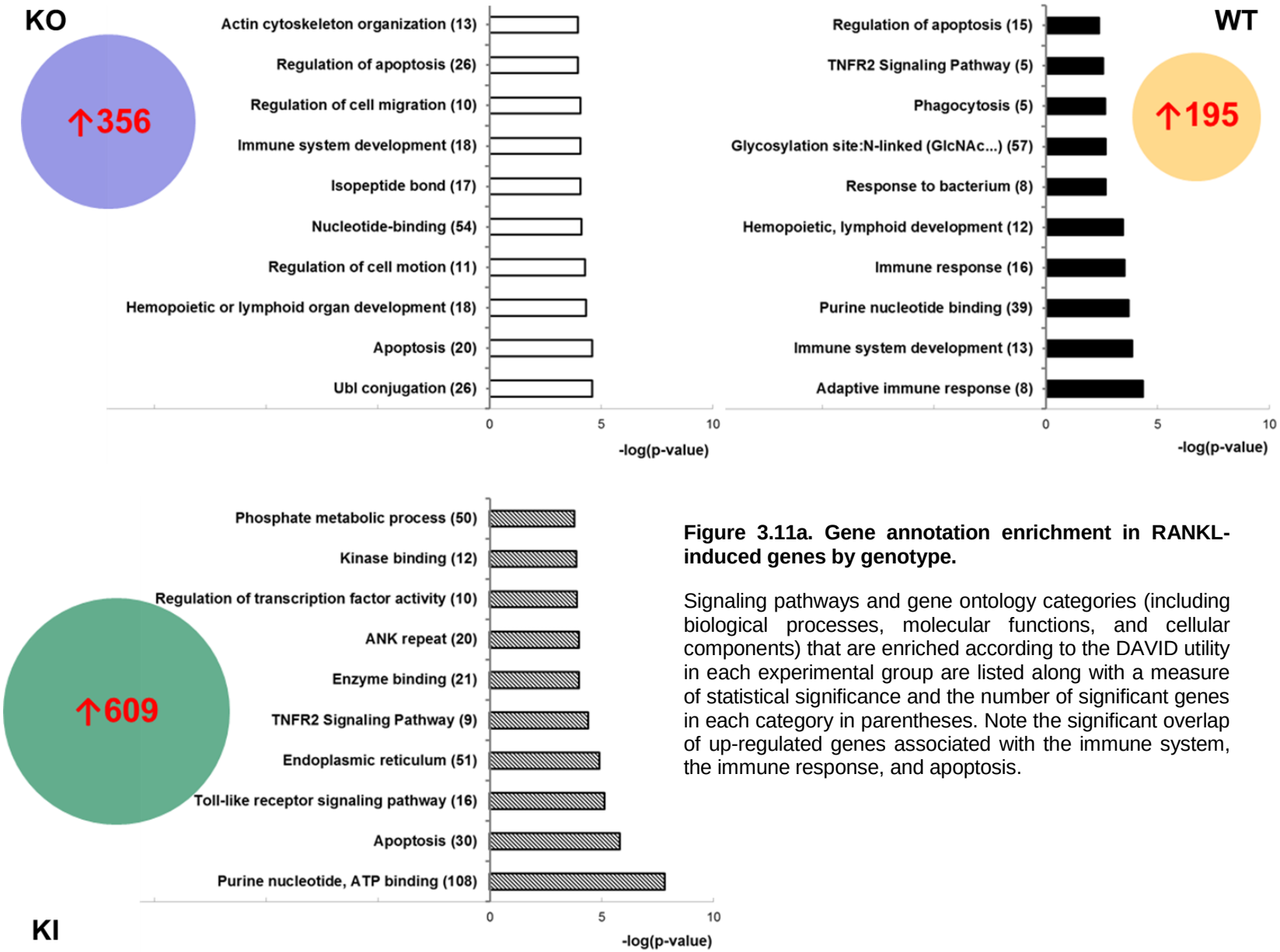

Figure 3.11a. Gene annotation enrichment in RANKL-induced genes by genotype.

Signaling pathways and gene ontology categories (including biological processes, molecular functions, and cellular components) that are enriched according to the DAVID utility in each experimental group are listed along with a measure of statistical significance and the number of significant genes in each category in parentheses. Note the significant overlap of up-regulated genes associated with the immune system, the immune response, and apoptosis.

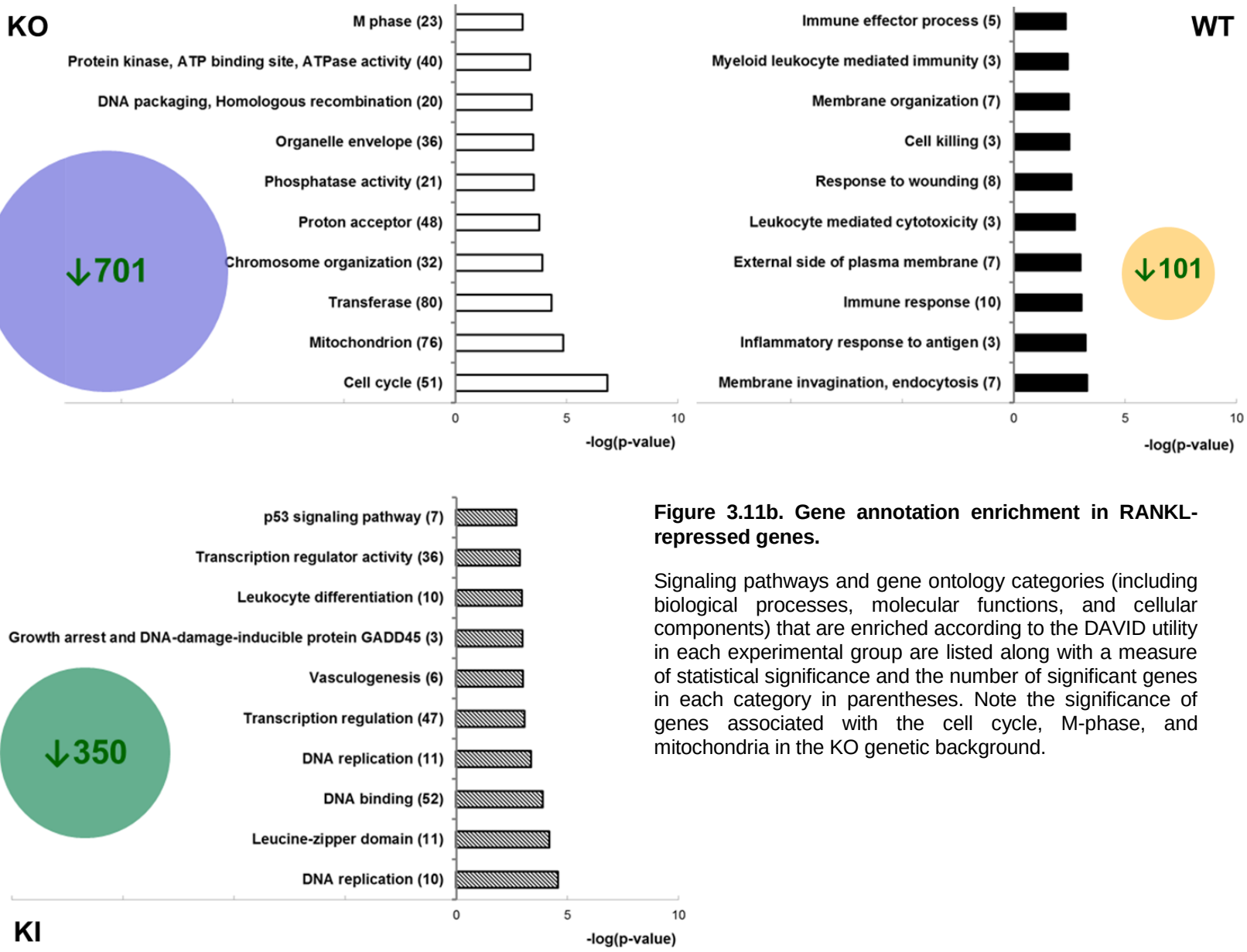

Figure 3.11b. Gene annotation enrichment in RANKL-repressed genes.

Signaling pathways and gene ontology categories (including biological processes, molecular functions, and cellular components) that are enriched according to the DAVID utility in each experimental group are listed along with a measure of statistical significance and the number of significant genes in each category in parentheses. Note the significance of genes associated with the cell cycle, M-phase, and mitochondria in the KO genetic background.

Next we sought to focus our analysis and improve the association between our enrichment results with our phenotypic profiles – i.e. osteoclast formation and activity that is impaired in KO cells, and enhanced in KI cells. We did so by systematically looking for specific patterns of overlap in our gene sets and submitting resultant lists to DAVID for further enrichment studies (Figures 3.12a, 3.12b). The results of three of the most biologically meaningful analyses are described below.

First, we noted that the 104 genes that were commonly up-regulated in response to RANKL across the three genotypes, WT, KO, and KI, were not likely to be regulated by p62 in a significant manner (Figure 3.12a). Many of the enrichment terms in this group (e.g. hematopoiesis, the immune response) are, once again, consistent with the cell type of origin – bone marrow derived hematopoietic precursors. Intriguingly, among the 104 genes in this subgroup, the NFκB cascade was predicted to be enriched with RANKL treatment of osteoclast progenitors, *irrespective* of p62 status – a finding at odds with the prevailing hypothesis about the important role played by p62 in this signaling pathway.

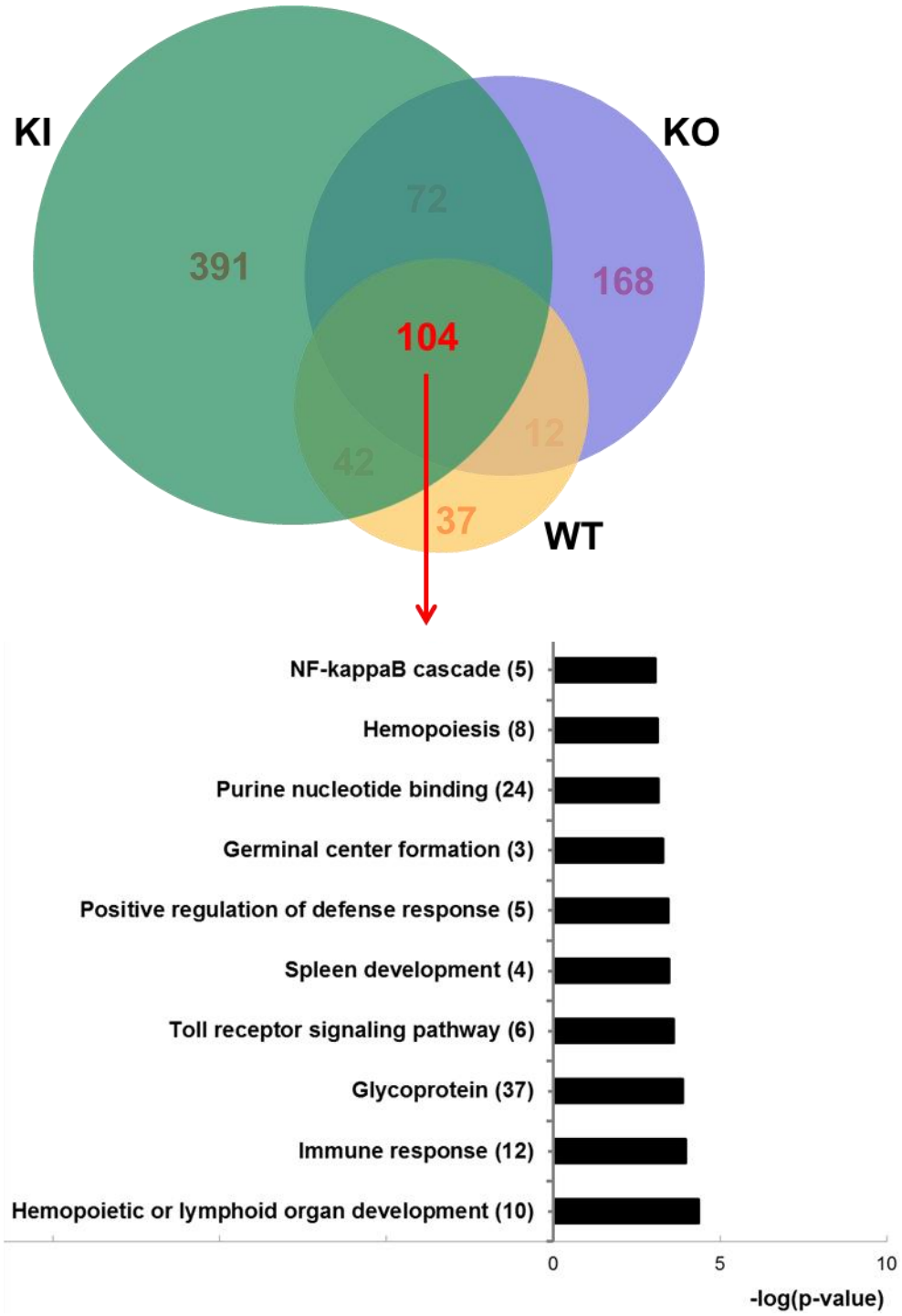

Figure 3.12a. Annotation enrichment of genes induced by RANKL independent of p62 status.

104 genes were commonly up-regulated in the three experimental groups in response to RANKL. Note the enrichment for the genes associated with hematopoiesis, the immune response, Toll-like receptor signaling and the NFκB signaling cascade.

Next, we explored the genes preferentially down-regulated by RANKL in the KO genetic background, finding that the most statistically enriched terms among these 552 genes were the cell cycle and the mitochondrial cellular component (Figure 3.12b). The genes associated with the cell cycle encode aurora kinases, E2F transcription factors, cyclins, and cyclin dependent kinases, which play important roles in mitosis and cellular proliferation, while the genes enriched for the mitochondrial component encode proteins associated with oxidative phosphorylation and the electron transport chain. Each of these results is broadly consistent with previously published findings. In the case of the cell cycle, investigators have demonstrated that p62 is phosphorylated by cdk1 in HEK293 cells, a process necessary for the maintenance of sufficient cyclin B1 levels to allow cells to properly enter and exit mitosis. In their hands, absence of p62 produced a lower fraction of cells in G1 that was attributable to a slower exit from mitosis (Linares et al., 2011). In the case of mitochondrial enrichment, Shin and colleagues have demonstrated that a subset of cellular p62 protein directly localizes within mitochondria obtained from murine brain tissue, forming heterogeneous protein complexes with several oxidation-prone proteins (including components of the electron transport chain, chaperone molecules, and redox enzymes) to support stable electron transport. They also demonstrated that p62-deficient mitochondria exhibited impaired electron transport, which was partially restored by in vitro delivery of p62 (Lee and Shin, 2011).

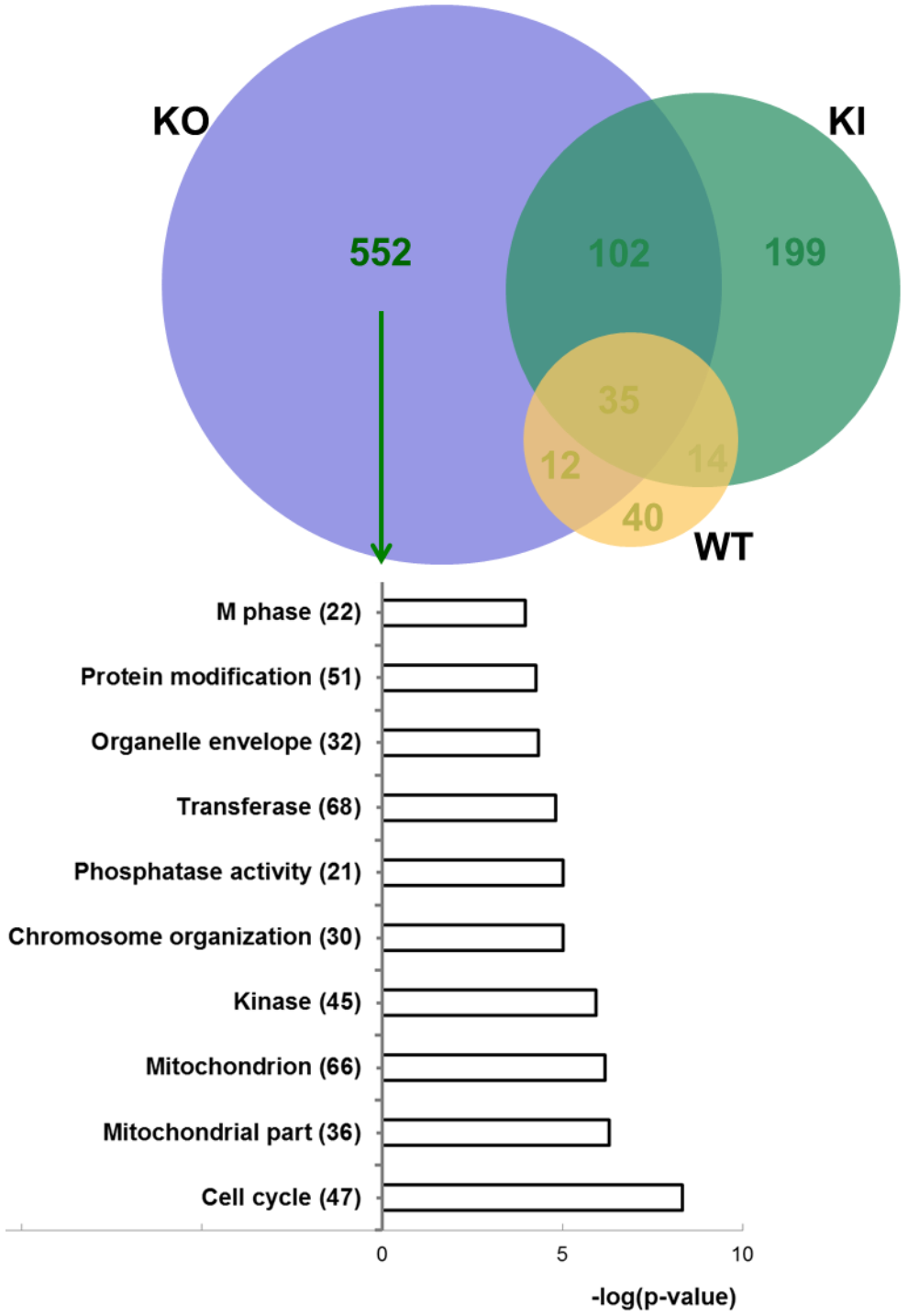

Figure 3.12b. Annotation enrichment of genes uniquely repressed by RANKL in KO cells.

552 genes were uniquely down-regulated in the KO group. Note the enrichment in genes associated with the cell cycle, chromosome organization, M-phase, and mitochondria.

How might these results correlate with the impaired osteoclastogenic phenotype of RANKL-treated KO cells? Osteoclasts, and, in particular, fully-differentiated, bone-resorbing osteoclasts, are characterized by an over-abundance of mitochondria, required to power energy-taxing activities such as bone resorption. In this manner, the absence of p62 may impair osteoclastogenesis by altering the expression of proteins involved in normal cell-cycle progression and the efficient function of the electron transport chain in these metabolically active cells.

Finally, we investigated transcripts that were uniquely up-regulated by RANKL in KI cells, reasoning that this subset of genes might be enriched for known pro-osteoclastogenic processes and pathways (Figure 3.12c). In this group, we found 391 genes that were enriched for association with the endoplasmic reticulum in terms of cellular component. Deeper investigation of these genes reveals further enrichment for genes associated with phosphate metabolism, redox reactions, catabolic processes, and protein folding and localization. Two possibilities for this pattern of expression present themselves. First, osteoclast progenitors obtained from KI mice are known to be hypersensitive to RANKL. It may be that these metabolically-hyperactive, differentiating cells have an increased requirement for protein-folding machinery. On the other hand, it is well known that p62 plays an important role in maintaining cellular homeostasis by mediating selective autophagy and the oxidative stress response. This pattern of gene expression, may, alternatively, reflect an impairment in either or both of these functions, generating an increased burden of intracellular cargo (including misfolded proteins) that may then activate the unfolded protein response (UPR), an evolutionarily-conserved, intracellular program of signal transduction that mitigates cellular stress or guides the cell to apoptose (Walter and Ron, 2011). Interestingly, it has been shown that selective autophagy is activated for cell survival after endoplasmic reticulum stress (Ogata et al., 2006).

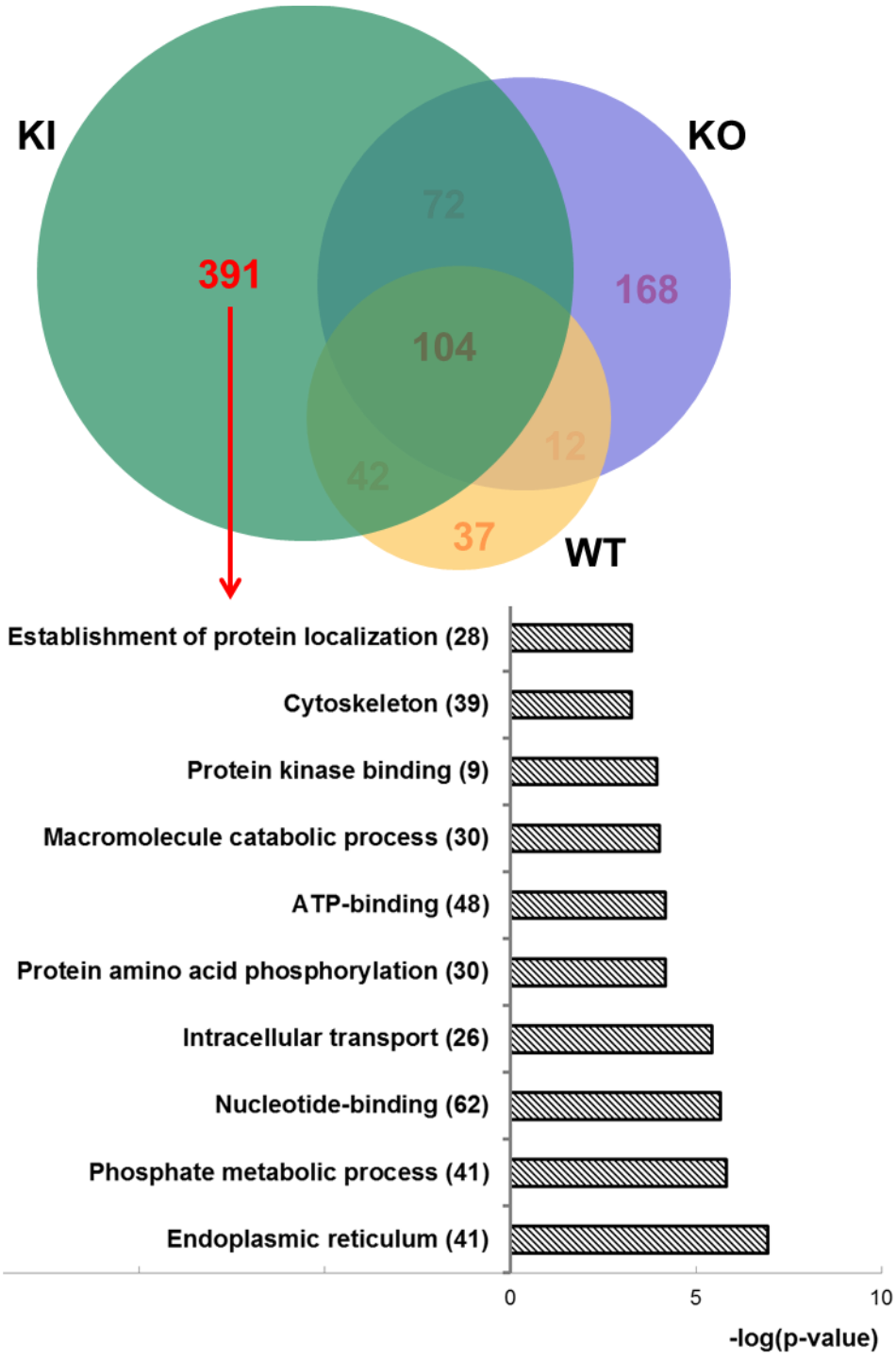

Figure 3.12c. Annotation enrichment of genes uniquely induced by RANKL in KI cells.

391 genes were uniquely up-regulated in the KI experimental group. Note the unique enrichment for genes associated with establishment of protein localization, catabolic processes, and the endoplasmic reticulum cellular component.

Mutations to p62's UBA domain, as in our KI cells, diminish its ability to bind ubiquitin, as well as ubiquitinated and misfolded proteins, then clear them via its (PB1-domain mediated) interaction with RPT1 of the 26S proteasome or its (LIR-domain mediated) interaction with LC3 in the autophagosome. In this manner, misfolded proteins that are normally directed toward proteasomal or autophagic degradation may accumulate in the ER lumen, prompting increased ER stress, and a more robust unfolded protein response (UPR). In this light, there is some evidence that induction of the ER stress response spurs osteoclast precursor differentiation (Wang K et al., 2011), but more work must be conducted to establish this more firmly.

To summarize, gene annotation enrichment analysis has led to a number of preliminary hypotheses about the role of p62 in RANKL-induced osteoclastogenesis: (a) that NFκB signaling may be largely p62-independent, (b) that ablation of p62 may alter osteoclast progenitor proliferation and mitochondrial function, indirectly diminishing osteoclastogenesis, and (c) that mutation of the UBA domain leads to the preferential up-regulation of ER-associated genes, possibly via an intensified ER-mediated unfolded protein response. To strengthen and refine these hypotheses, we next turned to upstream regulator analysis.

Upstream regulator analysis conducted on RANKL-treated osteoclast progenitors leads to several testable hypotheses

As noted earlier in the methods, DAVID and other broad-based gene annotation enrichment programs are very useful for providing generally enriched themes in user-specified gene expression sets. There is no specific mechanism, however, to distinguish between genes that are induced and genes that repressed in such sets. To deal with this deficiency we manually divided

our gene lists and submitted them in separate blocks of up and down-regulated genes for each of our three genotypes (Figure 3.9b, bottom panel), then re-performed this analysis after parsing out both overlapping and unique sets of genes that we hypothesized might correlate with our known phenotypes (Figures 3.11, 3.12). This analysis has provided important introductory themes about underlying pathways and biological processes, but is necessarily limited in two ways. First, real biological pathways and processes are composed of complex networks of genes, some of which may be up-regulated in response to external stimuli while others, in the same pathway and in response to the same stimulus, might be simultaneously down-regulated. Moreover, it may be that a pathway is composed of several genes whose expression and function are p62-independent with the exception of a key subset that is differentially-regulated by p62. In this manner parsing out genes to highlight differences in gene sets, as we did in Figures 3.12, may bias analyses away from more complex regulatory networks. The larger issue, though, as discussed earlier in the methods, is the absence of a prediction about the activation status of enriched biological pathways. To deal with these potential sources of bias and make more accurate predictions about potentially up and down-regulated networks, we made use of Ingenuity IPA's upstream regulator analysis tool.

Specifically, we submitted each list of genes represented by the middle panel of Figure 3.9, along with its fold change in response to RANKL treatment, and queried the system for quantitative predictions about the upstream regulators (very broadly defined, but includes cytokines, kinases, transcription factors and so on) most likely to be activated or inhibited in each data set (Figure 3.13a).

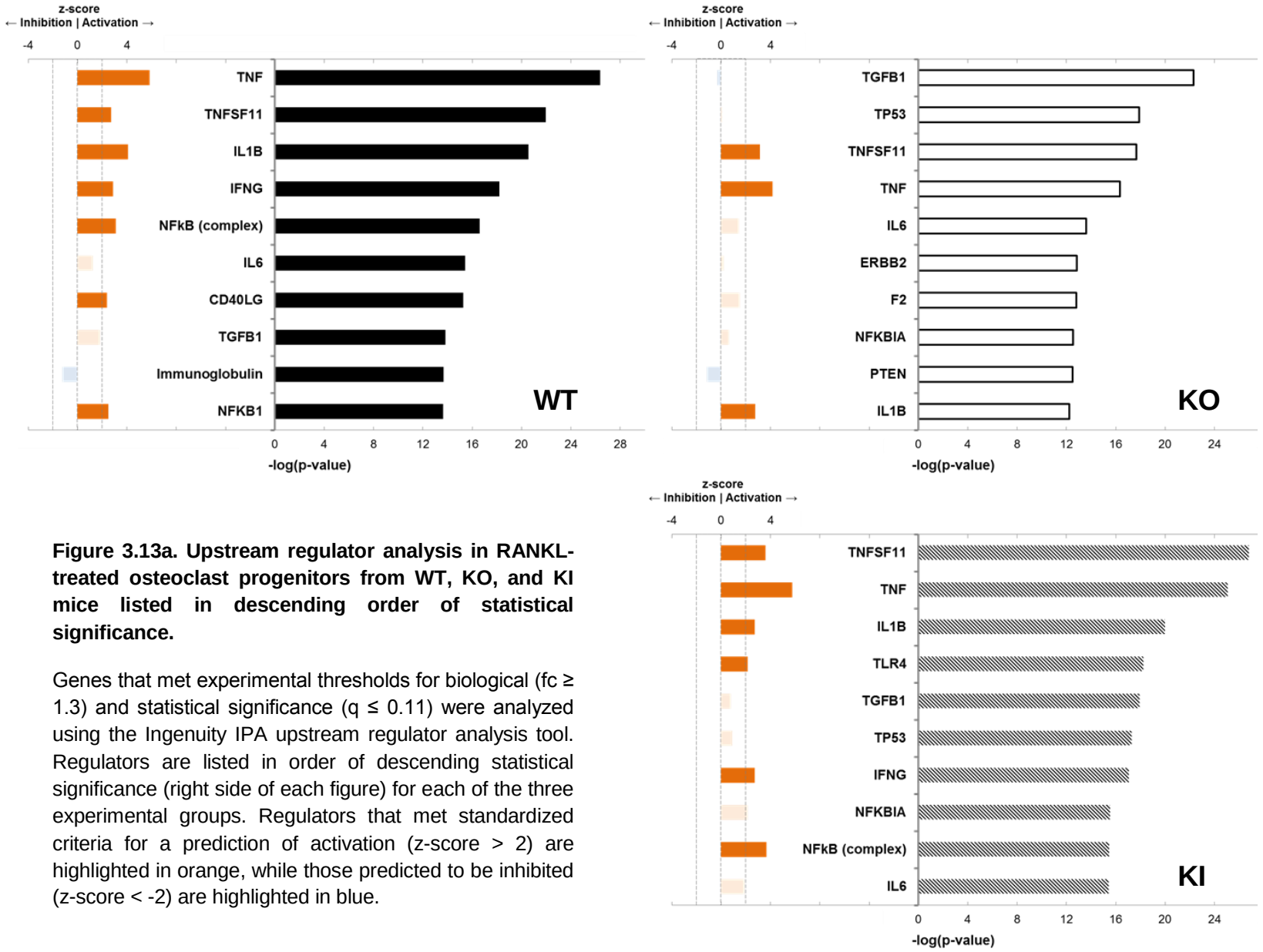

Figure 3.13a. Upstream regulator analysis in RANKL-treated osteoclast progenitors from WT, KO, and KI mice listed in descending order of statistical significance.

Genes that met experimental thresholds for biological (fc ≥ 1.3) and statistical significance (q ≤ 0.11) were analyzed using the Ingenuity IPA upstream regulator analysis tool. Regulators are listed in order of descending statistical significance (right side of each figure) for each of the three experimental groups. Regulators that met standardized criteria for a prediction of activation (z-score > 2) are highlighted in orange, while those predicted to be inhibited (z-score < -2) are highlighted in blue.

On the right hand side of each plot is a series of upstream regulators listed in descending order of enrichment strength (quantified, as noted above by a modified Fisher's exact score). On the left hand side, an independent, literature-based z-score offers a quantitative prediction about the activation status of each regulator.

A few points are noteworthy in this regard. First, for each genotype, the regulator that combines the highest prediction of activation and the greatest enrichment status is TNFSF11, otherwise known as RANKL, the very cytokine we used to stimulate our osteoclast progenitors (Figures 3.13b, 3.13c, 3.13d). This validation for the IPA URA tool, albeit internal, provided us with some measure of confidence for subsequent analyses.

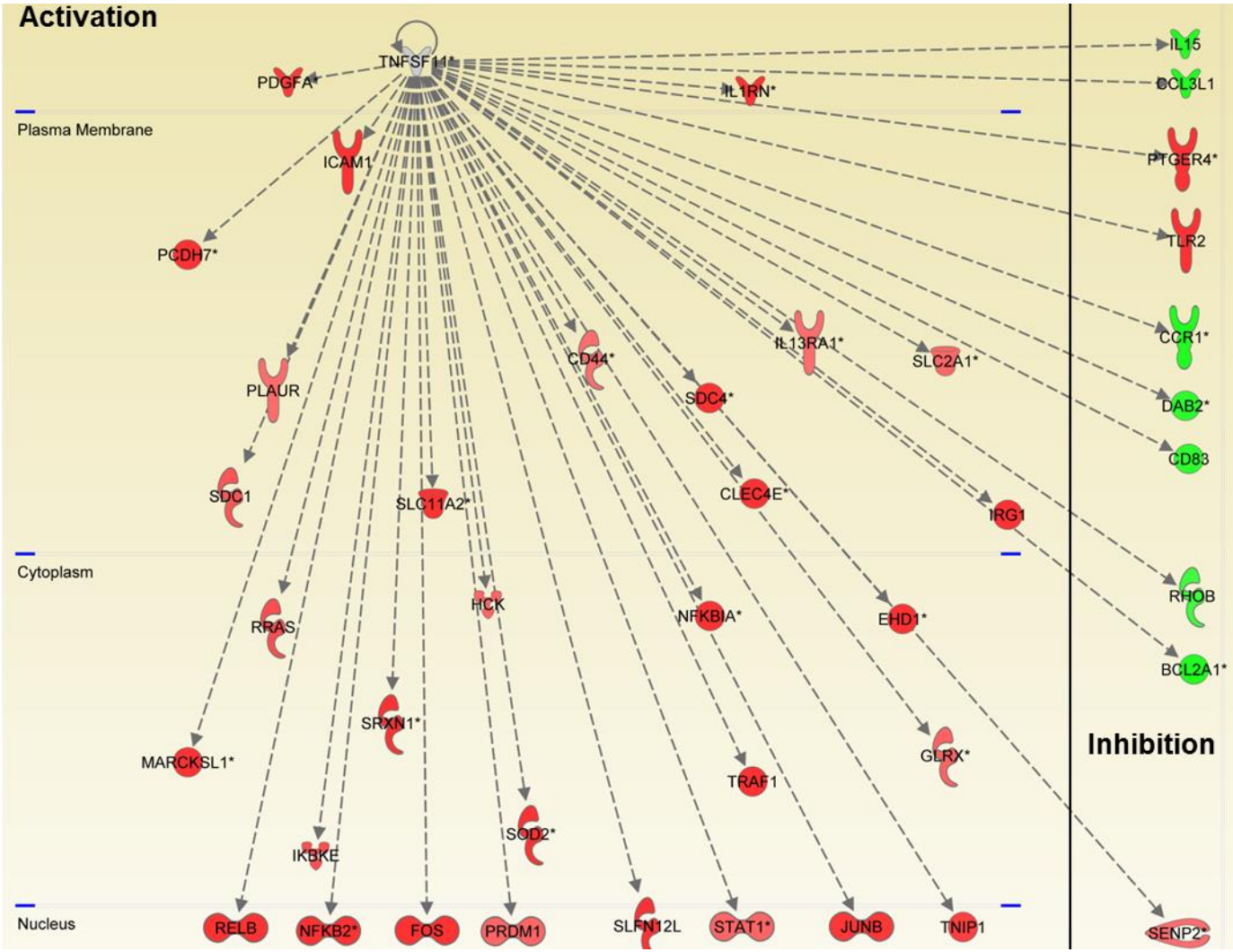

Figure 3.13b. Upstream regulator analysis of the WT gene expression set predicts that TNFSF11 (RANKL) is robustly activated. All 297 genes that were up- and down- regulated in the WT experimental group were submitted to IPA's URA tool. This chart displays the subset of gene products they encode that are regulated by RANKL. Gene products colored red and green were up- and down-regulated, respectively. Each gene product is listed on the left of the figure if its status (induction or repression) suggests that the upstream regulator is activated, and plotted on the right if its status (induction or repression) suggests that the upstream regulator is inhibited.

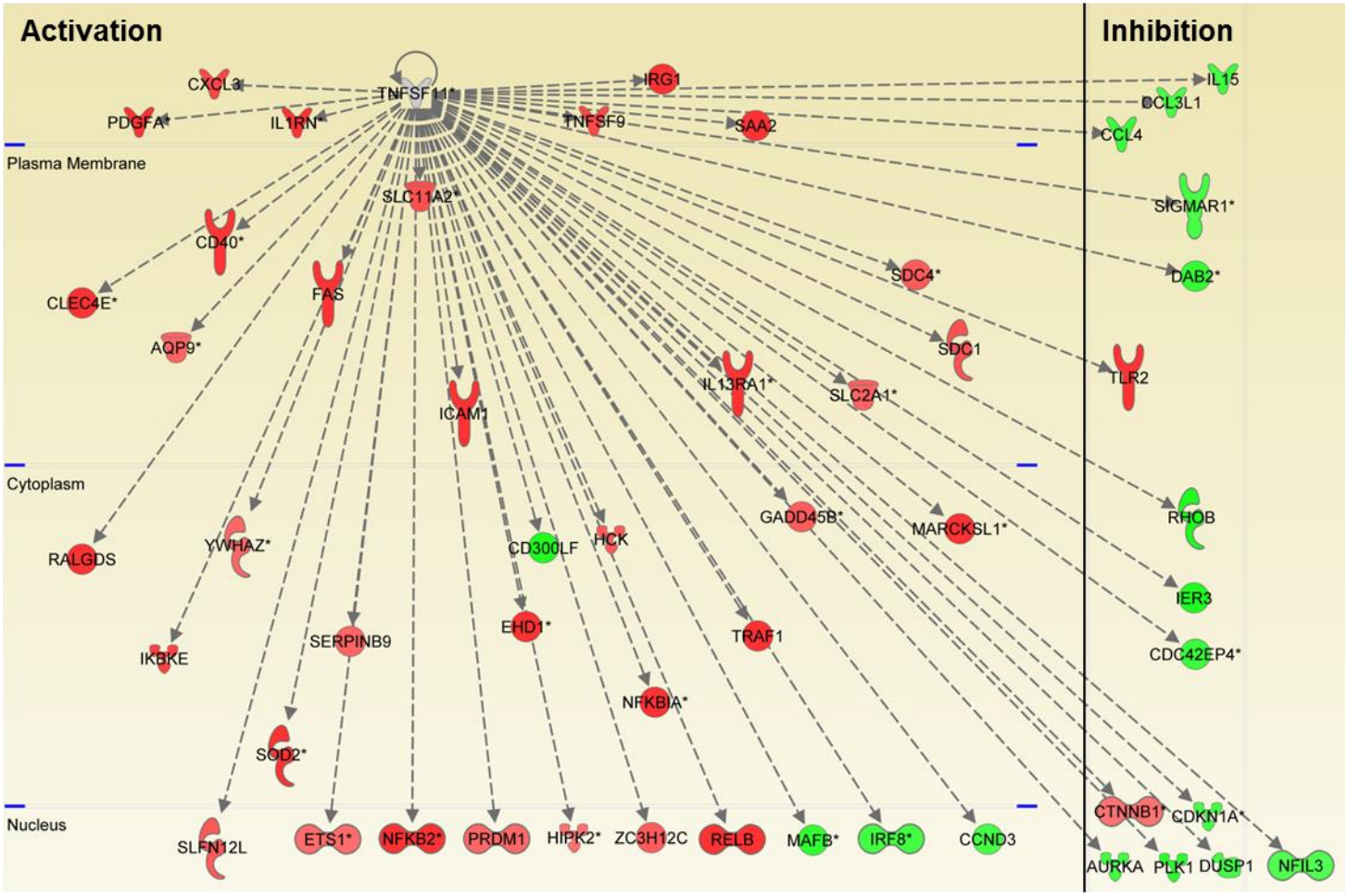

Figure 3.13c. Upstream regulator analysis of the KO gene expression set predicts that TNFSF11 (RANKL) is robustly activated. All 1057 genes that were up- and down- regulated in the KO experimental group were submitted to IPA's URA tool. This chart displays the subset of gene products they encode that are regulated by RANKL. Gene products colored red and green were up- and down-regulated, respectively. Each gene product is listed on the left of the figure if its status (induction or repression) suggests that the upstream regulator is activated, and plotted on the right if its status (induction or repression) suggests that the upstream regulator is inhibited.

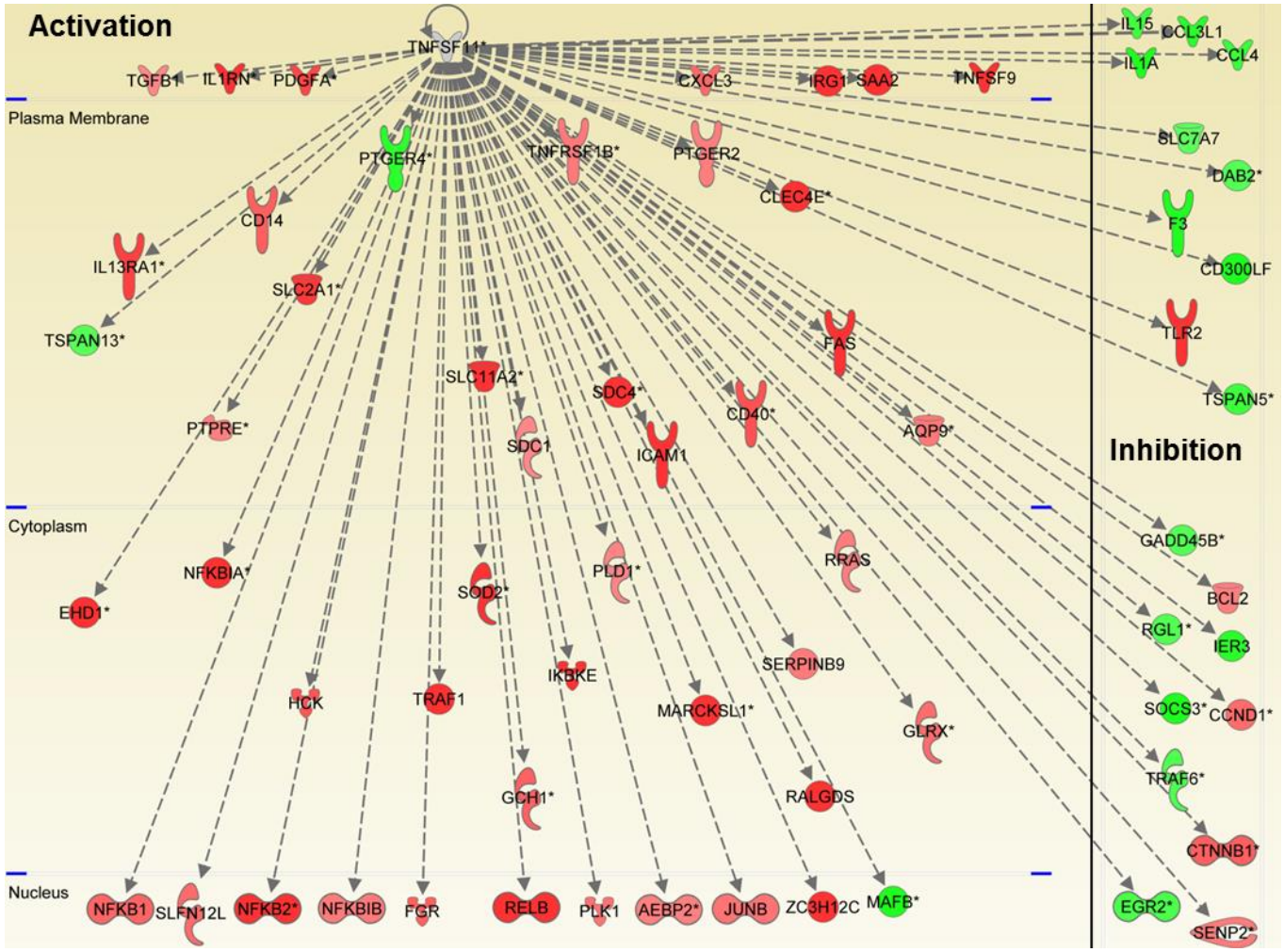

Figure 3.13d. Upstream regulator analysis of the KI gene expression set predicts that TNFSF11 (RANKL) is robustly activated. All 959 genes that were up- and down- regulated in the KI experimental group were submitted to IPA's URA tool. This chart displays the subset of gene products they encode that are regulated by RANKL. Gene products colored red and green were up- and down-regulated, respectively. Each gene product is listed on the left of the figure if its status (induction or repression) suggests that the upstream regulator is activated, and plotted on the right if its status (induction or repression) suggests that the upstream regulator is inhibited.

Next, we sorted enriched upstream regulators by predicted activation and inhibition. We were most struck by the abundance of regulators known to participate in the NFκB signaling pathway (Figure 3.14a).

Intriguingly, there was a greater divergence among the most inhibited regulators across the three genotypes. Specifically, several microRNAs were predicted to be inhibited in the WT and KI gene expression sets, but not in the p62 KO set (Figure 3.14b). This is most likely because a sufficient number of transcripts normally targeted for degradation or translational repression by these microRNAs are induced in KI and WT data sets to suggest that the pertinent microRNA are not active – and raises the interesting possibility that p62 may regulate microRNA function during osteoclastogenesis.

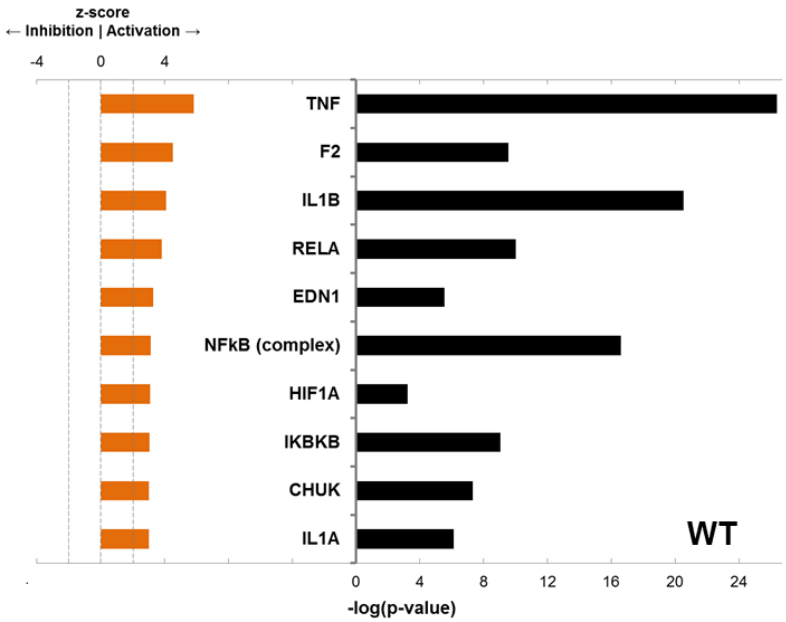

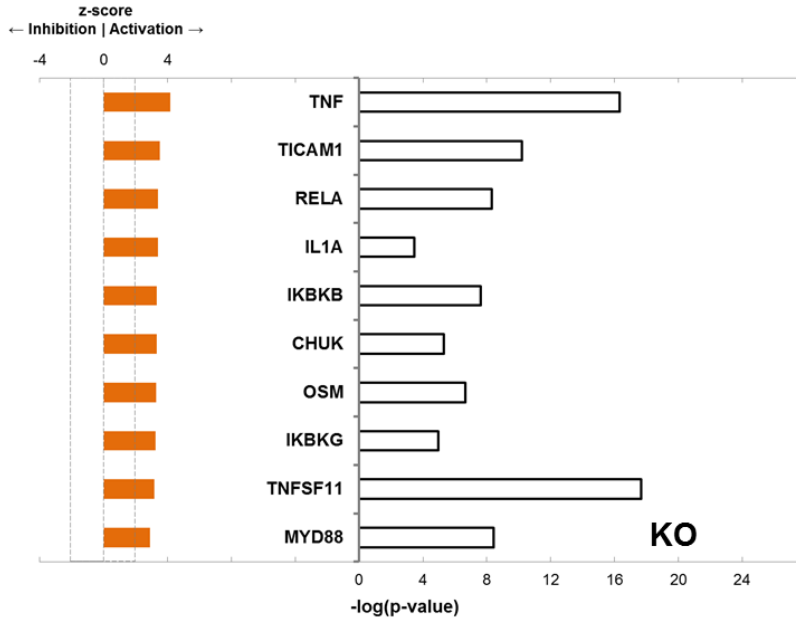

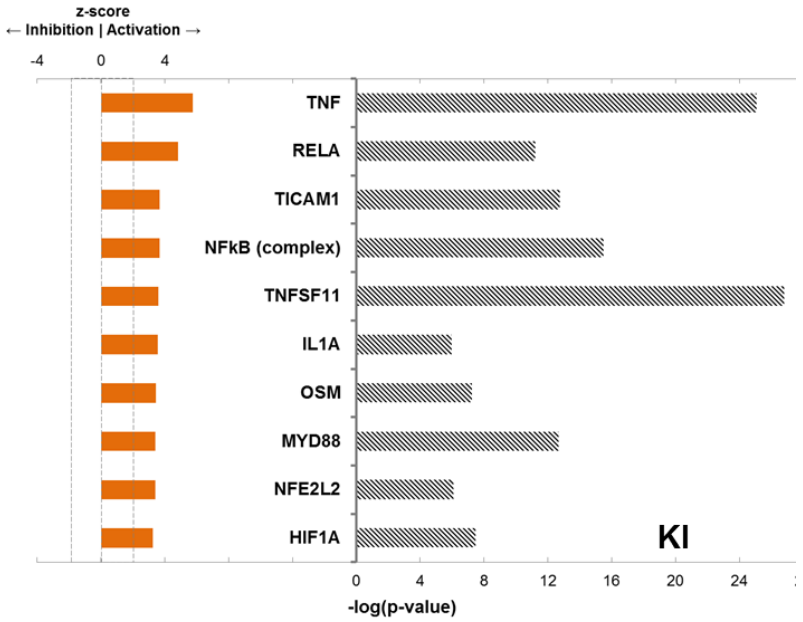

Figure 3.14a. Upstream regulator analysis in RANKL-treated osteoclast progenitors from WT, KO, and KI mice listed in descending order of predicted activation.

Genes that met experimental thresholds for biological (fc ≥ 1.3) and statistical significance (q ≤ 0.11) were analyzed using the Ingenuity IPA upstream regulator analysis tool. Regulators that met standardized criteria for a prediction of activation (z-score > 2) are highlighted in orange. Regulators are listed in descending order of activation (left side of each figure) for each of the three experimental groups.

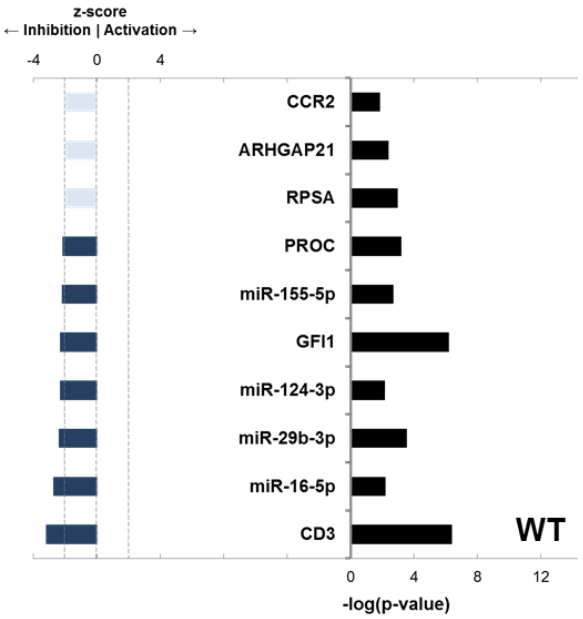

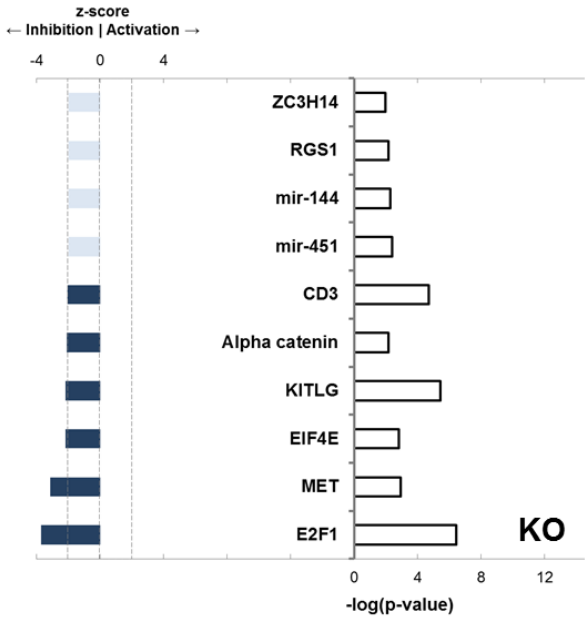

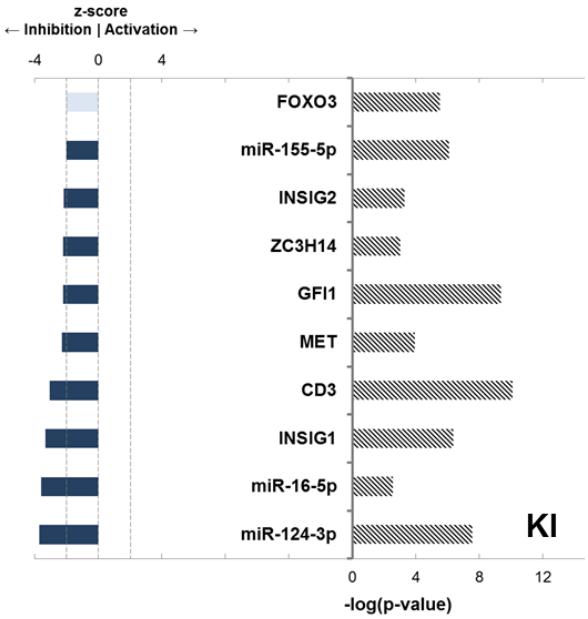

Figure 3.14b. Upstream regulator analysis in RANKL-treated osteoclast progenitors from WT, KO, and KI mice listed in descending order of predicted inhibition.

Genes that met experimental thresholds for biological (fc ≥ 1.3) and statistical significance (q ≤ 0.11) were analyzed using the Ingenuity IPA upstream regulator analysis tool. Regulators that met standardized criteria for a prediction of inhibition (z-score < -2) are highlighted in blue. Regulators are listed in increasing order of predicted inhibition (left side of each figure) for each of the three experimental groups.

To review the upstream regulators in a more systematic manner, and ideally develop and refine the hypotheses that originated with our gene annotation enrichment analyses, we generated Venn diagrams of overlap for our newly generated upstream regulators, relaxing inclusion criteria from a z-score of 2 to a z-score of 1.9 to reduce artifactual differences (Figure 3.15).

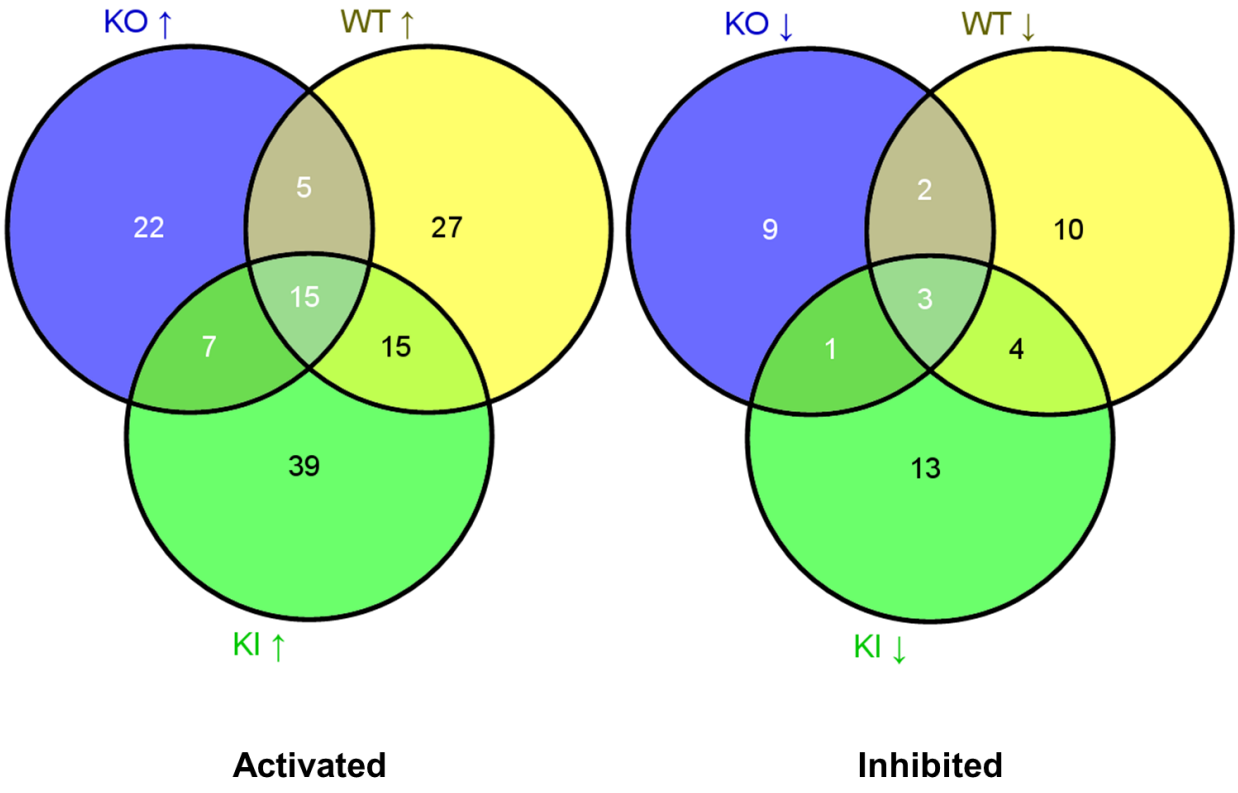

Figure 3.15. Overlap of upstream regulators predicted to be activated (↑) and inhibited (↓) in RANKL-treated osteoclast progenitors from KO, WT, and KI mice. Genes that met experimental thresholds for biological (fc ≥ 1.3) and statistical significance (q ≤ 0.11) were submitted to the Ingenuity IPA upstream regulator analysis tool. Regulators were then compared across genotypes as listed using Venny. A critical selection of regulators predicted to be phenotypically relevant is identified in the following figures.

As before, we observed that upstream regulators that were commonly predicted to be active or inhibited in response to RANKL across the three genotypes, WT, KO, and KI, were not likely to be significantly regulated by p62 (Figure 3.16). Most significantly, we were struck by the abundance of inflammatory mediators and members of NFκB signaling pathway, namely RelA (p65) a key transcription factor in the classical or canonical pathway, IKBKB (IKKβ) an upstream kinase, CHUK (IKKα) a member of the IKK complex, and so on (Figure 3.16). That NFκB signaling appears to be activated independent of p62 status was particularly striking to us given the important role previously ascribed to it in this cascade (Durán et al., 2004; Layfield, 2007). We returned to this hypothesis, testing the presence and interaction of several downstream intermediaries in the RANK-NFκB signaling pathway using immunoblotting and Co-immunoprecipitation, and report the results in the next chapter.

We also found the common prediction of inhibition for the regulators CD3 (the T-cell co-receptor protein complex) and GFI1 (growth factor 1 independent transcription repressor) very interesting. GFI1, in particular, plays a negative role in the proliferation of hematopoietic stem cells, maintaining their self-renewal and preserving their functional integrity (Duan and Horwitz, 2005). Moreover, GFI1 signaling is required for B and T-cell development, but antagonizes differentiation along the monocyte/macrophage lineage (Duan and Horwitz, 2005). That GFI1 and CD3 are predicted to be inhibited in RANKL-treated cells of all 3 genotypes supports the hypothesis that early differentiation of hematopoietic precursors along the monocyte/macrophage lineage, and apart from the lymphoid lineage, is also p62-independent (Figure 3.16). To this end, we used flow cytometry to measure the expression of osteoclast progenitor-specific cell surface markers during early RANKL-mediated osteoclastogenesis and report the results in the next chapter.

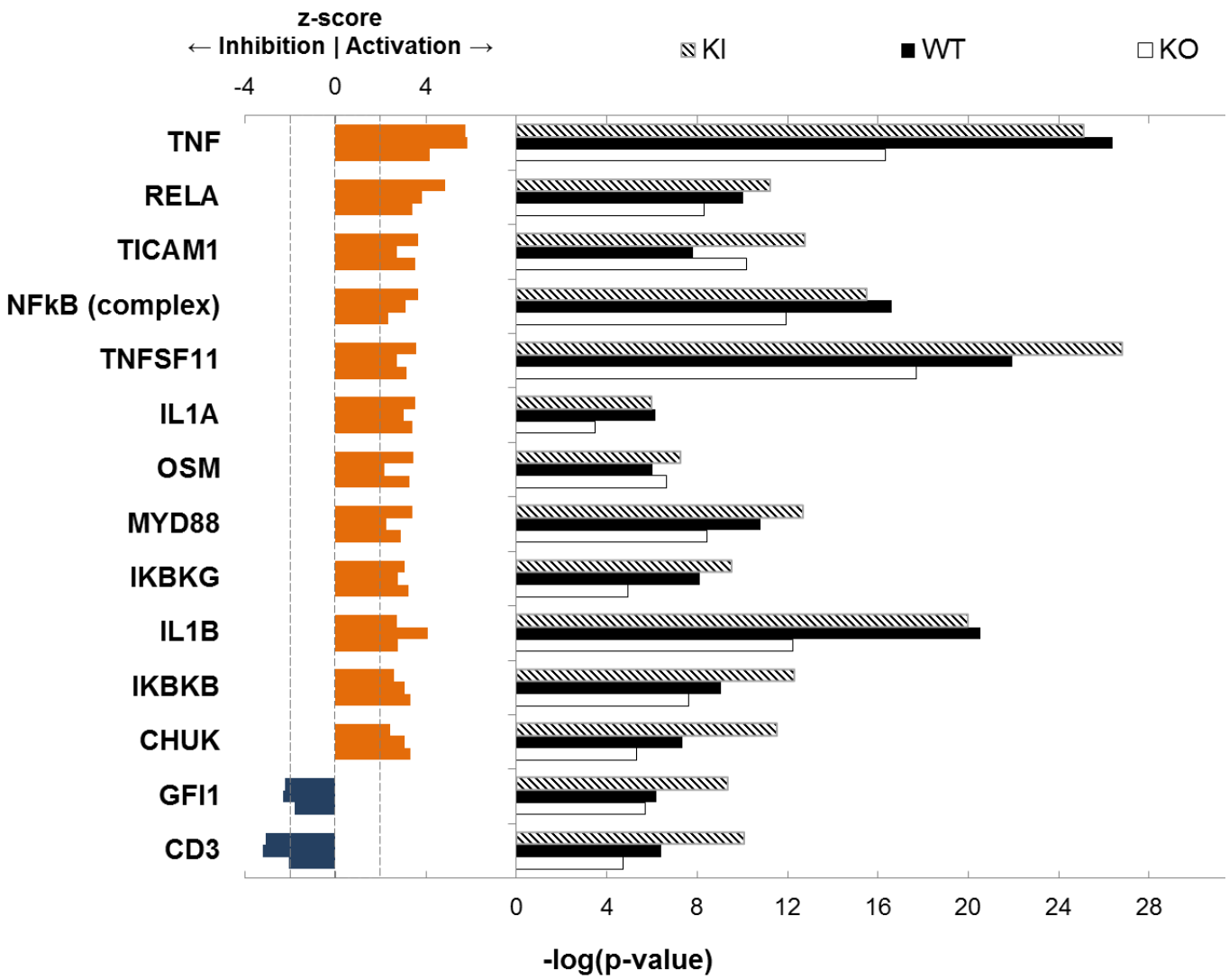

Figure 3.16. Overlap of upstream regulators predicted to be commonly activated (↑) and inhibited (↓) in RANKL-treated osteoclast progenitors from KI, WT, and KO mice.

Next, we reviewed the set of regulators predicted to be activated or inhibited in the WT and KI experimental sets, exclusively (Figure 3.17). Here, we reasoned that differentially activated mediators discovered in this set might better explain measured deficiencies in the KO phenotype. Most notably, Nuclear factor (erythroid-derived 2)-like 2 (NFE2L2 or NRF2), a transcription factor and master transcriptional regulator of the oxidative stress response, was predicted to be both highly activated and highly enriched in this data set in RANKL-treated WT and KI cells, but not in KO cells. As noted earlier, NRF2 is constitutively ubiquitinated and degraded by the proteasome under non-stressed conditions (Nezis and Stenmark, 2012). However, in the presence of electrophiles or ROS, its cytoplasmic inhibitor, KEAP1, is either inactivated or competitively displaced by p62, permitting NRF2 translocation into the nucleus, and the up-regulation of several detoxifying and antioxidant genes (Figure 1.7). It has previously shown that RANKL-stimulation of osteoclast progenitors increases intracellular ROS through a signaling cascade involving TRAF6 (Lee et al., 2005) and that p62 is also an NRF2-target, forming a positive-feedback loop in the antioxidant response (Jain et al., 2010). In this manner, two hypotheses present themselves: Either (1) KO cells have an impaired NRF2 signaling response because RANKL-mediated ROS production cannot displace the KEAP1-NRF2 interaction in the absence of p62, NRF2 remains persistently degraded and cannot translocate into the nucleus, and the antioxidant response is therefore never able to be appropriately mounted; or (2) RANKL-treated KO cells never generate sufficient ROS to stimulate NRF2 displacement and translocation. To help resolve this ambiguity, preliminary measures of RANKL-dependent ROS generation and NRF2 displacement into the nucleus were made. Results are described in the following chapter.

This analysis also suggests that during RANKL-stimulation of bone marrow derived precursors, p62 may regulate osteoclastogenesis through additional signaling pathways.

These include those mediated by protein kinase C-delta (PRKCD), mammalian target of rapamycin (activated), and mir-124 (repressed), in WT and KI, but not KO progenitors (Figure 3.17). When ablated genetically, PRKCD has been shown to impair lysosomal exocytosis of the critical secreted, proteolytic enzyme cathepsin K, resulting in mice with increased bone density (Cremasco et al., 2012). mTOR, an evolutionarily conserved serine/threonine protein kinase in the phosphoinositide 3-kinase (PI3K)-related kinase family, has been shown to promote osteoclastogenesis by altering translation initiation and isoform production of the critical transcription factor C/EBPβ in bone marrow derived osteoclast progenitors (Smink et al., 2009). When mTOR is inhibited genetically or pharmacologically, osteoclastogenesis is suppressed (Indo et al., 2013). Interestingly, p62 has been shown to interact with regulatory-associated protein of mTOR (Raptor), promoting nutrient sensing and cell growth by the mTOR complex 1 (Duran et al., 2011).

In contrast, microRNA-124 (miR-124) is a small non-coding RNA associated with inhibited proliferation and motility of osteoclast precursors, and decreased expression of the master osteoclastogenic transcription factor, NFATc1, but not NFκB or c-Fos (Lee Y et al., 2013). Interestingly, it has been previously documented that within 6 hours of RANKL-treatment in bone marrow derived osteoclast progenitors, endogenous expression of miR-124 falls by 50% (consistent with predictions made in WT and KI but not KO cells), and after 48 hours, less than 10% of miR-124 expression was detectable compared to that of untreated control, suggesting that this microRNA plays a physiological role (Lee, Y et al., 2013).

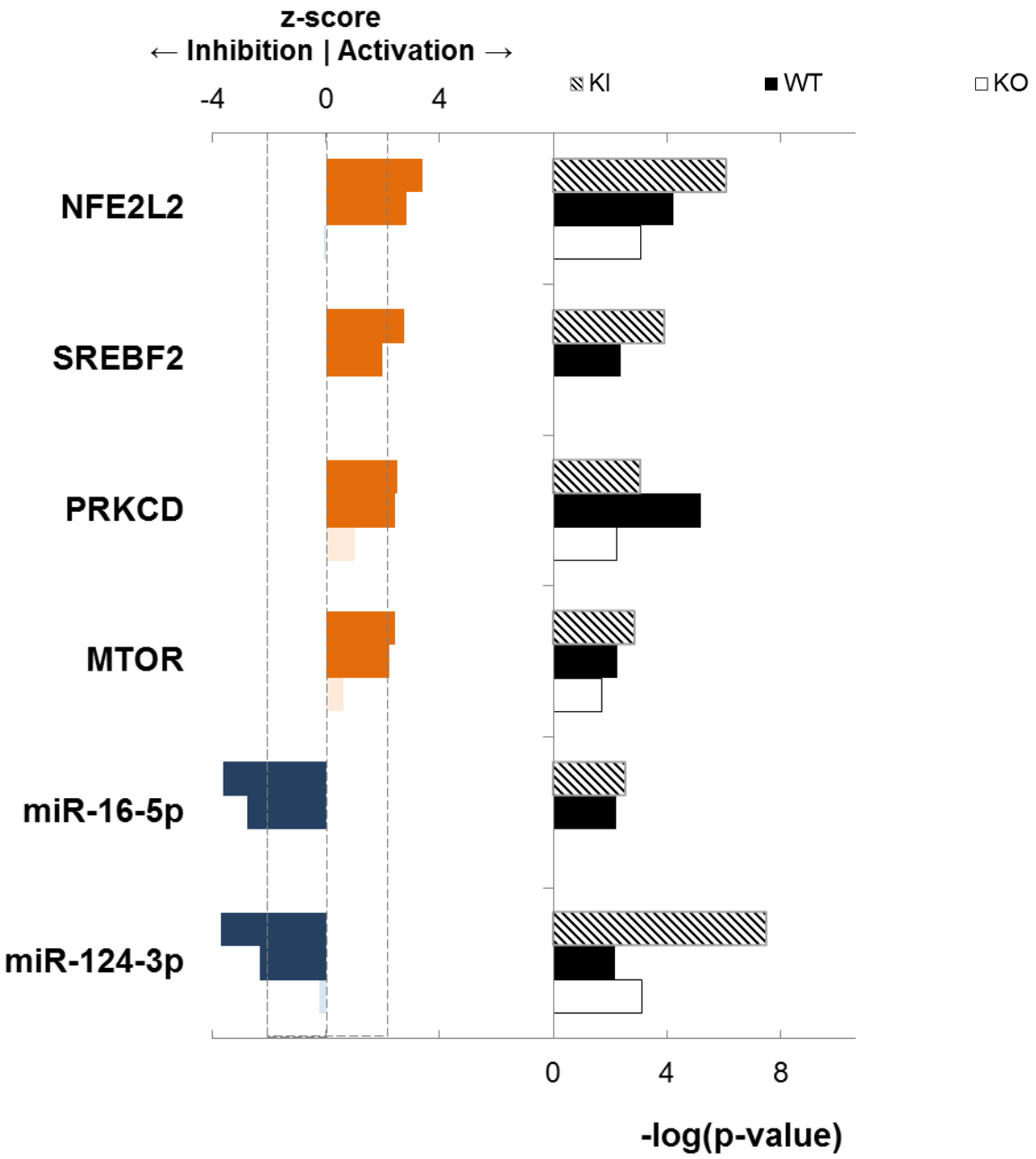

Figure 3.17. Upstream regulators predicted to be commonly activated (↑) and inhibited (↓) in RANKL-treated osteoclast progenitors from WT and KI mice.

Next, we investigated the upstream regulators that were predicted to be activated or inhibited in response to RANKL exclusively in KO cells (Figure 3.18). Several factors stood out in our analysis: RBL1 or p107, a key regulator of entry into cell division and potent inhibitor of cell cycle genes and let-7, a microRNA that has been shown to represses proliferation in human cells (Johnson et al., 2007), are predicted to be activated, while: E2F1, a transcription factor involved in cell proliferation; EIF4E, Eukaryotic translation initiation factor 4E, which plays a role in bringing mRNA to the pre-initiation complex during eukaryotic translation, are predicted to be inhibited. When taken individually, each regulator may only be modestly inhibited or activated. However, when taken together, a picture emerges of impaired cellular proliferation (Figure 3.18) in RANKL-treated KO cells that is not found in similarly treated WT or KI cells. The hypothesis that RANKL-treated KO cells are characterized by impaired proliferation was tested using a DNA synthesis assay (BrdU), while a cellular activity assay (MTT) was included to control for differing levels of viability. Results are reported in the following chapter.

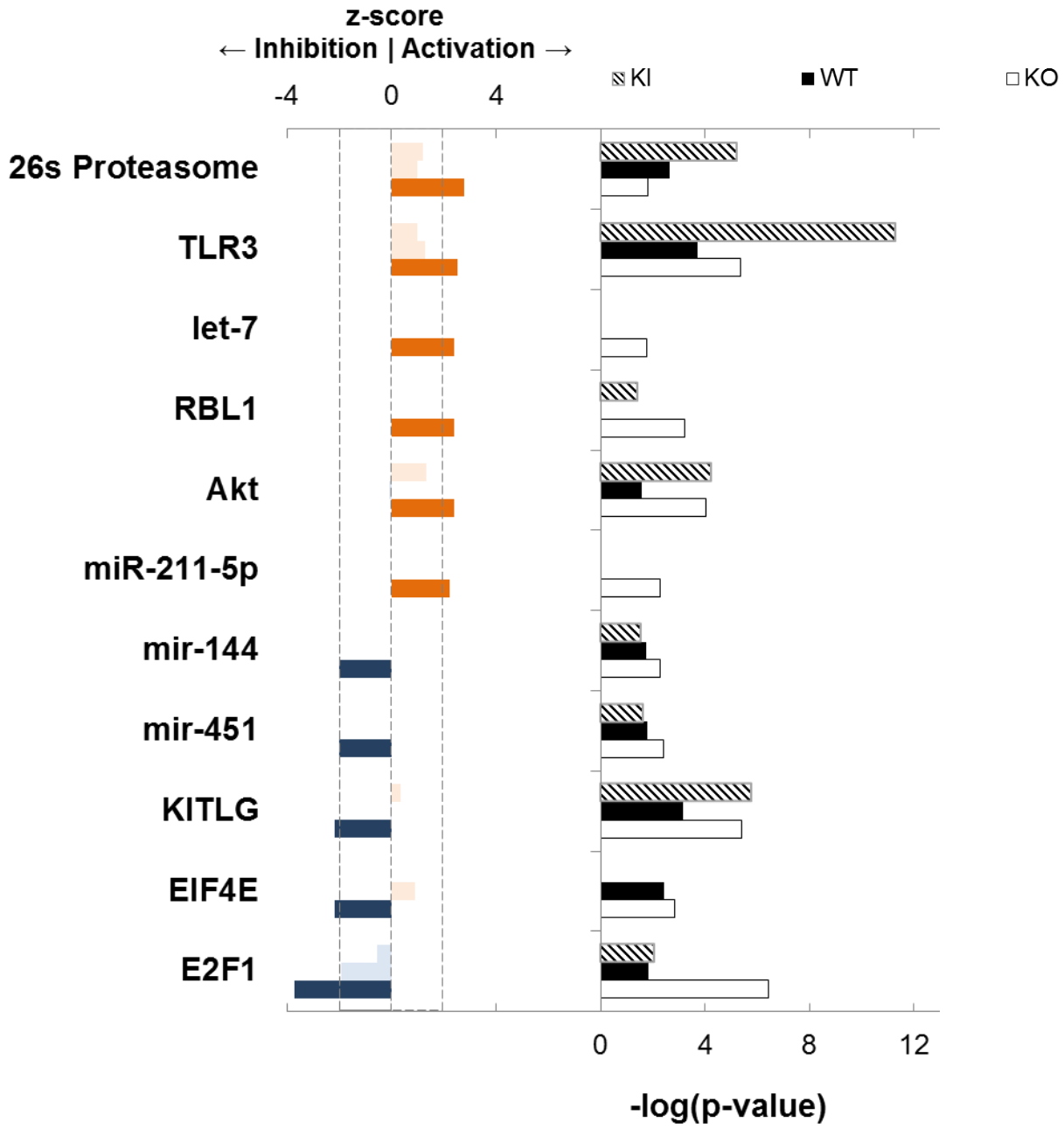

Figure 3.18. Upstream regulators predicted to be activated (↑) and inhibited (↓) in RANKL-treated osteoclast progenitors from KO mice only.

Finally, we turned to upstream regulators predicted to be activated and inhibited in RANKL-stimulated KI osteoclast progenitors, exclusively, hoping to gain insight into what drives hypersensitivity to RANKL in progenitors and osteopenia in vivo observed in the preceding chapter (Figure 3.19). Notably, two regulators previously associated with osteoclast phenotypes were predicted to be activated in KI cells alone. First among these was X-box binding protein 1 (XBP1), an evolutionarily conserved transcriptional effector that is activated in response to ER stress and required for the up-regulation of a host of genes that clear misfolded proteins (Acosta-Alvear et al., 2007) and has been previously shown to support myeloma cell growth and osteoclast formation (Xu et al., 2012). The second was CD38, an NAD+ degrading enzyme whose activation in the osteoclast triggers Ca^{2+} release and increased secretion of IL-6 (Sun et al., 2003). This is notable because IL-6 is elevated in PDB patients (Werner de Castro et al., 2014), and has been demonstrated to play a critical role in the formation of pagetic lesions, in vivo, and increased responsivity of osteoclast progenitors to 1,25-$(OH)_2D_3$, in vitro, in multiple PDB models (Kurihara et al., 2011; Teramichi et al., 2013). In contrast, B-cell lymphoma 6 protein (BCL6), a transcriptional repressor of NFATc1 whose overexpression inhibits osteoclastogenesis in vitro and ablation accelerates osteoclast differentiation and osteoporosis (Miyauchi et al., 2010), was predicted to be inhibited in KI cells alone (Figure 3.19).

Less has been published about the potential role played in osteoclastogenesis by additional factors identified in this analysis. IL-5, a cytokine that acts as a growth and differentiation factor for B cells and eosinophils, was also predicted to be activated exclusively in KI cells in our analysis (Figure 3.19). Interestingly, IL-5 has previously been shown not to affect osteoclast formation in vitro (Miyamoto et al., 2001), but has also been shown to dramatically increase extramedullary hematopoiesis and the numbers of granulocyte-macrophage, macrophage, eosinophil, and B-

lymphocyte progenitors in the peripheral blood and spleens of transgenic mice that overexpress this cytokine compared to wildtype (Khaldoyanidi et al., 2003). HDAC which in IPA's analysis refers to the broad category of histone deacetylases rather than a particular member of this group was also predicted to be activated in the present analysis in KI cells alone (Figure 3.19). Interestingly, the broad inhibitor of HDAC activity, trichostatin A (TSA) has been shown to suppress osteoclastogenesis (as well as RANKL formation, NFκB activation, bone resorption pit formation) by down-regulating c-Fos and NFATc1 in RAW 264.7 cells, likely by altering C/EBPβ (Williams et al., 2011). Moreover, different HDAC family members have differing effects on osteoclastogenesis, as suppression of HDAC3 and HDAC7 expression inhibits and accelerates osteoclast formation, respectively, in vitro (Pham et al., 2011). Finally, we may note that p62 has been shown to complex with HDAC6 (via an undefined region between p62's ZZ and TRAF6-binding domain) and that its ablation results in hyperactivation of HDAC6 and deacetylation of α-tubulin and cortactin in vitro (Yan et al., 2013). That said, drilling deeper into our data reveals that after 8 hours of RANKL-stimulation, none of the individual HDAC members queried (1, 3, 4, 5, 6, or 10) by IPA were predicted to be activated or repressed in our data set (data not shown), so further testing will be required to clarify whether PDB-associated mutations affect specific HDAC-mediated signaling during osteoclastogenesis.

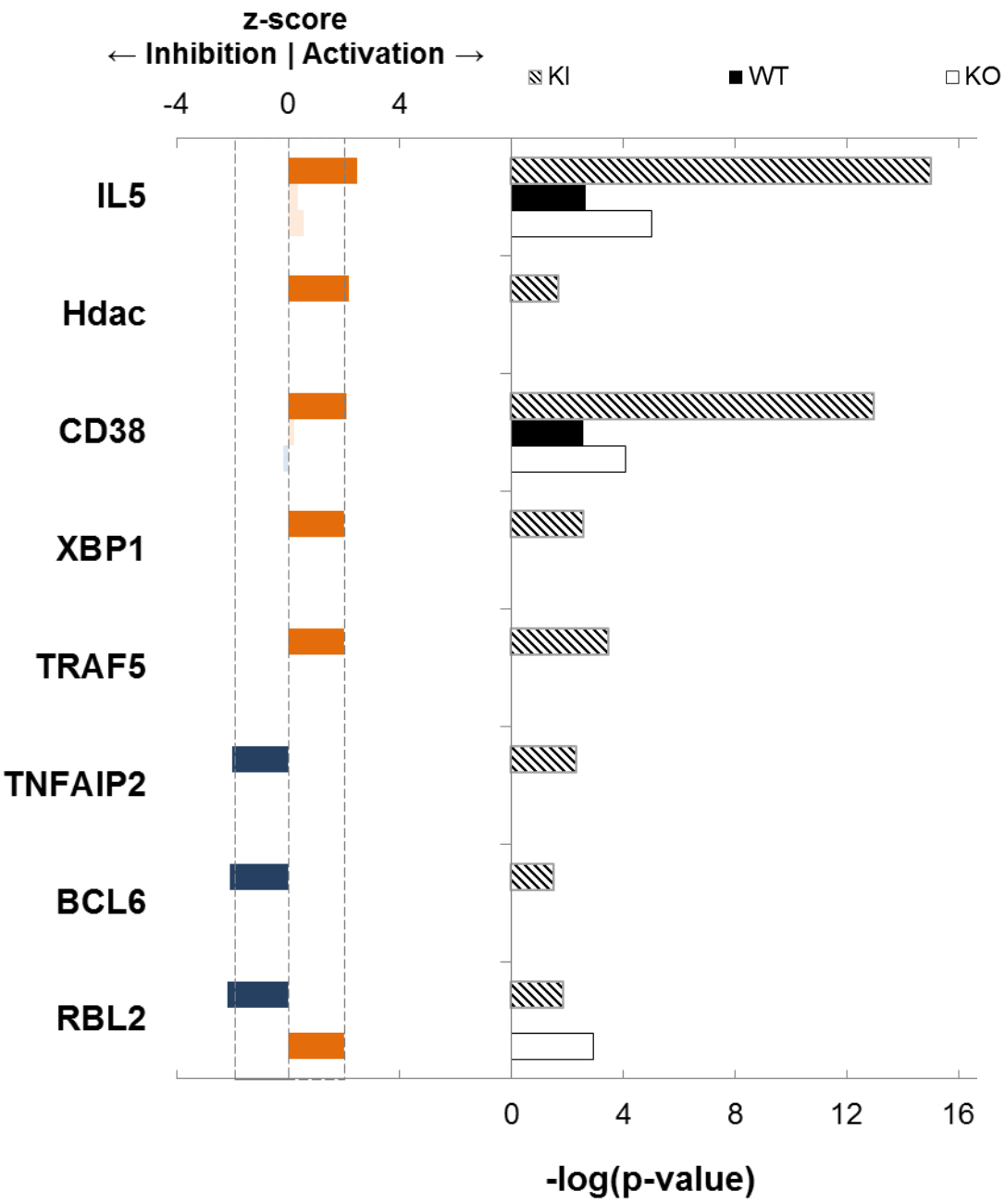

Figure 3.19. Upstream regulators predicted to be activated (↑) and inhibited (↓) in RANKL-treated osteoclast progenitors from KI mice only. Note that Rbl2 is predicted to be inhibited in KI cells and activated in KO cells.

3.4 Discussion

In this chapter, we sought to shed light on how genetic alteration at the p62 locus mediates normal and dysregulated osteoclastogenesis following RANKL stimulation - using gene expression profiling of bone marrow derived progenitors obtained from WT, KO, and KI mice. In the process, we have identified several hypotheses using gene annotation enrichment, upstream regulator analysis, and pattern analysis that may be summarized as follows. In bone marrow derived osteoclast progenitors treated with RANKL:

1. p62 may be dispensable for RANKL-mediated NFκB signaling and early differentiation of hematopoietic precursors toward the monocyte/macrophage lineage and apart from the lymphoid lineage during early osteoclastogenesis.
2. Ablation of p62 may impair cellular proliferation, cell cycle progression, or mitochondrial integrity, and thereby impair osteoclastogenesis.
3. Ablation of p62 may impair the NRF2-mediated oxidative stress response, protein kinase C delta (PRKCD) function, or mammalian target of rapamycin (mTOR) signaling, and thereby impair osteoclastogenesis.
4. p62 may mediate microRNA-124 turnover – and the absence of p62 may be associated with enhanced microRNA-124 signaling and impaired osteoclastogenesis.
5. P394L mutation of p62 may be associated with an increase in the unfolded protein stress response via XBP1, and thereby enhance osteoclastogenesis.
6. P394L mutation of p62 may be associated with increased CD38 signaling and IL-6 production, and thereby enhance osteoclastogenesis.
7. P394L mutation of p62 may be associated with decreased BCL6 signaling and thereby enhance osteoclastogenesis.

These results are significant because they are inconsistent with the most commonly accepted paradigm as to how p62 contributes to osteoclast formation, offer alternative explanations to results obtained by previous investigators, and present several novel, testable theories as to how PDB-associated mutation to p62 might contribute to increased osteoclastogenesis in PDB. Furthermore, they were generated via unbiased analysis of gene expression profiling data via DNA microarray on primary cultures obtained from genetically-modified animals on the C57Bl/6J background. This experimental design mitigates confounders such as inconsistent or supra-physiologic expression levels with pharmacologic models, strain-dependent background differential gene expression (Turk et al., 2004), and bias in target-selection inherent in limited gene expression profiling studies using RT-PCR. Indeed, the advantages conferred by using DNA microarray to develop our hypotheses, chief among them the ability to monitor expression levels of several thousand genes simultaneously in a time and cost-effective single experiment, are clear. Yet the task of searching for determinants of phenotype using gene expression levels is also fraught with many assumptions, potential sources of error, and limitations that must be acknowledged (Draghici et al., 2006).

First and foremost, we must acknowledge that our results are preliminary and must be reproduced via external validation and further experimentation, a process which is partially undertaken in the subsequent chapter. This is because reproducibility remains the greatest concern with gene expression profiling using microarray technology. Indeed, in 2009, three clinical trials were suspended at the Duke University Medical Center because genomic signatures used to select cancer therapies were found to be irreproducible (Baggerly, 2010). Although this particular case was later to have been complicated by additional personal and scientific misconduct, and later terminated (Reich, 2011), the challenge of inter-experimental reproducibility is well documented in the literature. In 2009, for example, 18 microarray articles that had been published in *Nature*

Genetics between 2005 and 2006 were evaluated for reproducibility. Of these, 2 were found to be reproducible, 6 were partially reproducible with some discrepancies, and 10 could not be reproduced (Ioannidis et al., 2009). Beyond insufficient data reporting and annotation, past challenges with this technology, including probe-set heterogeneity and change over time, laser-scanner readout variability, result platform-dependence, and additional sources of bias and artifact, have contributed to irreproducibility (Irizzary et al., 2005). Over time, however, multiple reviews and recommendations by organizations such as the MicroArray Quality Control (MAQC) consortium have led to the establishment of quality control standards, implemented in the design and analysis phases of the current study, that maximize accuracy, precision, sensitivity, and cross-platform reproducibility (MAQC Consortium, 2010). Further, intrinsic, limitations in gene expression profiling using microarray include deficiencies in our ability to measure products of alternative splicing or functionally important genes that are not highly expressed, as well as knowledge gaps in gene annotation, function, and correlation with translation (Oliver and Malone, 2011).

In the current study, more specific experimental design limitations include the number of experimental endpoints and biological replicates we were able to explore given financial and temporal constraints. We selected the 8 hour time point to assess how the transcriptome is altered during early osteoclast formation in response to RANKL treatment, while controlling for the effects of serum and M-CSF, which have been shown to increase, and thereby mask, or alter mRNA expression (Schmittgen TD and Zakrajsek, 2000; Cappellen et al., 2002). To have had an additional set of arrays at the zero time point as an additional control would have been ideal, and indeed, an initial attempt to conduct the experiment in this manner was attempted. However, insufficient RNA yields and the physical challenge of working with so many samples limited our

experimental design to the one employed presently. Additionally, our samples were not simply technical replicates because each of our 18 arrays (3 replicates x 2 treatments x 3 genotypes) came from a single plate of related, but not identical cells. It must be acknowledged, however, that these samples cannot be called true biological replicates, because samples were pooled by genotype early during progenitor preparation, before being aliquoted into individual plates. While not ideal, this step was required to control and normalize for gender, age, and, in the case of wildtype samples (which were culled from the progeny of both KO and KI heterozygotes) colony of origin.

In parallel with these design issues, several additional considerations must be borne in mind with respect to data analysis. First, as noted earlier, we selected cut-offs for significance at fold change ≥ 1.3 and false discovery rate ≤ 0.1. While these appear to be relatively relaxed criteria, we found that the patterns of analysis were relatively robust to cut-off value selections. Moreover, we reasoned that there may be patterns of gene expression change that, taken in aggregate, unveil greater information about broad patterns of regulation. Indeed, there are important historical precedents for such an approach. In one example, investigators published reports in which they identified sets of genes involved in oxidative phosphorylation with reduced expression in diabetic patients. None of the genes were repressed or down-regulated by more than 20% individually, but as a group their coordinated down-regulation was significant. Taken together with subsequent work, this analysis led to an improved understanding of the regulation of oxidative phosphorylation, as many of the components of this pathway turned out to be controlled by the PGC-1α transcription factor, which itself, was later found to be down-regulated in diabetic patients (Mootha et al., 2003; Mootha et al., 2004; Cunningham et al., 2007). Second, it might be argued the upstream regulator analysis tool utilized to generate hypotheses is built upon a database that is dynamic and constantly updated, on the one hand, yet proprietary, and, to a certain extent,

arbitrary. Do findings about relationships in other species always pertain to findings in mammalian cells? Is it then appropriate to always use such results in calculating whether a regulator is predicted to be activated or inhibited in our findings? The answer in both cases is clearly not. Furthermore, what does a quantitative difference in an upstream regulator's enrichment score (or activation level) mean? In Figure 3.14a, for example, the activation scores for TNF, the upstream regulator most highly enriched in KO, WT, and KI analyses, are 4.3, 6.0, and 5.7 (with $z > 2.0$ corresponding to activation). Does this suggest that there is greater activation of TNF signaling in WT than in KI cells, and that they are much greater than in KO cells? In reply to these questions we must speak with less conviction, for all that can be said with certainty is that the pattern of gene expression in each comparison (treatment vs. control) is consistent with what we might expect if the TNF signaling pathway were activated and that we have some measure of confidence in the biological relevance of our results in that they confirmed that TNFSF11 (RANKL), the very cytokine experimentally used to induce osteoclastogenesis, was predicted to be robustly activated in each assay (Figure 3.13a, b, c, d). More importantly, perhaps, we note that this portion of our analysis was aimed to be exploratory and generative rather than confirmatory and definitive and that external experimental validation is required to increase our confidence in these results.

To summarize, in this chapter we utilized gene expression profiling to develop several novel hypotheses about the role of wildtype and PDB-associated mutant p62 in normal and dysregulated osteoclastogenesis, respectively. Interestingly, preliminary results have called into question whether p62 plays an important role in early RANK-TRAF6-NFκB signaling during early osteoclast formation. We take up each of these issues in the following chapter.

CHAPTER 4

VALIDATION OF MICROARRAY-GENERATED HYPOTHESES

4.1 Introduction

In the preceding chapter, we generated several novel hypotheses about the role played by p62 in normal and dysregulated osteoclastogenesis associated with Paget's disease of bone (PDB). We did so by utilizing gene expression profiling on RANKL-treated primary osteoclast progenitors obtained from wildtype (WT), p62 knock-out (KO), and PDB-associated P394L p62 knock-in mutants (KI), and compared them with vehicle-treated controls. Surprisingly, preliminary results suggested that p62 may be dispensable for NFκB signaling during early osteoclast formation, but impair proliferation, cell cycle progression, mitochondrial integrity, or the NRF2-mediated oxidative stress response, and thereby impair osteoclastogenesis. In contrast, a common PDB-associated p62 mutant was associated with a prediction of an increased unfolded protein stress response, CD38 signaling, or decreased BCL6 signaling, each of which may be associated with enhanced osteoclastogenesis. Key questions remain answered, however. Do p62-mediated alterations in RANK and TRAF6 expression manifest at the level of protein? Is early osteoclastogenesis or NFκB signaling altered by changes at the p62 locus? Are cell viability and proliferation truly altered in a p62-dependent manner? To help clarify the role played by p62 in

osteoclast formation and activation, we sought to test a selection of these hypotheses in the present chapter by tracking protein expression and the interaction of critical intermediaries in the RANK-NFκB signaling in response to RANKL stimulation, and functionally probing p62's effects on cellular differentiation, proliferation, viability, and reactive oxygen species (ROS) production.

4.2 Methods

Osteoclast progenitor formation for validation experiments

For all post-array validation experiments, including the BrdU cell proliferation assay, MTT activity assay, ROS production assay, Flow Cytometry (FC), Western blotting (WB), and Co-Immunoprecipitation (Co-IP), the standard procedure to generate osteoclast progenitors was used. Briefly, non-adherent marrow cells were plated at the following densities (1 x 10^5cells/well: 96-well plate for BrdU, MTT, and ROS; 2.5 to 3 x 10^6cells/mL: 6-well, 6cm plates for Flow Cytometry; and 3 x 10^6cells/mL: 10cm plates for WB, Co-IP) as previously described (Hiruma et al., 2008), and cultured in conditioning media (α-MEM + 10% FBS + 1% antibiotic/antimycotic) for 2 days in the presence of recombinant murine M-CSF (20ng/mL, R&D). Additional quantities of M-CSF and RANKL were delivered as noted in each experiment.

Flow cytometry

Osteoclast progenitors obtained from KO, WT, and KI mice were generated in 96 well plates as noted above. Staining was conducted using combinations of the following conjugated antibodies:

APC-CSF-1R (Biolegend 135509 APC-conjugated anti-mouse, CD115, which is the receptor for M-CSF, and PE-RANK (Biolegend 119806 PE-conjugated anti-mouse RANK, CD265, the receptor for RANK-ligand). Briefly, cells in cultures plates were gently washed with PBS and detached manually, incubated with Fc Block for mice, and then with an optimal dilution of the conjugated antibodies noted above. After washing to remove nonspecific antibody, cells were analyzed on the BD FACSCantoII (BD Bioscience) in the VCU Flow Cytometry Shared Resource and analyzed using the FCS Express 4 (De Novo Software) software package.

Antibodies used in this study include:

p62 (Novus, Ms monoclonal (2C11), H00008878-M01; WB- 1:100,000; ineffective CoIP)

TRAF6 (Enzo lifesciences, Rb polyclonal, ADI-AAP-426; WB- 1:2500; CoIP- 1:50 to 1:100)

RANK (Novus, Rb polyclonal, NB100-56396; WB- 1:1000)

IKKβ (Cell Signaling, Rb polyclonal (L570), 2678S; WB- 1:1000)

NEMO (Cayman, aka IKKγ Ms monoclonal (72C627), 13931; WB- 1:1000)

IκBα (Cell Signaling, Ms monoclonal (L35A5), 4814S; WB- 1:1000)

p65 (Santa Cruz, Ms monoclonal (F-6) aka NFκB p65 or RelA, sc-8008; WB- 1:200)

NRF2 (Abcam, Rb ploYclonal, ab92946; WB-1:1000)

β-actin (Santa Cruz, Ms monoclonal (C4), sc-47778 HRP; WB- 1:20,000 to 1:50,000)

nucleolin (Santa Cruz, Ms monoclonal (H-6) aka C23: sc-55486; WB- 1:1000)

Western blot and immunoprecipitation

For RANKL or M-CSF signaling, osteoclast progenitors were cultured as described above in 10cm culture plates. Cells were then stimulated with 100ng/mL recombinant murine RANKL (R&D) for various times. Before lysis, 10x buffer (Cell signaling 9803), composed of 20 mM Tris-HCl (pH 7.5), 150 mM NaCl, 1 mM Na_2EDTA, 1 mM EGTA, 1% Triton, 2.5 mM sodium pyrophosphate, 1 mM beta-glycerophosphate, 1 mM Na_3VO_4, 1 µg/ml leupeptin (Cell signaling, 9803), was thawed with milliQ water, and combined with a mixture of protease and phosphatase inhibitors (Roche) immediately before use. Cells were initially washed twice with PBS, followed by the addition of lysis buffer at 4°C for 10-20min on ice, brief mild sonication, followed by vortexing, additional incubation on ice (10-20min), and centrifugation (10,000g, 10min, 4°C). Sample buffer (Bio-Rad) – to which SDS had been freshly added – were combined with supernatants or nuclear extracts obtained from pellets (Pierce NE-PER) in a 1:1 ratio. Combined solutions were boiled at 95-100°C before being resolved on SDS polyacrylamide gels. When appropriate, nuclear extracts were prepared using the NE-PER Nuclear and Cytoplasmic Extraction Kit (Thermo Scientific 78833).

For co-immunoprecipitation (Co-IP), lysates (0.5–1 mg) were pre-cleared by protein G (Invitrogen) or Trueblot Rabbit IgG-beads (eBiosciences), and then incubated with 1:50 to 1:100 µg of TRAF6 Ab (Enzo lifesciences, ADI-AAP-426-E) or control Rabbit IgG (Santa Cruz) at 4°C overnight, followed by incubation with protein G or Trueblot IgG for 2 to 4 hr at 4°C. Precipitates were washed at least four times in 1:1 dilution of PBS to lysis buffer, then eluted in 2× sample buffer. Eluted materials were resolved on SDS polyacrylamide gels (Bio-Rad TGX gel, 7.5% and any kD at 130V, 35minutes, RT), wet transferred (250mA, 2.5 hours, 4°C) onto nitrocellulose (Bio-Rad), and immunoblotted with indicated antibodies (overnight 4°C). Antibody binding was detected using the ECL kit (Pierce).

BrdU, MTT

To measure cellular proliferation of WT, KO, and KI osteoclast progenitors, we assessed DNA synthesis rates using a commercially available BrdU cell proliferation assay (kit #6813, Cell Signaling Technologies) and cellular dehydrogenase activity using the MTT assay (Sigma 5655). We generated primary osteoclast progenitors from mice of each of the three experimental genotypes, WT, KI, and KO (average age 4 months, all female, n = 3 for each genotype) in the manner described above. Independent biological replicates were plated in duplicate. After two days of culture, also at 37°C, 5% CO_2, osteoclast progenitors were treated with fresh conditioning media ± M-CSF ± RANKL for 24 hours, and then BrdU or MTT, as appropriate, for an additional 4 hours. In the BrdU assay this was followed by fixation and staining in accordance with manufacturer protocols. In the MTT assay, formazan generated by dehydrogenase-mediated cleavage of tetrazolium rings was solubilized by 10% SDS in 0.4N HCl. Plates were then read at 450nm (BrdU) or 600nm (MTT) via standard microplate reader (Modulus microplate reader, Turner biosystems).

Detection of superoxide and additional reactive oxygen species (ROS)

Osteoclast progenitors obtained from KO, WT, and KI mice were generated in 96 well plates as noted above. Total superoxide and ROS generated by these cells in response to varying doses of M-CSF and RANKL-treatment were measured over a period of days using the Total Superoxide/ROS kit from Enzo Lifesciences, in accordance with manufacturer instructions (ENZ-51010, Enzo). Measurements were made and recorded using appropriate fluorescent filters using a fluorescent-capable microplate reader (Modulus microplate reader, Turner Biosystems).

4.3 Results

p62 does not alter expression of key mediators in the RANK-NFκB signaling pathway

First, we sought to test whether p62 was truly dispensable for RANKL-mediated NFκB signaling. We accomplished this by looking for alterations in the expression and binding patterns of key intermediaries in the RANK-NFκB signaling cascade via temporally prescribed RANKL stimulation of primary osteoclast progenitor cultures (of non-adherent bone marrow cells obtained from KO, WT, and KI mice) followed by lysis and immunoblot or Co-IP. Here we observed that neither ablation nor P394L mutation of p62 altered expression levels of RANK, TRAF6, IKKβ, or IKKγ (Figures 4.1, 4.2, 4.4), and when adjusting for differences in protein loading, binding between TRAF6 and p62 (Figure 4.3). Additionally, TRAF6-binding to RANK, polyubiquitin, and CYLD appeared to be unaltered by p62 status (data not shown). Notably, the downstream target of the signaling complex, IκB, followed the expected pattern of rapid degradation in response to RANKL – decreased expression at 5 minutes of treatment, maximal degradation at 15 minutes – before returning to basal levels within the hour, without regard to p62 (Figure 4.5). Furthermore, p65, the mediator inhibited by IκB appears within the nuclear fraction in each of the three genotypes in a roughly coordinated manner after 5 minutes of RANKL induction (Figure 4.6) and may be free to mediate the induction of key genes as identified by the upstream regulator analysis (Figures 3.16). To summarize, then, western blot and co-immunoprecipitation experiments suggest that neither abrogation nor mutation of p62 appreciably alter the expression, protein-protein interaction, or downstream function of key NFκB signaling mediators, while gene expression profiling paired with upstream regulator analysis suggests that p65 (RelA) is activated after 8 hours of RANKL-treatment. Taken together, these results suggest that p62 is dispensable for NFκB signaling during early osteoclastogenesis.

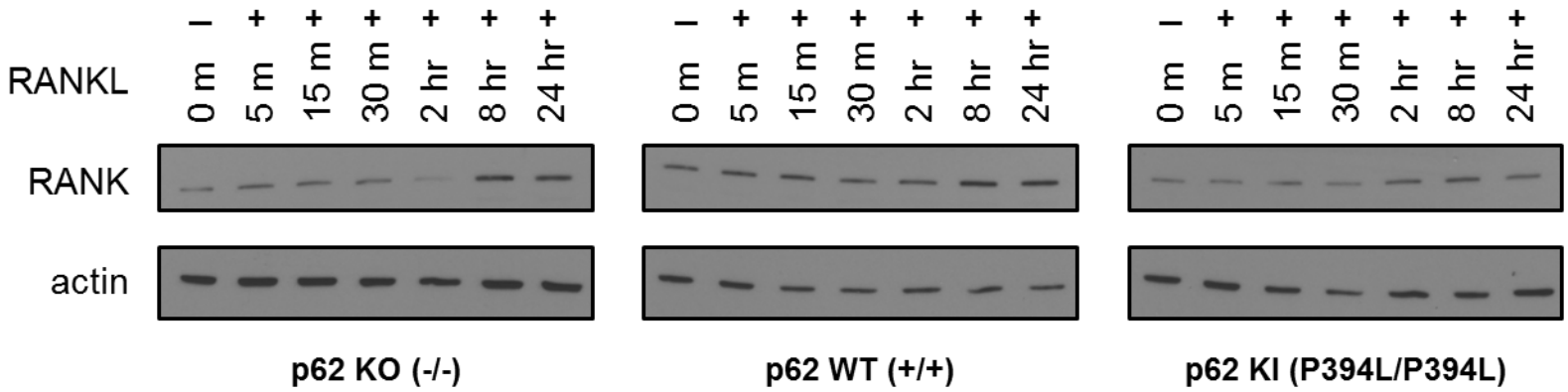

Figure 4.1. RANK up-regulation is unaffected by p62 status. Bone marrow derived progenitors obtained from p62 –/– (KO), wildtype (WT), and p62 P394L (KI) mice were primed with M-CSF for two days then cultured in the presence or absence of 100 ng/mL RANKL for the time periods shown, prior to processing and blotting with the antibodies as shown. Data represent results obtained in at least three independent experiments.

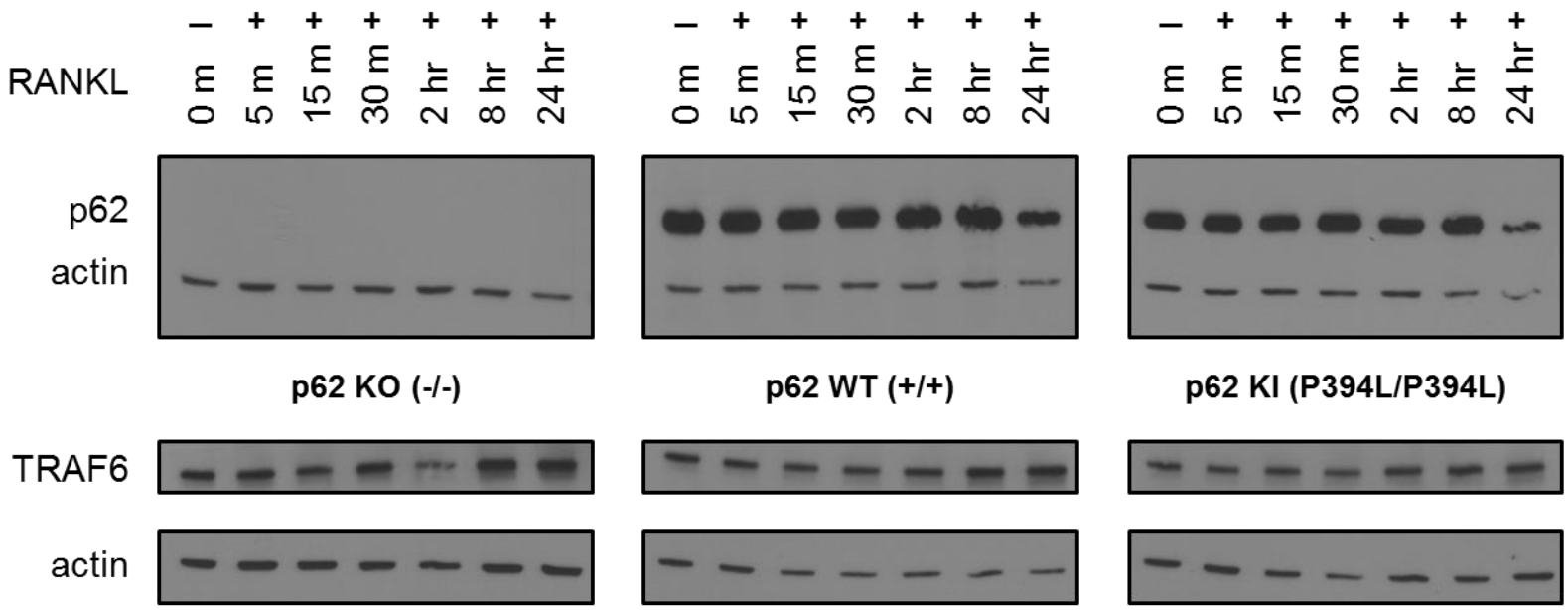

Figure 4.2. TRAF6 expression is unaffected by p62 status. Bone marrow derived progenitors obtained from p62 –/– (KO), wildtype (WT), and p62 P394L (KI) mice were primed with M-CSF for two days then cultured in the presence or absence of 100 ng/mL RANKL for the time periods shown, prior to processing and blotting with the antibodies as shown. Data represent results obtained in at least three independent experiments.

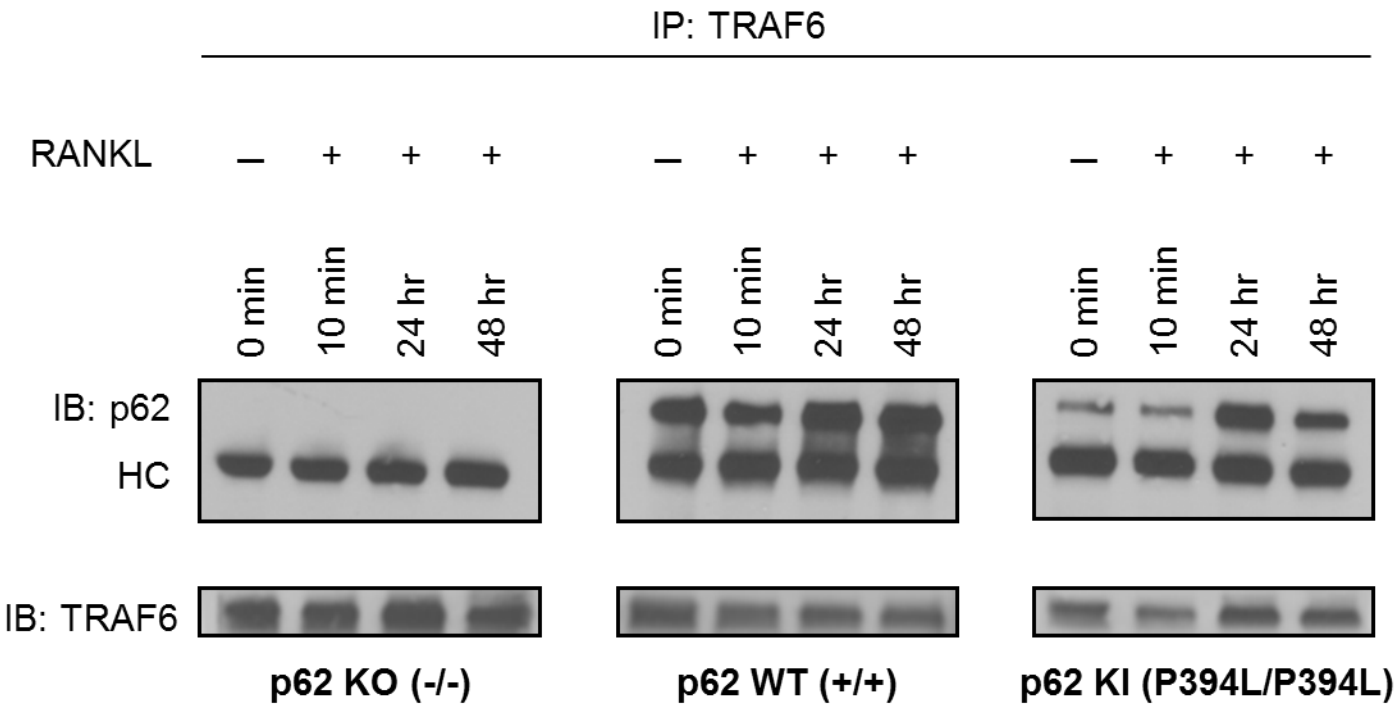

Figure 4.3. PDB-associated UBA-domain mutation does not alter p62 binding to TRAF6. Bone marrow derived progenitors obtained from p62 –/– (KO), wildtype (WT), and p62 P394L (KI) mice were primed with M-CSF for two days then cultured in the presence or absence of 100 ng/mL RANKL for the time periods shown, prior to processing and blotting with the antibodies as shown. Data represent results obtained in at least two independent experiments.

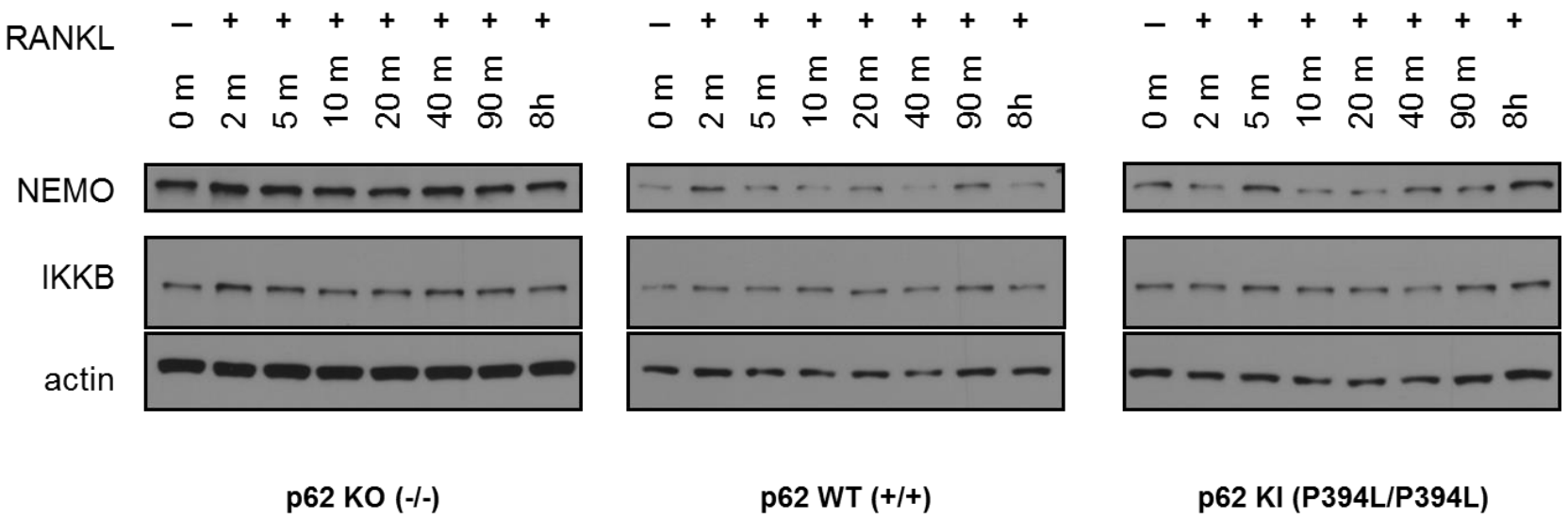

Figure 4.4. Expression levels of mediators downstream of TRAF6 in the NFκB pathway are not affected by p62 status. Bone marrow derived progenitors obtained from p62 –/– (KO), wildtype (WT), and p62 P394L (KI) mice were primed with M-CSF for two days then cultured in the presence or absence of 100 ng/mL RANKL for the time periods shown, prior to processing and blotting with the antibodies as shown. Data represent results obtained in at least three independent experiments.

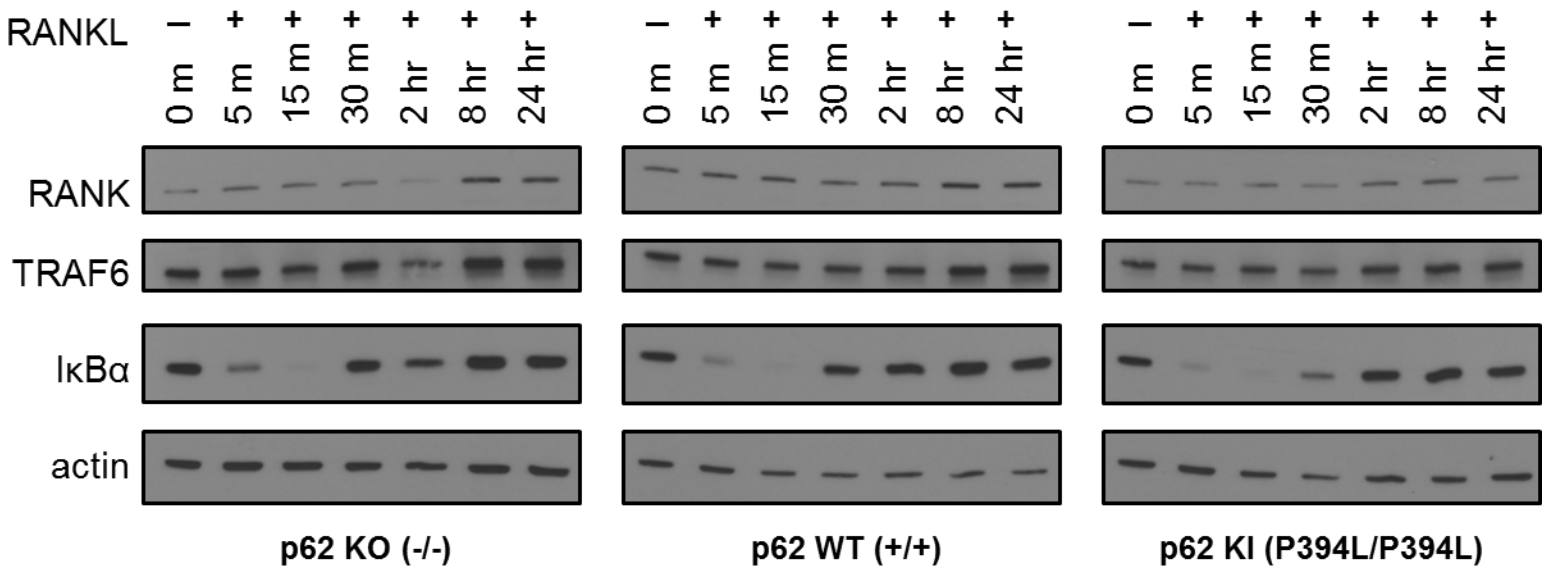

Figure 4.5. p62 is dispensable for RANKL-mediated IκB degradation. Bone marrow derived progenitors obtained from p62 –/– (KO), wildtype (WT), and p62 P394L (KI) mice were primed with M-CSF for two days then cultured in the presence or absence of 100 ng/mL RANKL for the time periods shown, prior to processing and blotting with the antibodies as shown. Data represent results obtained in at least three independent experiments.

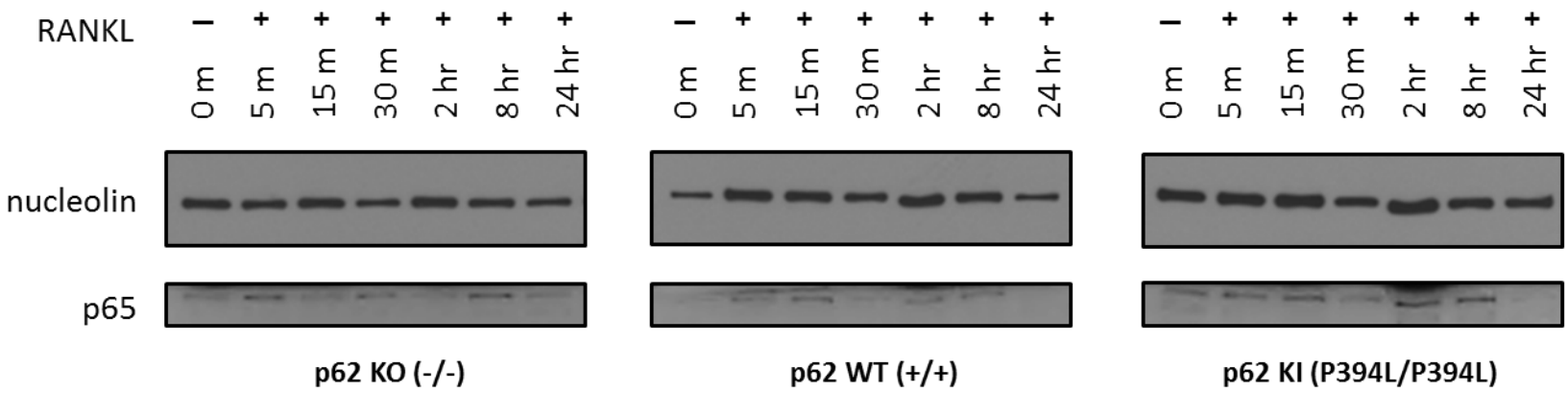

Figure 4.6. p62 is dispensable for RANKL-mediated p65 (RelA) nuclear translocation. Bone marrow derived progenitors obtained from p62 –/– (KO), wildtype (WT), and p62 P394L (KI) mice were primed with M-CSF for two days then cultured in the presence or absence of 100 ng/mL RANKL for the time periods shown, prior to processing and blotting with the antibodies as shown. Data represent results obtained in one preliminary experiment.

p62 regulates DNA synthesis but not viability or early osteoclast differentiation in response to M-CSF and RANKL

In previous sections, both gene set enrichment analysis and upstream regulator analysis suggested that the absence of p62 in RANKL-treated osteoclast progenitors might be associated with impaired proliferation. Traditionally, in vitro cellular proliferation has been determined by counting cells directly or performing clonogenic assays, which are time-consuming and impractical for evaluating large numbers of samples. In the present experiment, we have made use of two more common techniques, non-radioactive measurement of DNA synthesis (BrdU assay) and metabolic activity and viability (MTT assay).

The former relies on the observation that cellular proliferation requires the replication of cellular DNA. 5-bromo-2`-deoxyuridine (BrdU) is a pyrimidine analogue that is incorporated into the DNA of proliferating cells in place of thymidine. Subsequent immunodetection of BrdU using monoclonal antibodies allows labeling of cells in the S phase of the cell cycle, and thereby provides information about DNA synthesis directly, and cellular proliferation indirectly. To this end, we cultured non-adherent bone marrow cells obtained from the long bones of 2 to 4-month old KO, WT, and KI animals, treated them with 20 ng/mL of M-CSF for two days to generate osteoclast progenitors, then exposed the cells to various concentrations of M-CSF and RANKL for 24 hours and treated them with BrdU in accordance with manufacturer instructions. We observed that DNA synthesis increased significantly with M-CSF, consistent with what is known about M-CSF function in this cell type (Arai et al., 1999), independent of p62 status (Figure 4.7). RANKL treatment did not alter this increase in DNA synthesis except in KO cells, where there was a statistically significant, dose-dependent decrease in DNA synthesis, and presumably cellular proliferation (Figure 4.7).

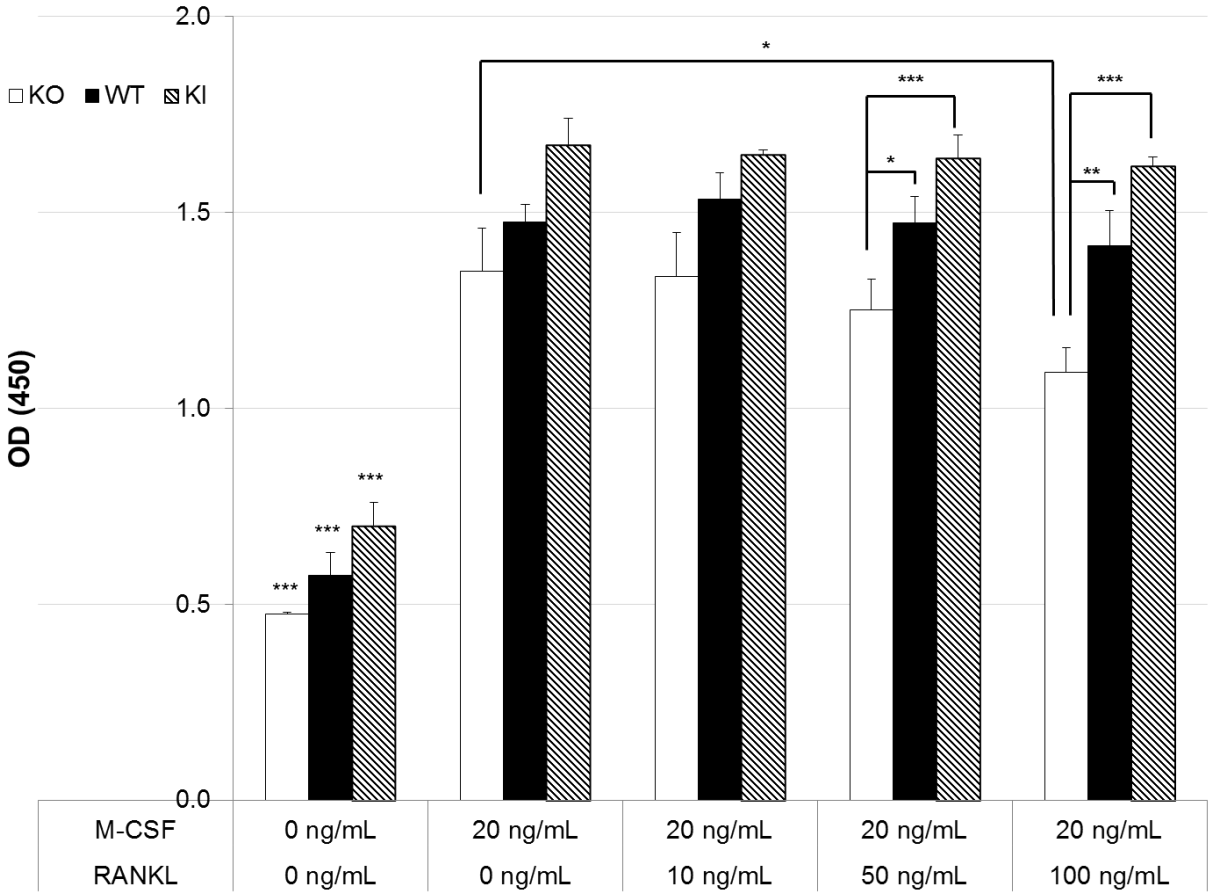

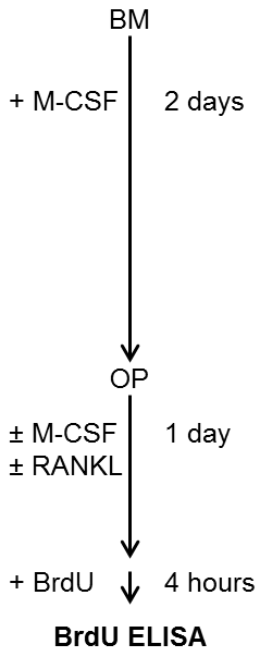

Figure 4.7. Quantification of DNA synthesis via BrdU incorporation in KO, WT, and KI osteoclast progenitors.

Bone marrow cells were obtained from 4-month old KO, WT, and KI animals, treated with 20 ng/mL of M-CSF for two days to generate osteoclast progenitors, exposed to various concentrations of M-CSF and RANKL for 24 hours, then treated with BrdU (n = 3, each genotype). Note that DNA synthesis increases significantly with M-CSF in all three genotypes, but is unaffected by RANKL treatment, except in the KO genetic background. * p<0.02, **p<0.001, ***p<0.0001

We next sought to assess cellular viability with the MTT assay, in which the tetrazolium salt Thiazolyl Blue Tetrazolium Blue (MTT) is metabolized in live cells to form a colored reaction product that is detectable by standard ELISA microplate reader. Indeed, this assay afforded us the dual opportunity to assess whether mitochondrial function was impaired, as suggested by the previous gene enrichment results, as an indirect measure of cellular viability. As before, we observed a dramatic increase in metabolic activity that was M-CSF-dependent, but in this instance p62-and RANKL-independent (Figure 4.8).

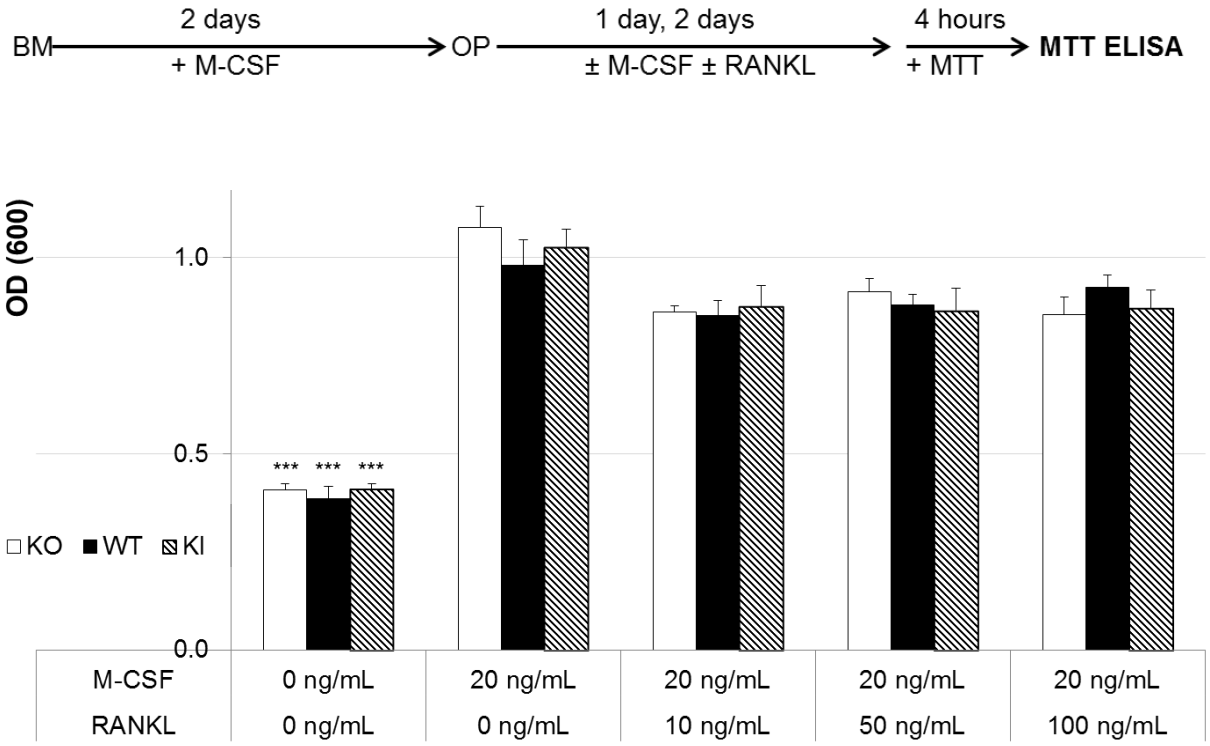

Figure 4.8. Quantification of cellular viability via the MTT assay in KO, WT, and KI osteoclast progenitors.

Bone marrow cells were obtained from 2-month old KO, WT, and KI animals, treated with 20 ng/mL of M-CSF for two days to generate osteoclast progenitors, exposed to various concentrations of M-CSF and RANKL for 24 hours (top panel) or 48 hours (bottom panel), then treated with MTT (n = 3). Metabolic activity increases significantly with M-CSF in all three genotypes, but is unaffected by RANKL treatment at 24 and 48 hours. ***p<0.0001

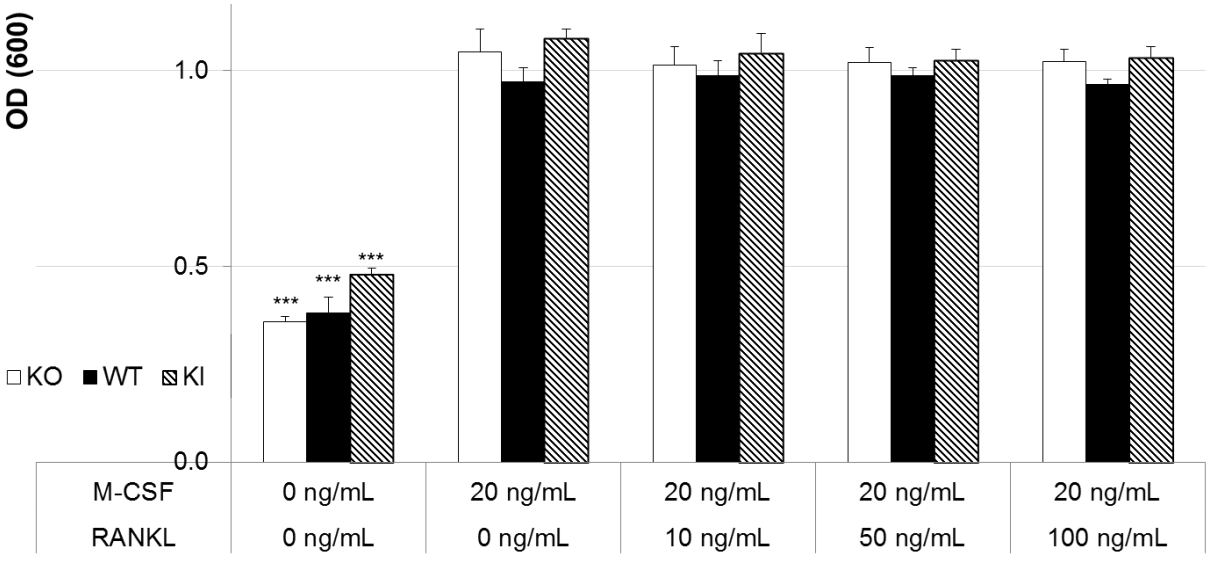

Next we sought to clarify whether the ablation or PDB-associated mutation of p62 played a role in the expression of two early osteoclast markers – the M-CSF receptor (CSF-1R), and receptor activator of NFκB (RANK). Data from the previous chapter suggested that RANK levels may have been diminished at the level of transcription in osteoclast progenitors obtained from mutants (both p62 KOs and KIs) compared to WT (Figure 3.10b), however Western blot data in the present chapter suggested that there were no obvious deficiencies in RANK protein expression in cells from all three genotypes (Figure 4.1). Still, we reasoned that decreased or delayed cell-surface expression of either key mediator, M-CSF receptor or RANK, may account for differences we observed proliferation and RNAKL-mediated osteoclastogenesis. Moreover, our upstream regulator suggested that all precursors may well have differentiated apart from the lymphoid lineages (Figure 3.16), but do not predict whether we might expect parallel increases in early osteoclast differentiation markers. For example, if these receptors were expressed robustly in WT and KI cells, but not in KO cells, we might reasonably assume that p62's role in osteoclastogenesis is direct, acting fairly early or upstream in the signaling cascade, and that alteration of this protein alters the nature of the progenitors. To these ends, we cultured non-adherent bone marrow cells, as before, treated them with 20 ng/mL of M-CSF for two days to generate osteoclast progenitors, then exposed them to 20 ng/mL of M-CSF and 100 ng/mL RANKL over 48 hours, fixing and staining cells for the expression of CSF-1R and RANK for flow cytometry analysis at time points, 0, 12 hours, 24 hours, and 48 hours post treatment (Figures 4.9a, 4.9b, 4.9c). Interestingly, all cell types expressed CSF-1R at fairly high levels initially, and were double positive for CSF-1R and RANK in proportions that, by the end of the experiment, were p62-independent. Taken together, these experiments suggest that p62 plays an important role in DNA synthesis and cell cycle progression, but does not alter early viability or directly mediate early osteoclast differentiation.

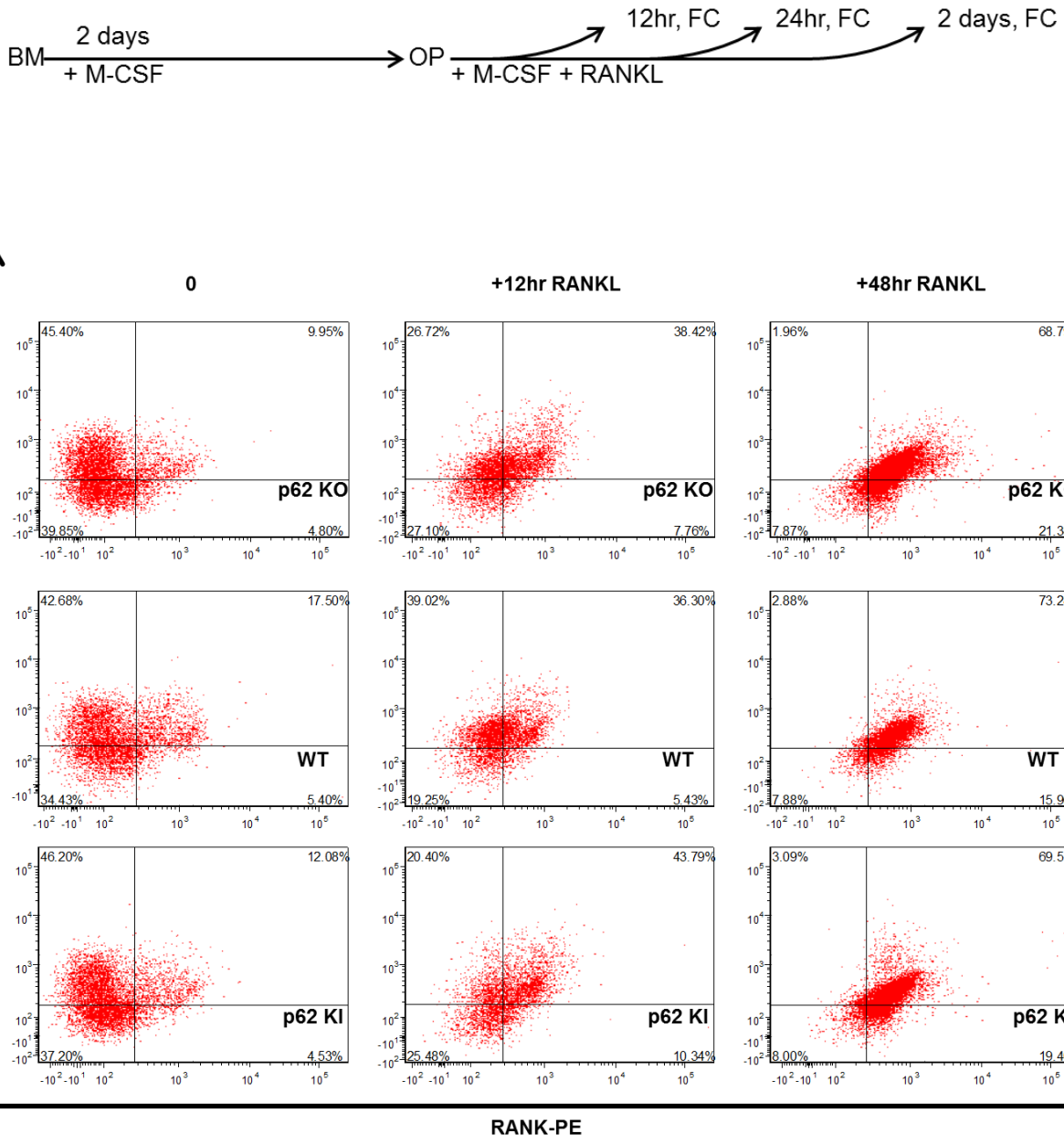

Figure 4.9a. Osteoclast progenitors are M-CSF receptor+, RANK+ during early osteoclast differentiation, independent of p62 status.

Bone marrow cells were obtained from 2-month old KO, WT, and KI animals, treated with 20 ng/mL of M-CSF for two days to generate osteoclast progenitors, exposed to 20 ng/mL of M-CSF and 100 ng/mL RANKL for 48 hours, then fixed and stained for the expression of receptor activator of NFκB (RANK) and CSF-1R, the receptor for M-CSF, via flow cytometry. Data represent results obtained in at least two independent experiments.

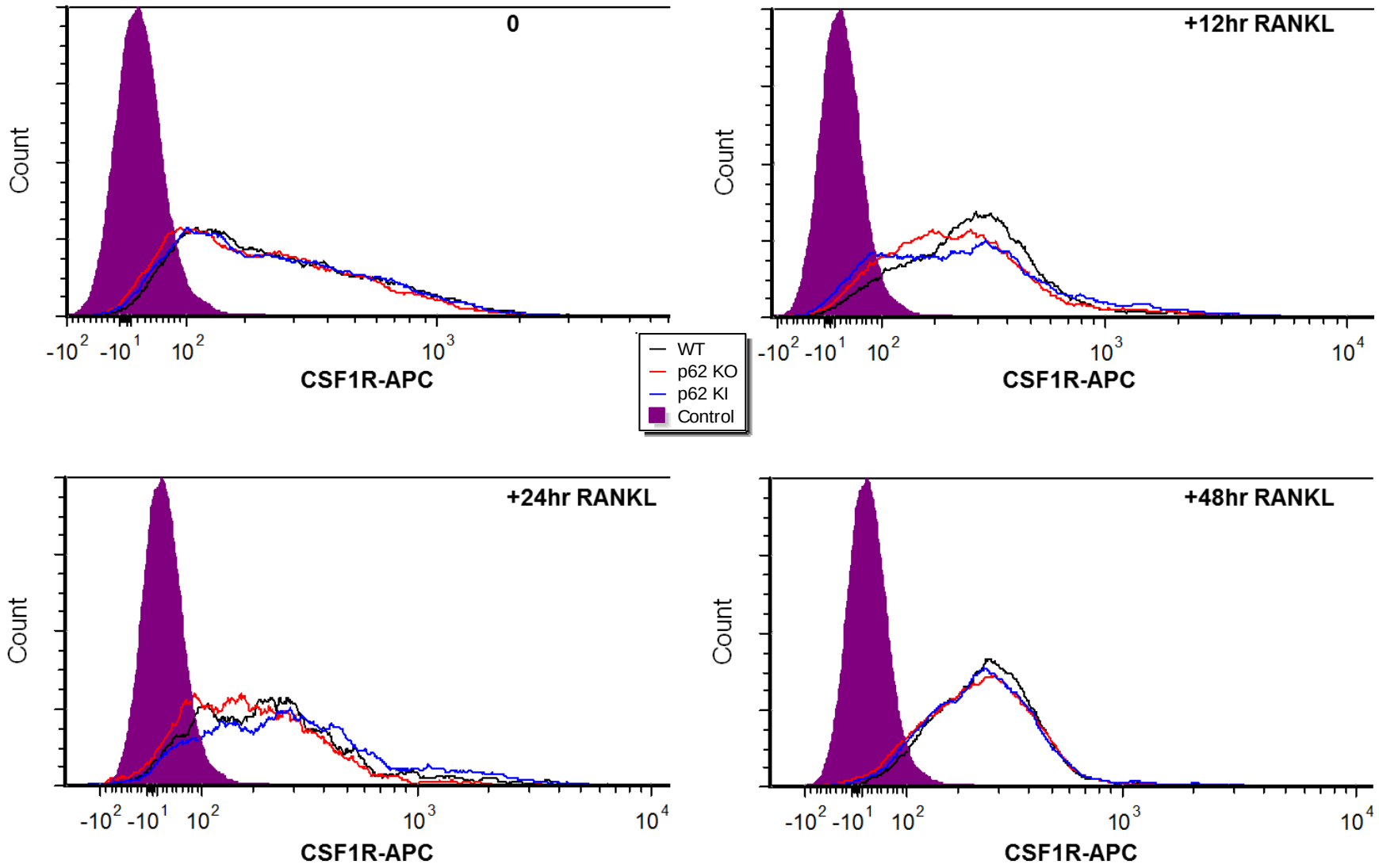

Figure 4.9b. M-CSF receptor expression increases during early osteoclast differentiation in a p62-independent manner.

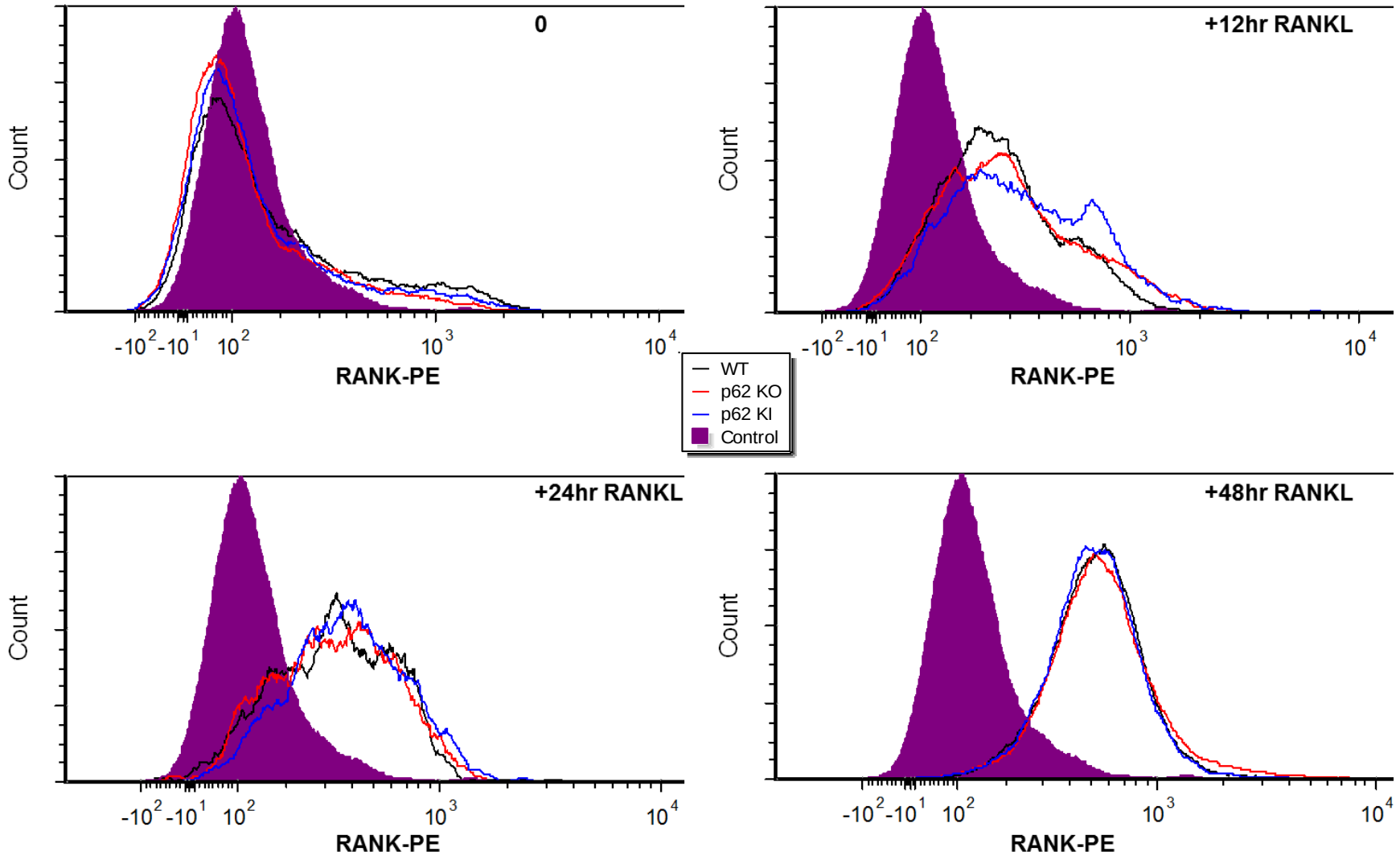

Figure 4.9c. RANK expression increases during early osteoclast differentiation in a p62-independent manner.

p62 mediates RANKL-induced production of reactive oxygen species (ROS)

The final experiment we conducted sought to test whether RANKL-treated KO cells exhibited an impaired NRF2-mediated oxidative stress response. We began by testing whether NRF2 could be located in nuclear fractions of osteoclast progenitors treated with RANKL. In preliminary testing, we found levels of NRF2 via Western blot that were essentially indistinguishable between KO, WT, and KI nuclear fractions (data not shown). Next, we tested whether ROS production varied by p62 status in osteoclast progenitors treated with RANKL, using previously published methods (Yang et al., 2011). We found that, in our hands, the kit did not detect dramatic increases RANKL-mediated ROS production over short durations (Figure 4.10a), as has been previously shown using fluorescence microscopy techniques (Lee et al., 2005). Nonetheless, a significant decrease in total ROS production was observed among KO cells relative to WT and KI cells. Moreover, a dramatic, dose-dependent up-regulation in RANKL-mediated ROS production was observed over a period of hours to days, particularly in WT and KI cells, a finding also consistent with previously published results (Kim et al., 2010). Interestingly, up-regulation of ROS also occurred in KO cells, but in a manner that was diminished relative to that in WT and KI cells, particularly at the 6 hour time point (Figure 4.10b). This suggests that the NRF2 mediated stress response may be impaired in KO cells, in part, because maximal levels of ROS production are not reached when they are stimulated by RANKL.

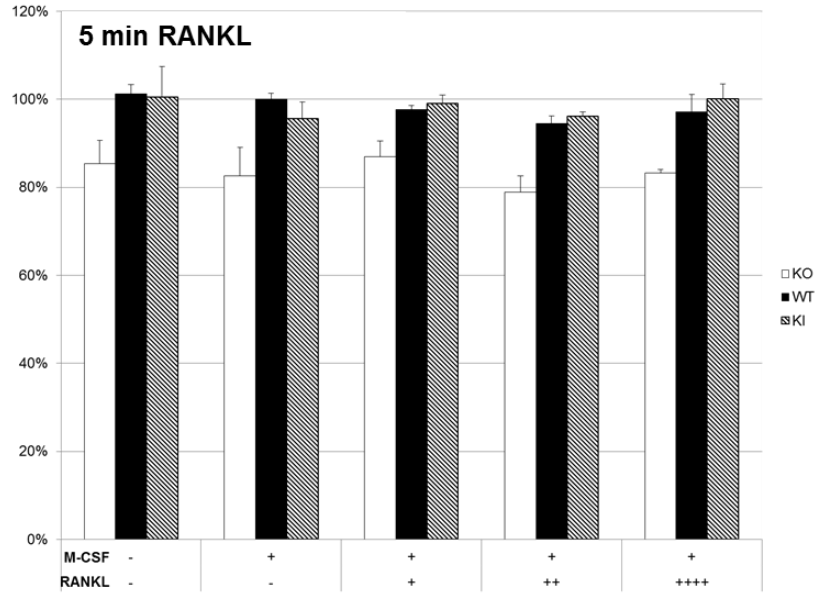

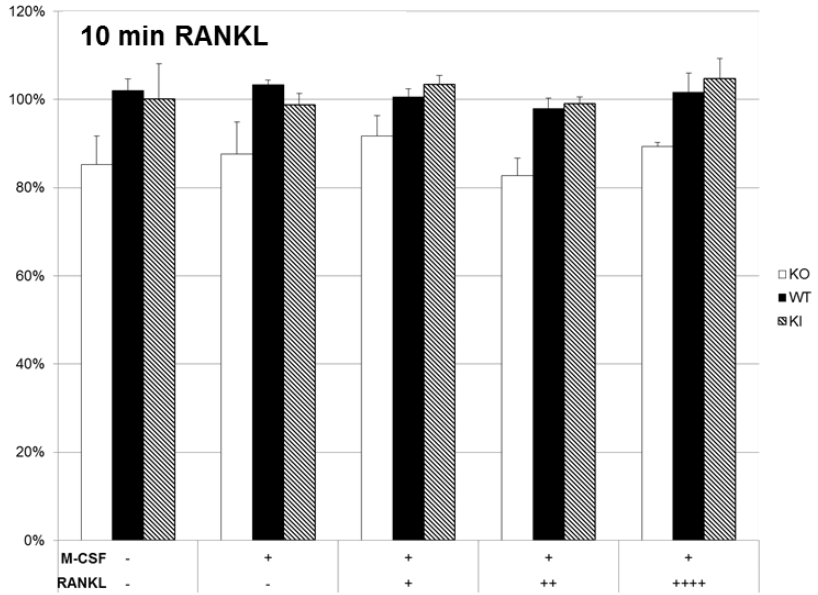

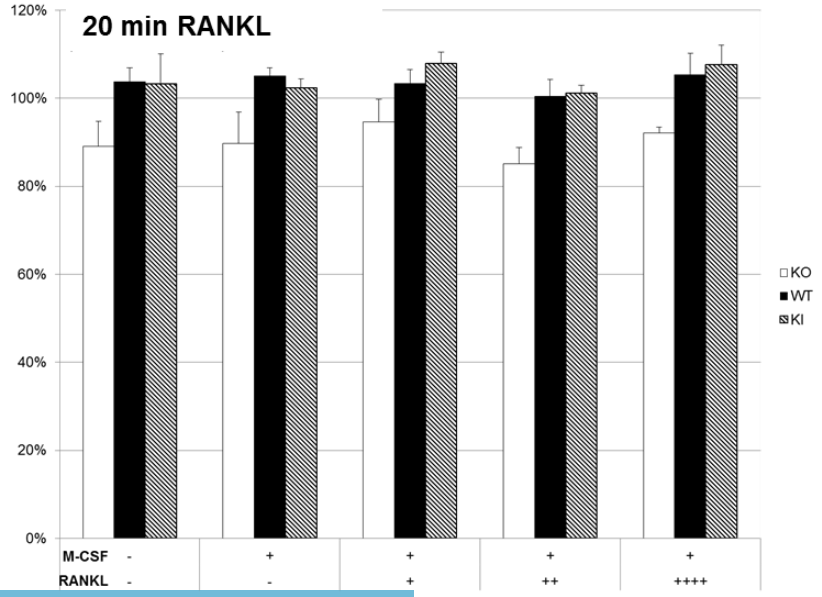

Figure 4.10a. Quantification of total ROS produced in response to RANKL stimulation in KO, WT, and KI osteoclast progenitors over immediate timepoints.

Bone marrow cells were obtained from 4-month old KO, WT, and KI animals, treated with 20 ng/mL of M-CSF for two days to generate osteoclast progenitors, incubated with ROS detection mix, then treated with various concentrations ± 20 ng/mL M-CSF and various doses of RANKL. Immediate measurements were made and reported as a percentage of the initial WT, M-CSF reading. Subsequent measures were taken at 10 and 20 minutes. Means ± SEM are reported for two independent experiments. RANKL concentrations of 25 ng/mL (+), 50 ng/mL (++), and 100 ng/mL were used (++++).

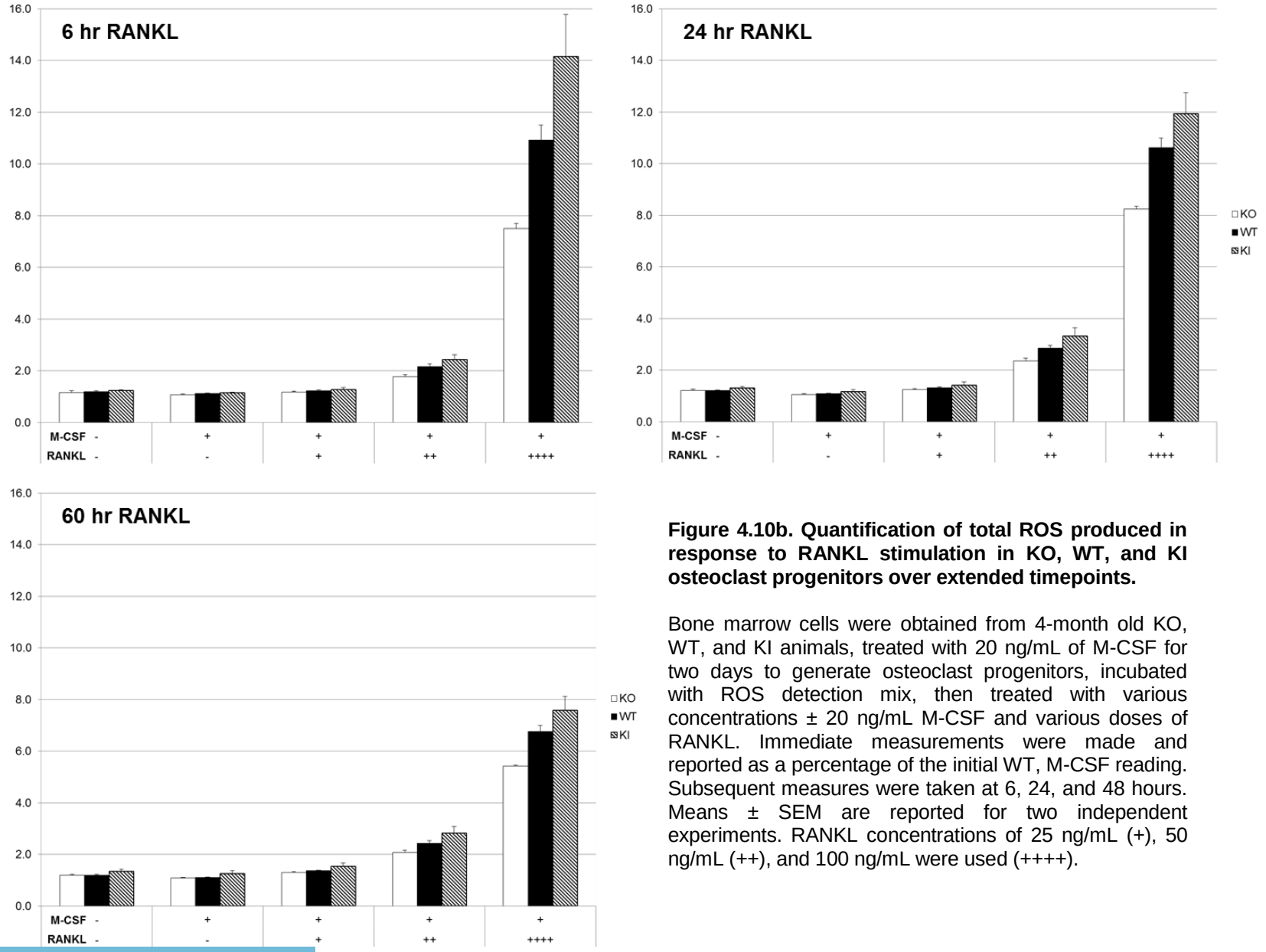

Figure 4.10b. Quantification of total ROS produced in response to RANKL stimulation in KO, WT, and KI osteoclast progenitors over extended timepoints.

Bone marrow cells were obtained from 4-month old KO, WT, and KI animals, treated with 20 ng/mL of M-CSF for two days to generate osteoclast progenitors, incubated with ROS detection mix, then treated with various concentrations ± 20 ng/mL M-CSF and various doses of RANKL. Immediate measurements were made and reported as a percentage of the initial WT, M-CSF reading. Subsequent measures were taken at 6, 24, and 48 hours. Means ± SEM are reported for two independent experiments. RANKL concentrations of 25 ng/mL (+), 50 ng/mL (++), and 100 ng/mL were used (++++).

4.4 Discussion

Experiments in this chapter revealed that key mediators in the RANK-NFκB signaling pathway including RANK, TRAF6, IKKβ, and IKKγ were expressed at levels that were p62-independent, that RANK-TRAF6 and RANK-p62 binding did not differ appreciably with p62 status in preliminary pull-down experiments, and that the kinetics of IκB degradation did not appreciably change in the absence of p62 or presence of PDB-associated mutant p62 during early osteoclastogenesis. How can we understand this set of results in light of the phenotypes we described in the previous chapter and what has been previously published in the literature? On the one hand, genetic abrogation of p62 does not lead to a detectable phenotype in the absence of external stimuli, a result that was previously published for 2 month old mice (Durán et al., 2004), and confirmed in the present project, in year-old mice about which there had been some uncertainty. Yet genetic knock-out mouse models for any of the following mediators: RANKL, RANK, NFκB1 and NFκB2, or TRAF6, result in a severe, osteoclast-poor, osteopetrotic phenotype under similar conditions. If p62 were a key mediator in this pathway, we might have expected a similar phenotype. On the other hand, as noted earlier, there is some evidence from in vitro studies that an intact p62 UBA domain is required for the proper function of CYLD, a TRAF6 de-ubiquitinase and feedback inhibitor of NFκB signaling. Yet, when CYLD is knocked-out, mice exhibit severe osteoporosis, a phenotype that neither KO nor KI mutant mice demonstrate. Taken together, these findings suggest that p62 may not play a role in modulating the effects of the RANK-NFκB in a biologically relevant manner, or that its absence or genetic alteration is countered by the presence of some yet-unidentified factor. That said, the inability of KO mice or cells to mount an appropriate osteoclastogenic response to cytokine stimulation in vivo (whether it is indirect such as via PTHrP or direct via TNF-α) or in vitro (with RANKL), is unmistakable. As

such, we next turned to alternative hypotheses generated by our gene expression profiling experiments.

Specifically, in chapter three we observed that a constellation of regulators of cellular proliferation were predicted to be inhibited in KO cells relative to their WT and KI counterparts (Figures 3.16 and 3.17) and that a bevy of genes, including aurora kinases, E2F transcription factors, cyclins, and cyclin dependent kinases associated with cell cycle progression, were uniquely down-regulated in RANKL-treated KO cells (Figure 3.12b). We tested these results functionally with BrdU and MTT assays for proliferation and viability, respectively. Interestingly, we confirmed that proliferation was diminished in a RANKL dose-dependent manner in KO, but not WT or KI, cells, while cell viability was p62-independent. Possible sources of error must be acknowledged – it has been reported, for example, that over 50% of the MTT dye that penetrates the cell membrane can be reduced by non-mitochondrial, cytosolic and microsomal enzymes (Jaszcyszyn and Gasiorowski, 2008), that reactive oxygen species (ROS) such as superoxide can efficiently reduce tetrazolium salts, and that the simultaneous use of ROS-inducers with the MTT or XTT assays leads to inaccurate predictions about cell toxicity and overestimated cell viability (Wang and Wickliffe, 2011). Yet, the fact that these observations are broadly consistent with the previously published findings that absence of p62 facilitates a slower exit of cells from mitosis (Linares et al., 2011) but also disrupts mitotic catastrophe, a p53-mediated oncosuppressive cell death cascade (Bui and Shin, 2011), strengthen our confidence in these results.

Our final set of experiments were motivated by the prediction, generated in chapter three, that activation of antioxidant NRF2 signaling cascade may be impaired in the absence of p62. We tested this indirectly by measuring ROS production in response to RANKL in cells of each

genotype, reasoning that in the absence of p62, the antioxidant response would be muted, and ROS would be elevated, especially on the scale of hours to days, in KO cells compared with WT and KI cells. In our preliminary data, the trend was consistent with *diminished* ROS production in KO cells compared to WT and KI cells, contrary to our expectation. How can we make sense of these results? As noted earlier, investigators have shown that p62 localizes within mitochondria and forms protein complexes with several oxidation-prone proteins (including components of the electron transport chain, chaperone molecules, and redox enzymes) to support stable electron transport, and that p62-deficient mitochondria exhibit impaired electron transport, which is partially restored by in vitro delivery of p62 (Lee and Shin, 2011). Another group recently confirmed these results, demonstrating that p62 is localized to mitochondria in basal, non-stressed conditions, and that p62 deficiency disrupts mitochondrial morphology, function (e.g. ATP production), and mitochondrial genome stability (Seibenhener et al., 2013). Furthermore, it has been previously shown that RANKL stimulation of osteoclast progenitors transiently increases intracellular ROS (Lee et al., 2005), while application of the antioxidant N-acetylcysteine (NAC) or suppression of the activity of Nox (an enzyme that catalyzes ROS production) inhibit the responses of progenitors to RANKL and osteoclast differentiation (Lee et al., 2005). Because ROS are produced endogenously as by-products of the incomplete reduction of cellular oxygen and p62-/- mitochondria exhibit impaired electron transport, it stands to reason that such mitochondria may also produce diminished ROS in response to RANKL stimulation, leading to deficient osteoclastogenesis (and diminished ROS production would also presumably diminish the NRF2-mediated antioxidant response, hence our findings in chapter three). One way to test this hypothesis would be to be culture osteoclast progenitors from WT and KO mice in the presence of NAC and H_2O_2, respectively, and characterize the structural and functional responses.

Before concluding, we must acknowledge some of the experimental challenges and limitations to the work chronicled in this chapter. First, conducting experiments where endogenous proteins and protein-protein interactions are probed from primary cultures is an inherently difficult task. Biological heterogeneity, the increased time and cost involved in simultaneously generating cell cultures from mice of three different genotypes for each experiment, and the difficulty in identifying appropriate antibodies for endogenous proteins were significant hurdles to overcome to increase the biological relevance of our studies. Consequently, some interactions appeared to be somewhat non-specific and would benefit from repeat experimentation. Second, time and financial constraints limited the number of hypotheses generated in chapter three that could be tested here. To this end, while an additional external validation of differentially expressed genes has already been conducted (the parameters of which are outlined in the following chapter), additional hypothesis testing may yet reveal additional, novel therapeutic targets for Paget's disease specifically, and bone disease characterized by overly exuberant or dysregulated osteoclastogenesis, such as multiple myeloma and cancer metastasis, more generally.

Despite these limitations, we have tested a significant subset of hypotheses developed in chapters two and three. We have provided additional evidence that p62 may mediate early osteoclastogenesis not by regulation of the RANK-NFκB signaling pathway, alteration of cellular differentiation, or disruption of viability, but by mediating proliferation and the production of reactive oxygen species. Taken together these experiments provide a novel framework to advance our understanding of p62 function in osteoclastogenesis and the pathophysiology of Paget's disease of bone, which we discuss in the final chapter.

SUMMARY AND CONCLUDING REMARKS

This dissertation was undertaken to elucidate the role played by the multifunctional adaptor protein p62 in the cellular physiology of osteoclasts in health and disease. We began with a broad structural and functional characterization of congenic mice in which the gene encoding p62 was left intact (wildtype or WT), genetically knocked-out (KO), or altered to produce the murine equivalent of a common mutant associated with Paget's disease of bone, p62 P394L (KI). Next, we assessed the signaling changes underlying differential osteoclastogenesis in progenitors obtained from these mice using gene expression profiling via DNA microarray. Finally, we tested predictions about specific signaling pathways culled from the microarray results, confirming a subset of them, and in the process, altered our view of the role p62 plays in osteoclast formation.

In the original study of p62-/- mice, investigators found that the absence of p62 did not affect skeletal architecture under basal conditions in 6 to 8 week old mice, but impaired osteoclast formation in response to induction by PTHrP and RANKL, in vivo and in vitro, respectively (Durán et al., 2004). To account for these and other findings, they proposed a model in which p62 forms a complex with TRAF6 to enhance NFκB signaling, up-regulate NFATc1, the master transcriptional regulator of osteoclastogenesis, and ultimately form new osteoclasts.

Despite the fact that knock-out mouse models of key RANK-NFκB signaling mediators, including RANKL, RANK, and TRAF6, develop osteopetrosis under basal conditions, and p62-/- mice do not, this model took hold, and has gained broad acceptance in the literature through the years. Of note, in a later paper, this group demonstrated that KO mice develop mature-onset obesity, and suggested, but never experimentally demonstrated, that such mice also exhibit increased bone mineral density as they age, implying a possible aging-induced osteopetrotic phenotype (Rodriguez et al., 2006). In this study, we confirmed that p62-/- mice and cells demonstrate impaired osteoclastogenesis in response to cytokine stimulation and that genetic ablation of p62 results in mature-onset obesity, but found no statistically appreciable differences in skeletal architecture in KO mice compared to WT controls at one year of age. That we observed the obesity phenotype, but did not observe any significant changes to skeletal architecture suggested to us that either p62 plays a minor role in normal bone homeostasis or that a sufficient number of compensatory pathways are active to mask the effects of its loss. In contrast, KI mice exhibited an osteopenic phenotype (i.e. increased osteoclastogenesis) under basal conditions, a finding that differed from previously reported results (Hiruma et al., 2008; Daroszewska et al., 2011). Though this may be attributable to strain-dependence, we suspect that this discrepancy is better accounted for by the fact that we characterized older and greater numbers of mice in the present study compared to previous ones. Taken together with the fact that cytokine-induced osteoclastogenesis was also enhanced in KI mice and cells relative to WT controls, these data indicated to us that PDB-associated mutations result in a true physiologic gain of osteoclast function.

These findings prompted us to re-evaluate p62's accepted role in osteoclastogenesis and probe it in an unbiased fashion using gene expression profiling. Importantly, we generated several novel hypotheses, which include: (a) that p62 may be dispensable for RANKL-mediated NFκB signaling

and early differentiation of hematopoietic precursors toward the monocyte/macrophage lineage, (b) that ablation of p62 may impair cellular proliferation, cell cycle progression, mitochondrial integrity, or the NRF2-mediated oxidative stress response, among other signaling pathways, and thereby inhibit osteoclastogenesis, and (c) that P394L mutation of p62 may be associated with an increase in the unfolded protein stress response, increased CD38 signaling and IL-6 production, or decreased BCL6 signaling and thereby enhance osteoclastogenesis. We then tested a subset of these hypotheses. First, we observed that key mediators in RANK signaling were expressed and co-precipitated at levels that were p62-independent and, that, moreover, the kinetics of IκB degradation, the rate-limiting step in NFκB activation, did not change in the absence of p62 or presence of mutant p62 during early osteoclastogenesis, casting further doubt on the putative role ascribed to p62 in the RANK-NFκB signaling pathway. Next, we found that the absence of p62 was associated with diminished cellular proliferation and reactive oxygen species production in a RANKL dose-dependent manner, but did not alter cellular viability, while PDB-associated mutation of p62 increased ROS production alone.

Taken together, our results suggest that a new narrative of p62's place in osteoclastogenesis may be in order, favoring its role in maintaining cellular homeostasis through selective autophagy, the maintenance of mitochondrial integrity, ROS production, and the NRF2-mediated antioxidant response, above its putative role in RANK-NFκB signaling. A natural extension to Paget's disease of bone follows. We propose that p62 P394L, and other UBA-domain mutants may alter the ability of p62 to sequester ubiquitinated proteins that are to be degraded via autophagy or the 26S proteasome, increasing the cellular burden of misfolded proteins. We speculate that this may increase ER stress, trigger a robust unfolded protein response, possibly mediated by XBP1, which may lead to increased levels of endogenous inflammatory mediators that then may increase the

general osteoclastogenic milieu of the bone microenvironment. How we may reconcile these results with the body of literature discussing viral contributions to PDB is beyond the scope of the present work, but we may note that a recent publication suggests that the attenuated measles virus-Edmonston strain (used in oncolytic virotherapy trials) triggers p62-mediated mitophagy (Xia et al., 2014). In this vein, we speculate that true infection with measles virus may act in a similar fashion to alter normal cellular homeostasis.

It must be acknowledged that several further experiments should be conducted to increase our confidence in these findings and help confirm our hypotheses. In fact, an additional validation experiment where samples of WT, KO, and KI bone-marrow derived osteoclast progenitors were treated with RANKL or vehicle at 0, 8, 24, and 48 hours has already been conducted. Moreover, RNA samples have been purified and assessed for quality, and probes for quantitative RT-PCR to evaluate differential regulation of key NFκB signaling mediators and targets (RANK, TRAF6, CYLD, NFATc1, RelB, NFκB1), NRF2 targets (SRXN1, SOD2, ICAM-1), and highly expressed genes from our microarray data (DUSP6, FOS, MAPK3) have already been purchased and obtained. Additional targets to consider prior to final experimentation include NQO-1 and NQO-2, critical targets of NRF2 known to play an important role in the maintenance of mitochondrial integrity. Moreover, additional external validation of mammalian target of rapamycin (mTOR) signaling, protein kinase C delta (PRKCD) function, and microRNA-124 turnover are warranted in KO and WT cells, while methods for measuring the unfolded stress response have been established in mammalian cell system (Oslowski and Urano, 2011), and should also be explored along with CD38, IL-6, and BCL6 signaling pathways in p62 P394L cells. Such studies may extend our understanding of normal osteoclastogenesis and provide further novel targets for intervention in bone disease.

REFERENCES

Acosta-Alvear D, Zhou Y, Blais A, Tsikitis M, Lents NH, Arias C, Lennon CJ, Kluger Y, Dynlacht BD. XBP1 controls diverse cell type- and condition-specific transcriptional regulatory networks. Mol Cell. 2007 Jul 6;27(1):53-66.

Aliprantis AO. NFATc1 in mice represses osteoprotegerin during osteoclastogenesis and dissociates systemic osteopenia from inflammation in cherubism. J Clin Invest. 2008; 118:3775-3789.

Arai F, Miyamoto T, Ohneda O, Inada T, Sudo T, Brasel K, Miyata T, Anderson DM, Suda T. Commitment and differentiation of osteoclast precursor cells by the sequential expression of c-Fms and receptor activator of nuclear factor kappaB (RANK) receptors. J Exp Med. 1999; 190:1741-1754.

Ashrafi G, Schwarz TL. The pathways of mitophagy for quality control and clearance of mitochondria. Cell Death Differ. 2013 Jan;20(1):31-42.

Baggerly K. Disclose all data in publications. Nature. 2010 Sep 23;467(7314):401.

Baslé M, Rebel A, Pouplard A, Kouyoumdjian S, Filmon R, Lepatezour A. [Demonstration of measles virus antigens in osteoclasts in Paget's disease of bone.] C R Seances Acad Sci D. 1979; 289:225-228. French.

Baslé M, Rebel A, Pouplard A, Kouyoumdjian S, Filmon R, Loepatezour A. [Demonstration by immunofluorescence and immunoperoxidase of an antigen of the measles type in the osteoclasts of Paget's disease of bone]. Bull Assoc Anat (Nancy). 1979; 63:263-272. French.

Baslé MF, Fournier JG, Rozenblatt S, Rebel A, Bouteille M. Measles virus RNA detected in Paget's disease bone tissue by in situ hybridization. J Gen Virol. 1986; 67(Pt 5):907-913.

Bax BE, Alam AS, Banerji B, Bax CM, Bevis PJ, Stevens CR, Moonga BS, Blake DR, Zaidi M. Stimulation of osteoclastic bone resorption by hydrogen peroxide. Biochem Biophys Res Commun. 1992; 183:1153-1158.

Benford HL, McGowan NW, Helfrich MH, Nuttall ME, Rogers MJ. Visualization of bisphosphonate-induced caspase-3 activity in apoptotic osteoclasts in vitro. Bone. 2001 May;28(5):465-73.

Beyens G, Van Hul E, Van Driessche K, Fransen E, Devogelaer JP, Vanhoenacker F, Van Offel J, Verbruggen L, De Clerck L, Westhovens R, Van Hul W. Evaluation of the role of the SQSTM1 gene in sporadic Belgian patients with Paget's disease. Calcif Tissue Int 2004; 75:144-152.

Birch MA, Taylor W, Fraser WD, Ralston SH, Hart CA, Gallagher JA. Absence of paramyxovirus RNA in cultures of pagetic bone cells and in pagetic bone. J Bone Miner Res. 1994; 9:11-16.

Bucay N, Sarosi I, Dunstan CR, Morony S, Tarpley J, Capparelli C, Scully S, Xu W, Lacey DL, Boyle WJ, Simonet WS. Osteoprotegerin-deficient mice develop early onset osteoporosis and arterial calcification. Genes Dev. 1998; 12:1260-1268.

Bui CB, Shin J. Persistent expression of Nqo1 by p62-mediated Nrf2 activation facilitates p53-dependent mitotic catastrophe. Biochem Biophys Res Commun. 2011 Aug 26;412(2):347-52.

Cappellen D, Luong-Nguyen NH, Bongiovanni S, Grenet O, Wanke C, Susa M. Transcriptional program of mouse osteoclast differentiation governed by the macrophage colony-stimulating factor and the ligand for the receptor activator of NFkappa B. J Biol Chem. 2002 Jun 14;277(24):21971-82.

Carles D, Rivel J, Devars F, Honton JL, Basle MF, Coquet M, Coindre JM. Giant cell tumors developing in Paget's disease. Presentation of 2 cases with an ultrastructural study. Ann Pathol. 1989; 9:47-53.

Chae HJ, Park RK, Chung HT, Kang JS, Kim MS, Choi DY, Bang BG, Kim HR. Nitric oxide is a regulator of bone remodelling. J Pharm Pharmacol. 1997; 49:897-902.

Chamoux E, Couture J, Bisson M, Morissette J, Brown JP, Roux S. The p62 P392L mutation linked to Paget's disease induces activation of human osteoclasts. Mol Endocrinol. 2009 Oct;23(10):1668-80.

Chapuy MC, Zucchelli P, Meunier PJ. Parathyroid function in Paget's disease of bone. Rev Rhum Mal Osteoartic 1982; 49:99-102.

Chen HY, White E. Role of autophagy in cancer prevention. Cancer Prev Res (Phila). 2011; 4:973-983.

Chung PY, Van Hul W. Paget's disease of bone: evidence for complex pathogenetic interactions. Semin Arthritis Rheum. 2012; 41:619-641.

Ciani B, Layfield R, Cavey JR, Sheppard PW, Searle MS. Structure of the ubiquitin-associated domain of p62 (SQSTM1) and implications for mutations that cause Paget's disease of bone. J Biol Chem. 2003; 278:37409-37412.

Cody JD, Singer FR, Roodman GD, Otterund B, Lewis TB, Leppert M, Leach RJ. Genetic linkage of Paget disease of the bone to chromosome 18q. Am J Hum Genet. 1997; 61:1117-1122.

Copple IM, Lister A, Obeng AD, Kitteringham NR, Jenkins RE, Layfield R, Foster BJ, Goldring CE, Park BK. Physical and functional interaction of sequestosome 1 with Keap1 regulates the Keap1-Nrf2 cell defense pathway. J Biol Chem. 2010; 285:16782-16788.

Courtois G. Tumor suppressor CYLD: negative regulation of NF-kappaB signaling and more. Cell Mol Life Sci. 2008; 65:1123-1132.

Cremasco V, Decker CE, Stumpo D, Blackshear PJ, Nakayama KI, Nakayama K, Lupu TS, Graham DB, Novack DV, Faccio R. Protein kinase C-delta deficiency perturbs bone homeostasis by selective uncoupling of cathepsin K secretion and ruffled border formation in osteoclasts. J Bone Miner Res. 2012 Dec;27(12):2452-63.

Cunningham JT, Rodgers JT, Arlow DH, Vazquez F, Mootha VK, Puigserver P. mTOR controls mitochondrial oxidative function through a YY1-PGC-1alpha transcriptional complex. Nature. 2007; 450:736-740.

Darnay BG, Haridas V, Ni J, Moore PA, Aggarwal BB. Characterization of the intracellular domain of receptor activator of NF-κB (RANK): Interaction with tumor necrosis factor receptor-associated factors and activation of NF-κB and c-Jun N terminal kinase. J Biol Chem. 1998; 273:2055 -20555.

Daroszewska A, Ralston SH. Genetics of Paget's disease of bone. Clin Sci. 2005; 109:257-263.

Daroszewska A, van 't Hof RJ, Rojas JA, Layfield R, Landao-Basonga E, Rose L, Rose K, Ralston SH. A point mutation in the ubiquitin-associated domain of SQSMT1 is sufficient to cause a Paget's disease-like disorder in mice. Hum Mol Genet. 2011; 20:2734-2744.

Datta HK, Rathod H, Manning P, Turnbull Y, McNeil CJ. Parathyroid hormone induces superoxide anion burst in the osteoclast: evidence for the direct instantaneous activation of the osteoclast by the hormone. J Endocrinol. 1996; 149:269-275.

De Chiara A, Apice G, Fazioli F, Silvestro P, Carone G, Manco A. Multicentric giant cell tumor with viral-like inclusions associated with Paget's disease of bone: A case treated by steroid therapy. Oncol Rep. 1998; 5:317-320.

Draghici S, Khatri P, Eklund AC, Szallasi Z. Reliability and reproducibility issues in DNA microarray measurements. Trends Genet. 2006 Feb;22(2):101-9.

Demulder A, Takahashi S, Singer FR, Hosking DJ, Roodman GD. Abnormalities in osteoclast precursors and marrow accessory cells in Paget's disease. Endocrinology 1993; 133:1978-1982.

Dougall WC, Glaccum M, Charrier K, Rohrbach K, Brasel K, De Smedt T, Daro E, Smith J, Tometsko ME, Maliszewski CR, Armstrong A, Shen V, Bain S, Cosman D, Anderson D, Morrissey PJ, Peschon JJ, Schuh J. RANK is essential for osteoclast and lymph node development. Genes Dev. 1999; 13:2412-2424.

Duan Z, Horwitz M. Gfi-1 takes center stage in hematopoietic stem cells. Trends Mol Med. 2005 Feb;11(2):49-52.

Durán A, Serrano M, Leitges M, Flores JM, Picard S., Brown JP, Moscat J, Diaz-Meco MT. The atypical PKC-interacting protein p62 is an important mediator of RANK-activated osteoclastogenesis. Devel Cell. 2004; 6:303-309.

Duran A, Amanchy R, Linares JF, Joshi J, Abu-Baker S, Porollo A, Hansen M, Moscat J, Diaz-Meco MT. p62 is a key regulator of nutrient sensing in the mTORC1 pathway. Mol Cell. 2011 Oct 7;44(1):134-46.

Eekhoff EW, Karperien M, Houtsma D, Zwinderman AH, Dragoiescu C, Kneppers AL, Papapoulos SE. Familial Paget's disease in The Netherlands: occurrence, identification of

new mutations in the sequestosome 1 gene, and their clinical associations. Arthritis Rheum. 2004; 50:1650-1654.

el-Labban NG 1984 Ultrastructural study of intranuclear tubulo-filaments in a giant cell tumour of bone in a patient with Paget's disease. J Oral Pathol. 1984; 13:650-660.

Falchetti A, Di Stefano M, Marini F, Del Monte F, Gozzini A, Masi L, Tanini A, Amedei A, Carossino A, Isaia G, Brandi ML. Segregation of a M404V mutation of the p62/sequestosome 1 (p62/SQSTM1) gene with polyostotic Paget's disease of bone in an Italian family. Arthritis Res Ther. 2005; 7:R1289-1295.

Fotino M, Haymovits A, Falk CT. Evidence for linkage between HLA and Paget's disease Transplant Proc. 1977; 9:1867-1868.

Galibert L, Tometsko ME, Anderson DM, Cosman D, Dougall WC. The involvement of multiple tumor necrosis factor receptor (TNFR)-associated factors in the signaling mechanisms of receptor activator of NF-κB, a member of the TNFR superfamily. J Biol. Chem. 1998; 273:34120-34127.

Garner TP, Long J, Layfield R, Searle MS. Impact of p62/SQSTM1 UBA domain mutations linked to Paget's disease of bone on ubiquitin recognition. Biochem. 2011; 50:4665-4674.

Geetha T, Wooten MW. Structure and functional properties of the ubiquitin binding protein p62. FEBS Let. 2002; 512:19-24.

Gibbings D, Mostowy S, Jay F, Schwab Y, Cossart P, Voinnet O. Selective autophagy degrades DICER and AGO2 and regulates miRNA activity. Nat Cell Biol. 2012 Dec;14(12):1314-21.

Glaser B, Furth J, Stanley CA, Baker L, Thornton PS, Landau H, Permutt MA. Intragenic single nucleotide polymorphism haplotype analysis of SUR1 mutations in familial hyperinsulinism. Hum Mutat. 1999; 14:23-29.

Gohda J, Akiyama T, Koga T, Takayanagi H, Tanaka S, Inoue J. RANK-mediated amplification of TRAF6 signaling leads to NFATc1 induction during osteoclastogenesis. EMBO J. 2005; 24:790-799.

Gonzales F, Karnovsky MJ. Electron microscopy of osteoclasts in healing fractures of rat bone. J Biophys Biochem Cytol. 1961 Feb;9:299-316.

Good DA, Busfield F, Fletcher BH, Lovelock PK, Duffy DL, Kesting JB, Andersen J, Shaw JT. Identification of SQSTM1 mutations in familial Paget's disease in Australian pedigrees. Bone. 2004; 35:277-282.

Good DA, Busfield F, Fletcher BH, Duffy DL, Kesting JB, Andersen J, Shaw JT. Linkage of Paget disease of bone to a novel region on human chromosome 18q23. Am J Hum Genet. 2002; 70:517-525.

Gordon MT, Anderson DC, Sharpe PT. Canine distemper virus localised in bone cells of patients with Paget's disease. Bone. 1991; 12:195-201.

Ha H, Kwak HB, Lee SW, Jin HM, Kim HM, Kim HH, Lee ZH. Reactive oxygen species mediate RANK signaling in osteoclasts. Exp Cell Res. 2004; 301:119-127.

Hamdy RC. Clinical features and pharmacologic treatment of Paget's disease. Endocr Metab Clin North Am. 1995; 24:421-436.

Hansen MF, Nellissery MJ, Bhatia P. Common mechanisms of osteosarcoma and Paget's disease. J Bone Miner Res. 1999; 14 Suppl. 2:39-44.

Harada H1, Warabi E, Matsuki T, Yanagawa T, Okada K, Uwayama J, Ikeda A, Nakaso K, Kirii K, Noguchi N, Bukawa H, Siow RC, Mann GE, Shoda J, Ishii T, Sakurai T. Deficiency of p62/Sequestosome 1 causes hyperphagia due to leptin resistance in the brain. J Neurosci. 2013 Sep 11;33(37):14767-77.

Haslam SI, Van Hul W, Morales-Piga A, Balemans W, San-Millan JL, Nakatsuka K, Willems P, Haites NE, Ralston SH. Paget's disease of bone: evidence for a susceptibility locus on chromosome 18q and for genetic heterogeneity. J Bone Miner Res. 1998; 13:911-917.

Helfrich MH, Hobson RP, Grabowski PS, Zurbriggen A, Cosby SL, Dickson GR, Fraser WD, Ooi CG, Selby PL, Crisp AJ, Wallace RG, Kahn S, Ralston SH. A negative search for a paramyxoviral etiology of Paget's disease of bone: molecular, immunological, and ultrastructural studies in UK patients. J Bone Miner Res. 2000; 15:2315-2329.

Hiruma Y, Kurihara N, Subler MA, Zhou H, Boykin CS, Zhang H, Ishizuka S, Dempster DW, Roodman GD, Windle JJ. A SQSTM1/p62 mutation linked to Paget's disease increases the osteoclastogenic potential of the bone microenvironment. Hum Mol Genet. 2008; 17:3708-3719.

Hocking LJ, Herbert CA, Nicholls RK, Williams F, Bennett ST, Cundy T, Nicholson GC, Wuyts W, Van Hul W, Ralston SH. Genomewide search in familial Paget disease of bone shows evidence of genetic heterogeneity with candidate loci on chromosomes 2q36, 10p13, and 5q35 Am J Hum Genet. 2001; 69:1055-1061.

Hocking LJ, Herbert CA, Nicholls RK, Williams F, Bennett ST, Cundy T, Nicholson GC, Wuyts W, Van Hul W, Ralston SH. Genomewide search in familial Paget disease of bone shows evidence of genetic heterogeneity with candidate loci on chromosomes 2q36, 10p13, and 5q35. Am J Hum Genet. 2001; 69:1055-1061.

Hocking LJ, Lucas GJ, Daroszewska A, Mangion J, Olavesen M, Cundy T, Nicholson GC, Ward L, Bennett ST, Wuyts W, Van Hul W, Ralston SH. Domain-specific mutations in sequestosome 1 (SQSTM1) cause familial and sporadic Paget's disease. Hum Mol Genet. 2002; 11:2735-2739.

Hocking LJ, Lucas GJ, Daroszewska A, Cundy T, Nicholson GC, Donath J, Walsh JP, Finlayson C, Cavey JR, Ciani B, Sheppard PW, Searle MS, Layfield R, Ralston SH. Novel UBA domain mutations of SQSTM1 in Paget's disease of bone: genotype phenotype correlation, functional analysis, and structural consequences. J Bone Miner Res. 2004;19:1122-1127.

Hosking DJ. Paget's disease of bone. Br Med J (Clin Res Ed). 1981; 283:686-288.

Huang DW, Sherman BT, Lempicki RA. Systematic and integrative analysis of large gene lists using DAVID Bioinformatics Resources. Nature Protoc. 2009;4(1):44-57.

Huang DW, Sherman BT, Lempicki RA. Bioinformatics enrichment tools: paths toward the comprehensive functional analysis of large gene lists. Nucleic Acids Res. 2009;37(1):1-13.

Ichimura Y, Waguri S, Sou YS, Kageyama S, Hasegawa J, Ishimura R, Saito T, Yang Y, Kouno T, Fukutomi T, Hoshii T, Hirao A, Takagi K, Mizushima T, Motohashi H, Lee MS, Yoshimori T, Tanaka K, Yamamoto M, Komatsu M. Phosphorylation of p62 activates the Keap1-Nrf2 pathway during selective autophagy. Mol Cell. 2013 Sep 12;51(5):618-31.

Indo Y, Takeshita S, Ishii KA, Hoshii T, Aburatani H, Hirao A, Ikeda K. Metabolic regulation of osteoclast differentiation and function. J Bone Miner Res. 2013 Nov;28(11):2392-9.

Ioannidis JP, Allison DB, Ball CA, Coulibaly I, Cui X, Culhane AC, Falchi M, Furlanello C, Game L, Jurman G, Mangion J, Mehta T, Nitzberg M, Page GP, Petretto E, van Noort V. Repeatability of published microarray gene expression analyses. Nat Genet. 2009 Feb;41(2):149-55.

Iotsova V, Caamano J, Loy J, Yang Y, Lewin A, Bravo R. Osteopetrosis in mice lacking NF-kappaB1 and NF-kappaB2. Nat Med. 1997; 3:1285-1289.

Irizarry RA, Warren D, Spencer F, Kim IF, Biswal S, Frank BC, Gabrielson E, Garcia JG, Geoghegan J, Germino G, Griffin C, Hilmer SC, Hoffman E, Jedlicka AE, Kawasaki E,

Martínez-Murillo F, Morsberger L, Lee H, Petersen D, Quackenbush J, Scott A, Wilson M, Yang Y, Ye SQ, Yu W. Multiple-laboratory comparison of microarray platforms. Nat Methods. 2005 May;2(5):345-50.

Ishii T, Yanagawa T, Kawane T, Yuki K, Seita J, Yoshida H, Bannai S. Murine peritoneal macrophages induce a novel 60-kDa protein with structural similarity to a tyrosine kinase p56lck-associated protein in response to oxidative stress. Biochem Biophys Res Commun. 1996; 226:456-460.

Ishii T, Yanagawa T, Yuki K, Kawane T, Yoshida H, Bannai S. Low micromolar levels of hydrogen peroxide and proteasome inhibitors induce the 60-kDa A170 stress protein in murine peritoneal macrophages. Biochem Biophys Res Commun. 1997; 232:33-37.

Ishimura R, Tanaka K, Komatsu M. Dissection of the role of p62/Sqstm1 in activation of Nrf2 during xenophagy. FEBS Lett. 2014 Mar 3;588(5):822-8.

Isogai S, Morimoto D, Arita K, Unzai S, Tenno T, Hasegawa J, Sou YS, Komatsu M, Tanaka K, Shirakawa M, Tochio H. Crystal structure of the ubiquitin-associated (UBA) domain of p62 and its interaction with ubiquitin. J Biol Chem. 2011; 286:31864-31874.

Jain A, Lamark T, Sjøttem E, Larsen KB, Awuh JA, Øvervatn A, McMahon M, Hayes JD, Johansen T. p62/SQSTM1 is a target gene for transcription factor NRF2 and creates a positive feedback loop by inducing antioxidant response element-driven gene transcription. J Biol Chem. 2010; 285:22576-22591.

Jänicke RU, Sprengart ML, Wati MR, Porter AG. Caspase-3 is required for DNA fragmentation and morphological changes associated with apoptosis. J Biol Chem. 1998 Apr 17;273(16):9357-60.

Jilka RL. The relevance of mouse models for investigating age-related bone loss in humans. J Gerontol A Biol Sci Med Sci. 2013 Oct;68(10):1209-17.

Jin W, Chang M, Paul EM, Babu G, Lee AJ, Reiley W, Wright A, Zhang M, You J, Sun SC. Deubiquitinating enzyme CYLD negatively regulates RANK signaling and steoclastogenesis in mice. J Clin Invest. 2008; 118:1858-1866.

Johnson CD, Esquela-Kerscher A, Stefani G, Byrom M, Kelnar K, Ovcharenko D, Wilson M, Wang X, Shelton J, Shingara J, Chin L, Brown D, Slack FJ. The let-7 microRNA represses cell proliferation pathways in human cells. Cancer Res. 2007 Aug 15;67(16):7713-22.

Johnson-Pais TL, Wisdom JH, Weldon KS, Cody JD, Hansen MF, Singer FR, Leach RJ. Three novel mutations in SQSTM1 identified in familial Paget's disease of bone. J Bone Miner Res. 2003; 18:1748-1753.

Jono H, Lim JH, Chen LF, Xu H, Trompouki E, Pan ZK, Mosialos G, Li JD. NF-kappaB is essential for induction of CYLD, the negative regulator of NFkappaB: evidence for a novel inducible autoregulatory feedback pathway. J Biol Chem. 2004; 279:36171-36174.

Joung I, Strominger JL, Shin J. Molecular cloning of a phosphotyrosine-independent ligand of the p56lck SH2 domain. Proc Natl Acad Sci USA. 1996; 93:5991-5995.

Kall L, Storey JD, Noble WS. QVALITY: non-parametric estimation of q-values and posterior error probabilities. Bioinformatics. 2009; 25:964-966.

Kanis JA. Pathophysiology and treatment of Paget's disease of bone. 2nd ed. London: Martin Dunitz; 1998.

Khaldoyanidi S, Sikora L, Broide DH, Rothenberg ME, Sriramarao P.Constitutive overexpression of IL-5 induces extramedullary hematopoiesis in the spleen. Blood. 2003 Feb 1;101(3):863-8.

Kim N, Kadono Y, Takami M, Lee J, Lee SH, Okada F, Kim JH, Kobayashi T, Odgren PR, Nakano H, Yeh WC, Lee SK, Lorenzo JA, Choi Y. Osteoclast differentiation independent of the TRANCE-RANK-TRAF6 axis. J Exp Med. 2005; 202:589-595.

Kim Y, Sato K, Asagiri M, Morita I, Soma K, Takayanagi H. Contribution of nuclear factor of activated T cells c1 to the transcriptional control of immunoreceptor osteoclast-associated receptor but not triggering receptor expressed by myeloid cells-2 during osteoclastogenesis. J Biol Chem. 2005 Sep 23;280(38):32905-13.

Kim H, Kim IY, Lee SY, Jeong D. Bimodal actions of reactive oxygen species in the differentiation and bone-resorbing functions of osteoclasts. FEBS Lett. 2006; 580:5661-5665.

Kim K, Lee SH, Ha Kim J, Choi Y, Kim N. NFATc1 induces osteoclast fusion via up-regulation of Atp6v0d2 and the dendritic cell-specific transmembrane protein (DC-STAMP). Mol Endocrinol. 2008 Jan;22(1):176-85.

Kim JY, Ozato K. The sequestosome 1/p62 attenuates cytokine gene expression in activated macrophages by inhibiting IFN regulatory factor 8 and TNF receptor-associated factor 6/NF-kappaB activity. J Immunol. 2009; 182:2131-2140.

Kim MS, Yang YM, Son A, Tian YS, Lee SI, Kang SW, Muallem S, Shin DM. RANKL-mediated reactive oxygen species pathway that induces long lasting Ca2+ oscillations essential for osteoclastogenesis. J Biol Chem. 2010 Mar 5;285(10):6913-21.

Kirkin V, McEwan DG, Novak I, Dikic I. A role for ubiquitin in selective autophagy. Mol Cell. 2009 May 15;34(3):259-69.

Kobayashi K, Takahashi N, Jimi E, Udagawa N, Takami M, Kotake S, Nakagawa N, Kinosaki M, Yamaguchi K, Shima N, Yasuda H, Morinaga T, Higashio K, Martin TJ, Suda T. Tumor

necrosis factor alpha stimulates osteoclast differentiation by a mechanism independent of the ODF/RANKL-RANK interaction. J Exp Med. 2000; 191:275-286.

Kobayashi N, Kadono Y, Naito A, Maatsumoto K, Yamamoto T, Tanaka S, Inoue J. Segregation of TRAF6-mediated signaling pathways clarifies its role in osteoclastogenesis. EMBO J. 2001; 20:1271-1280.

Kobayashi T1, Walsh PT, Walsh MC, Speirs KM, Chiffoleau E, King CG, Hancock WW, Caamano JH, Hunter CA, Scott P, Turka LA, Choi Y. TRAF6 is a critical factor for dendritic cell maturation and development. Immunity. 2003 Sep;19(3):353-63.

Kobayashi A, Kang MI, Okawa H, Ohtsuji M, Zenke Y, Chiba T, Igarashi K, Yamamoto M. Oxidative stress sensor Keap1 functions as an adaptor for Cul3-based E3 ligase to regulate proteasomal degradation of Nrf2. Mol Cell Biol. 2004; 24:7130-7139.

Komatsu M, Waguri S, Koike M, Sou YS, Ueno T, Hara T, Mizushima N, Iwata J, Ezaki J, Murata S, Hamazaki J, Nishito Y, Iemura S, Natsume T, Yanagawa T, Uwayama J, Warabi E, Yoshida H, Ishii T, Kobayashi A, Yamamoto M, Yue Z, Uchiyama Y, Kominami E, Tanaka K. Homeostatic levels of p62 control cytoplasmic inclusion body formation in autophagy-deficient mice. Cell. 2007 Dec 14;131(6):1149-63.

Kong YY, Yoshida H, Sarosi I, Tan HL, Timms E, Capparelli C, Morony S, Oliveira-dos-Santos AJ, Van G, Itie A, Khoo W, Wakeham A, Dunstan CR, Lacey DL, Mak TW, Boyle WJ, Penniinger JM. OPGL is a key regulator of osteoclastogenesis, lymphocyte development and lymph-node organogenesis. Nature. 1999; 397:315-323.

Kovalenko A, Chable-Bessia C, Cantarella G, Israël A, Wallach D, Courtois G. The tumour suppressor CYLD negatively regulates NF-kappaB signalling by deubiquitination. Nature. 2003; 424:801-805.

Kukita A, Chenu C, McManus LM, Mundy GR, Roodman GD. Atypical multinucleated cells form in long-term marrow cultures from patients with Paget's disease. J Clin Invest. 1990; 85:1280-1286.

Kurihara N, Reddy SV, Araki N, Ishizuka S, Ozono K, Cornish J, Cundy T, Singer FR, Roodman GD. Role of TAFII-17, a VDR binding protein, in the increased osteoclast formation in Paget's Disease. J Bone Miner Res. 2004; 19:1154-1164.

Kurihara N, Reddy SV, Menaa C, Anderson D, Roodman GD. Osteoclasts expressing the measles virus nucleocapsid gene display a pagetic phenotype. J Clin Invest. 2000; 105:607-614.

Kurihara N, Zhou H, Reddy SV, Garcia Palacios V, Subler MA, Dempster DW, Windle JJ, Roodman GD. Expression of measles virus nucleocapsid protein in osteoclasts induces Paget's disease-like bone lesions in mice. J Bone Miner Res. 2006; 21:446-455.

Kwon J, Han E, Bui CB, Shin W, Lee J, Lee S, Choi YB, Lee AH, Lee KH, Park C, Obin MS, Park SK, Seo YJ, Oh GT, Lee HW, Shin J. Assurance of mitochondrial integrity and mammalian longevity by the p62-Keap1-Nrf2-Nqo1 cascade. EMBO Rep. 2012 Feb 1;13(2):150-6.

Lamark T, Perander M, Outzen H, Kristiansen K, Øvervatn A, Michaelsen E, Bjørkøy G, Johansen T. Interaction codes within the family of mammalian Phox and Bem1p domain-containing proteins. J Biol Chem. 2003; 278:34568-34581.

Lamothe B, Besse A, Campos AD, Webster WK, Wu H, Darnay BG. Site-specific Lys-63-linked tumor necrosis factor receptor-associated factor 6 auto-ubiquitination is a critical determinant of IκB kinase activation. J Biol Chem. 2007; 282:4102-4112.

Lamothe B, Webster WK, Gopinathan A, Besse A, Campos AD, Carnay BG. TRAF6 ubiquitin ligase is essential for RANKL signaling and osteoclast differentiation . Biochem Biophys Res Commun. 2008; 359:1044-1049.

Langston AL, Ralston SH. Management of Paget's disease of bone. Rheumatology. 2004; 43:955-959.

Laurin N, Brown JP, Lemainque A, Duchesne A, Huot D, Lacourciere Y, Drapeau G, Verreault J, Raymond V, Morissette J. Paget disease of bone: mapping of two loci at 5q35-qter and 5q31. Am J Hum Genet. 2001; 69:528-543.

Laurin N, Brown JP, Lemainque A, Duchesne A, Huot D, Lacourcière Y, Drapeau G, Verreault J, Raymond V, Morissette J. Paget disease of bone: mapping of two loci at 5q35-qter and 5q31. Am J Hum Genet. 2001; 69:528-543.

Laurin N, Brown JP, Morissette J, Raymond V. Recurrent mutation of the gene encoding sequestosome 1 (SQSTM1/p62) in Paget disease of bone. Am J Hum Genet. 2002;70:1582-8.

Layfield R, Shaw B. Ubiquitin-mediated signalling and Paget disease of bone. BMC Biochemistry. 2007; 8(suppl 1):S5.

Leach RJ, Singer FR, Roodman GD. The genetics of Paget's disease of the bone. J Clin Endocrinol Metab. 2001; 86:24-28.

Leitges M, Sanz L, Martin P, Duran A, Braun U, García JF, Camacho F, Diaz-Meco MT, Rennert PD, Moscat J. Targeted disruption of the zetaPKC gene results in the impairment of the NF-kappaB pathway. Mol Cell. 2001 Oct;8(4):771-80.

Lee M, Shin J. Triage of oxidation-prone proteins by SQSTM1/p62 within the mitochondria. Biochem Biophys Res Commun. 2011; 413:122-127.

Lee NK, Choi YG, Baik JY, Han SY, Jeong DW, Bae YS, Kim N, Lee SY. A crucial role for reactive oxygen species in RANKL-induced osteoclast differentiation. Blood. 2005; 106:852-859.

Lee Y, Kim HJ, Park CK, Kim YG, Lee HJ, Kim JY, Kim HH. MicroRNA-124 regulates osteoclast differentiation. Bone. 2013 Oct;56(2):383-9.

Linares JF, Amanchy R, Greis K, Diaz-Meco MT, Moscat J. Phosphorylation of p62 by cdk1 controls the timely transit of cells through mitosis and tumor cell proliferation. Mol Cell Biol. 2011; 31:105-117.

Lomaga MA, Yeh WC, Sarosi I, Duncan GS, Furlonger C, Ho A, Morony S, Capparelli C, Van G, Kaufman S, van der Heiden A, Itie A, Wakeham A, Khoo W, Sasaki T, Cao Z, Penninger JM, Paige CJ, Lacey DL, Dunstan CR, Boyle WJ, Goeddel DV, Mak TW. TRAF6 deficiency results in osteopetrosis and defective interleukin-1, CD40, and LPS signaling. Genes Dev. 1999; 13:1015-1024.

Lomaga MA, Yeh WC, Sarosi I, Duncan, GS, Furlonger C, Ho A, Morony S, Capparelli C, Van G, Kaufman S, van der Heiden A, Itie A, Wakeham A, Khoo W, Sasaki T, Cao Z, Penninger JM, Paige CJ, Lacey DL, Dunstan CR, Boyle WJ, Goeddel DV, Mak TW. TRAF6 deficiency results in osteopetrosis and defective interleukin-1, CD40, and LPS signaling. Genes Dev. 1999; 13:1015-1024.

Long J, Garner TP, Pandya MJ, Craven CJ, Chen P, Shaw B, Williamson MP, Layfield R, Searle MS. Dimerisation of the UBA domain of p62 inhibits ubiquitin binding and regulates NF-kappaB signalling. J Mol Biol. 2010; 396:178-194.

MAQC Consortium. The MicroArray Quality Control (MAQC)-II study of common practices for the development and validation of microarray-based predictive models. Nat Biotechnol. 2010 Aug;28(8):827-38.

Magitsky S, Lipton JF, Reidy J, Vigorita VJ, Bryk E. Ultrastructural features of giant cell tumors in Paget's disease. Clin Orthop Relat Res. 2002; 402:213-219.

Malone JH, Oliver B. Microarrays, deep sequencing and the true measure of the transcriptome. BMC Biol. 2011 May 31;9:34.

Martin TJ. Osteoblast-derivde PTHrP is a physiological regulator of bone formation. J Clin Invest. 2005: 115:2322-2324.

Matthews BG, Afzal MA, Minor PD, Bava U, Callon KE, Pitto RP, Cundy T, Cornish J, Reid IR, Naot D. Failure to detect measles virus ribonucleic acid in bone cells from patients with Paget's disease. J Clin Endocrinol Metab. 2008; 93:1398-1401.

McGill GG, Horstmann M, Widlund HR, Du J, Motyckova G, Nishimura EK, Lin YL, Ramaswamy S, Avery W, Ding HF, Jordan SA, Jackson IJ, Korsmeyer SJ, Golub TR, Fisher DE. Bcl2 regulation by the melanocyte master regulator Mitf modulates lineage survival and melanoma cell viability. Cell. 2002 Jun 14;109(6):707-18.

McHugh KP, Hodivala-Dilke K, Zheng MH, Namba N, Lam J, Novack D, Feng X, Ross FP, Hynes RO, Teitelbaum SL. Mice lacking beta3 integrins are osteosclerotic because of dysfunctional osteoclasts. J Clin Invest. 2000 Feb;105(4):433-40.

Mee AP, Dixon JA, Hoyland JA, Davies M, Selby PL, Mawer EB. Detection of canine distemper virus in 100% of Paget's disease samples by in situ-reverse transcriptase-polymerase chain reaction. Bone. 1998; 23:171-175.

Menaa C, Barsony J, Reddy SV, Cornish J, Cundy T, Roodman GD. 1,25-dihydroxyvitamin D3 hypersensitivity of osteoclast precursors from patients with Paget's disease. J Bone Miner Res. 2000;.15:228-236.

Menaa C, Kurihara N, and Roodman GD. CFU-GM-derived cells form osteoclasts at a very high efficiency. Biochem Biophys Res Commun, 2000; 267:943-946.

Menaa C, Reddy SV, Kurihara N, Maeda H, Anderson D, Cundy T, Cornish J, Singer FR, Bruder JM, Roodman GD. Enhanced RANK ligand expression and responsivity of bone marrow cells in Paget's disease of bone. J Clin Invest. 2000; 105:1833-1838.

Meunier PJ, Coindre JM, Edouard CM, Arlot ME. Bone histomorphometry in Paget's disease. Quantitative and dynamic analysis of pagetic and nonpagetic bone tissue. Arthritis Rheum. 1980; 23:1095-1103.

Michou L, Chamoux E, Couture J, Morissette J, Brown JP, Roux S. Gene expression profile in osteoclasts from patients with Paget's disease of bone. Bone. 2010 Mar;46(3):598-603. Erratum in: Bone. 2010 Jun;46(6):1668-9.

Mills BG, Singer FR, Weiner LP, Holst PA. Immunohistological demonstration of respiratory syncytial virus antigens in Paget disease of bone. Proc Natl Acad Sci USA. 1981; 78:1209-1213.

Mirra JM, Bauer FC, Grant TT. Giant cell tumor with viral-like intranuclear inclusions associated with Paget's disease. Clin Orthop Relat Res. 1981; 158:243-251.

Miyamoto T, Ohneda O, Arai F, Iwamoto K, Okada S, Takagi K, Anderson DM, Suda T. Bifurcation of osteoclasts and dendritic cells from common progenitors. Blood. 2001 Oct 15;98(8):2544-54.

Miyauchi Y, Ninomiya K, Miyamoto H, Sakamoto A, Iwasaki R, Hoshi H, Miyamoto K, Hao W, Yoshida S, Morioka H, Chiba K, Kato S, Tokuhisa T, Saitou M, Toyama Y, Suda T, Miyamoto T. The Blimp1-Bcl6 axis is critical to regulate osteoclast differentiation and bone homeostasis. J Exp Med. 2010 Apr 12;207(4):751-62.

Miyazaki T, Iwasawa M, Nakashima T, Mori S, Shigemoto K, Nakamura H, Katagiri H, Takayanagi H, Tanaka S. Intracellular and extracellular ATP coordinately regulate the inverse correlation between osteoclast survival and bone resorption. J Biol Chem. 2012 Nov 2;287(45):37808-23.

Mizushima N, Levine B, Cuervo AM, Klionsky DJ. Autophagy fights disease through cellular self-digestion. Nature. 2008 Feb 28;451(7182):1069-75.

Mizukami J, Takaesu G, Akatsuka H, Sakurai H, Ninomiya-Tsuji J, Matsumoto K, Sakurai N. Receptor activator of NF-kappaB ligand (RANKL) activates TAK1 mitogen-activated protein kinase kinase kinase through a signaling complex containing RANK, TAB2, and TRAF6. Mol Cell Biol. 2002; 22:992-1000.

Mootha VK, Lindgren CM, Eriksson KF, Subramanian A, Sihag S, Lehar J, Puigserver P, Carlsson E, Ridderstråle M, Laurila E, Houstis N, Daly MJ, Patterson N, Mesirov JP, Golub TR, Tamayo P, Spiegelman B, Lander ES, Hirschhorn JN, Altshuler D, Groop LC. PGC-1alpha-responsive genes involved in oxidative phosphorylation are coordinately down-regulated in human diabetes. Nat Genet. 2003; 34:267-273.

Mootha VK, Handschin C, Arlow D, Xie X, St Pierre J, Sihag S, Yang W, Altshuler D, Puigserver P, Patterson N, Willy PJ, Schulman IG, Heyman RA, Lander ES, Spiegelman BM. Erralpha and Gabpa/b specify PGC-1alpha-dependent oxidative phosphorylation gene

expression that is altered in diabetic muscle. Proc Natl Acad Sci USA. 2004; 101:6570-6575.

Morales-Piga AA, Rey-Rey JS, Corres-Gonzalez J, Garcia-Sagredo JM, Lopez-Abente G. Frequency and characteristics of familial aggregation of Paget's disease of bone. J Bone Miner Res. 1995; 10:663-670.

Moscat J, Diaz-Meco MT, Wooten MW. Signal integration and diversification through the p62 scaffold protein. Trends Biochem Sci. 2007; 32:95-100.

Müller TD, Lee SJ, Jastroch M, Kabra D, Stemmer K, Aichler M, Abplanalp B, Ananthakrishnan G, Bhardwaj N, Collins S, Divanovic S, Endele M, Finan B, Gao Y, Habegger KM, Hembree J, Heppner KM, Hofmann S, Holland J, Küchler D, Kutschke M, Krishna R, Lehti M, Oelkrug R, Ottaway N, Perez-Tilve D, Raver C, Walch AK, Schriever SC, Speakman J, Tseng YH, Diaz-Meco M, Pfluger PT, Moscat J, Tschöp MH. p62 links β-adrenergic input to mitochondrial function and thermogenesis. J Clin Invest. 2013 Jan 2;123(1):469-78.

Muroi M, Tanamoto K. TRAF6 distinctively mediates MyD88- and IRAK-1-induced activation of NF-kappaB. J Leukoc Biol. 2008; 83:702-707.

Nagy ZB, Gergely P, Donáth J, Borgulya G, Csanád M, Poór G. Gene expression profiling in Paget's disease of bone: upregulation of interferon signaling pathways in pagetic monocytes and lymphocytes. J Bone Miner Res. 2008 Feb;23(2):253-9.

Naito A, Azuma S, Tanaka S, Miyazaki T, Takaki S, Takatsu K, Nakao K, Nakamura K, Katsuki M, Yamamoto T, Inoue J. Severe osteopetrosis, defective interleukin-1 signalling and lymph node organogenesis in TRAF6-deficient mice. Genes Cells. 1999; 4:353-362.

Najat D, Garner T, Hagen T, Shaw B, Sheppard PW, Falchetti A, Marini F, Brandi ML, Long JE, Cavey JR, Searle MS, Layfield R. Characterization of a non-UBA domain missense mutation

of sequestosome 1 (SQSTM1) in Paget's disease of bone. J Bone Miner Res. 2009 Apr;24(4):632-42.

Naot D, Bava U, Matthews B, Callon KE, Gamble GD, Black M, Song S, Pitto RP, Cundy T, Cornish J, Reid IR. Differential gene expression in cultured osteoblasts and bone marrow stromal cells from patients with Paget's disease of bone. J Bone Miner Res. 2007; 22:298-309.

Neale SD, Schulze E, Smith R, Athanasou NA. The influence of serum cytokines and growth factors on osteoclast formation in Paget's disease. Q J Med. 2002; 95:233-240.

Nezis IP, Simonsen A, Sagona AP, Finley K, Gaumer S, Contamine D, Rusten TE, Stenmark H, Brech A. Ref(2)P, the Drosophila melanogaster homologue of mammalian p62, is required for the formation of protein aggregates in adult brain. J Cell Biol. 2008 Mar 24;180(6):1065-71.

Nezis IP, Stenmark H. p62 at the interface of autophagy, oxidative stress signaling, and cancer. Antioxid Redox Signal. 2012; 17:786-793.

Ogata M, Hino S, Saito A, Morikawa K, Kondo S, Kanemoto S, Murakami T, Taniguchi M, Tanii I, Yoshinaga K, Shiosaka S, Hammarback JA, Urano F, Imaizumi K. Autophagy is activated for cell survival after endoplasmic reticulum stress. Mol Cell Biol. 2006 Dec;26(24):9220-31.

Oliveros JC. VENNY. An interactive tool for comparing lists with Venn diagrams. http://bioinfogp.cnb.csic.es/tools/venny/index.html.

Oslowski CM, Urano F. Measuring ER stress and the unfolded protein response using mammalian tissue culture system. Methods Enzymol. 2011;490:71-92

Pankiv S, Clausen TH, Lamark T, Brech A, Bruun JA, Outzen H, Øvervatn A, Bjørkøy G, Johansen T. p62/SQSTM1 binds directly to Atg8/LC3 to facilitate degradation of

ubiquitinated protein aggregates by autophagy. J Biol Chem. 2007 Aug 17;282(33):24131-45.

Pham L, Kaiser B, Romsa A, Schwarz T, Gopalakrishnan R, Jensen ED, Mansky KC. HDAC3 and HDAC7 have opposite effects on osteoclast differentiation. J Biol Chem. 2011 Apr 8;286(14):12056-65.

Puls A, Schmidt S, Grawe F, Stabel S. Interaction of protein kinase C zeta with ZIP, a novel protein kinase C-binding protein. Proc Natl Acad Sci USA. 1997; 94:6191-6196.

Räisänen SR, Halleen J, Parikka V, Väänänen HK. Tartrate-resistant acid phosphatase facilitates hydroxyl radical formation and colocalizes with phagocytosed Staphylococcus aureus in alveolar macrophages. Biochem Biophys Res Commun. 2001; 288:142-150.

Ralston SH, Afzal MA, Helfrich MH, Fraser WD, Gallagher JA, Mee A, Rima B. Multicenter blinded analysis of RT-PCR detection methods for paramyxoviruses in relation to Paget's disease of bone. J Bone Miner Res. 2007; 22:569-577.

Ralston SH, Helfrich MH. Are paramyxoviruses involved in Paget's disease? A negative view. Bone. 1999; 24(5 Suppl):17S-18S.

Ralston SH, Layfield R. Pathogenesis of Paget disease of bone. Calcif Tissue Int. 2012; 91:97-113.

Rea SL, Walsh JP, Ward L, Yip K, Ward BK, Kent GN, Steer JH, Xu J, Ratajczak T. A novel mutation (K378X) in the sequestosome 1 gene associated with increased NF-kappaB signaling and Paget's disease of bone with a severe phenotype. J Bone Miner Res. 2006 Jul;21(7):1136-45.

Rea SL, Walsh JP, Ward L, Magno AL, Ward BK, Shaw B, Layfield R, Kent GN, Xu J, Ratajczak T. Sequestosome 1 mutations in Paget's disease of bone in Australia: prevalence, genotype/phenotype correlation, and a novel non-UBA domain mutation (P364S) associated

with increased NF-kappaB signaling without loss of ubiquitin binding. J Bone Miner Res. 2009 Jul;24(7):1216-23.

Rebel A, Baslé M, Pouplard A, Kouyoumdjian S, Filmon R, Lepatezour A. Viral antigens in osteoclasts from Paget's disease of bone. Lancet. 1980; 2:344-346.

Rebel A, Basle M, Pouplard A, Malkani K, Filmon R, Lepatezour A. Towards a viral etiology for Paget's disease of bone. Metab Bone Dis Relat Res. 1981; 3:235-238.

Reich ES. Cancer trial errors revealed. Nature. 2011 Jan 13;469(7329):139-40.

Reddy SV, Singer FR, Roodman GD. Bone marrow mononuclear cells from patients with Paget's disease contain measles virus nucleocapsid messenger ribonucleic acid that has mutations in a specific region of the sequence. J Clin Endocrinol Metab. 1995; 80:2108-2111.

Rodriguez A, Durán A, Selloum M, Champy MF, Diez-Guerra FJ, Flores JM, Serrano M, Auwerx J, Diaz-Meco MT, Moscat J. Mature-onset obesity and insulin resistance in mice deficient in the signaling adapter p62. Cell Metab. 2006; 3:211-222.

Roodman GD, Windle JJ. Paget disease of bone. J Clin Invest. 2005; 115:200-208.

Ron D, Walter P. Signal integration in the endoplasmic reticulum unfolded protein response. Nat Rev Mol Cell Biol. 2007 Jul;8(7):519-29.

Rusten TE, Stenmark H. p62, an autophagy hero or culprit? Nat Cell Biol. 2010;12:207-209.

Salminen A, Kaarniranta K, Haapasalo A, Hiltunen M, Soininen H, Alafuzoff I. Emerging role of p62/sequestosome-1 in the pathogenesis of Alzheimer's disease. Prog Neurobiol. 2012; 96:87-95.

Sanchez P, De Carcer G, Sandoval IV, Moscat J, Diaz-Meco MT. Localization of atypical protein kinase C isoforms into lysosome-targeted endosomes through interaction with p62. Mol Cell Biol. 1998; 18:3069-3080.

Schmittgen TD, Zakrajsek BA. Effect of experimental treatment on housekeeping gene expression: validation by real-time, quantitative RT-PCR. J Biochem Biophys Methods. 2000 Nov 20;46(1-2):69-81.

Searle MS, Garner TP, Strachan J, Long J, Adlington J, Cavey JR, Shaw B, Layfield R. Structural insights into specificity and diversity in mechanisms of ubiquitin recognition by ubiquitin-binding domains. Biochem Soc Trans. 2012; 40:404-408.

Seibenhener ML, Geetha T, Wooten MW. Sequestosome 1/p62-More than just a scaffold. FEBS Lett. 2007; 581:175-179.

Seibenhener ML, Du Y, Diaz-Meco MT, Moscat J, Wooten MC, Wooten MW. A role for sequestosome 1/p62 in mitochondrial dynamics, import and genome integrity. Biochim Biophys Acta. 2013 Mar;1833(3):452-9.

Singer FR, Mills BG. Giant cell tumor arising in Paget's disease of bone. Recurrences after 36 years. Clin Orthop Relat Res. 1993; 293:293-301.

Singer FR, Roodman GD. Paget's Disease of Bone: Pathogenesis and Treatment. Bone-Metabolic Functions and Modulators: Topics Bone Biol. 2012; 7:197-215.

Singer FR. Paget's disease of bone possible viral basis. Trends Endocrinol Metab. 1996; 7:258-261.

Siris ES, Canfield RE. Paget's disease of bone. In: Becker KL, editor. Principles and practice of endocrinology and metabolism. Philadelphia: J.B. Lippincott; 1990. p. 504-12.

Siris ES, Clemens TP, McMahon D, Gordon A, Jacobs TP, Canfield RE. Parathyroid function in Paget's disease of bone. J Bone Miner Res. 1989;.4:75-79.

Siris ES, Ottman R, Flaster E, Kelsey JL. Familial aggregation of Paget's disease of bone. J Bone Miner Res. 1991; 6:495-500.

Smink JJ, Bégay V, Schoenmaker T, Sterneck E, de Vries TJ, Leutz A. Transcription factor C/EBPbeta isoform ratio regulates osteoclastogenesis through MafB. EMBO J. 2009 Jun 17;28(12):1769-81.

Szymczyk KH, Freeman TA, Adams CS, Srinivas V, Steinbeck MJ. Active caspase-3 is required for osteoclast differentiation. J Cell Physiol. 2006 Dec;209(3):836-44.

Song I, Kim JH, Kim K, Jin HM, Youn BU, Kim N. Regulatory mechanism of NFATc1 in RANKL-induced osteoclast activation. FEBS Lett. 2009 Jul 21;583(14):2435-40.

Sofaer JA, Holloway SM, Emery AE. A family study of Paget's disease of bone. J Epidemiol Community Health. 1983;3 7:226-231

Srinivasan S, Koenigstein A, Joseph J, Sun L, Kalyanaraman B, Zaidi M, Avadhani NG. Role of mitochondrial reactive oxygen species in osteoclast differentiation. Ann N Y Acad Sci. 2010 Mar;1192:245-52.

Stepkowski TM, Kruszewski MK. Molecular cross-talk between the NRF2/KEAP1 signaling pathway, autophagy, and apoptosis. Free Radic Biol Med. 2011; 50:1186-1195.

Suda N, Morita I, Kuroda T, Murota S. Participation of oxidative stress in the process of osteoclast differentiation. Biochim Biophys Acta. 1993; 1157:318-323.

Sun L, Iqbal J, Dolgilevich S, Yuen T, Wu XB, Moonga BS, Adebanjo OA, Bevis PJ, Lund F, Huang CL, Blair HC, Abe E, Zaidi M. Disordered osteoclast formation and function in a CD38 (ADP-ribosyl cyclase)-deficient mouse establishes an essential role for CD38 in bone resorption. FASEB J. 2003 Mar;17(3):369-75.

Sun SG, Lau YS, Itonaga I, Sabokbar A, Athanasou NA. Bone stromal cells in pagetic bone and Paget's sarcoma express RANKL and support human osteoclast formation. J Pathol. 2006; 209:114-120.

Sundaram K, Nishimura R, Senn J, Youssef RF, London SD, Reddy SV. RANK ligand signaling modulates the matrix metalloproteinase-9 gene expression during osteoclast differentiation. Exp Cell Res. 2007 Jan 1;313(1):168-78.

Sundaram K, Shanmugarajan S, Rao DS, Reddy SV. Mutant p62P392L stimulation of osteoclast differentiation in Paget's disease of bone. Endocrinology. 2011; 152:4180-4189.

Taguchi K, Fujikawa N, Komatsu M, Ishii T, Unno M, Akaike T, Motohashi H, Yamamoto M. Keap1 degradation by autophagy for the maintenance of redox homeostasis. Proc Natl Acad Sci USA. 2012; 109:13561-13566.

Takahashi N, Udagawa N, Kobayashi Y, Takami M, Martin TJ, Suda T. Osteoclast Generation, Ch. 9 in Principles of Bone Biology, 3rd Edition. Edited by T. J. Martin, L. G. Raisz and J. P. Bilezikian. Academic Press 2008.

Takayanagi H, Kim S, Koga T, Nishina H, Isshiki M, Yoshida H, Saiura A, Isobe M, Yokochi T, Inoue J, Wagner EF, Mak TW, Kodama T, Taniguchi T. Induction and activation of the transcription factor NFATc1 (NFAT2) integrate RANKL signaling in terminal differentiation of osteoclasts. Dev Cell. 2002 Dec;3(6):889-901.

Takayanagi H. Osteoimmunology: shared mechanisms and crosstalk between the immune and bone systems. Nature Rev. Immunology 2007; 7:292-304.

Takayanagi H. Receptor Activator of NFκB (RANK) Signaling, Ch. 11 in Principles of Bone Biology, 3rd Edition. Edited by T. J. Martin, L. G. Raisz and J. P. Bilezikian. Academic Press 2008.

Teramachi J, Zhou H, Subler MA, Kitagawa Y, Galson DL, Dempster DW, Windle JJ, Kurihara N, Roodman GD. Increased IL-6 Expression in Osteoclasts is Necessary but not Sufficient for

the Development of Paget's Disease of Bone. J Bone Miner Res. 2013 Dec 11. doi: 10.1002/jbmr.2158. [Epub ahead of print]

Teitelbaum SL, Ross FP. Genetic regulation of osteoclast development and function. Nat Rev Genet. 2003; 4:638-649.

Tohmonda T, Yoda M, Mizuochi H, Morioka H, Matsumoto M, Urano F, Toyama Y, Horiuchi K. The IRE1α-XBP1 pathway positively regulates parathyroid hormone (PTH)/PTH-related peptide receptor expression and is involved in pth-induced osteoclastogenesis. J Biol Chem. 2013 Jan 18;288(3):1691-5.

Turk R, 't Hoen PA, Sterrenburg E, de Menezes RX, de Meijer EJ, Boer JM, van Ommen GJ, den Dunnen JT. Gene expression variation between mouse inbred strains. BMC Genomics. 2004 Aug 18;5(1):57.

USDHHS. Bone Health and Osteoporosis: A Report of the Surgeon General 2004. http://www.surgeongeneral.gov/library/reports/bonehealth/executive_summary.html.

Vadlamudi RK, Joung I, Strominger JL, Shin J. p62, a phosphotyrosine-independent ligand of the SH2 domain of p56lck, belongs to a new class of ubiquitin-binding proteins. J Biol Chem. 1996; 271:20235-20237.

Walter P, Ron D. The unfolded protein response: from stress pathway to homeostatic regulation. Science. 2011 Nov 25;334(6059):1081-6.

Wang K, Niu J, Kim H, Kolattukudy PE. Osteoclast precursor differentiation by MCPIP via oxidative stress, endoplasmic reticulum stress, and autophagy. J Mol Cell Biol. 2011; 3:360-368.

Wang S, Yu H, Wickliffe JK. Limitation of the MTT and XTT assays for measuring cell viability due to superoxide formation induced by nano-scale TiO2. Toxicol In Vitro. 2011; 25:2147-2151.

Wang FM, Sarmasik A, Hiruma Y, Sun Q, Sammut B, Windle JJ, Roodman GD, Galson DL. Measles virus nucleocapsid protein, a key contributor to Paget's disease, increases IL-6 expression via down-regulation of FoxO3/Sirt1 signaling. Bone. 2013 Mar;53(1):269-76.

Wei S, Kitaura H, Zhou P, Ross FP, Teitelbaum SL. IL-1 mediates TNF-induced osteoclastogenesis. J Clin Invest. 2005; 115:282-290.

Werner de Castro GR1, Buss Z2, Da Rosa JS2, Fröde TS2. Inflammatory cytokines in Paget's disease of bone. Int Immunopharmacol. 2014 Feb;18(2):277-81.

Williams PJ, Nishu K, Rahman MM. HDAC inhibitor trichostatin A suppresses osteoclastogenesis by upregulating the expression of C/EBP-β and MKP-1. Ann N Y Acad Sci. 2011 Dec;1240:18-25.

Wong BR, Besser D, Kim N, Arron JR, Vologodskaia M, Hanafusa H, Choi Y. TRANCE, a TNF family member, activates Akt/PKB through a signaling complex involving TRAF6 and c-Src. Mol. Cell. 1999; 4:1041-1049.

Wong BR, Rho J, Arron J, Robinson E, Orlinick J, Chao M, Kalachikov S, Cayani E, Bartlett FS III, Frankel WN, Lee SY, Choi Y. TRANCE is a novel ligand of the tumor necrosis factor receptor family that activates c-Jun N-terminal kinase in T cells. J Biol Chem. 1998; 272:25190-25194.

Wooten MW, Geetha T, Seibenhener ML, Babu JR, Diaz-Meco MT, Moscat J. The p62 scaffold regulates nerve growth factor-induced NF-kappaB activation by influencing TRAF6 polyubiquitination. J Biol Chem. 2005;.280:35625-35629.

Wooten MW, Geetha T, Babu JR, Seibenhener ML, Peng J, Cox N, Diaz-Meco MT, Moscat J. Essential role of SQSTM1/p62 in regulating accumulation of K63-ubiquitinated proteins. J Biol Chem. 2008;283:6783-6789.

Wright T, Rea SL, Goode A, Bennett AJ, Ratajczak T, Long JE, Searle MS, Goldring CE, Park BK, Copple IM, Layfield R. The S349T mutation of SQSTM1 links Keap1/Nrf2 signalling to Paget's disease of bone. Bone. 2013 Feb;52(2):699-706.

Xia M, Gonzalez P, Li C, Meng G, Jiang A, Wang H, Gao Q, Debatin KM, Beltinger C, Wei J. Mitophagy enhances oncolytic measles virus replication by mitigating RLRs signaling. J Virol. 2014 Feb 26. [Epub ahead of print]

Xu G, Liu K, Anderson J, Patrene K, Lentzsch S, Roodman GD, Ouyang H. Expression of XBP1s in bone marrow stromal cells is critical for myeloma cell growth and osteoclast formation. Blood. 2012 May 3;119(18):4205-14.

Yamashita T, Yao Z, Li F, Zhang Q, Badell IR, Schwarz EM, Takeshita S, Wagner EF, Noda M, Matsuo K, Xing L, Boyce BF. NF-kappaB p50 and p52 regulate receptor activator of NF-kappaB ligand (RANKL) and tumor necrosis factor-induced osteoclast precursor differentiation by activating c-Fos and NFATc1. J Biol Chem. 2007; 282:18245-18253.

Yan J, Seibenhener ML, Calderilla-Barbosa L, Diaz-Meco MT, Moscat J, Jiang J, Wooten MW, Wooten MC. SQSTM1/p62 interacts with HDAC6 and regulates deacetylase activity. PLoS One. 2013 Sep 27;8(9):e76016.

Yanagawa T, Yuki K, Yoshida H, Bannai S, Ishii T. Phosphorylation of A170 stress protein by casein kinase II-like activity in macrophages. Biochem Biophys Res Commun. 1997; 241:157-163.

Yang L, Wu D, Wang X, Cederbaum AI. Depletion of cytosolic or mitochondrial thioredoxin increases CYP2E1-induced oxidative stress via an ASK-1-JNK1 pathway in HepG2 cells. Free Radic Biol Med. 2011 Jul 1;51(1):185-96.

Yang DQ, Feng S, Chen W, Zhao H, Paulson C, Li YP. V-ATPase subunit ATP6AP1 (Ac45) regulates osteoclast differentiation, extracellular acidification, lysosomal trafficking, and protease exocytosis in osteoclast-mediated bone resorption. J Bone Miner Res. 2012 Aug;27(8):1695-707.

Yip KH, Feng H, Pavlos NJ, Zheng MH, Xu J. p62 ubiquitin binding-associated domain mediated the receptor activator of nuclear factor-kappaB ligand-induced osteoclast formation: a new insight into the pathogenesis of Paget's disease of bone. Am J Pathol. 2006 Aug;169(2):503-14.

Zhang DE, Hetherington CJ, Chen HM, Tenen DG.The macrophage transcription factor PU.1 directs tissue-specific expression of the macrophage colony-stimulating factor receptor. Mol Cell Biol. 1994 Jan;14(1):373-81.

Zhang P, Zhang H. Autophagy modulates miRNA-mediated gene silencing and selectively degrades AIN-1/GW182 in C. elegans. EMBO Rep. 2013 Jun;14(6):568-76.

APPENDIX A

INHIBITION OF BCL6 SIGNALING IS PREDICTED IN KI CELLS ALONE

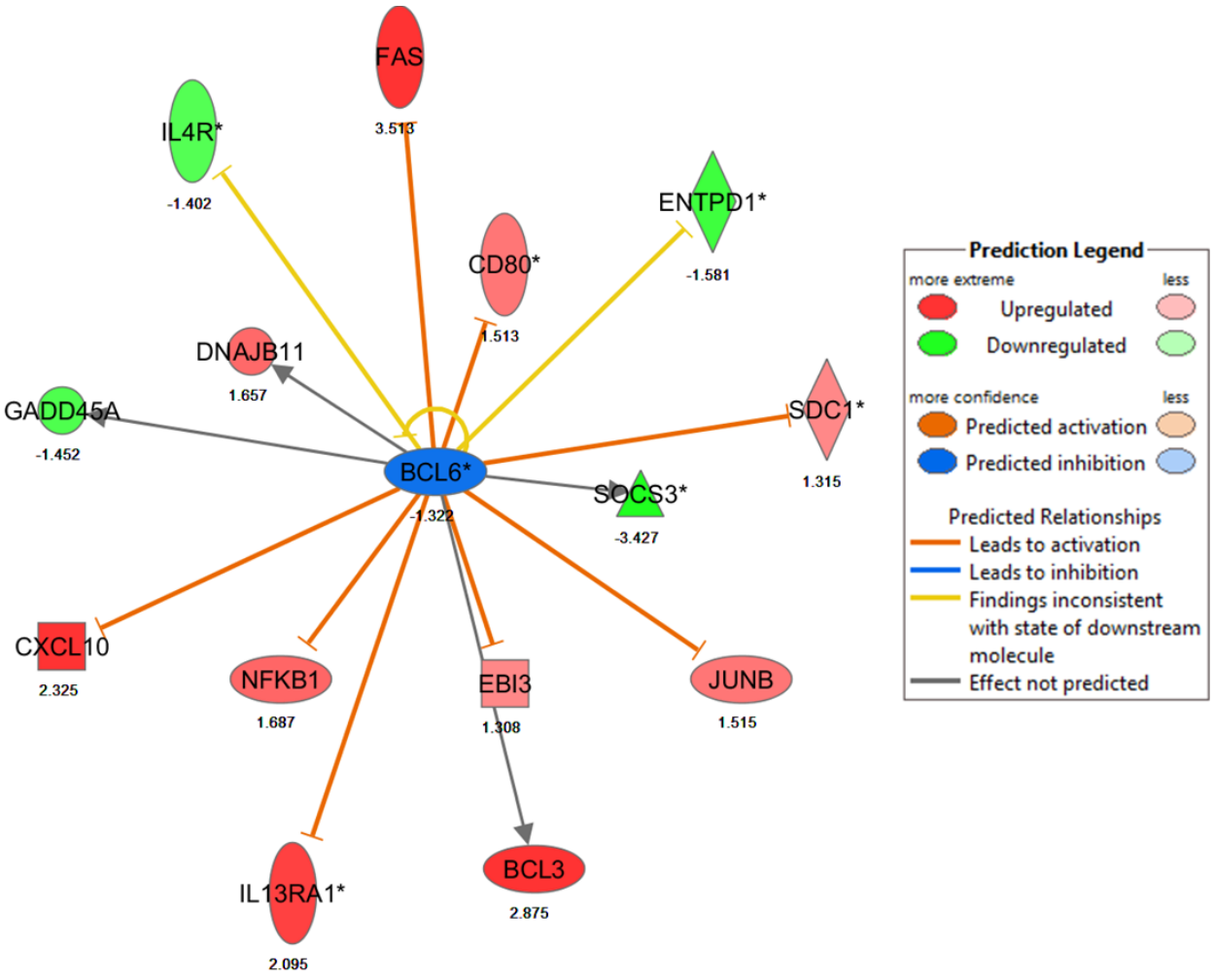

APPENDIX B

ACTIVATION OF XBP1 SIGNALING IS PREDICTED IN KI CELLS ALONE

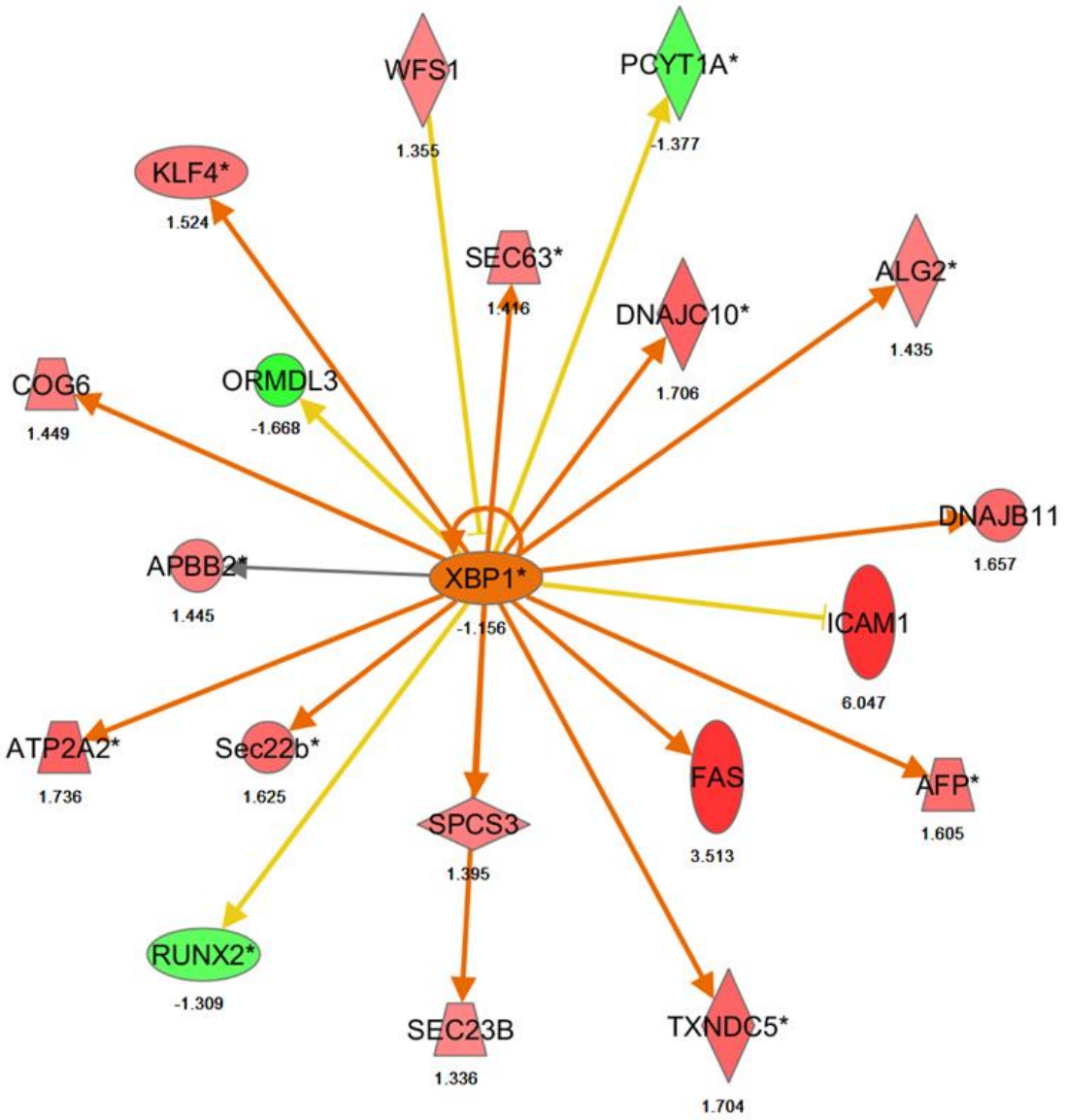

APPENDIX C

ACTIVATION OF CD38 SIGNALING IS PREDICTED IN KI CELLS ALONE

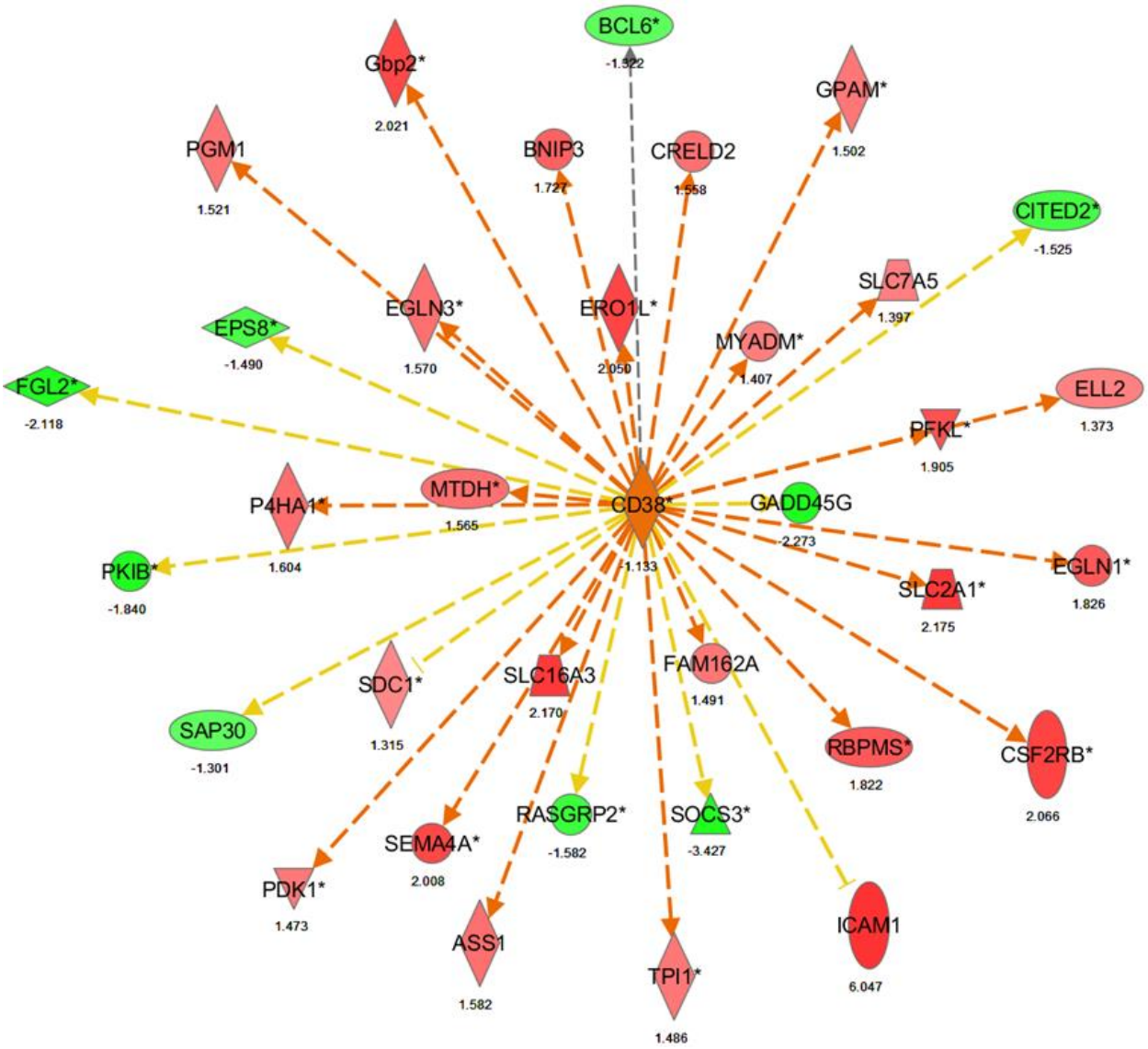

APPENDIX D

ACTIVATION OF MTOR SIGNALING IS PREDICTED IN WT (SHOWN) AND KI, BUT NOT KO, CELLS

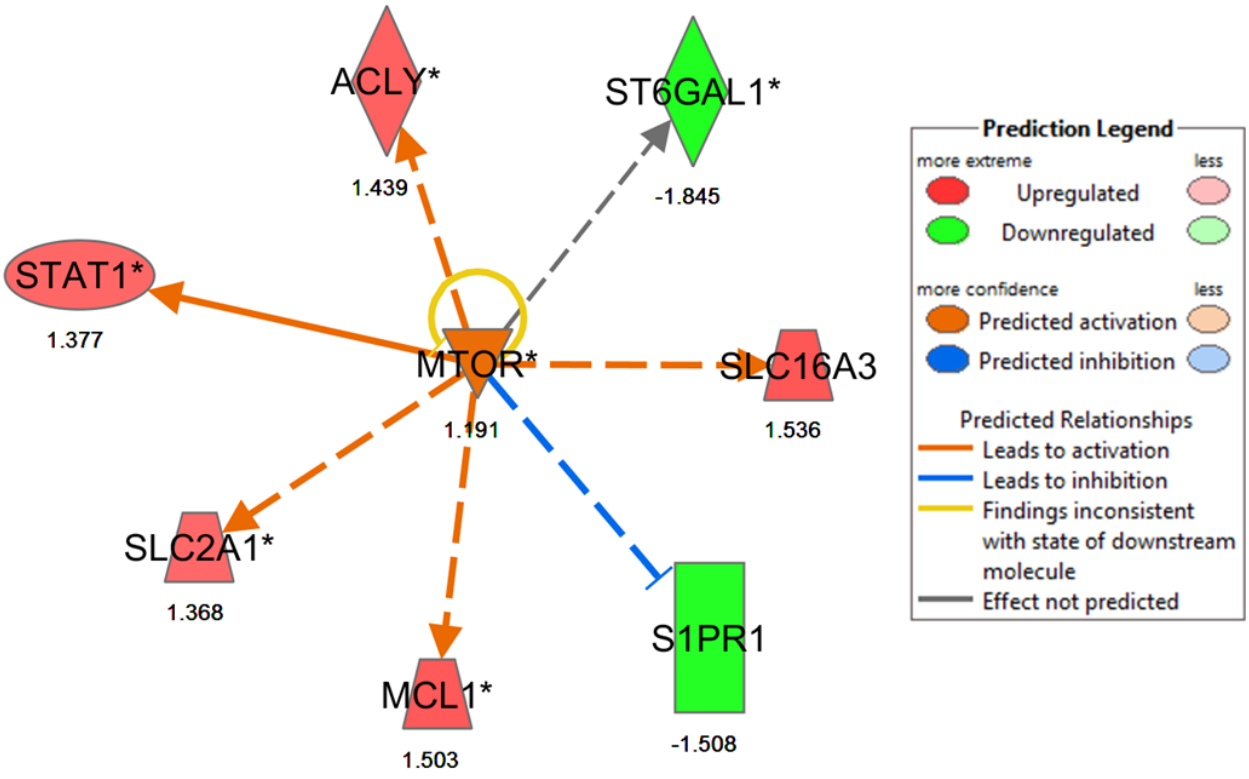

APPENDIX E

ACTIVATION OF NFE2L2 SIGNALING IS PREDICTED IN WT (SHOWN) AND KI, BUT NOT KO, CELLS

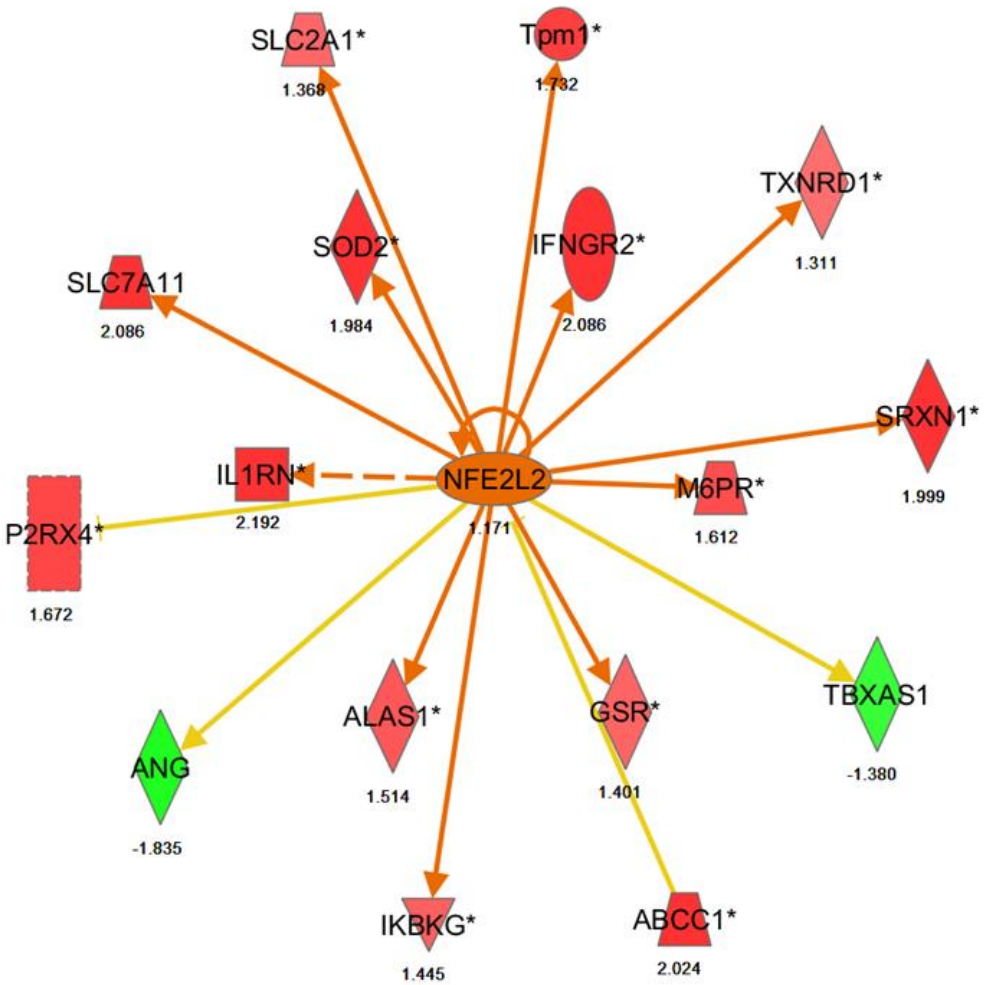

APPENDIX F

INHIBITION OF EUKARYOTIC TRANSLATION INITIATION FACTOR 4E (EIF4E) FUNCTION IS PREDICTED IN KO CELLS ALONE

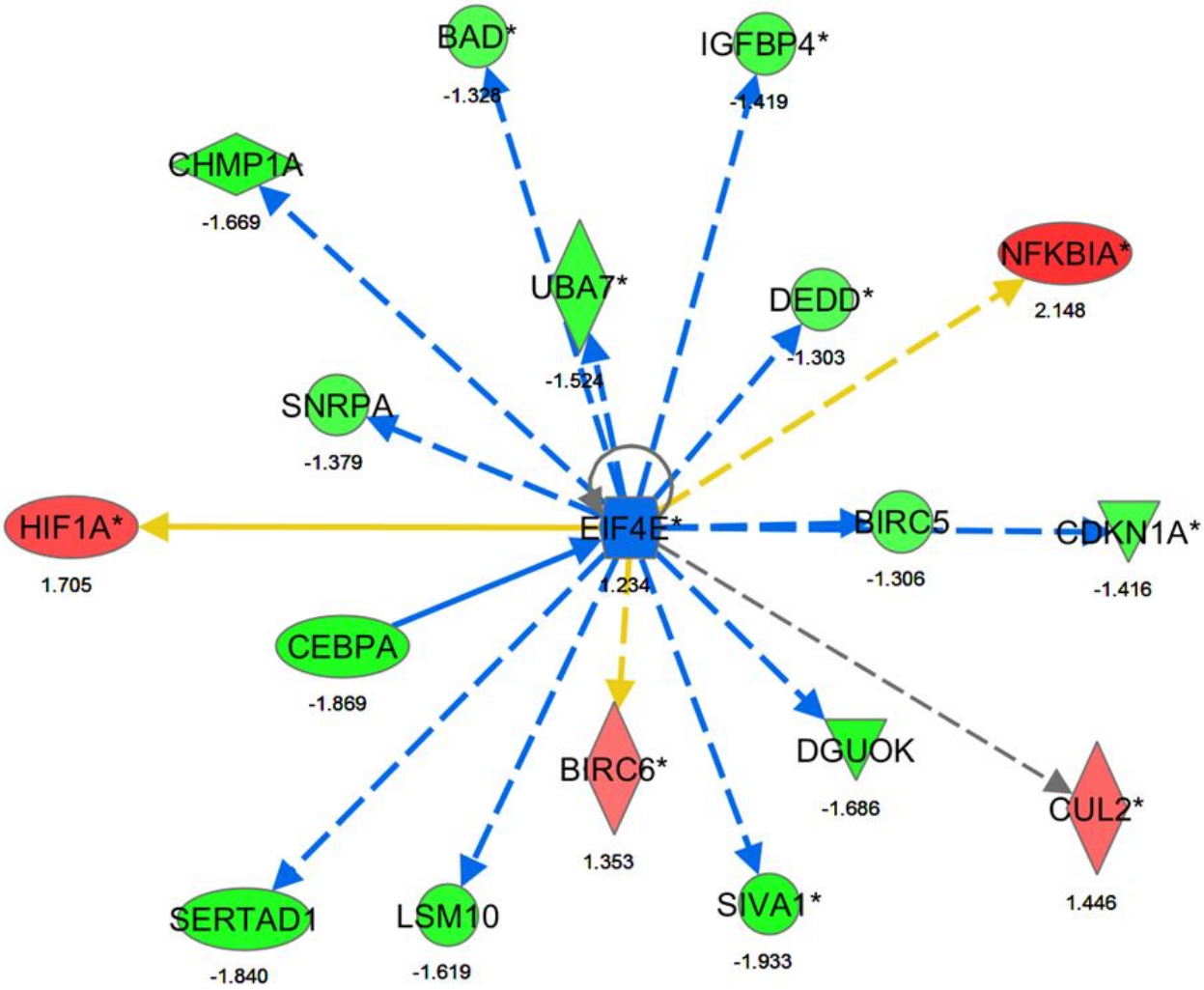

APPENDIX G

INHIBITION OF E2F1 FUNCTION IS PREDICTED IN KO CELLS ALONE

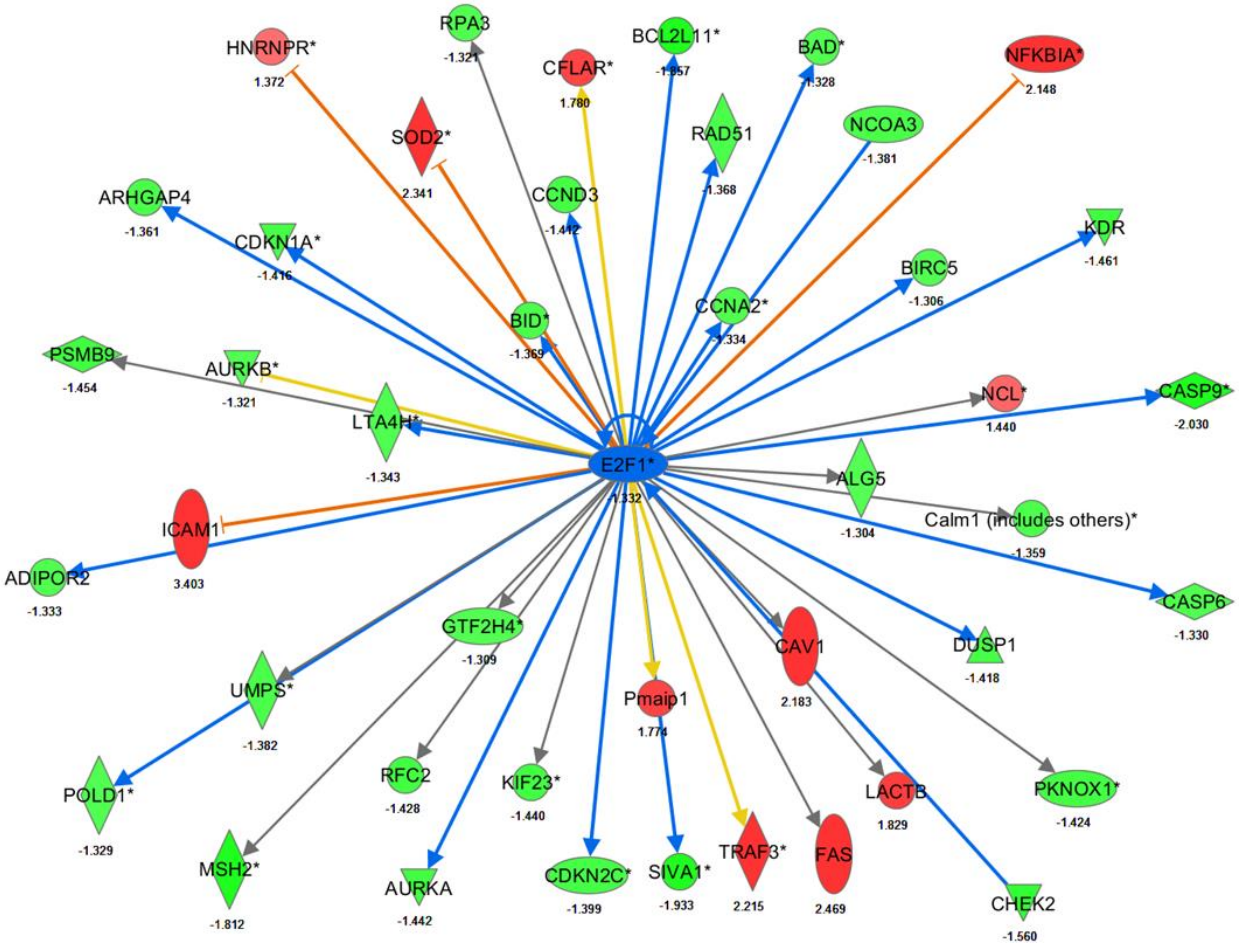

APPENDIX H

INHIBITION OF MIRNA-124 IS PREDICTED IN WT (SHOWN) AND KI, BUT NOT KO, CELLS

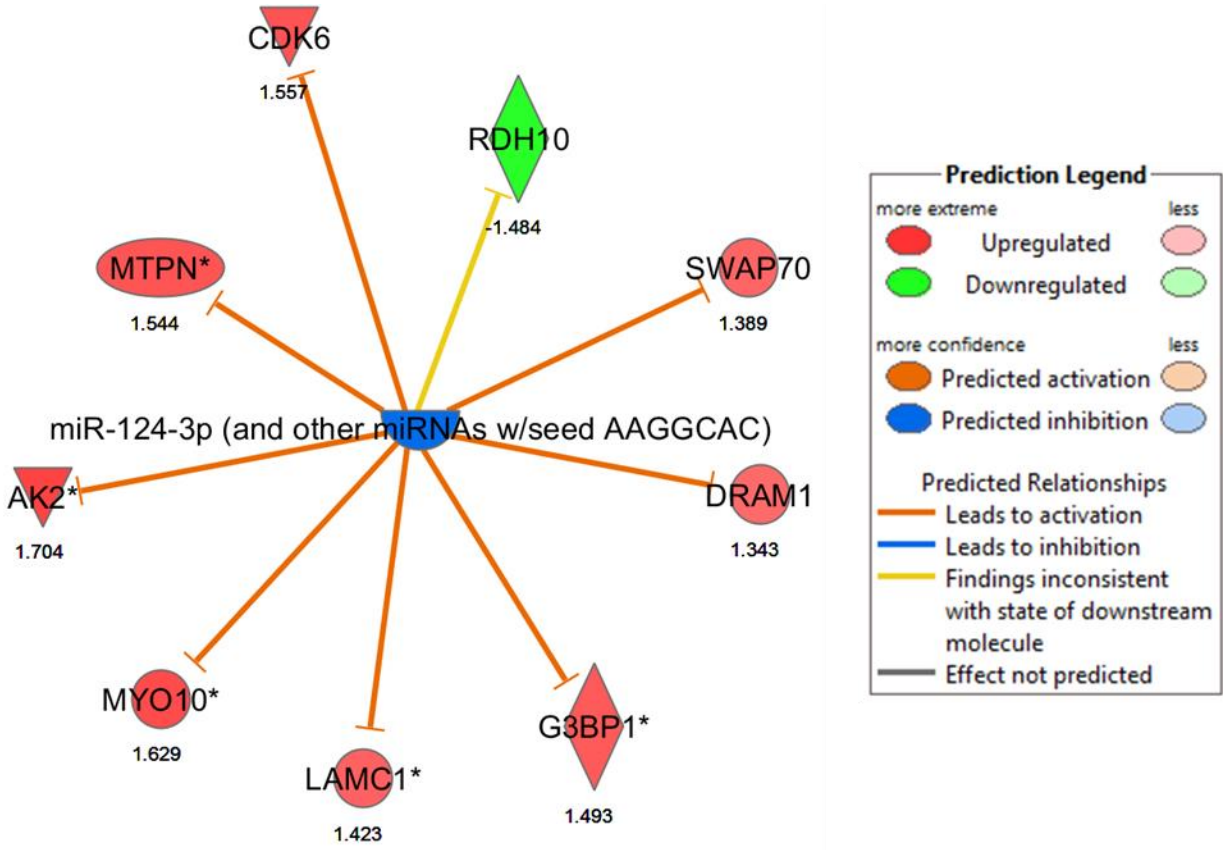

APPENDIX I

INHIBITION OF MIRNA-16-5 IS PREDICTED IN WT (SHOWN) AND KI, BUT NOT KO, CELLS

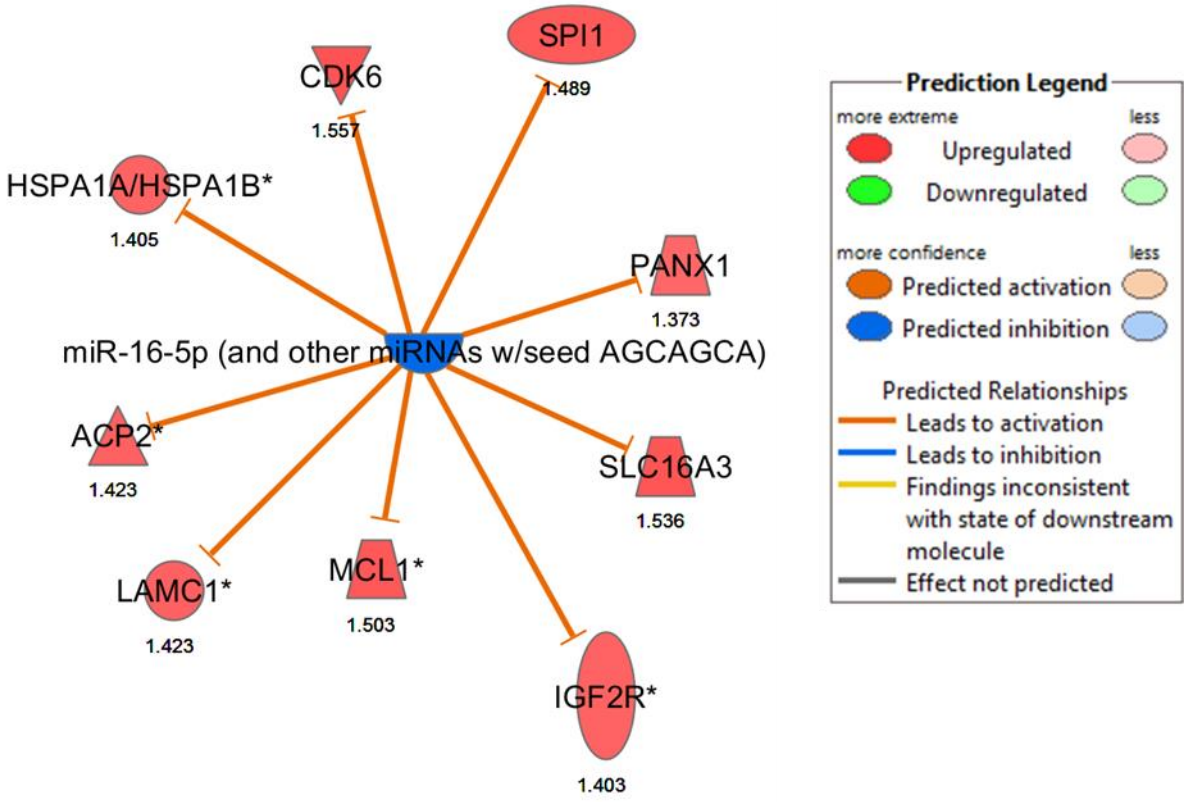

APPENDIX J

INHIBITION OF LET-7 FUNCTION IS PREDICTED IN KO CELLS ALONE

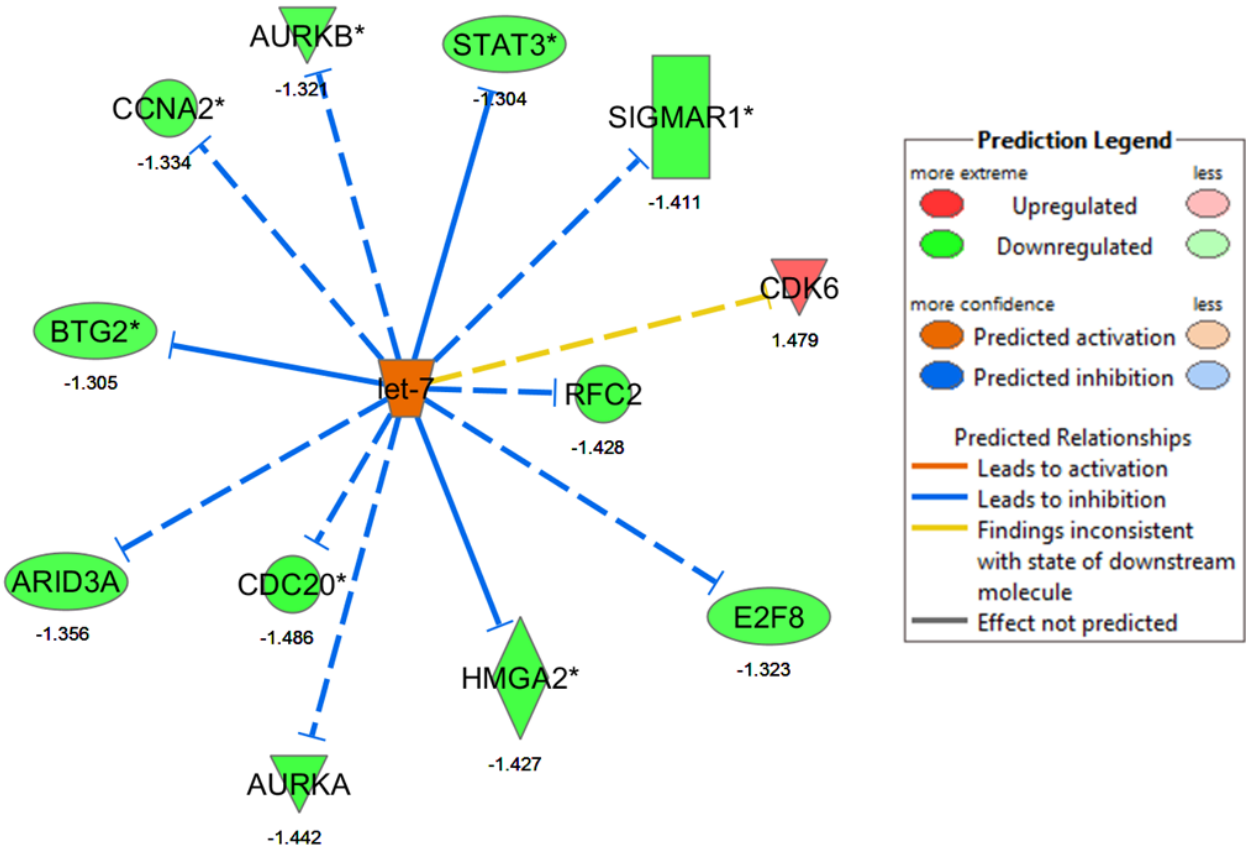

VITA

Tamer M. Hadi was born in Mountain View, California, USA, on March 30, 1977. He received a BS degree in Bioengineering from University of California, Berkeley in 1998, and an MS degree in Biomedical Engineering from University of California, Davis in 2006. He entered medical school at Virginia Commonwealth University in August, 2006, and transitioned into the MD-PhD program the following semester. In August, 2008, he initiated his dissertation research project in the laboratory of Dr. Jolene Windle in the Molecular Biology and Genetics graduate program in the Department of Human and Molecular Genetics. He was inducted into the Phi Kappa Phi Honors Society in 2009, and received Young Investigator Awards from the American Society for Bone and Mineral Research in both 2010 and 2011.

Tamer currently resides in Richmond, VA with his wife, Marwa El-Messidi, and their two children, Ismael and Maryam. He plans to pursue a career as a physician-scientist upon the completion of his training.